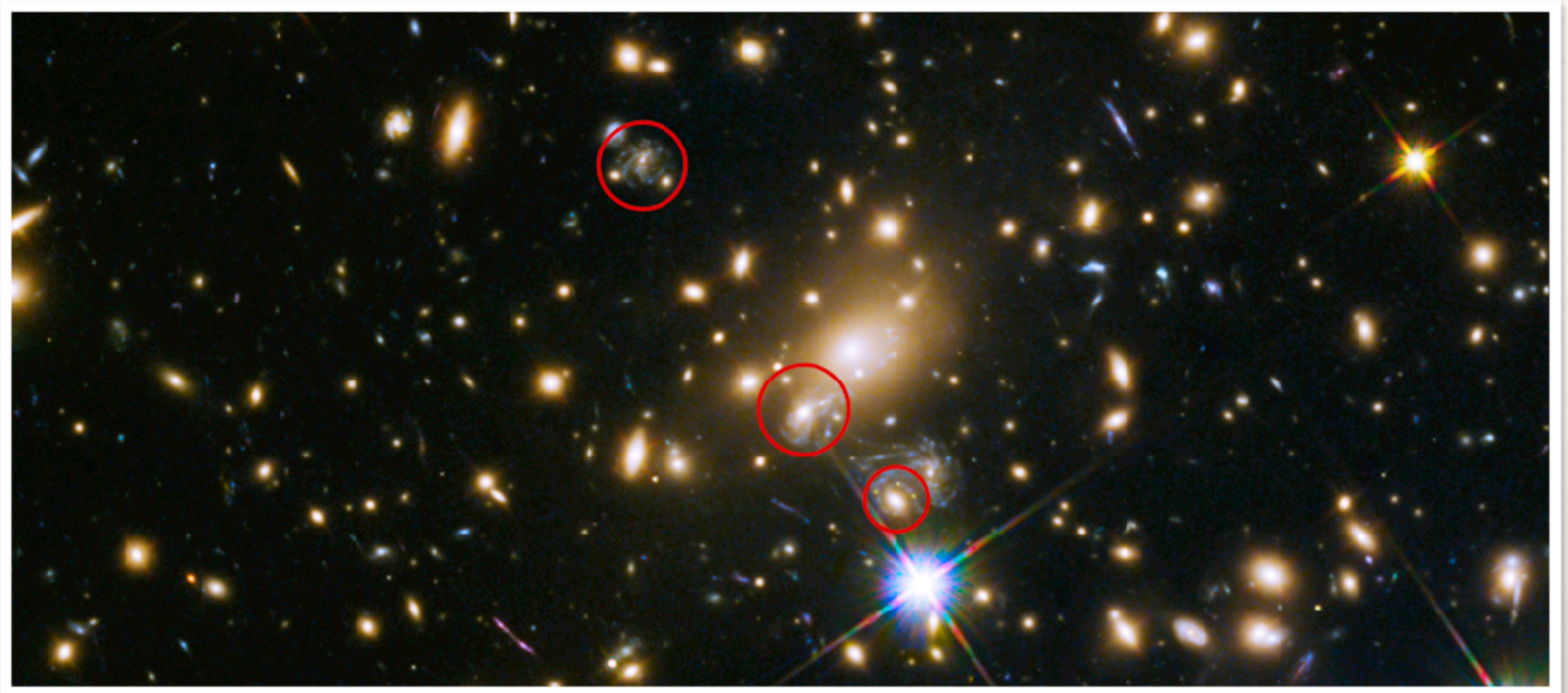

Marco Lombardi

Probing galaxy clusters with strong gravitational lensing

with P. Rosati, C. Grillo,
A. Mercurio, I. Balestra,
M. Nonino, M. Bonamigo,
G.B. Carminha, A. Biviano
and the Clash-VLT team

Open questions in modern cosmology

–

Open questions in modern cosmology

Fundamental cosmology

- Why $\Omega_b > \Omega_{\bar{b}}$?
- What is the dark matter?
- What is the dark energy?
- Did inflation occur?
- Are the physical constants changing with time?
- Do we need to modify GR?

Open questions in modern cosmology

Fundamental cosmology

- Why $\Omega_b > \Omega_{\bar{b}}$?
- What is the dark matter?
- What is the dark energy?
- Did inflation occur?
- Are the physical constants changing with time?
- Do we need to modify GR?

Observational cosmology

- Understand reionization
- Formation of first stars
- How are galaxies assembled?
- How is LSS distributed?
- What is the contribution of baryin physics in galaxies?
- Measure the Ω's

Open questions in modern cosmology

Fundamental cosmology

- Why $\Omega_b > \Omega_{\bar{b}}$?
- What is the dark matter?
- What is the dark energy?
- Did inflation occur?
- Are the physical constants changing with time?
- Do we need to modify GR?

Observational cosmology

- Understand reionization
- Formation of first stars
- How are galaxies assembled?
- How is LSS distributed?
- What is the contribution of baryon physics in galaxies?
- Measure the Ω's

Gravitational lensing can help us to understand many of the current open questions.

Open questions in modern cosmology

Fundamental cosmology

- Why $\Omega_b > \Omega_{\bar{b}}$?
- What is the dark matter?
- What is the dark energy?
- Did inflation occur?
- Are the physical constants changing with time?
- Do we need to modify GR?

Observational cosmology

- Understand reionization
- Formation of first stars
- How are galaxies assembled?
- How is LSS distributed?
- What is the contribution of baryon physics in galaxies?
- Measure the Ω's

Gravitational lensing can help us to understand many of the current open questions.

Many types of phenomena

Many types of phenomena

Microlensing. Lens: star or planet; source: star

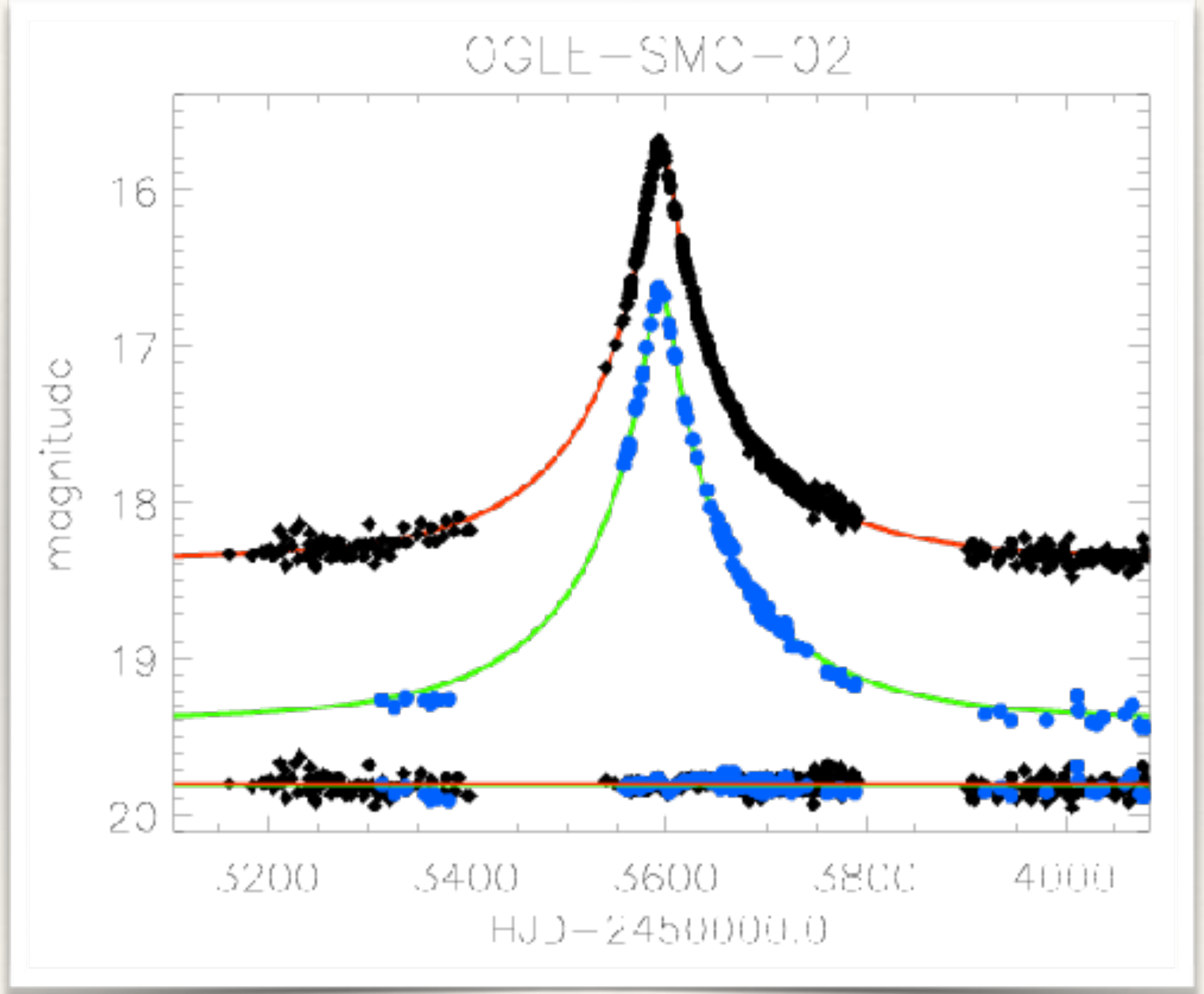

Many types of phenomena

Microlensing. Lens: star or planet; source: star

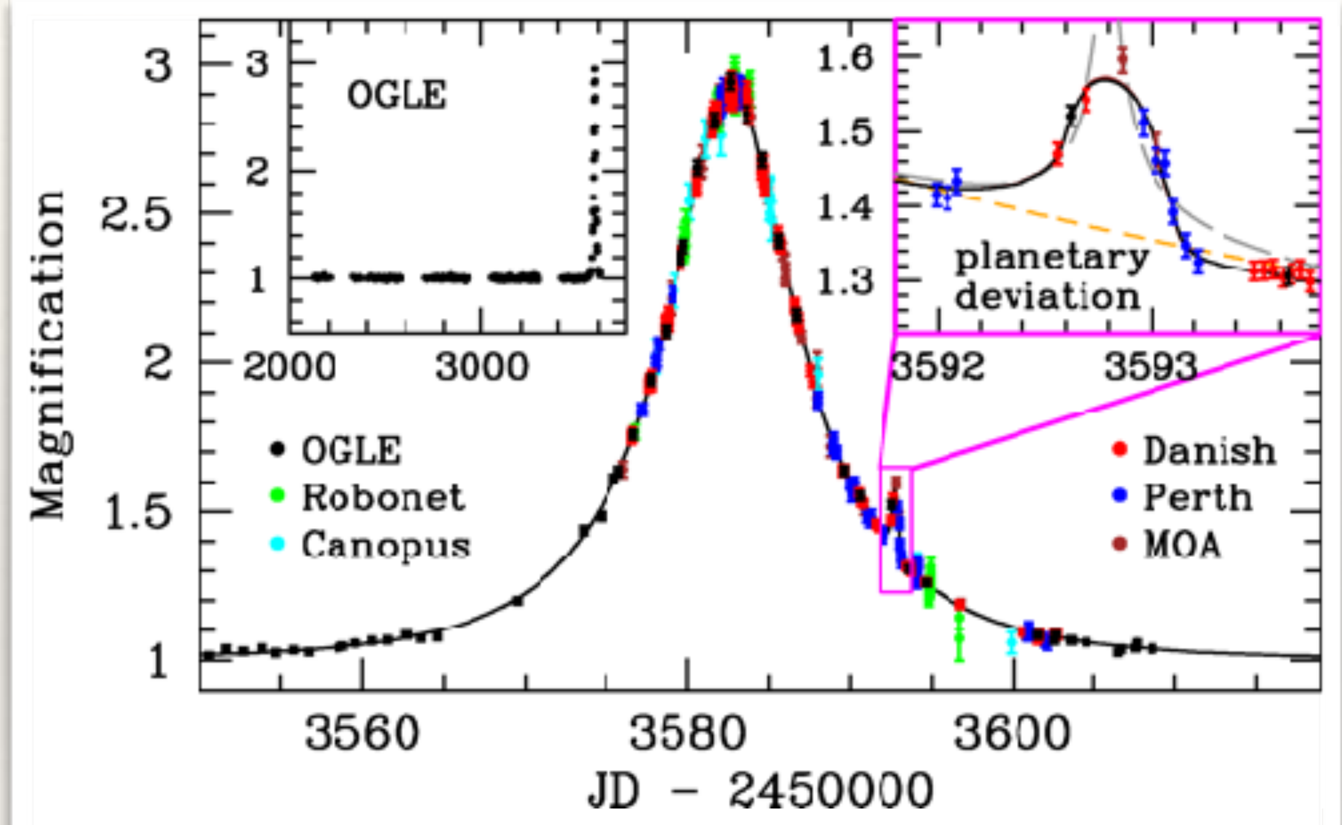

Planet collab. (Beaulieu et al. 2006)

Many types of phenomena

Microlensing. Lens: star or planet; source: star

Strong lensing. Lens: galaxy or galaxy cluster; source: QSO, galaxy

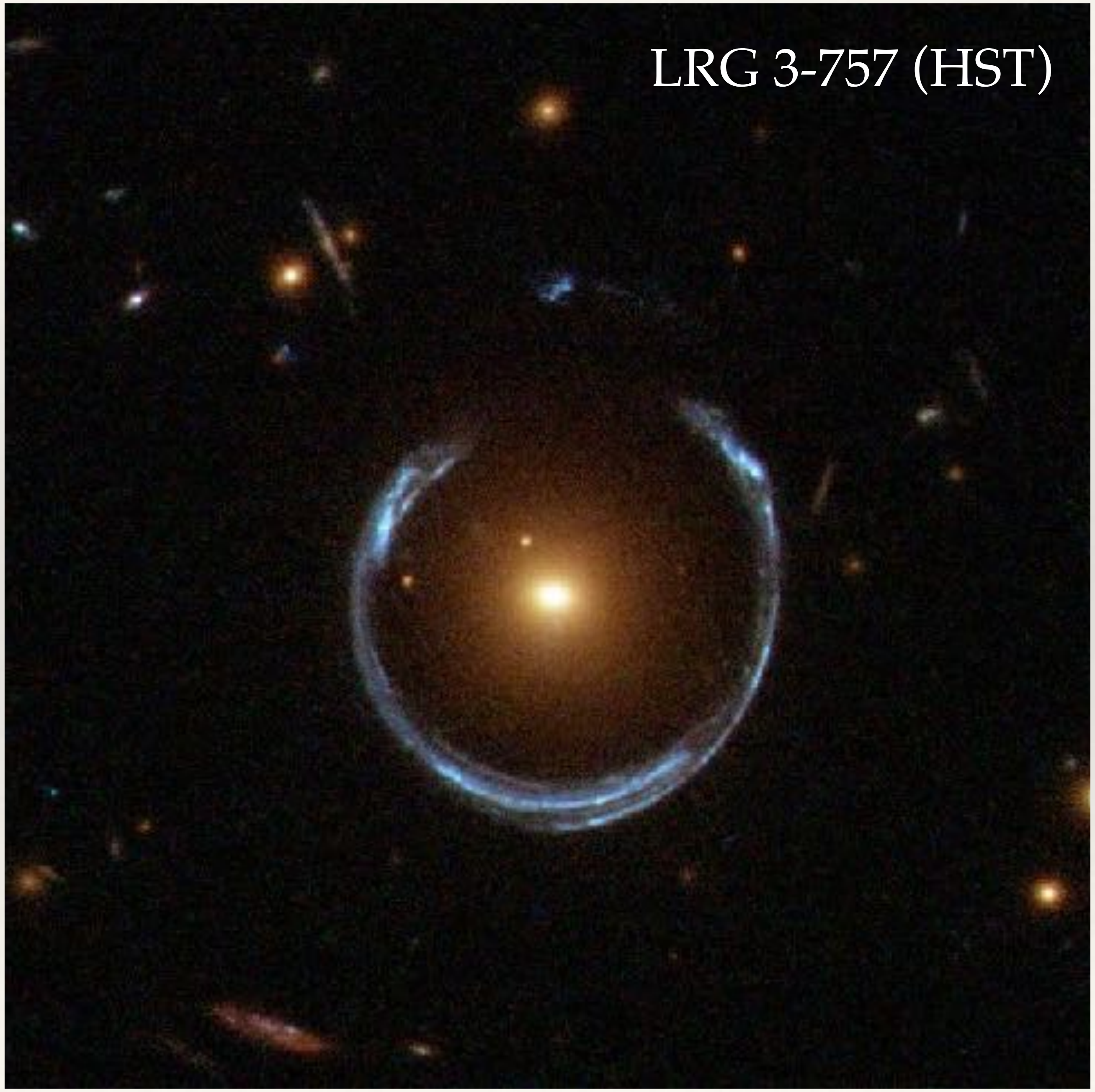

Many types of phenomena

Microlensing. Lens: star or planet; source: star

Strong lensing. Lens: galaxy or galaxy cluster; source: QSO, galaxy

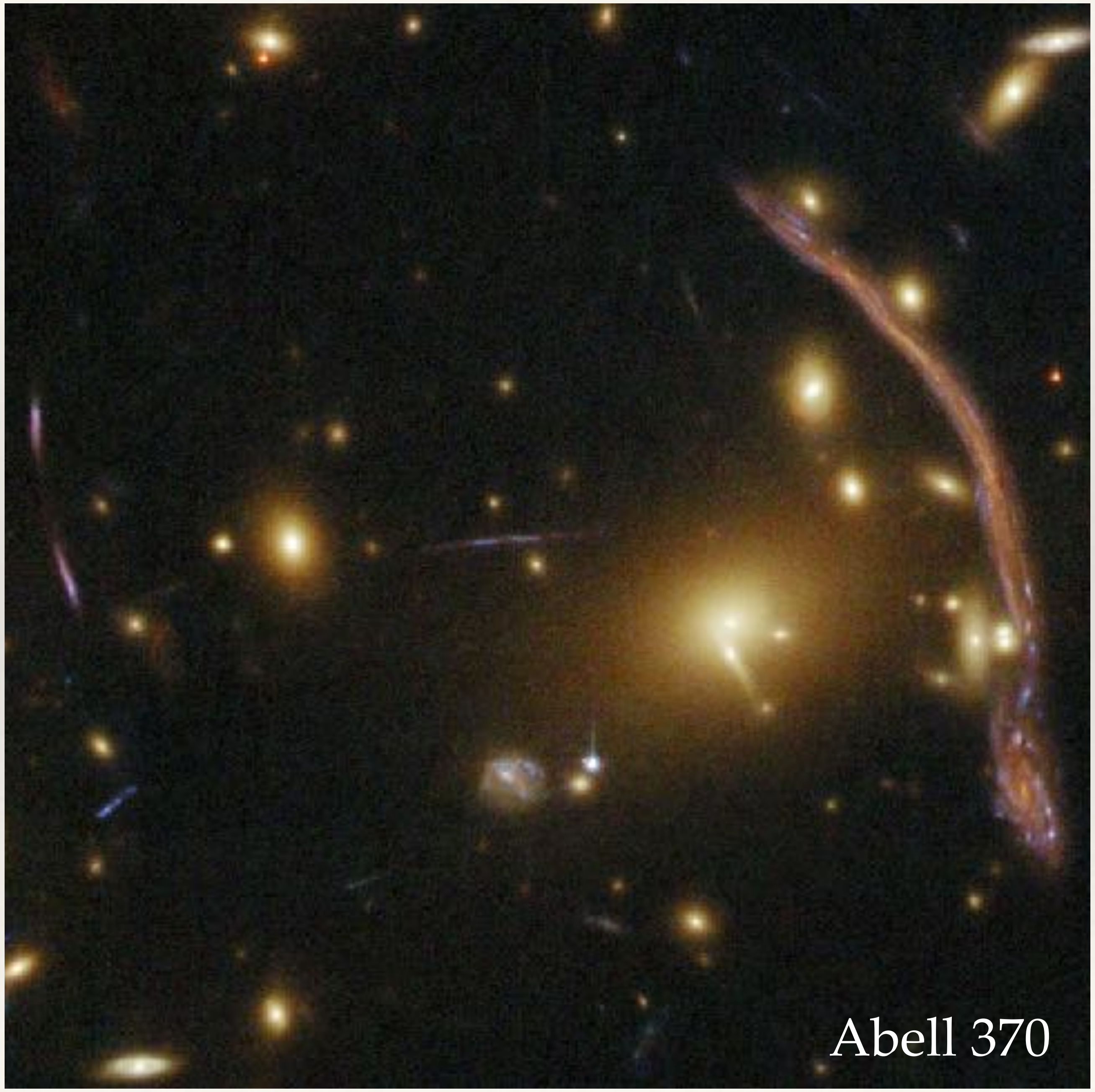

Many types of phenomena

Microlensing. Lens: star or planet; source: star

Strong lensing. Lens: galaxy or galaxy cluster; source: QSO, galaxy

Weak lensing. Lens: galaxy or galaxy cluster; source: galaxy

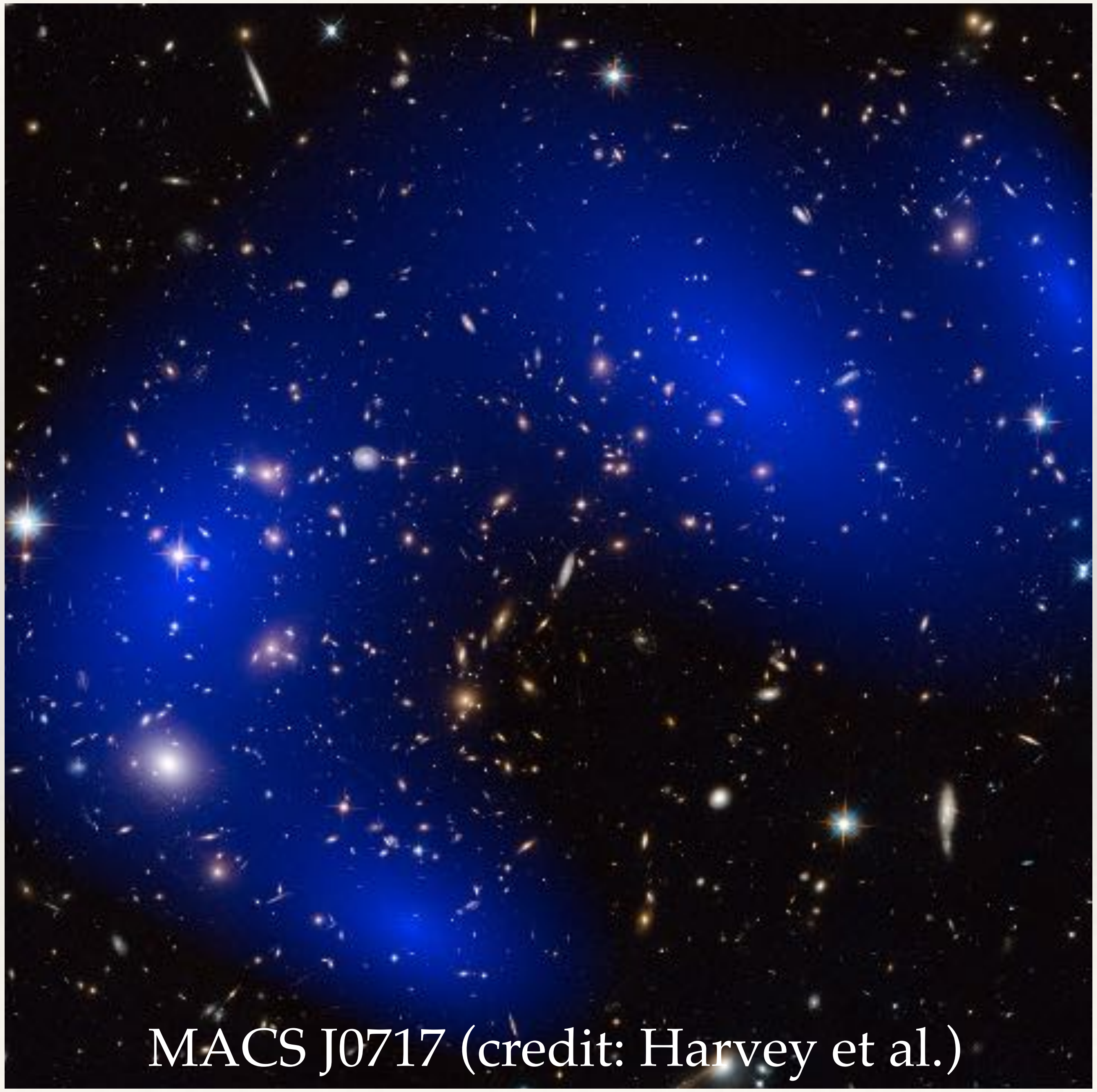
MACS J0717 (credit: Harvey et al.)

Many types of phenomena

Microlensing. Lens: star or planet; source: star

Strong lensing. Lens: galaxy or galaxy cluster; source: QSO, galaxy

Weak lensing. Lens: galaxy or galaxy cluster; source: galaxy

Cosmic shear. Lens: large scale structure; source: galaxies (or CMB)

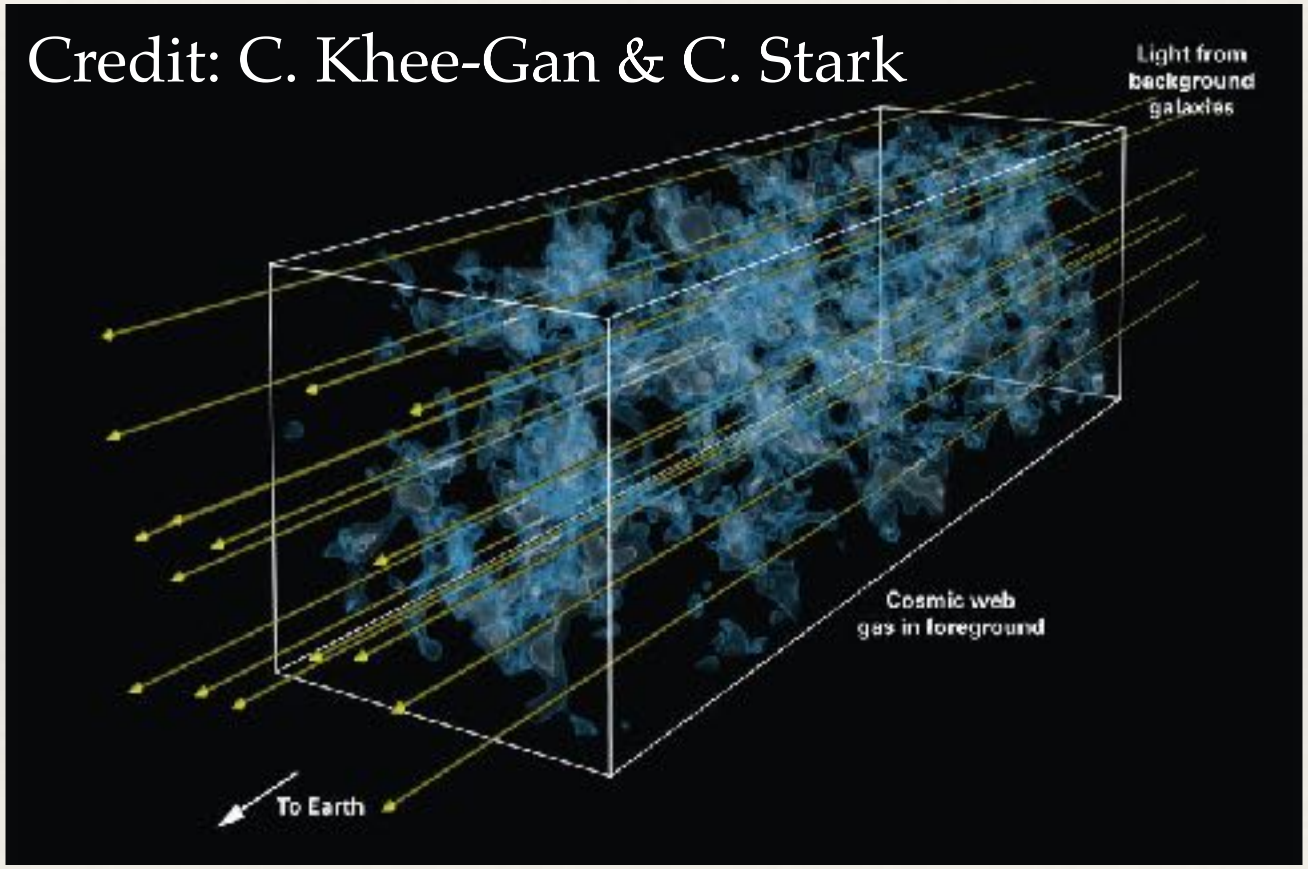

Many types of phenomena

Microlensing. Lens: star or planet; source: star

Strong lensing. Lens: galaxy or galaxy cluster; source: QSO, galaxy

Weak lensing. Lens: galaxy or galaxy cluster; source: galaxy

Cosmic shear. Lens: large scale structure; source: galaxies (or CMB)

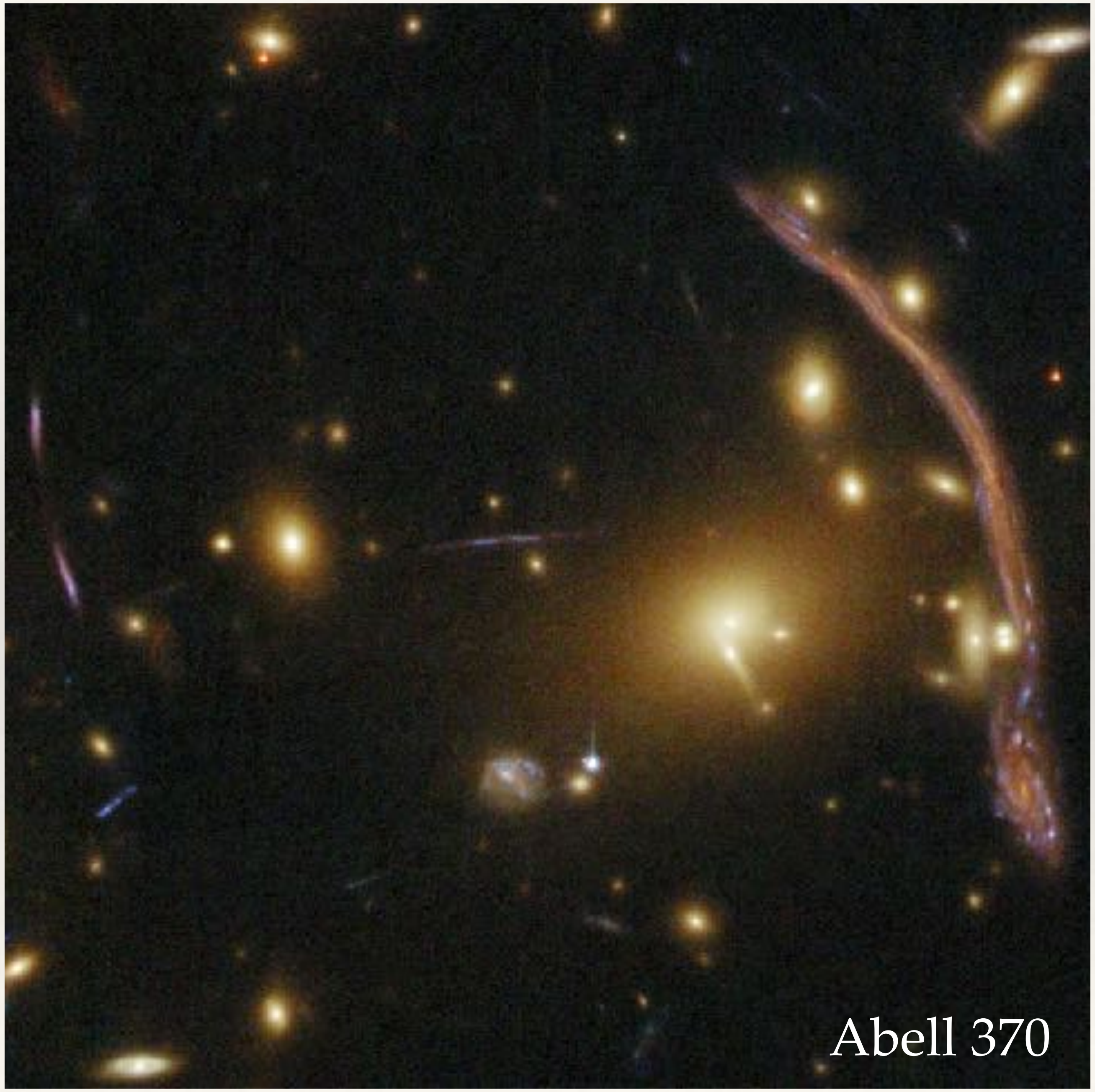

Uses of gravitational lensing

Uses of gravitational lensing

Magnification effect. Lenses allow us to detect and study objects which are **too distant** or **too faint** to be observed without lensing (e.g., Salmon et al. 2018)

Uses of gravitational lensing

Magnification effect. Lenses allow us to detect and study objects which are **too distant** or **too faint** to be observed without lensing (e.g., Salmon et al. 2018)

Mass distribution of the lens. Gravitational lensing depends solely on the projected, two-dimensional mass distribution of the lens. Lensing is thus an ideal tool to study **dark matter**.

Uses of gravitational lensing

Magnification effect. Lenses allow us to detect and study objects which are **too distant** or **too faint** to be observed without lensing (e.g., Salmon et al. 2018)

Mass distribution of the lens. Gravitational lensing depends solely on the projected, two-dimensional mass distribution of the lens. Lensing is thus an ideal tool to study **dark matter**.

Cosmology. Many properties of individual lens systems or samples of lensed objects depend on the **age**, the **scale**, and the overall **geometry of the Universe**.

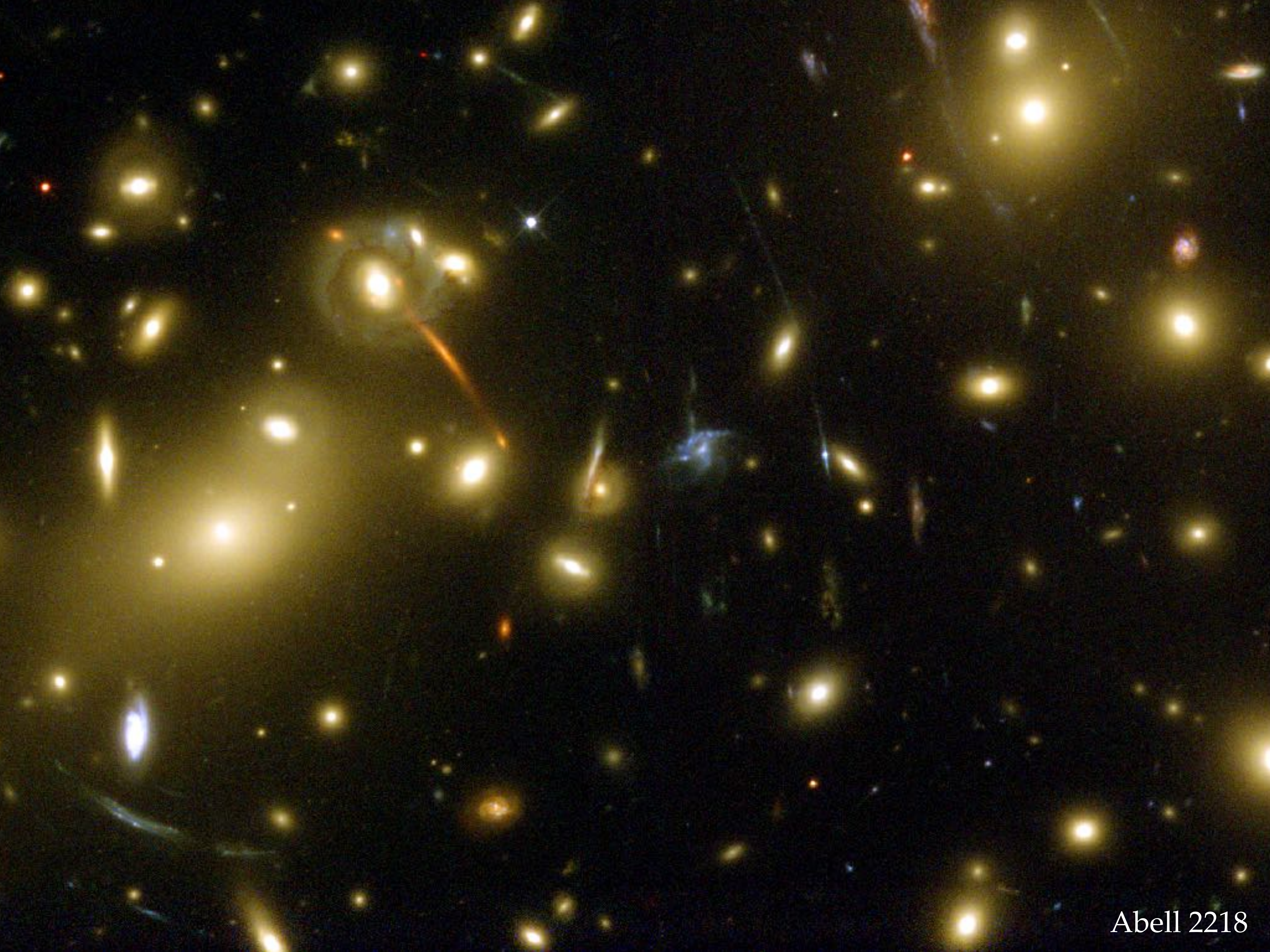
Abell 2218

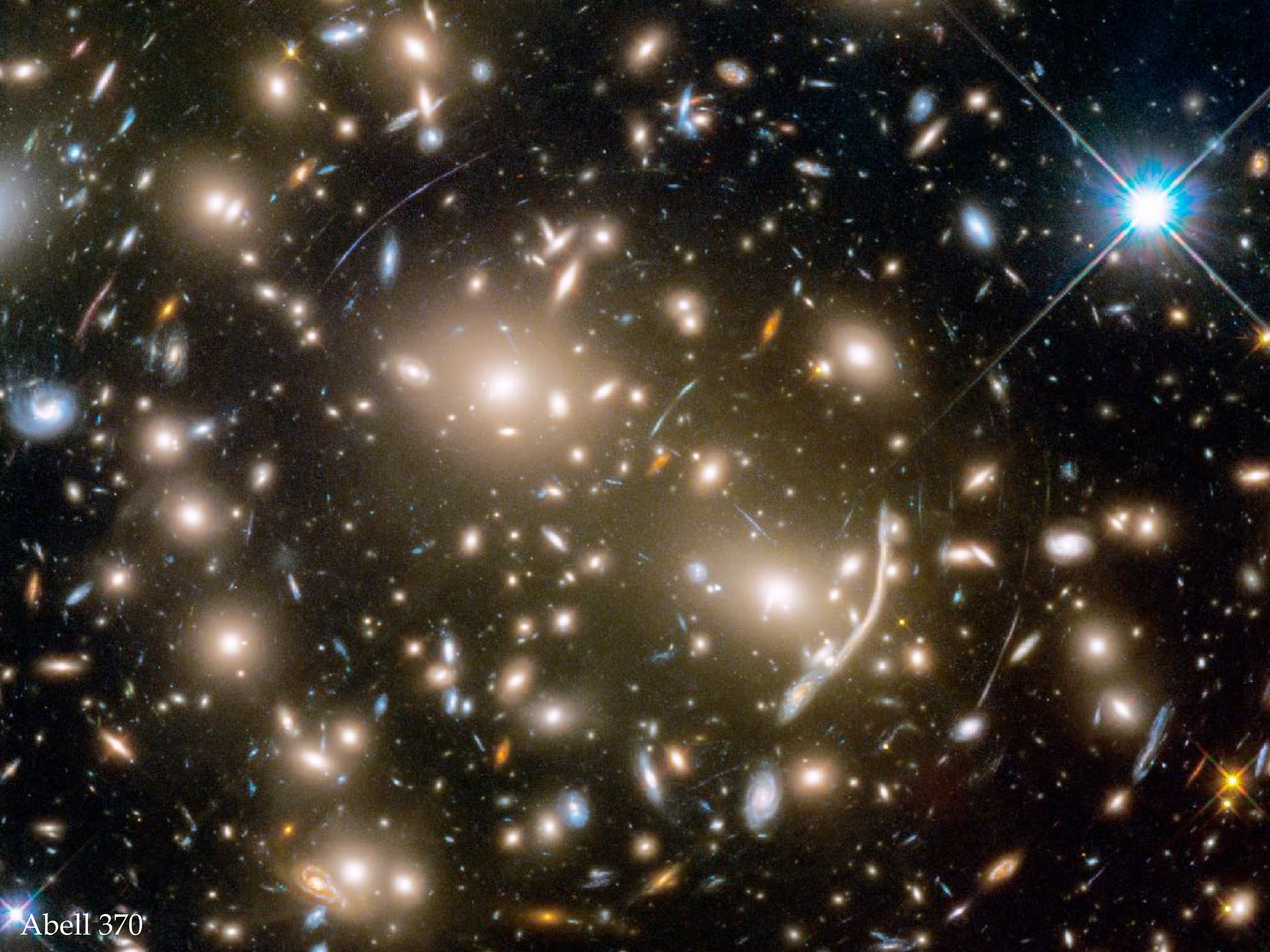
Abell 370

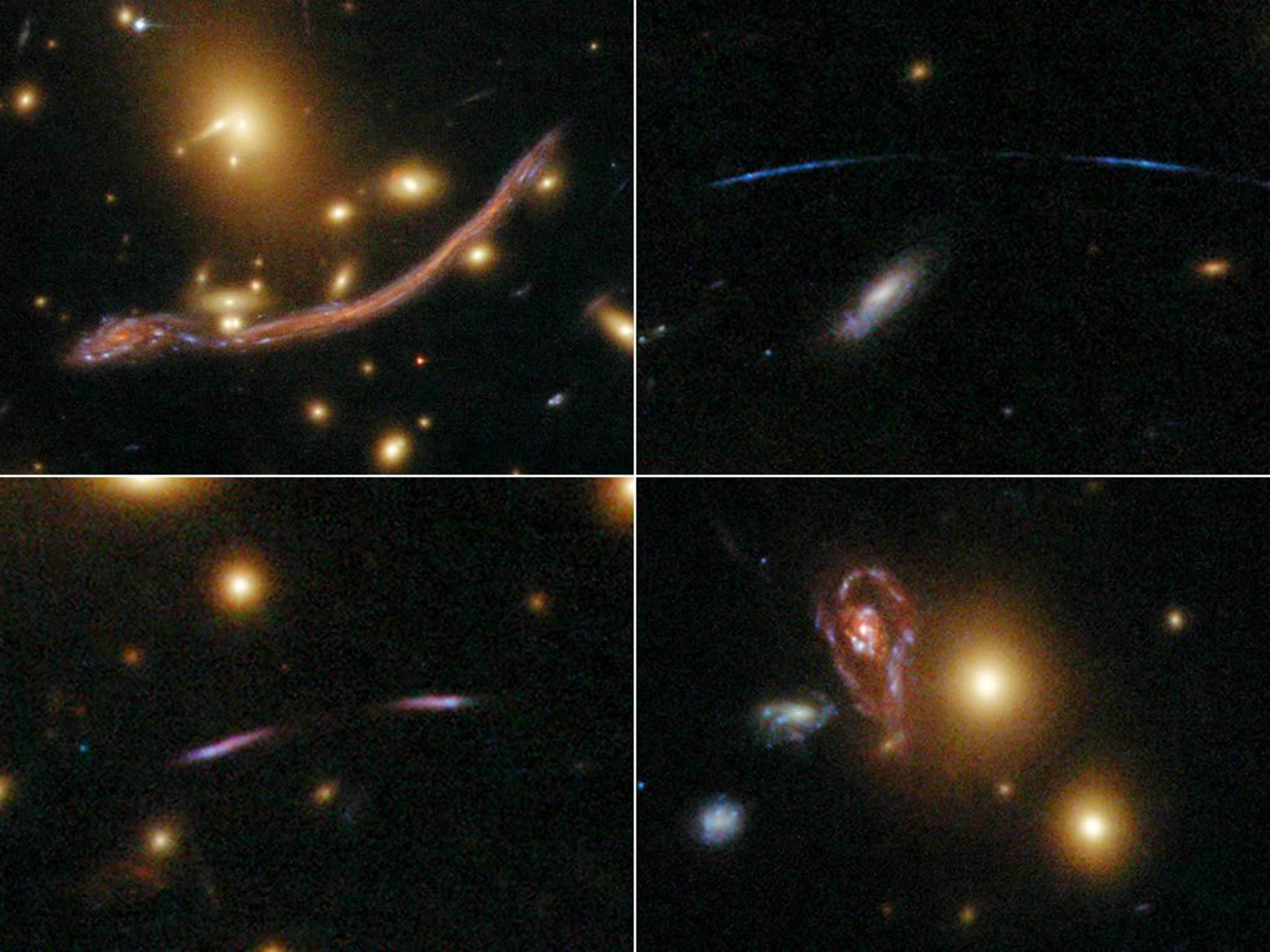

Macs J 1149 (CLASH)

Weak lensing of CL 0152

(Jee et al. 2005)

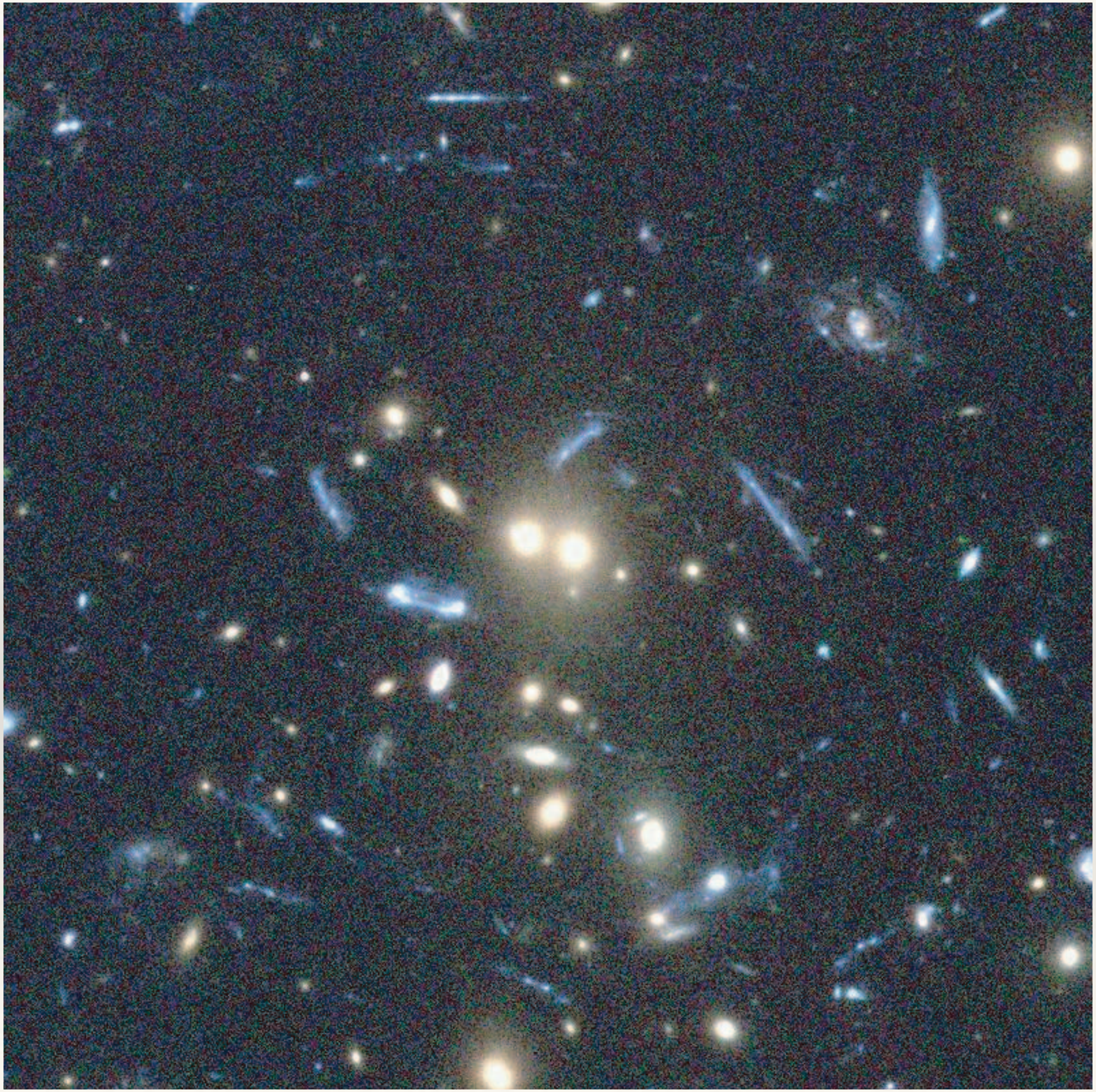

Weak lensing of CL 0152

(Jee et al. 2005)

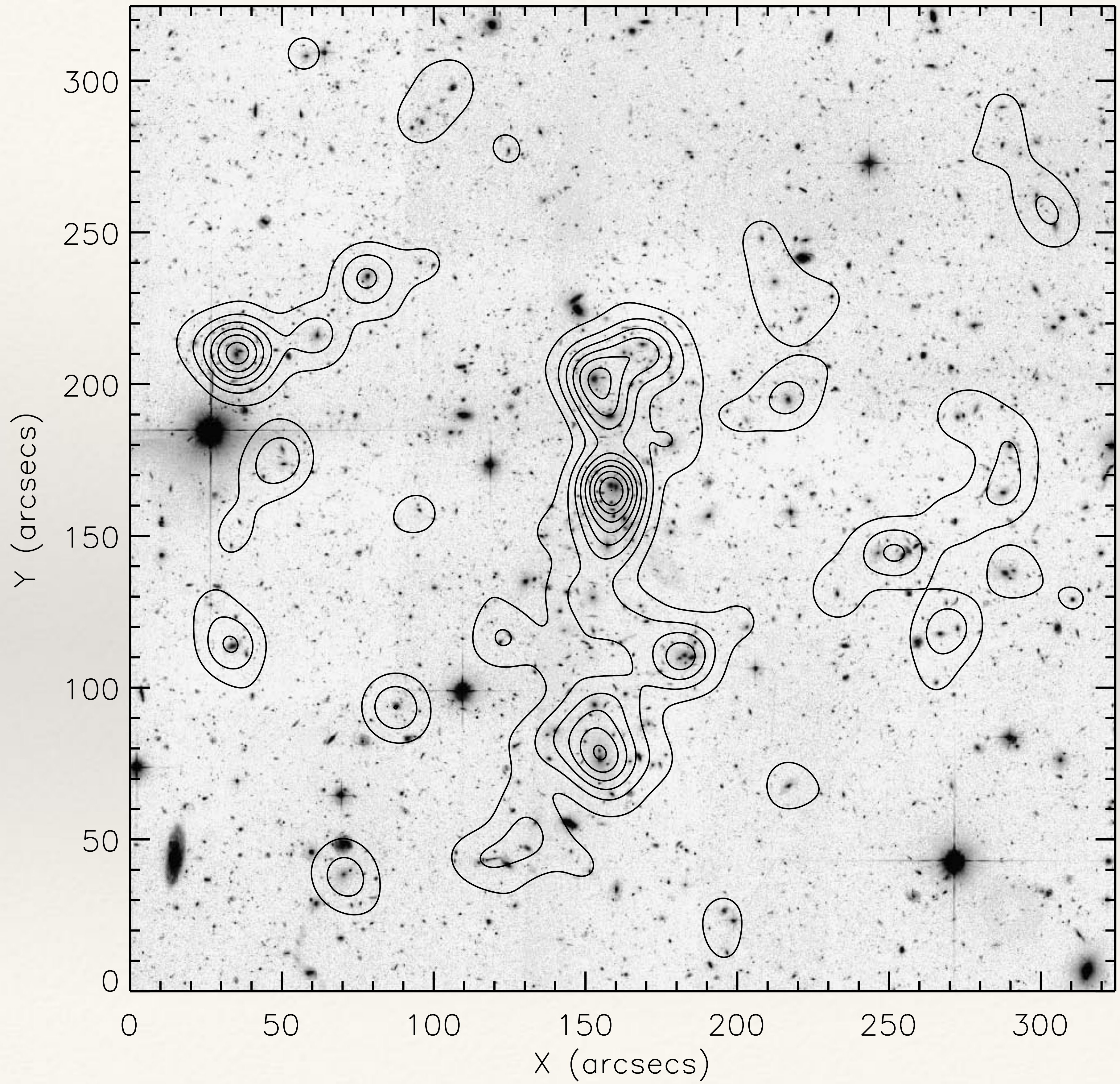

Weak lensing of CL 0152

(Jee et al. 2005)

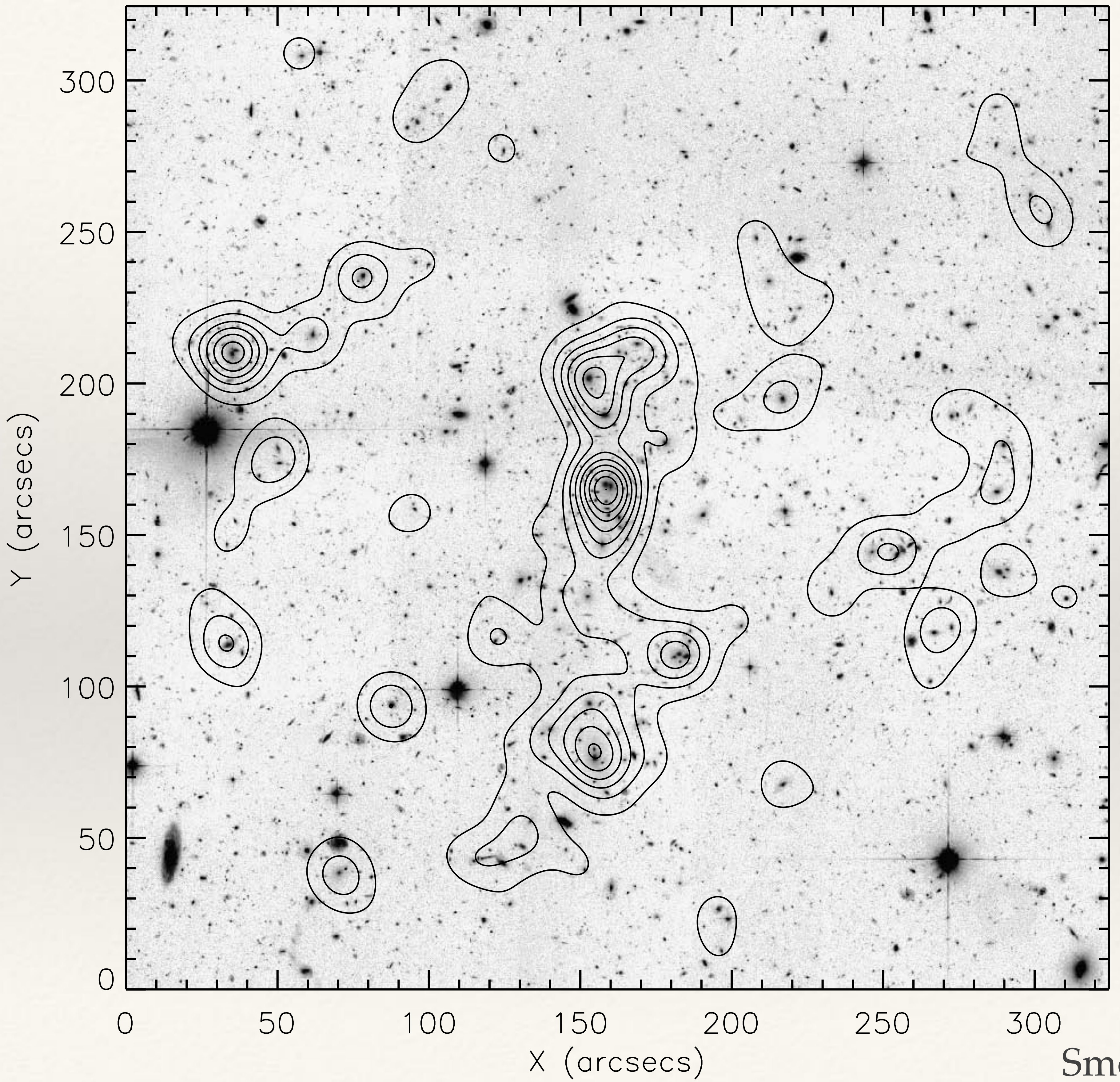

Smoothed luminosity

Weak lensing of CL 0152

(Jee et al. 2005)

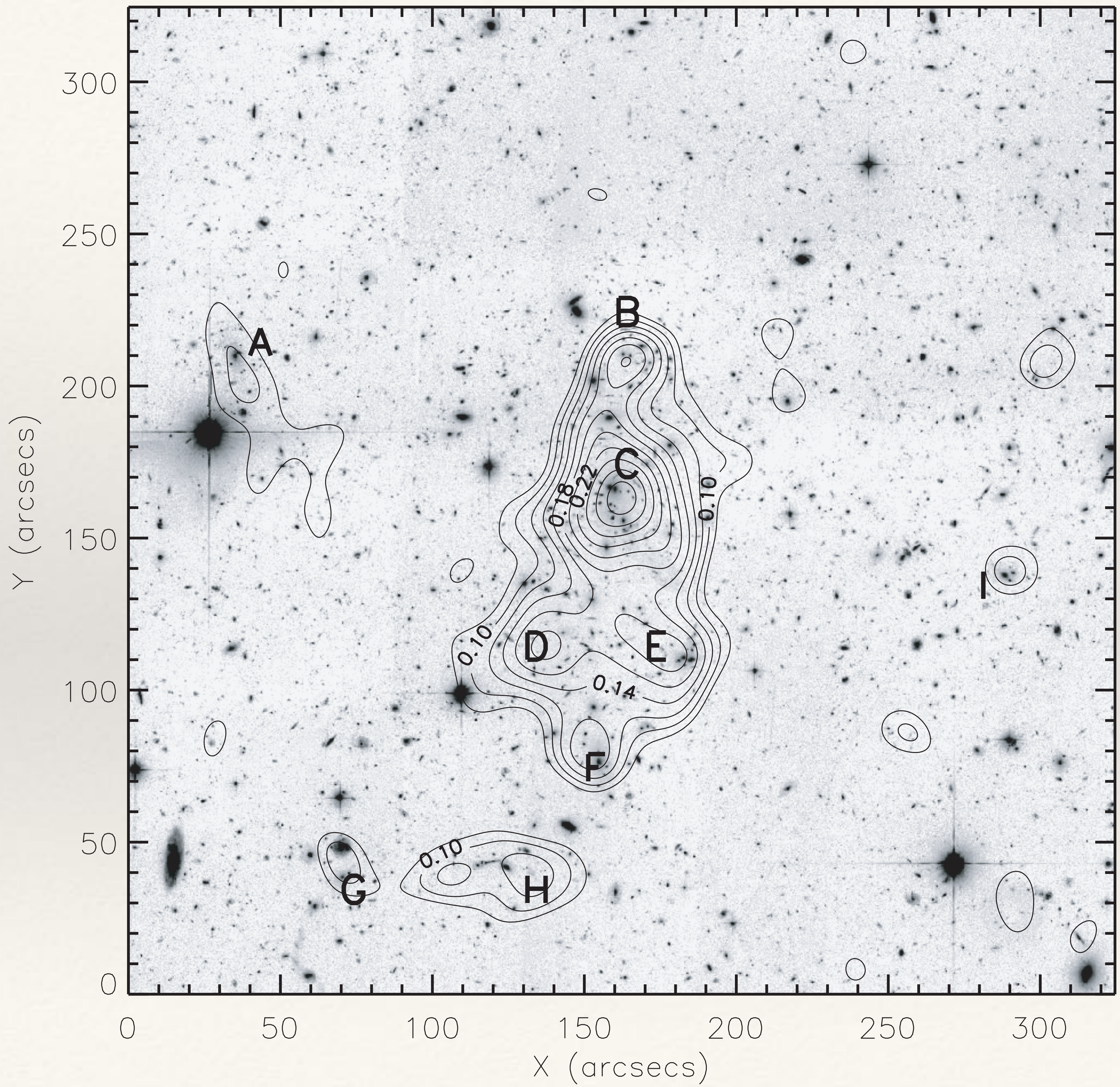

Weak lensing of CL 0152

(Jee et al. 2005)

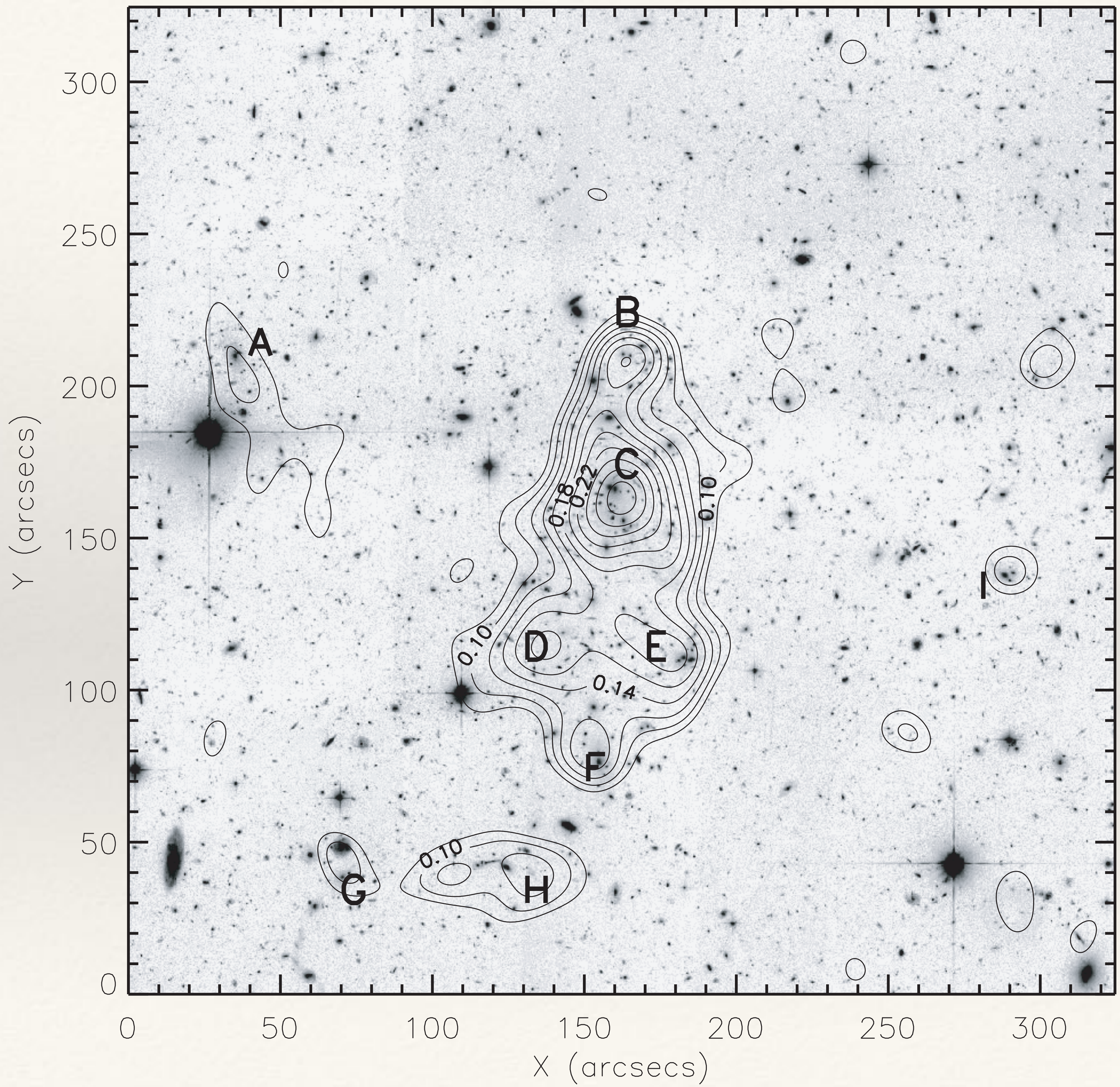

Weak lensing map

Weak lensing of CL 0152

(Jee et al. 2005)

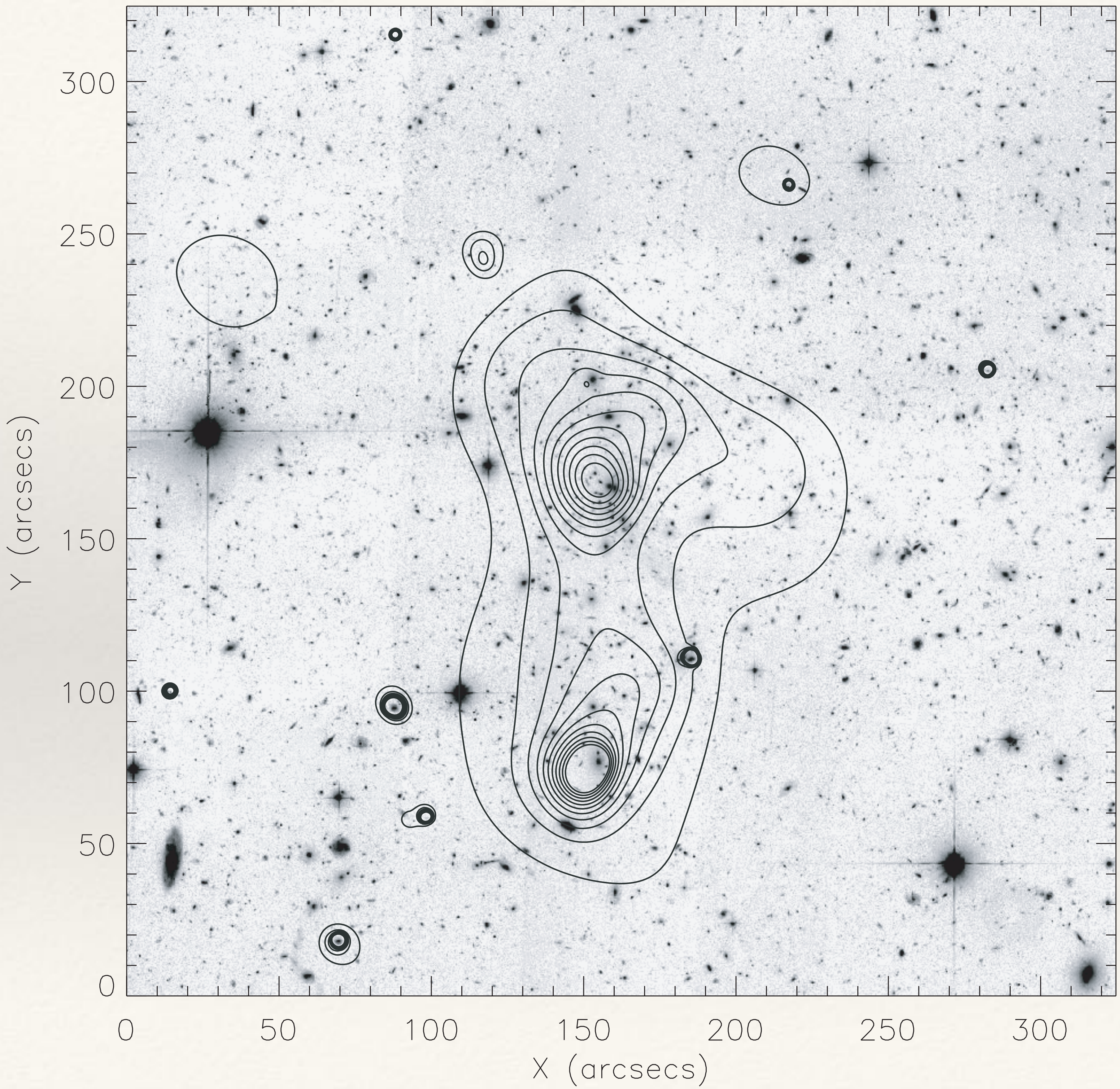

Weak lensing of CL 0152

(Jee et al. 2005)

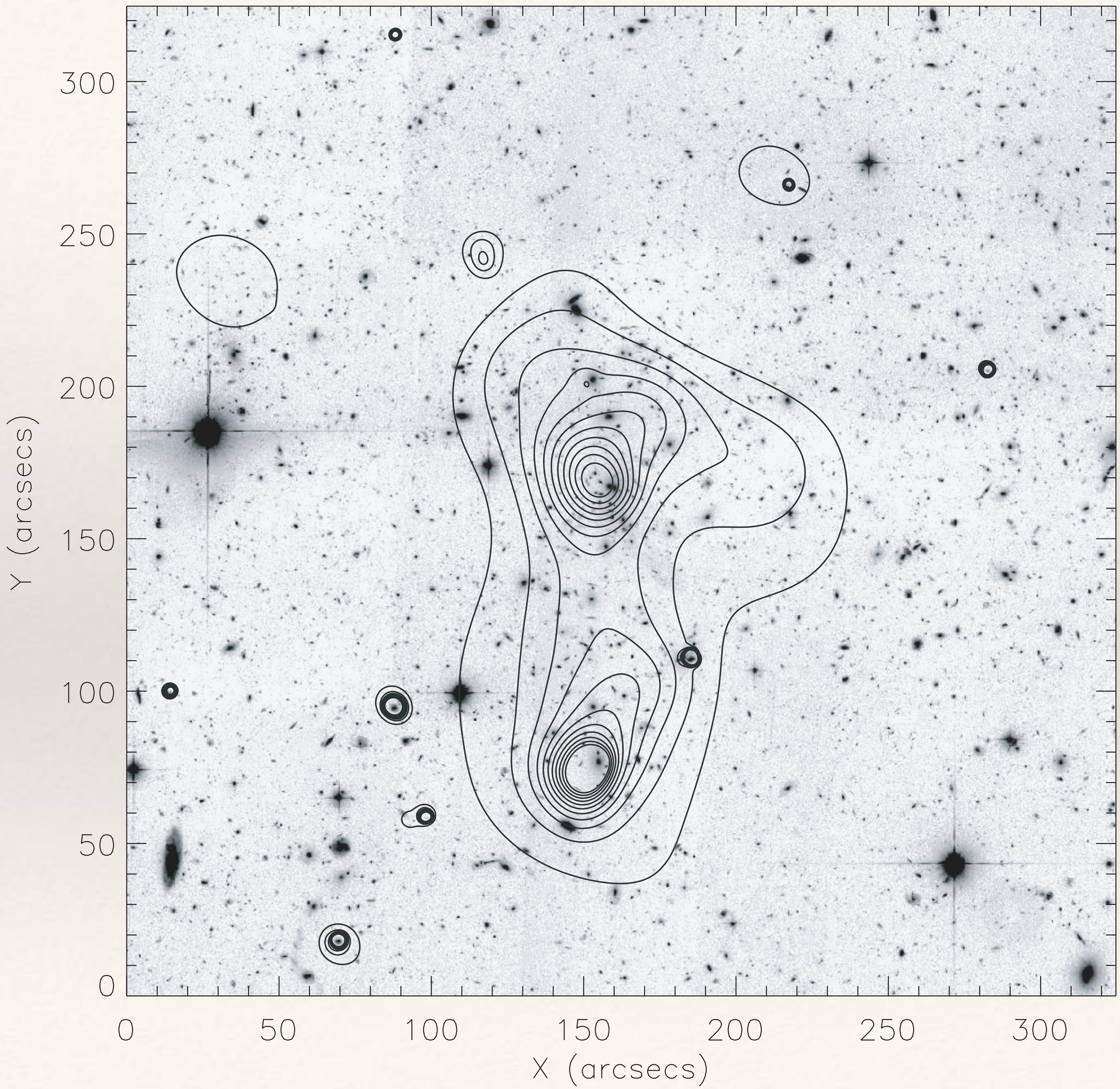

X-ray flux

Principles of gravitational lensing

- Gravity acts on light as a medium with (variable) **refractive index** $n = 1 - 2\,\phi / c^2$
    - Gravitational lenses are **perfectly acromatic**
    - Can produce both a delay and a bending of light rays
- The entire phenomenon can be described in terms of **classical optics** (magnification, caustics, time delay…)

Principles of gravitational lensing

- Gravity acts on light as a medium with (variable) **refractive index** $n = 1 - 2\,\phi / c^2$
  - Gravitational lenses are **perfectly acromatic**
  - Can produce both a delay and a bending of light rays
- The entire phenomenon can be described in terms of **classical optics** (magnification, caustics, time delay…)

Principles of gravitational lensing

- Gravity acts on light as a medium with (variable) **refractive index** $n = 1 - 2\,\phi / c^2$
  - Gravitational lenses are **perfectly acromatic**
  - Can produce both a delay and a bending of light rays
- The entire phenomenon can be described in terms of **classical optics** (magnification, caustics, time delay…)

Principles of gravitational lensing

- Gravity acts on light as a medium with (variable) **refractive index** $n = 1 - 2\,\phi / c^2$
  - Gravitational lenses are **perfectly acromatic**
  - Can produce both a delay and a bending of light rays
- The entire phenomenon can be described in terms of **classical optics** (magnification, caustics, time delay…)

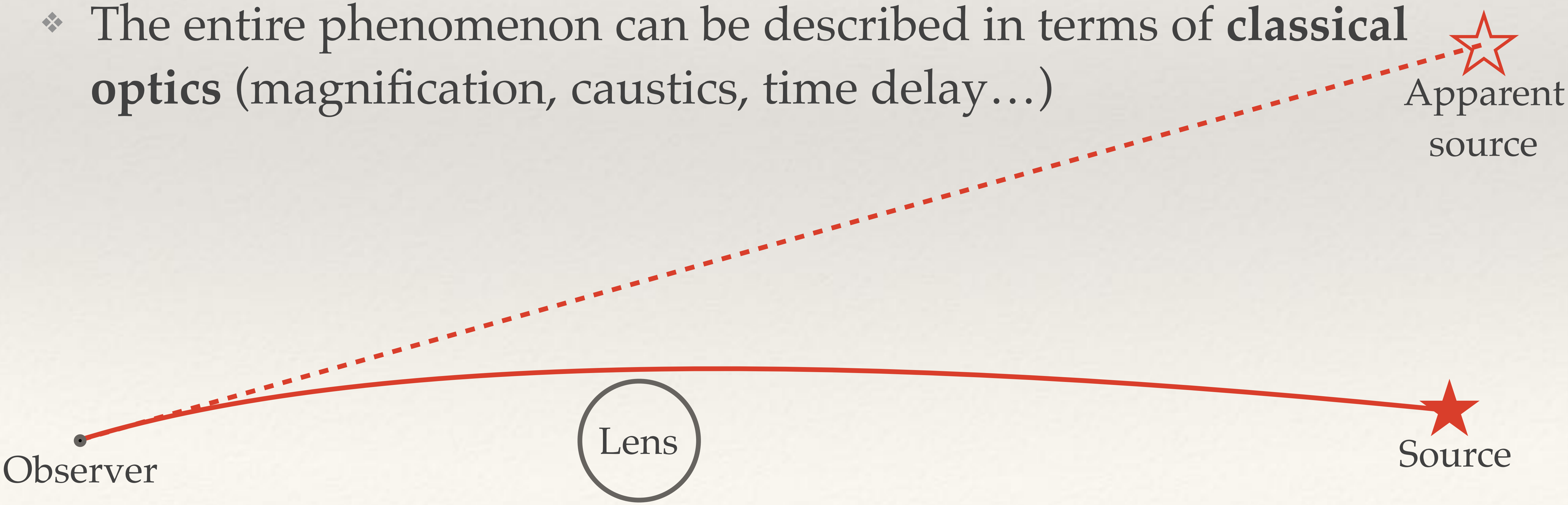

Gravitational time delay

Gravitational time delay

- The time it takes the light to travel through a lens is

$$ct = \int_\gamma n(\boldsymbol{x})\,\mathrm{d}\ell = |\gamma| + \frac{2}{c^2}\int_\gamma \phi(\boldsymbol{x})\,\mathrm{d}\ell$$

Gravitational time delay

- The time it takes the light to travel through a lens is

$$ct = \int_\gamma n(\boldsymbol{x})\,\mathrm{d}\ell = |\gamma| + \frac{2}{c^2}\int_\gamma \phi(\boldsymbol{x})\,\mathrm{d}\ell$$

  - Sum of a geometric term…

Gravitational time delay

- The time it takes the light to travel through a lens is

$$ct = \int_\gamma n(\boldsymbol{x})\,\mathrm{d}\ell = |\gamma| + \frac{2}{c^2}\int_\gamma \phi(\boldsymbol{x})\,\mathrm{d}\ell$$

  - Sum of a geometric term…
  - …and of a gravitational term

Gravitational time delay

- The time it takes the light to travel through a lens is

$$ct = \int_\gamma n(\boldsymbol{x})\,\mathrm{d}\ell = |\gamma| + \frac{2}{c^2}\int_\gamma \phi(\boldsymbol{x})\,\mathrm{d}\ell$$

  - Sum of a geometric term…
  - …and of a gravitational term
- For a "thin lens" the this can be written as

$$ct = (1 + z_\mathrm{d})\frac{D_\mathrm{d}D_\mathrm{s}}{D_\mathrm{ds}}\left[\frac{1}{2}\|\boldsymbol{\theta} - \boldsymbol{\theta}^\mathrm{s}\|^2 - \Psi(\boldsymbol{\theta})\right] + \mathrm{const}$$

Gravitational time delay

- The time it takes the light to travel through a lens is

$$ct = \int_\gamma n(\boldsymbol{x})\,\mathrm{d}\ell = |\gamma| + \frac{2}{c^2}\int_\gamma \phi(\boldsymbol{x})\,\mathrm{d}\ell$$

  - Sum of a geometric term…
  - …and of a gravitational term
- For a “thin lens” the this can be written as

$$ct = (1 + z_\mathrm{d})\frac{D_\mathrm{d} D_\mathrm{s}}{D_\mathrm{ds}}\Bigg[\underbrace{\frac{1}{2}\|\boldsymbol{\theta} - \boldsymbol{\theta}^\mathrm{s}\|^2 - \Psi(\boldsymbol{\theta})}_{\text{Fermat's potential}}\Bigg] + \mathrm{const}$$

Fermat’s potential

Time delays

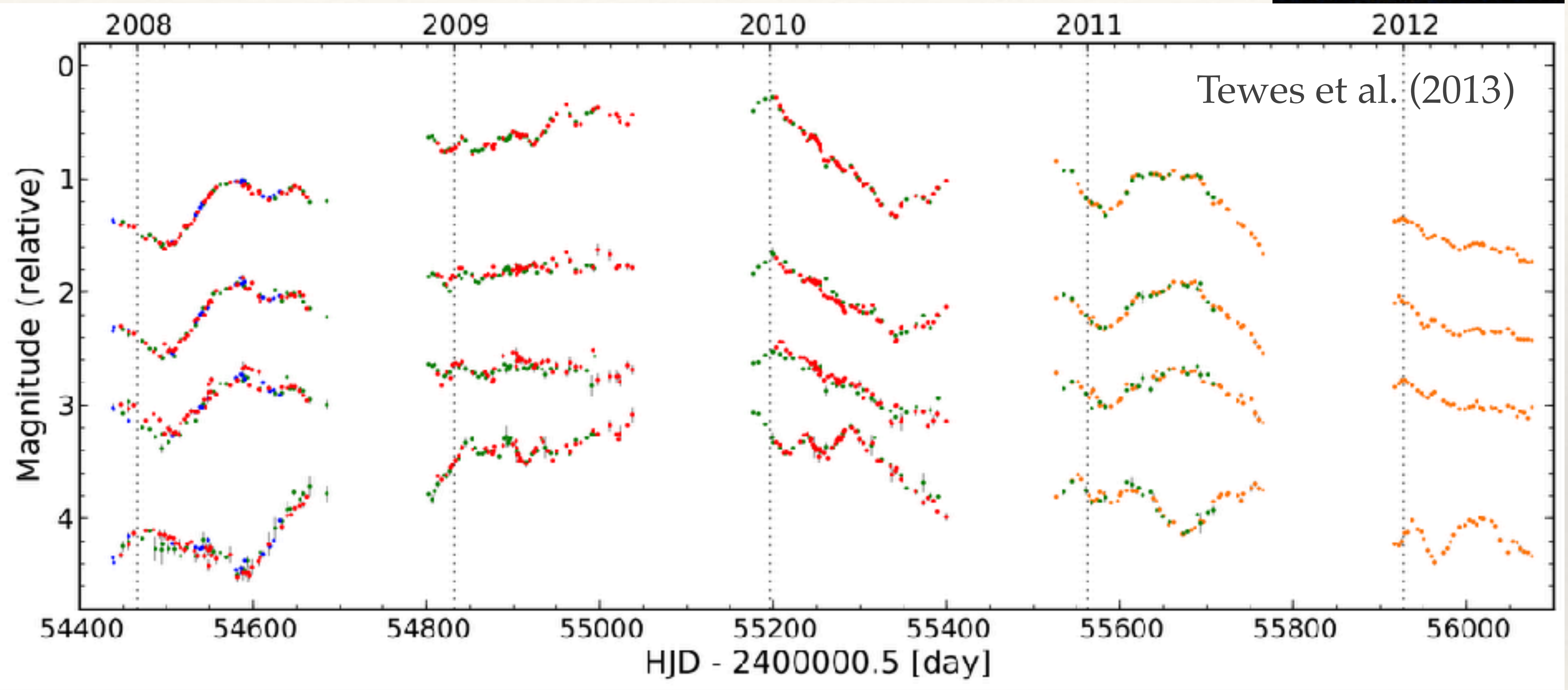

A variable source observed through a lens allows one to measure the time delays among the multiple images.

Fermat's potential

- **Fermat's principle** holds in General Relativity
- As a consequence, Fermat's potential

$$ct = (1 + z_{\mathrm{d}}) \frac{D_{\mathrm{d}} D_{\mathrm{s}}}{D_{\mathrm{ds}}} \left[\frac{1}{2} \|\boldsymbol{\theta} - \boldsymbol{\theta}^{\mathrm{s}}\|^2 - \Psi(\boldsymbol{\theta}) \right] + \mathrm{const}$$

can be used to find the image(s) associated to a source:

$$\nabla_\theta (ct) = 0 \implies \boldsymbol{\theta}_s = \boldsymbol{\theta} - \nabla\Psi(\boldsymbol{\theta})$$

- The associated "**ray-tracing**" equation is solved (numerically) and is a fundamental step of strong lensing modeling

Fermat's potential and image configurations

No lens

Fermat's potential and image configurations

No lens

Fermat's potential is just an **axisymmetric paraboloid**.

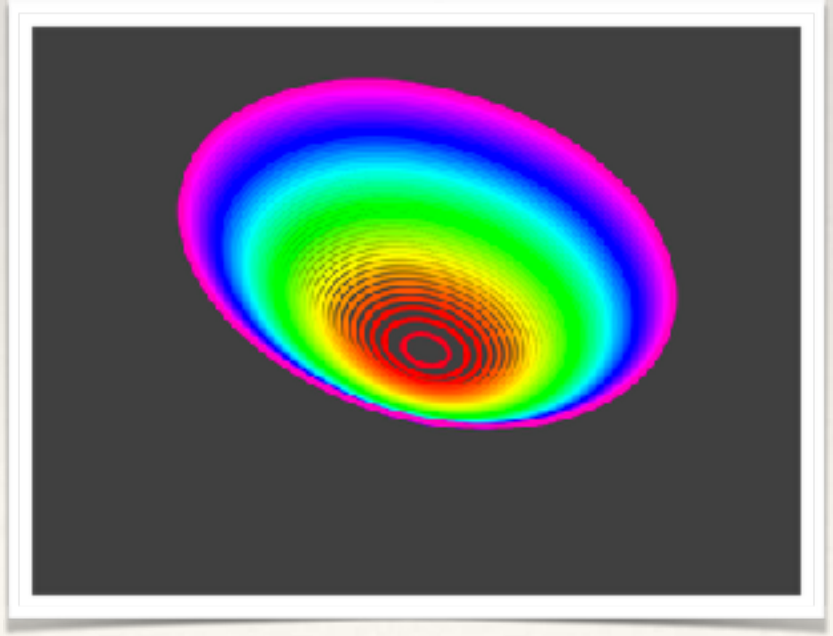

Fermat's potential and image configurations

No lens

Fermat's potential is just an **axisymmetric paraboloid**.

A single image is observed, corresponding to the minimum of the potential, where $\boldsymbol{\theta}^{\mathrm{s}} = \boldsymbol{\theta}$ (no lensing).

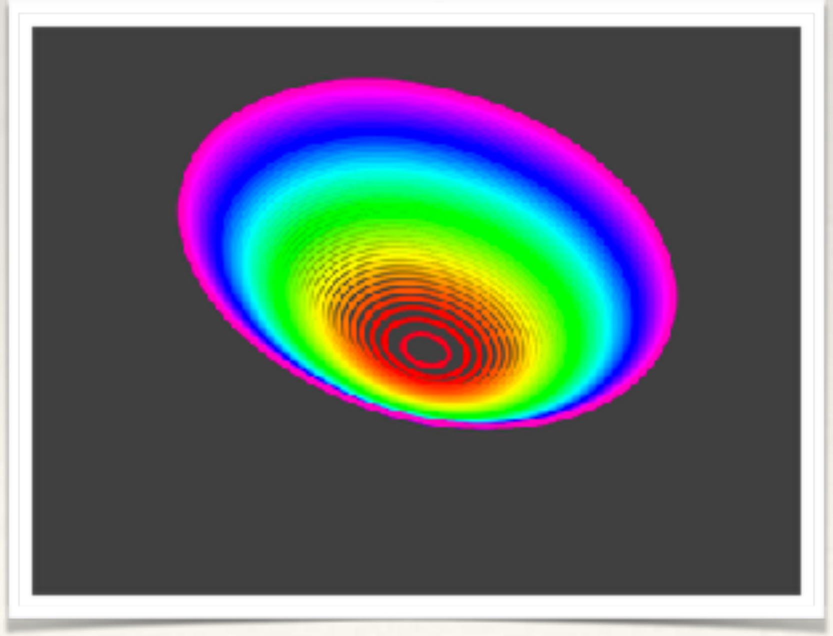

Fermat's potential and image configurations

Axisymmetric lens

Fermat's potential and image configurations

Axisymmetric lens

Fermat's potential has a **central peak**, a **saddle point**, and a **minimum**.

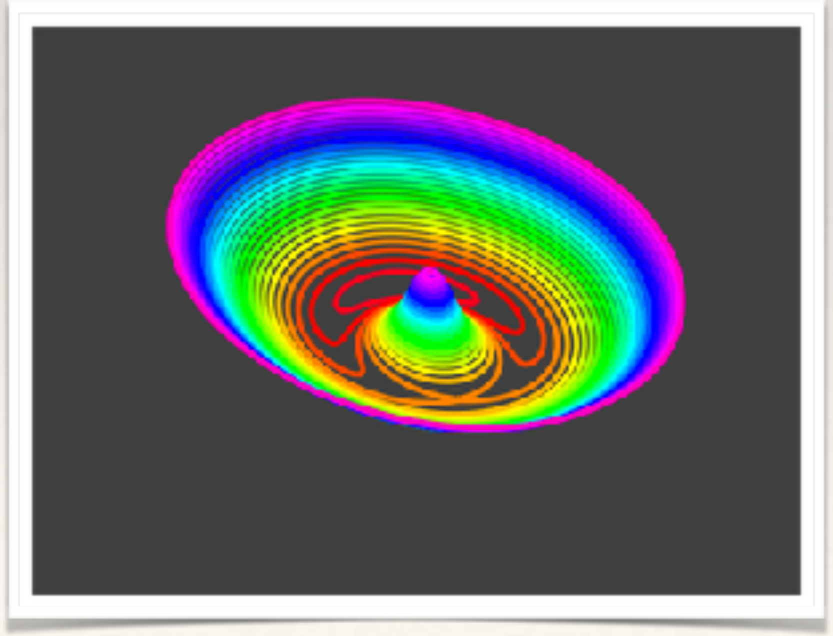

Fermat’s potential and image configurations

Axisymmetric lens

Fermat’s potential has a **central peak**, a **saddle point**, and a **minimum**.

Image corresponding to the peak usually very faint.

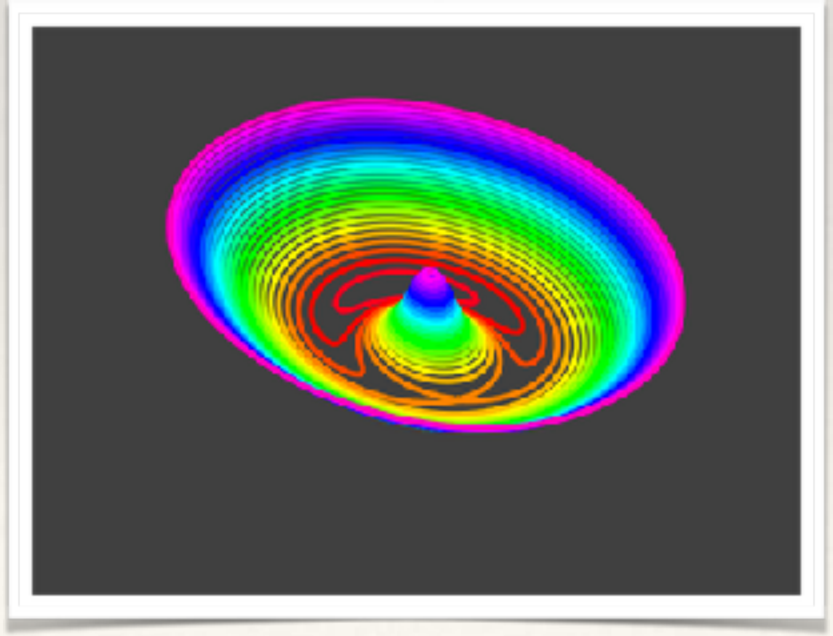

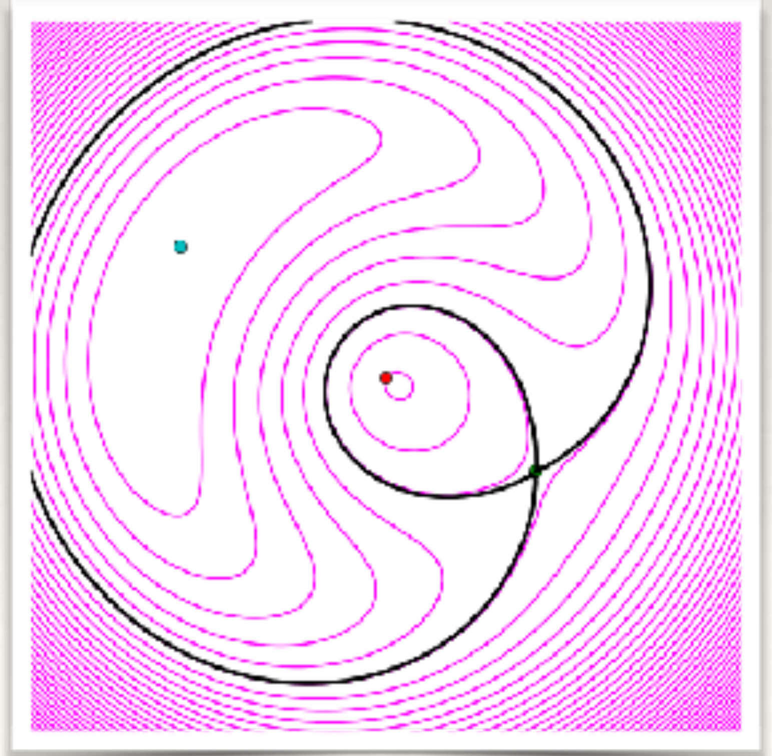

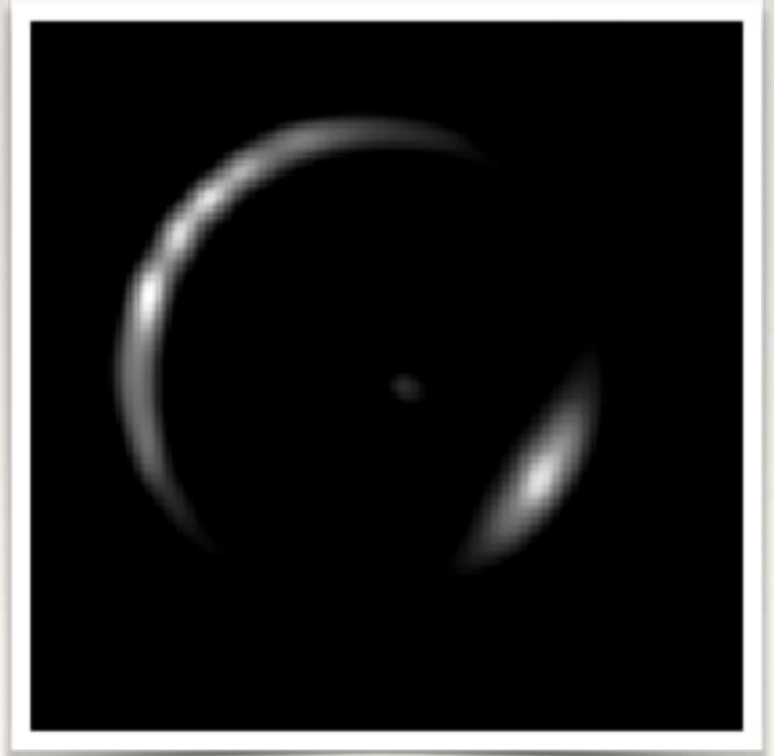

Fermat's potential & image configurations

Non-axisymmetric lens

Fermat's potential has a **central peak**, and **several points**, and **minimuma**.

Image corresponding to the peak usually very faint.

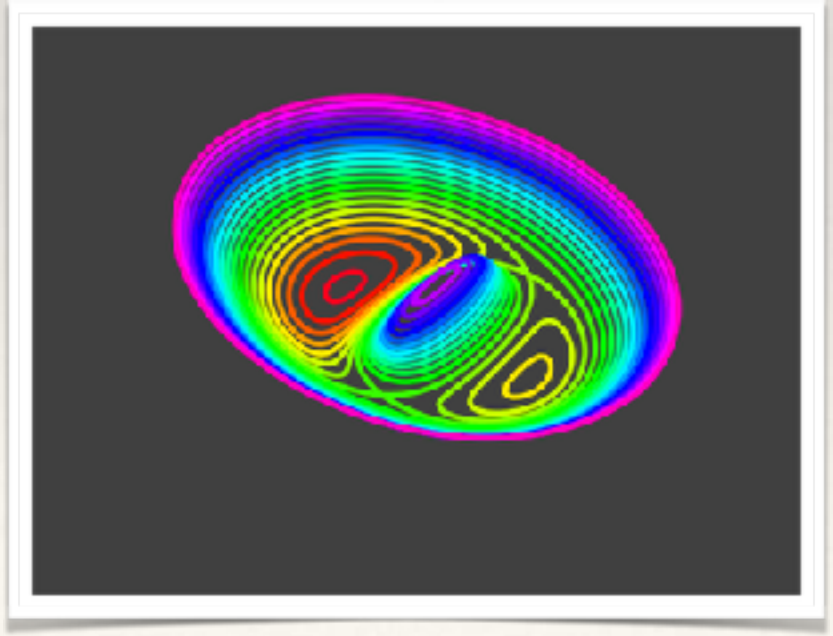

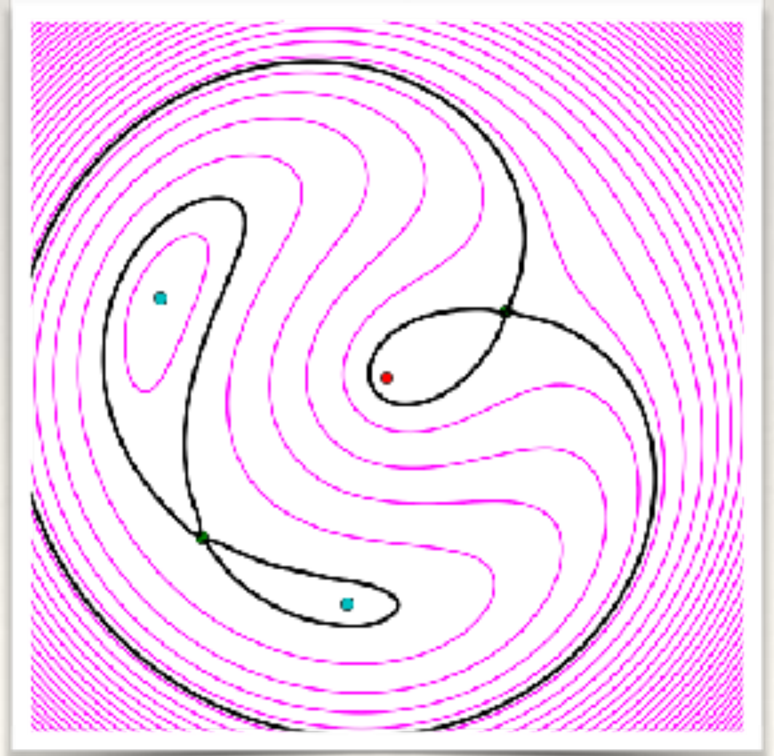

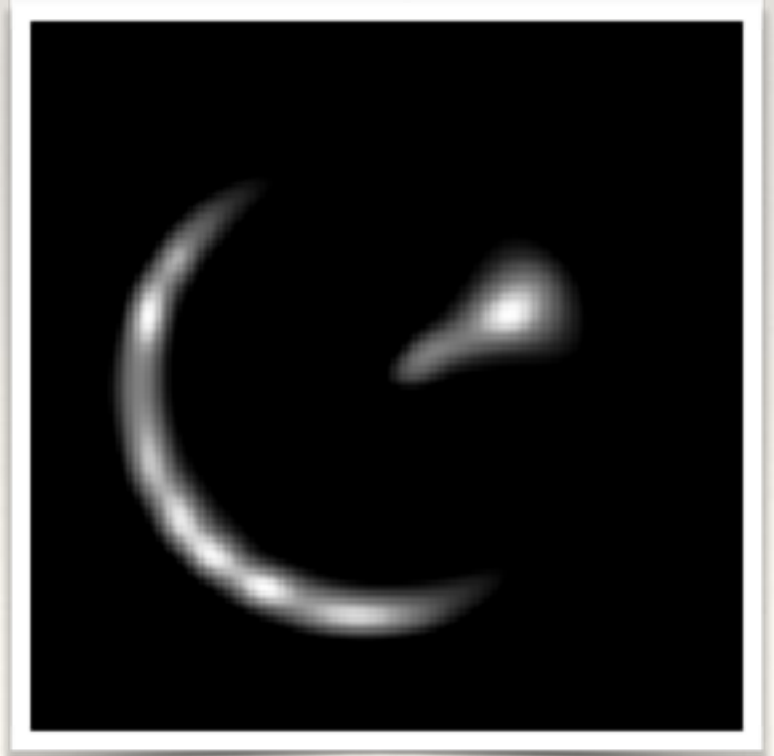

Magnification effect

Gravitational lensing generally increases the luminosity of sources.

Magnification effect

Gravitational lensing generally increases the luminosity of sources.

Gravitational lensing

Seeing

Magnification effect

Gravitational lensing generally increases the luminosity of sources.

Gravitational lensing

- is described by a **simple mapping** (ray tracing)

Seeing

- is described by a **convolution** with a kernel

Magnification effect

Gravitational lensing generally increases the luminosity of sources.

Gravitational lensing

- is described by a **simple mapping** (ray tracing)
- conserves the **surface brightness**

Seeing

- is described by a **convolution** with a kernel
- does not conserve the **surface brightness**

Magnification effect

Gravitational lensing generally increases the luminosity of sources.

Gravitational lensing

- is described by a **simple mapping** (ray tracing)
- conserves the **surface brightness**
- does not conserve the **flux**

Seeing

- is described by a **convolution** with a kernel
- does not conserve the **surface brightness**
- conserves the **flux**

Magnification effect

Gravitational lensing generally increases the luminosity of sources.

Gravitational lensing

- is described by a **simple mapping** (ray tracing)
- conserves the **surface brightness**
- does not conserve the **flux**

Seeing

- is described by a **convolution** with a kernel
- does not conserve the **surface brightness**
- conserves the **flux**

When studying a strong lensing system both effects needs to be taken into account.

Problems of Cold Dark Matter

Problems of Cold Dark Matter

- **The cusp-core problem**
  - (Dwarf) galaxies show a core not predicted by simulations

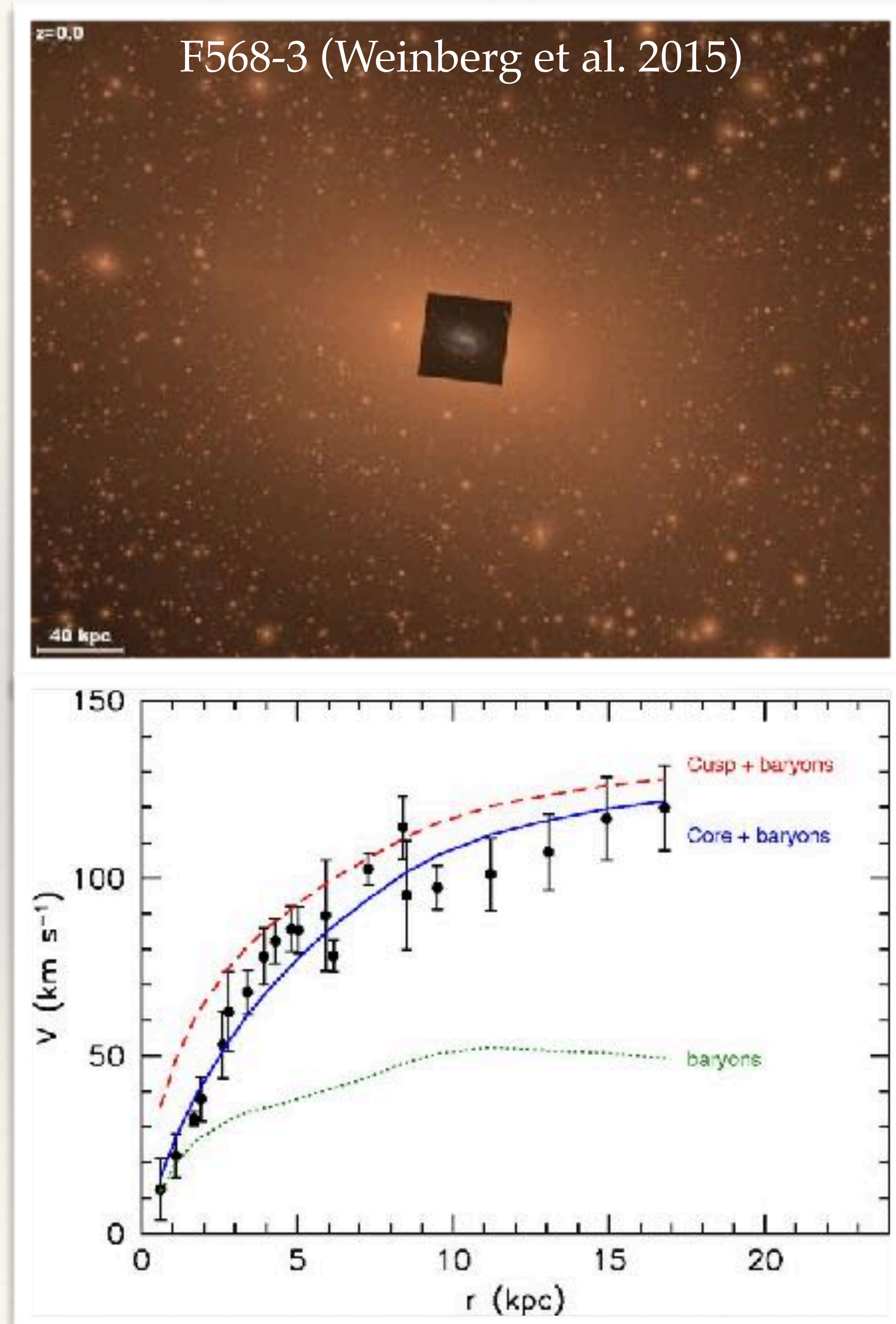

Problems of Cold Dark Matter

- **The cusp-core problem**
  - (Dwarf) galaxies show a core not predicted by simulations
- **Missing satellites problem**
  - Too few satellites observed around massive halos

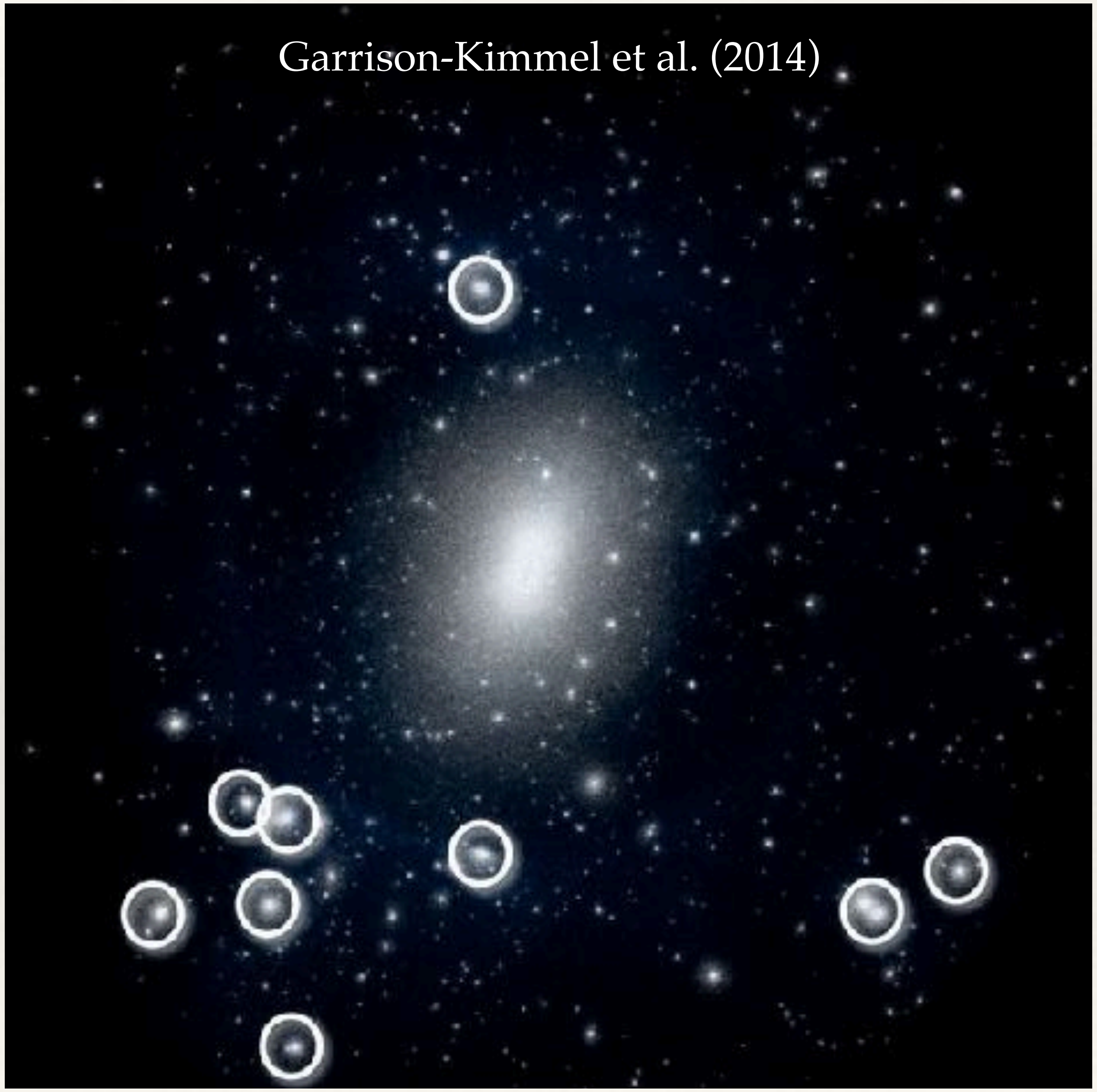

Problems of Cold Dark Matter

- **The cusp-core problem**
  - (Dwarf) galaxies show a core not predicted by simulations
- **Missing satellites problem**
  - Too few satellites observed around massive halos

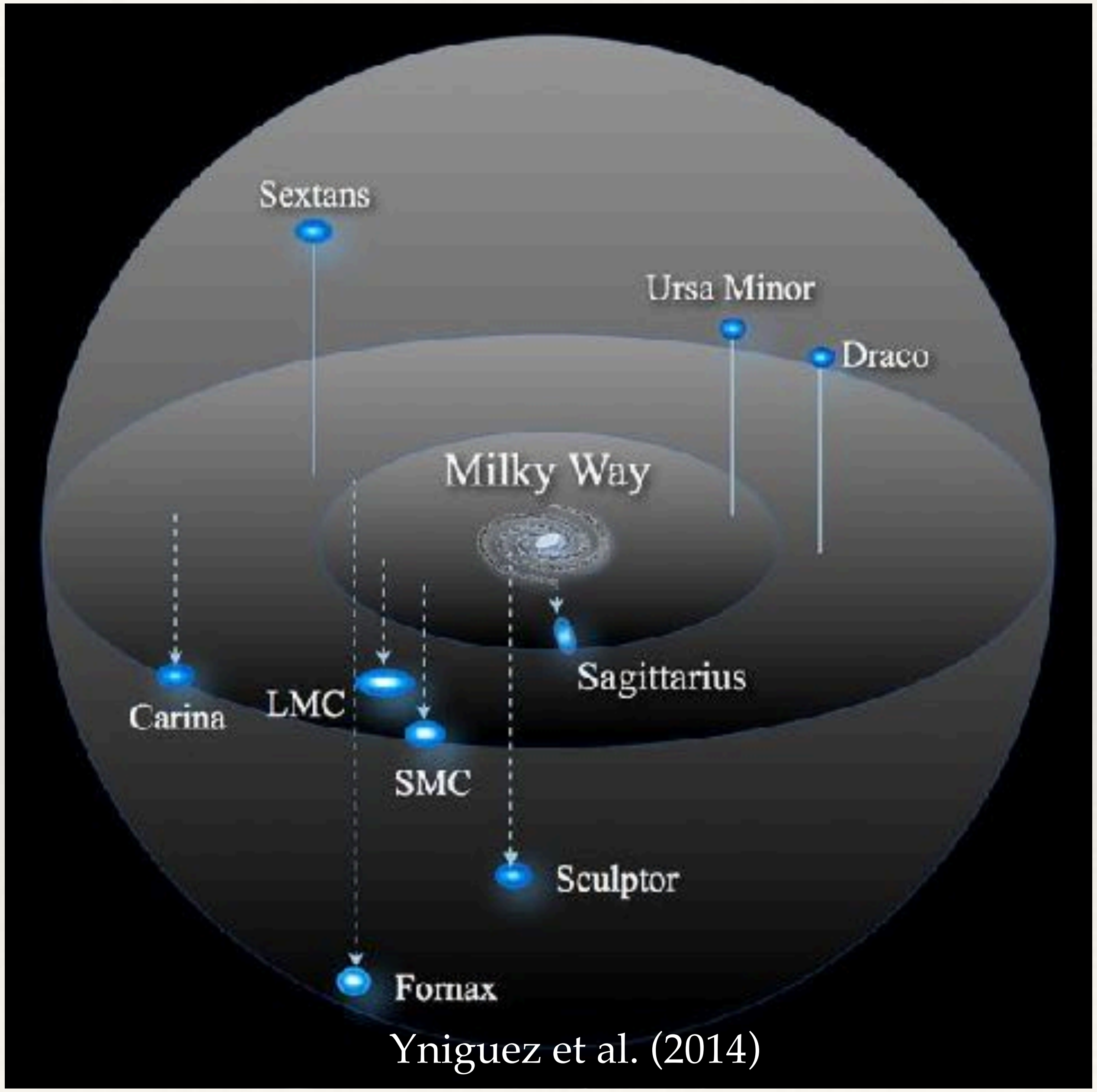

Yniguez et al. (2014)

Problems of Cold Dark Matter

- **The cusp-core problem**
  - (Dwarf) galaxies show a core not predicted by simulations
- **Missing satellites problem**
  - Too few satellites observed around massive halos
- **Early mass assembly**
  - Massive clusters form earlier than expected

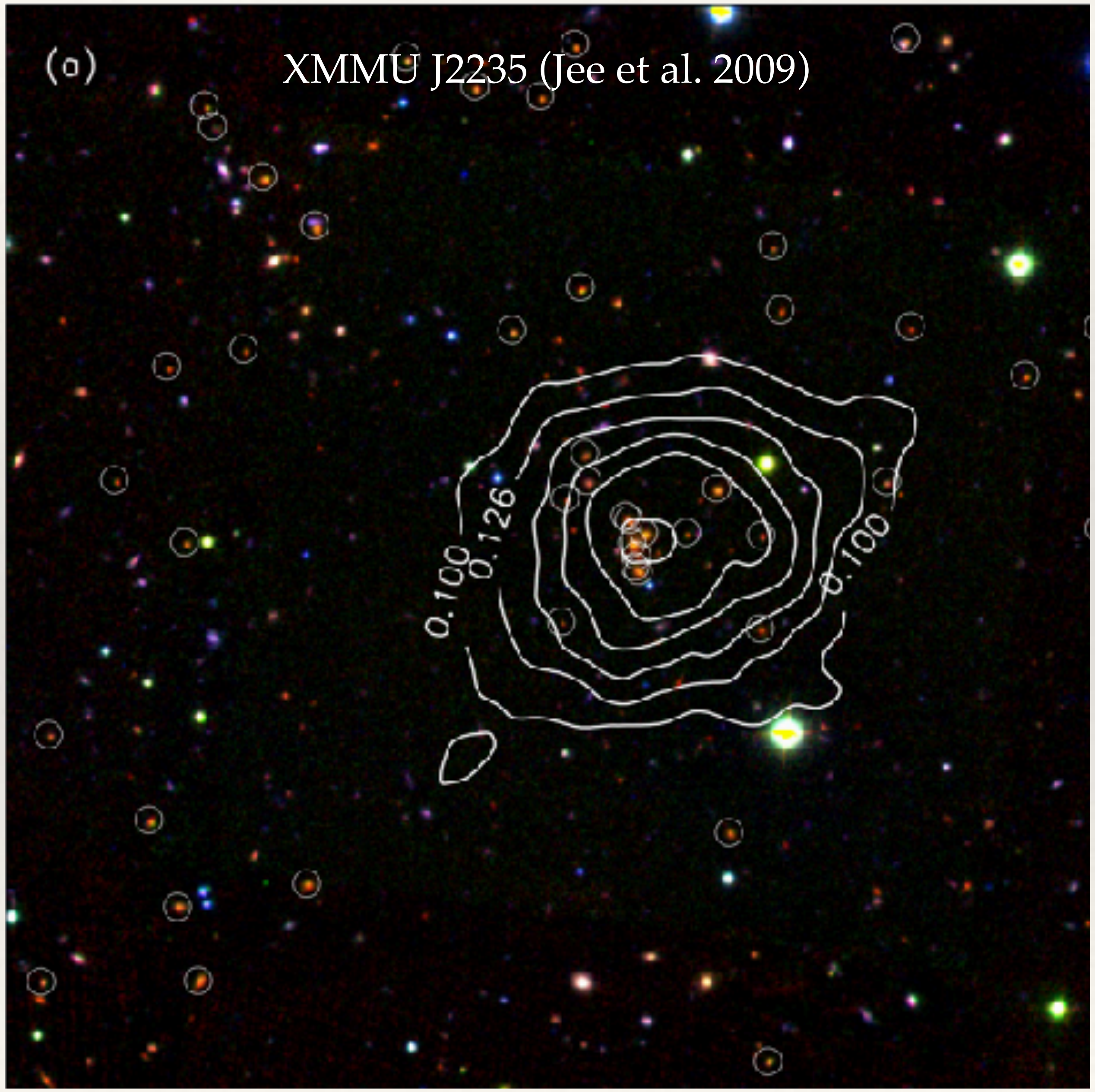

Simulations and Observations

- Cosmological simulations predict the structure of halos
- Run different cosmological simulations with different properties of DM particles
  - CDM predicts more structures than WDM or HDM
  - Self-interacting CDM can make halos with cores
- Compare simulations and observations

Simulations and Observations

- Cosmological simulations predict the structure of halos
- Run different cosmological simulations with different properties of DM particles
  - CDM predicts more structures than WDM or HDM
  - Self-interacting CDM can make halos with cores
- Compare simulations and observations

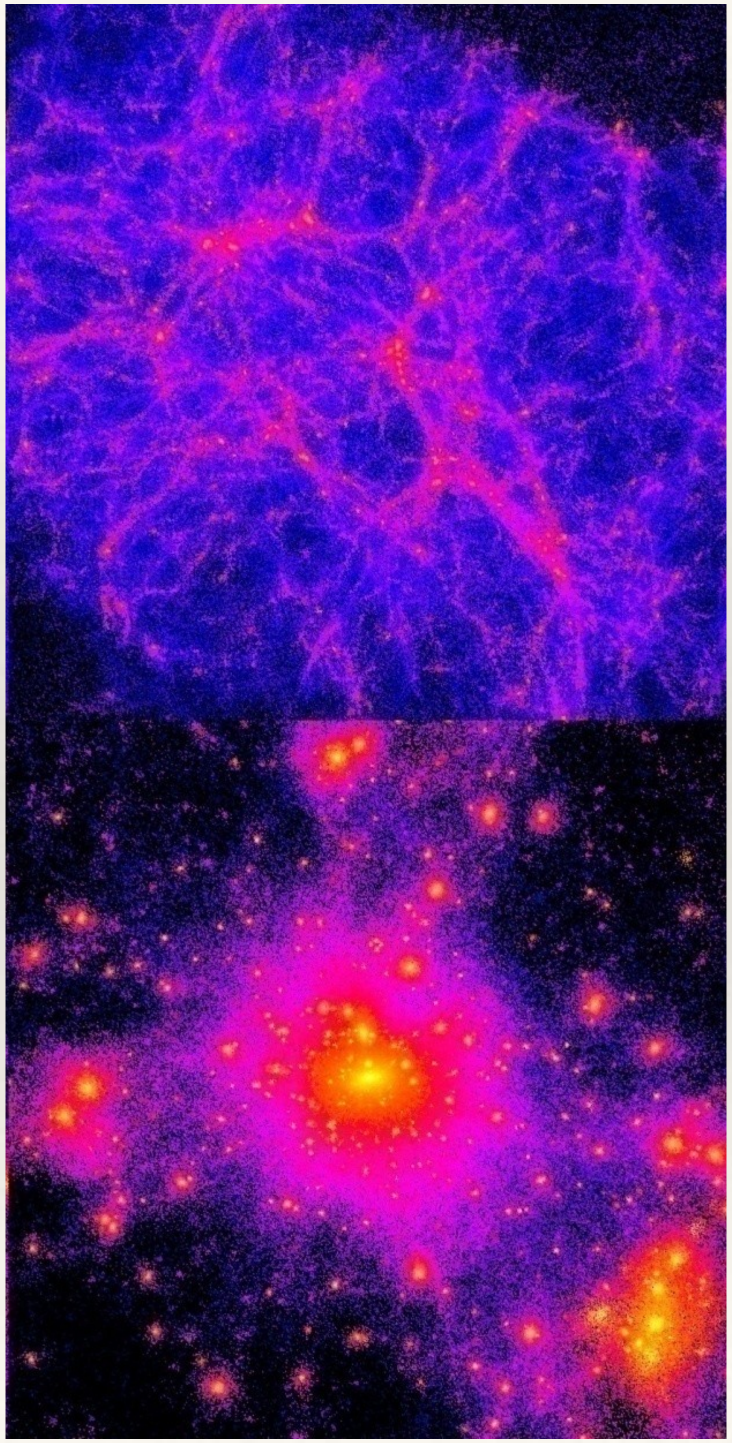

Credit: Ben Moore, University of Zurich

Simulations and Observations

- Cosmological simulations predict the structure of halos
- Run different cosmological simulations with different properties of DM particles
  - CDM predicts more structures than WDM or HDM
  - Self-interacting CDM can make halos with cores
- Compare simulations and observations

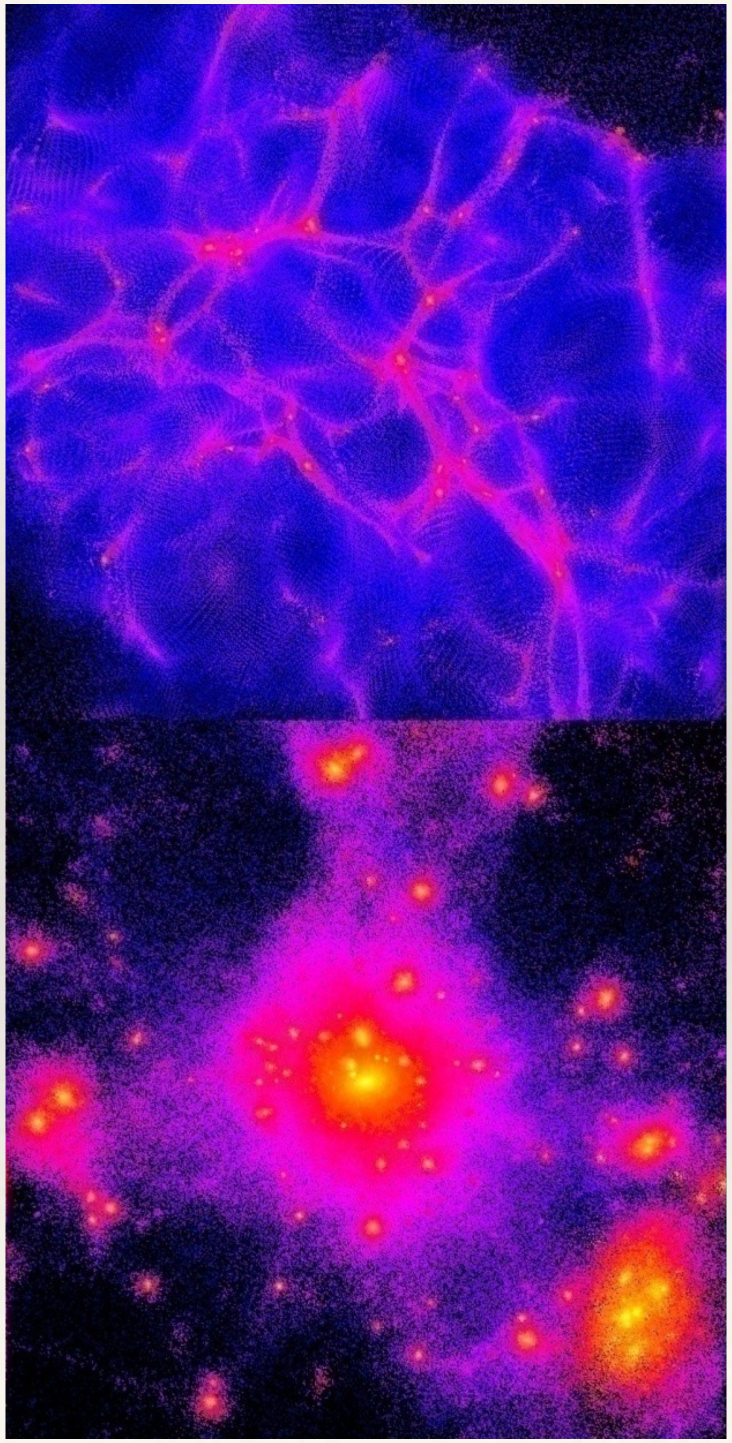

Credit: Ben Moore, University of Zurich

Simulations and Observations

- Cosmological simulations predict the structure of halos
- Run different cosmological simulations with different properties of DM particles
  - CDM predicts more structures than WDM or HDM
  - Self-interacting CDM can make halos with cores
- Compare simulations and observations

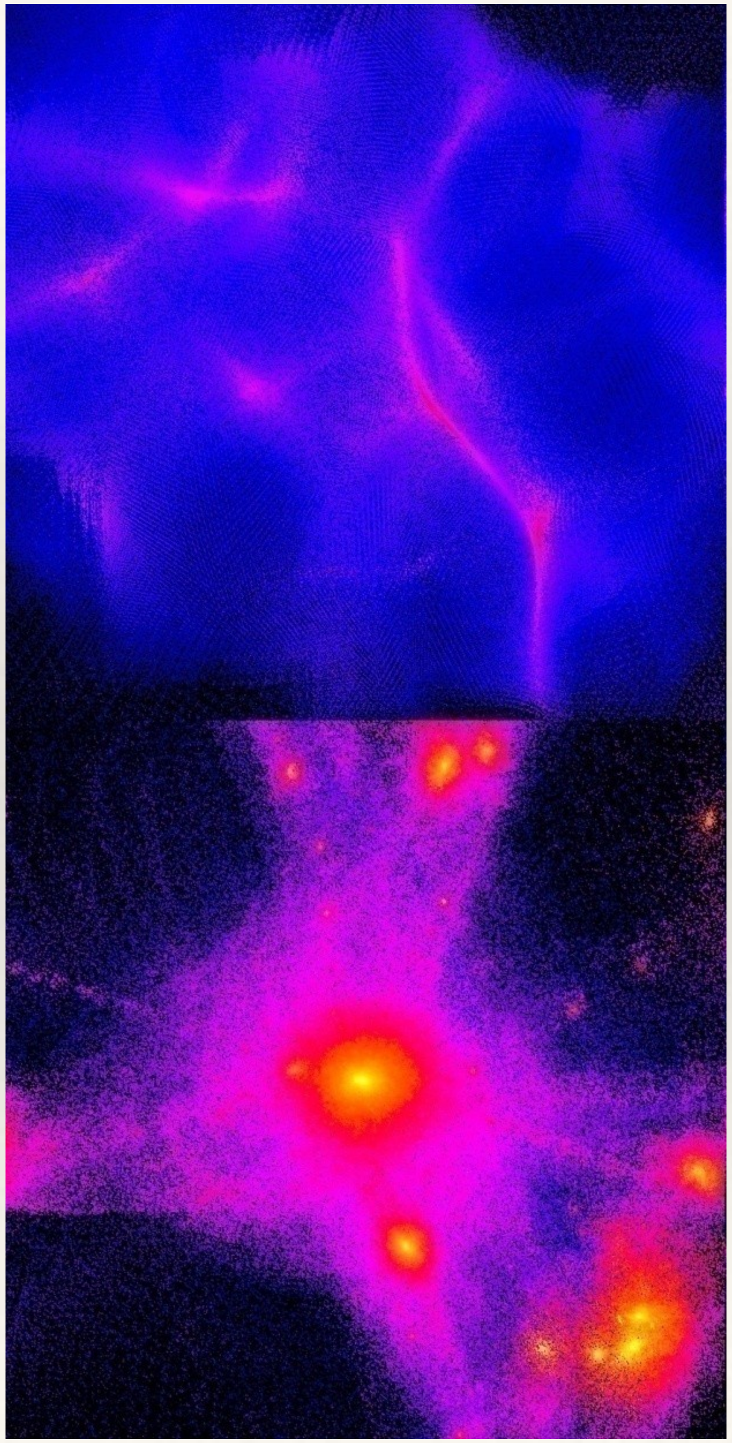

Credit: Ben Moore, University of Zurich

Simulations and Observations

- Cosmological simulations have reached the **resolution** to distinguish among various DM models
- Observations now contain **exquisite details** to perform accurate strong lensing modeling

Simulations and Observations

- Cosmological simulations have reached the **resolution** to distinguish among various DM models
- Observations now contain **exquisite details** to perform accurate strong lensing modeling

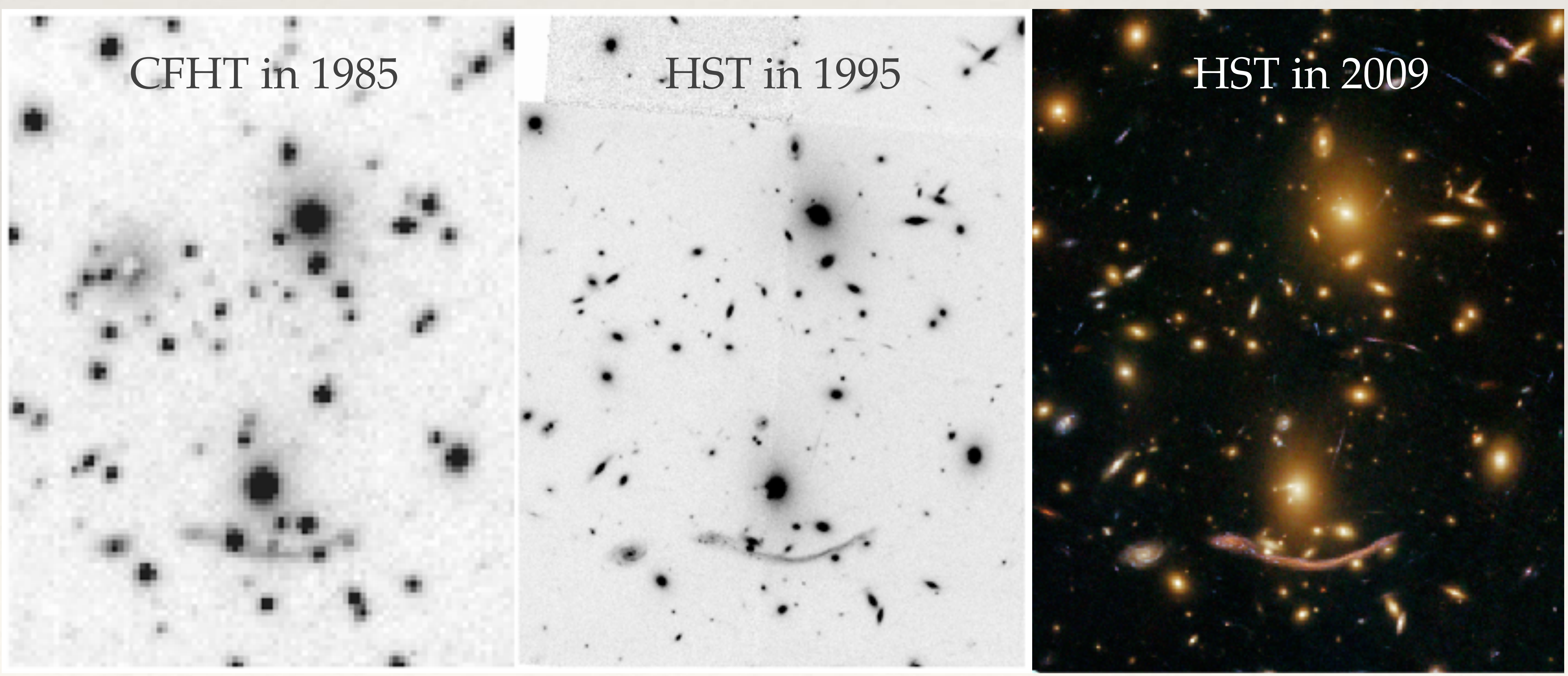

CLASH

CLASH

Cluster Lensing And Supernovae survey with Hubble

CLASH

Cluster Lensing And Supernovae survey with Hubble

- **524-orbit** HST multi-cycle treasury program (PI: M. Postman)

CLASH

Cluster Lensing And Supernovae survey with Hubble

- **524-orbit** HST multi-cycle treasury program (PI: M. Postman)
- **25** massive intermediate-*z* **galaxy clusters** (4 HFF) observerd with **16** (ACS+WFC3) broadband **filters**

CLASH

Cluster Lensing And Supernovae survey with Hubble

- **524-orbit** HST multi-cycle treasury program (PI: M. Postman)
- **25** massive intermediate-*z* **galaxy clusters** (4 HFF) observerd with **16** (ACS+WFC3) broadband **filters**
    - Study **DM mass profiles** and **substructures** with unprecedented precision and resolution

CLASH

Cluster Lensing And Supernovae survey with Hubble

- **524-orbit** HST multi-cycle treasury program (PI: M. Postman)
- **25** massive intermediate-z **galaxy clusters** (4 HFF) observerd with **16** (ACS+WFC3) broadband **filters**
  - Study **DM mass profiles** and **substructures** with unprecedented precision and resolution
  - Detect some of the **most distant** ($z > 7$) **galaxies** through the gravitational lensing **magnification effect**

CLASH

Cluster Lensing And Supernovae survey with Hubble

- **524-orbit** HST multi-cycle treasury program (PI: M. Postman)
- **25** massive intermediate-z **galaxy clusters** (4 HFF) observerd with **16** (ACS+WFC3) broadband **filters**
    - Study **DM mass profiles** and **substructures** with unprecedented precision and resolution
    - Detect some of the **most distant** ($z > 7$) **galaxies** through the gravitational lensing **magnification effect**
    - Find in parallel fields **new Type Ia SNae** up to $z \sim 2.5$

CLASH-VLT

- **200-hr VLT/VIMOS** Large Program (PI: P. Rosati)
- **Spectroscopic follow-up** of the 14 southern CLASH galaxy clusters (2 HFF)
- **Dynamical study** beyond R_{vir} with ~500 members per cluster
- Spectroscopic confirmation of the **multiple-image systems**
- **Galaxy formation** and evolution analyses of lens and lensed galaxies

CLASH-VLT data reduction summary

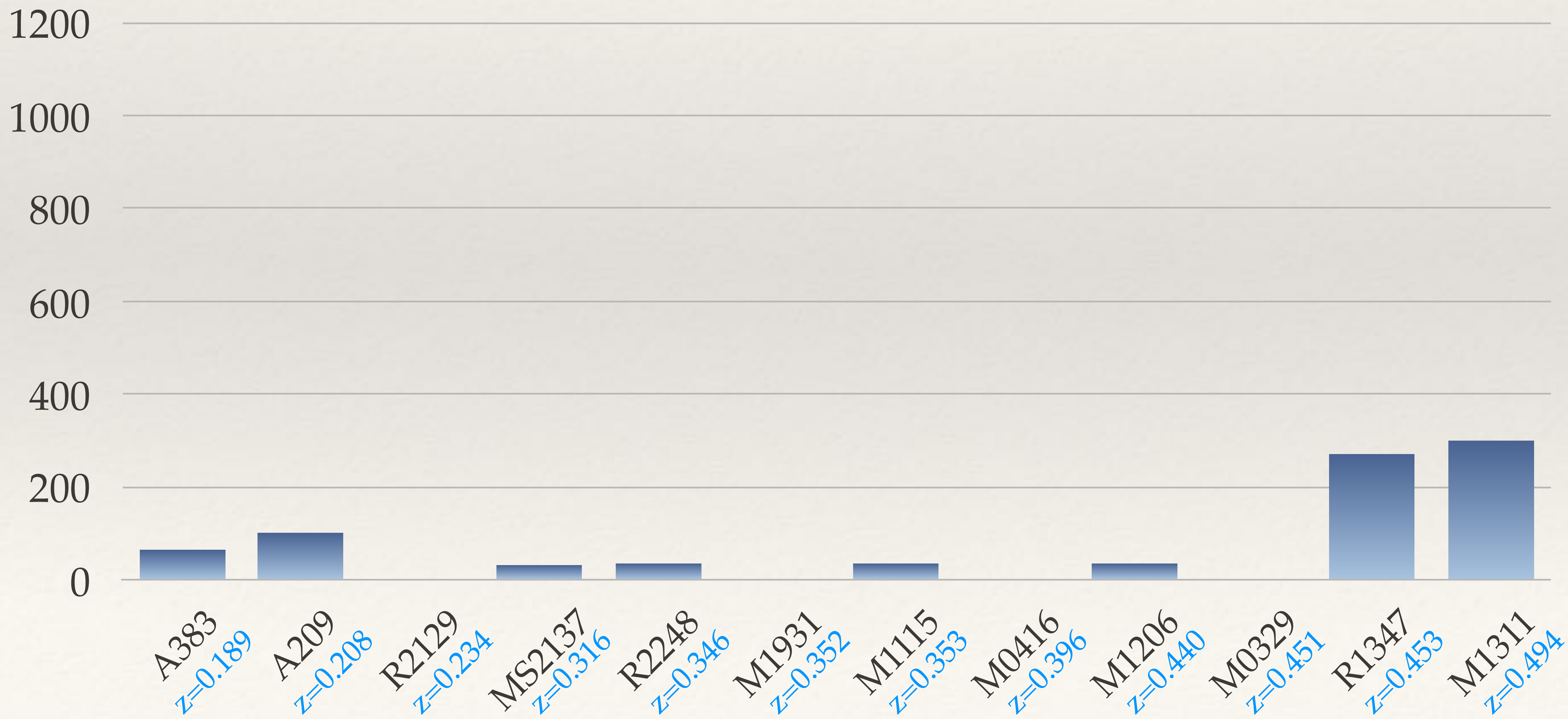

CLASH-VLT data reduction summary

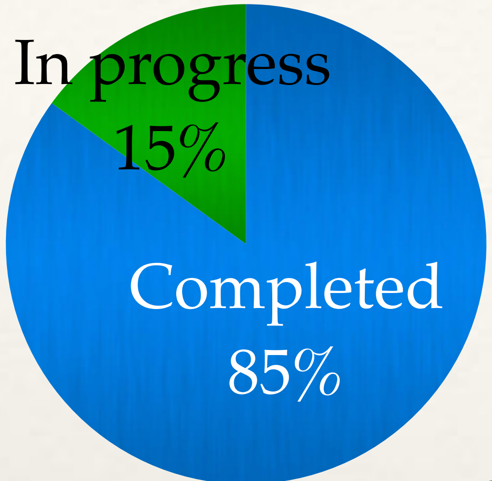

Specz	Total	Members	"Arcs"	X-ray
Now	26000	6400	260	390
Final	30000	7300	300	450

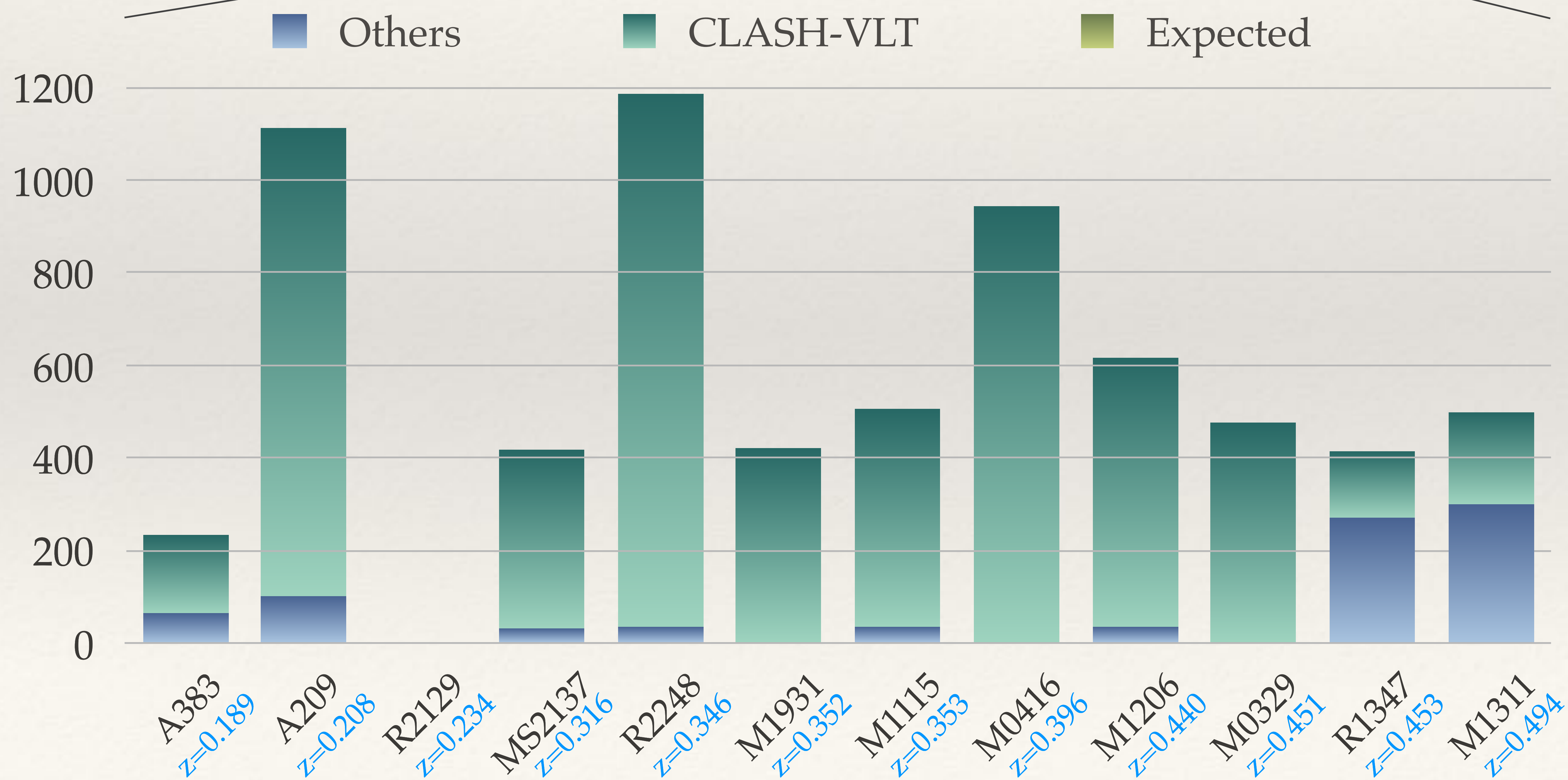

CLASH-VLT data reduction summary

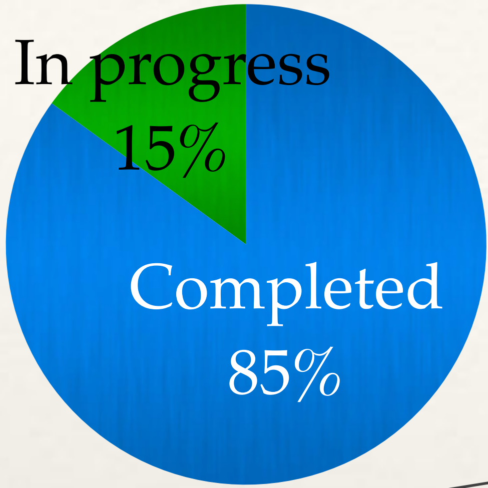

Specz	Total	Members	"Arcs"	X-ray
Now	26000	6400	260	390
Final	30000	7300	300	450

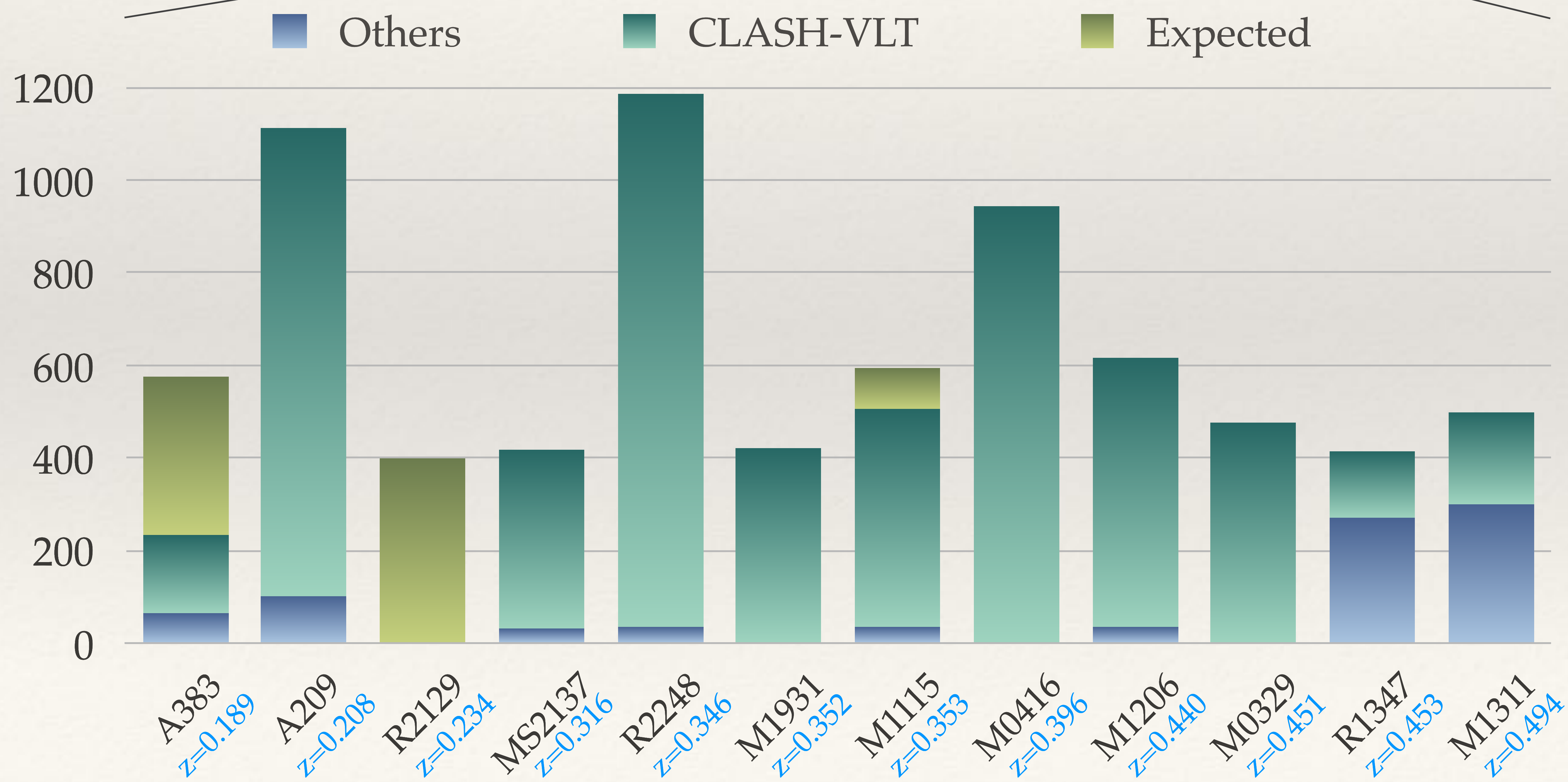

CLASH-VLT data reduction summary

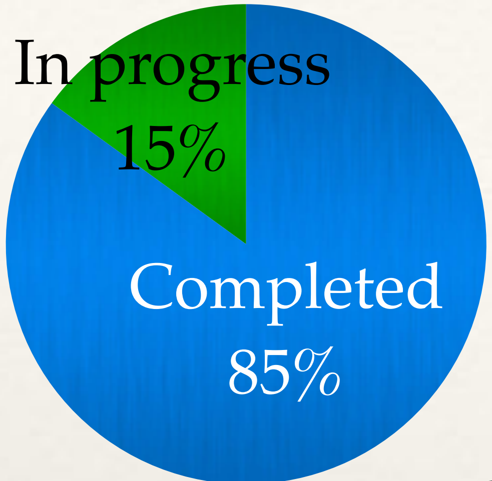

Specz	Total	Members	"Arcs"	X-ray
Now	26000	6400	260	390
Final	30000	7300	300	450

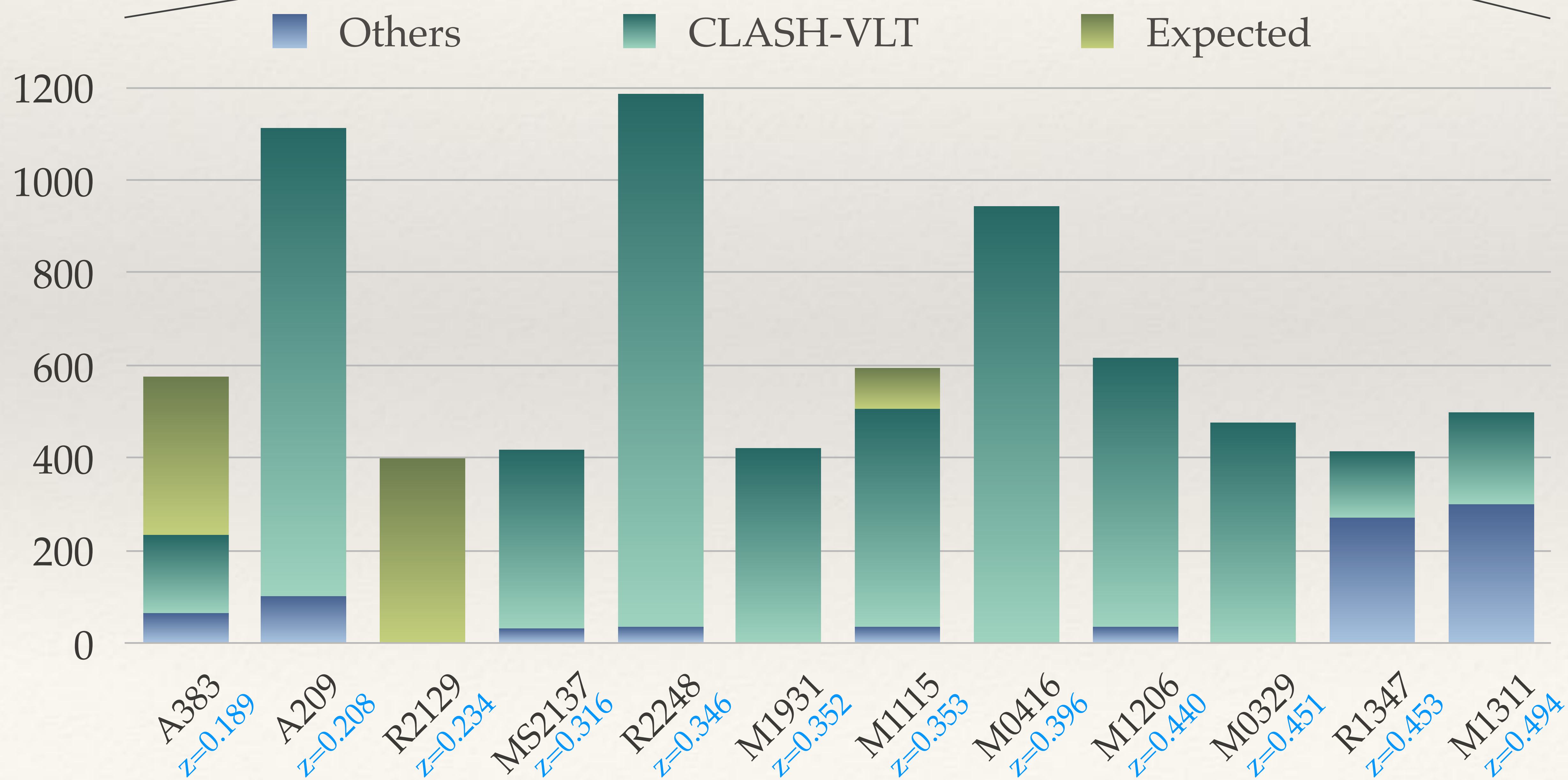

CLASH-VLT data reduction summary

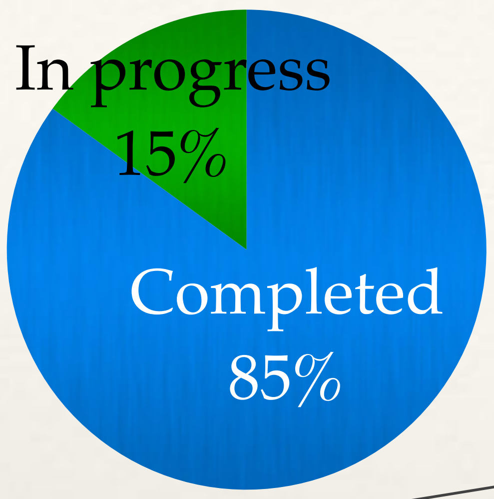

Specz	Total	Members	"Arcs"	X-ray
Now	26000	6400	260	390
Final	30000	7300	300	450

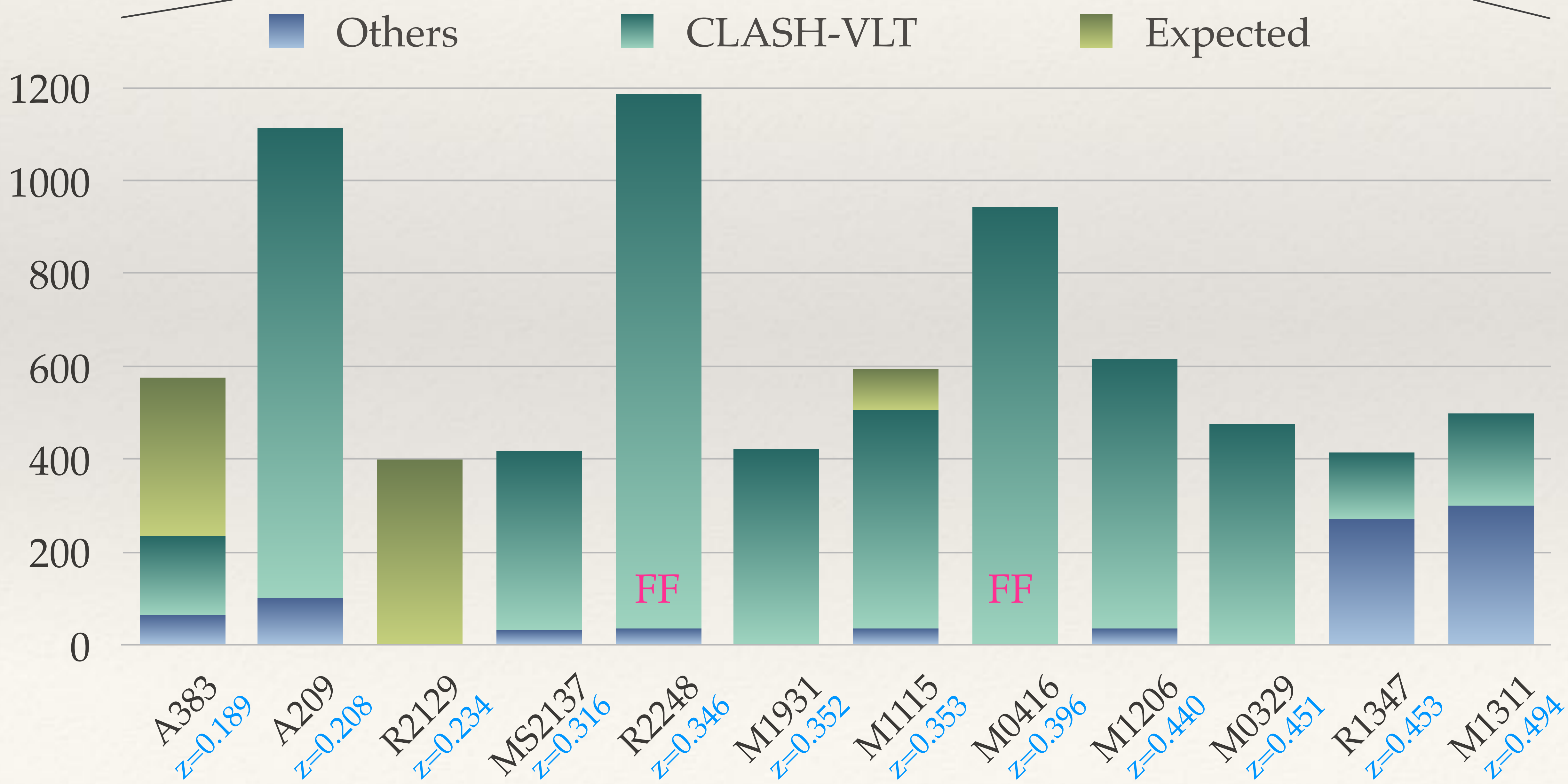

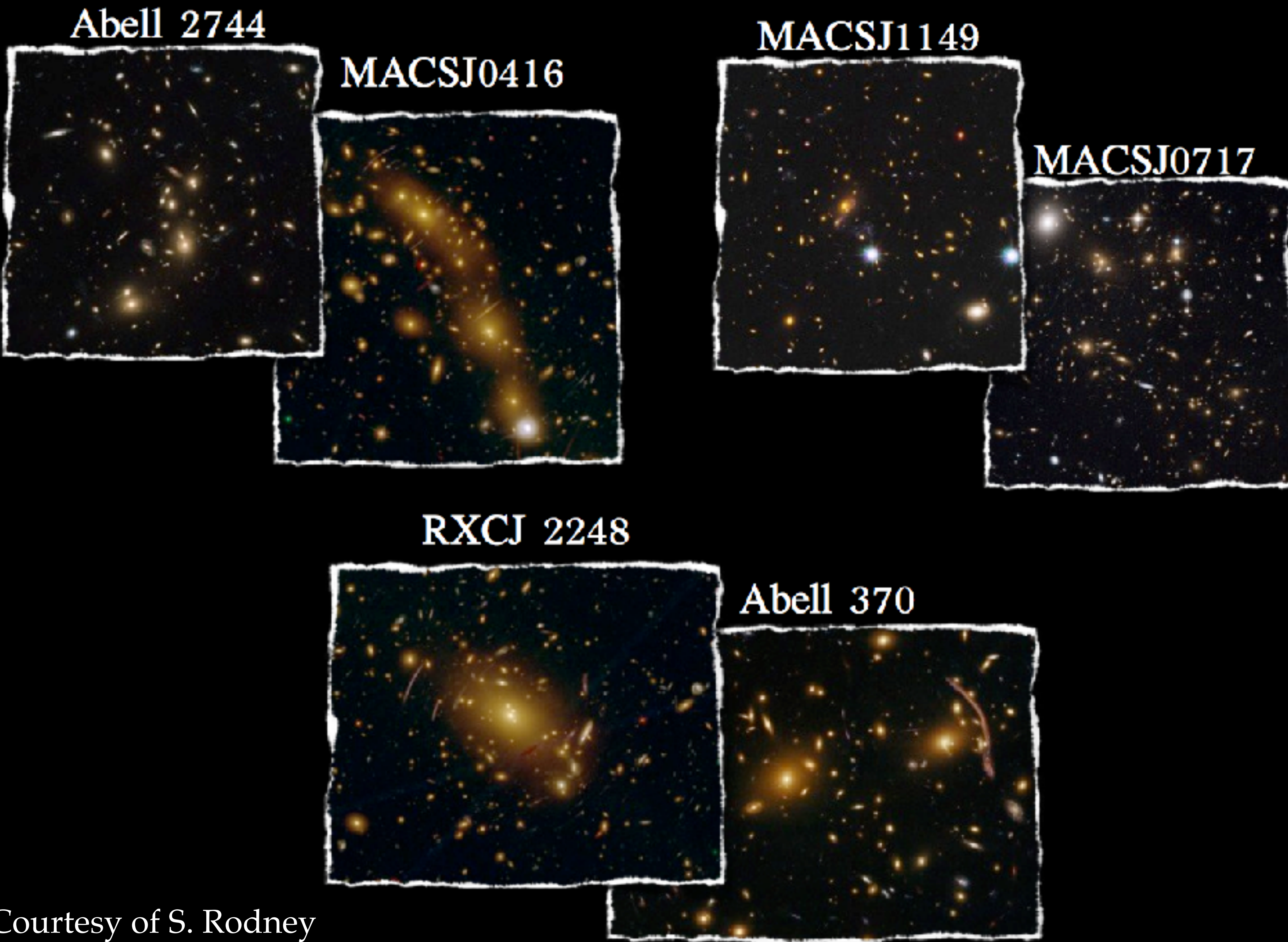

Courtesy of S. Rodney

HFF in CLASH-VLT

HFF in CLASH-VLT

RXJ 2248. 16 VIMOS masks (12 LR-Blue & 4 MR)

- Total exposure time: 15 hours
- 3734 reliable redshifts (area: 23x26 $arcmin^2$)
- ~1100 cluster members ($z = 0.346$)

HFF in CLASH-VLT

RXJ 2248. 16 VIMOS masks (12 LR-Blue & 4 MR)

- Total exposure time: 15 hours
- 3734 reliable redshifts (area: 23x26 arcmin^2)
- ~1100 cluster members (z = 0.346)

MACS 0416. 21 VIMOS masks (15 LR-Blue & 6 MR)

- Total exposure time: 20 hours
- 4386 reliable redshifts (area: 23x26 arcmin^2)
- ~900 cluster members (z = 0.396)

HFF in CLASH-VLT

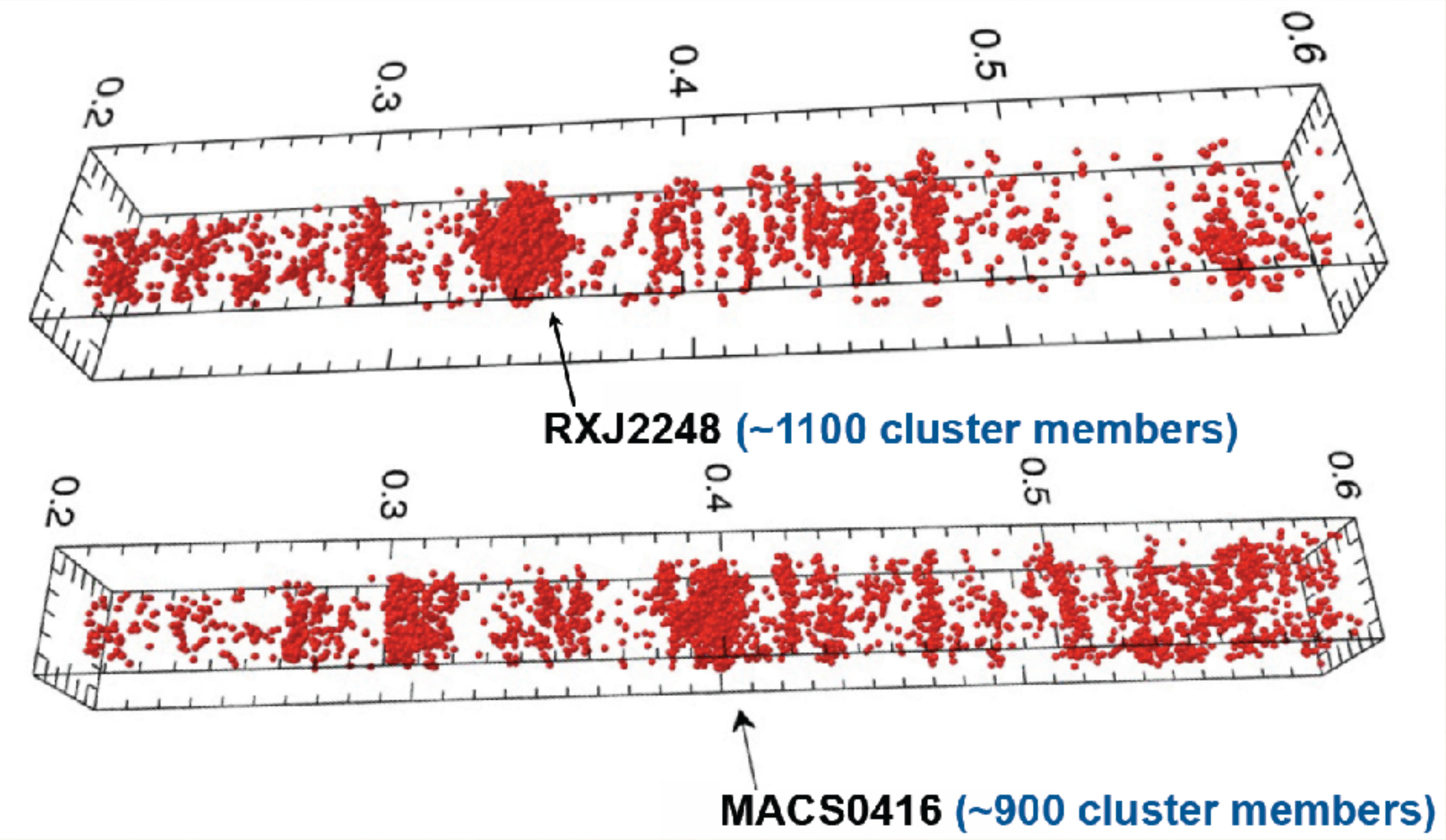

Complex dynamical structure of MACS 0416

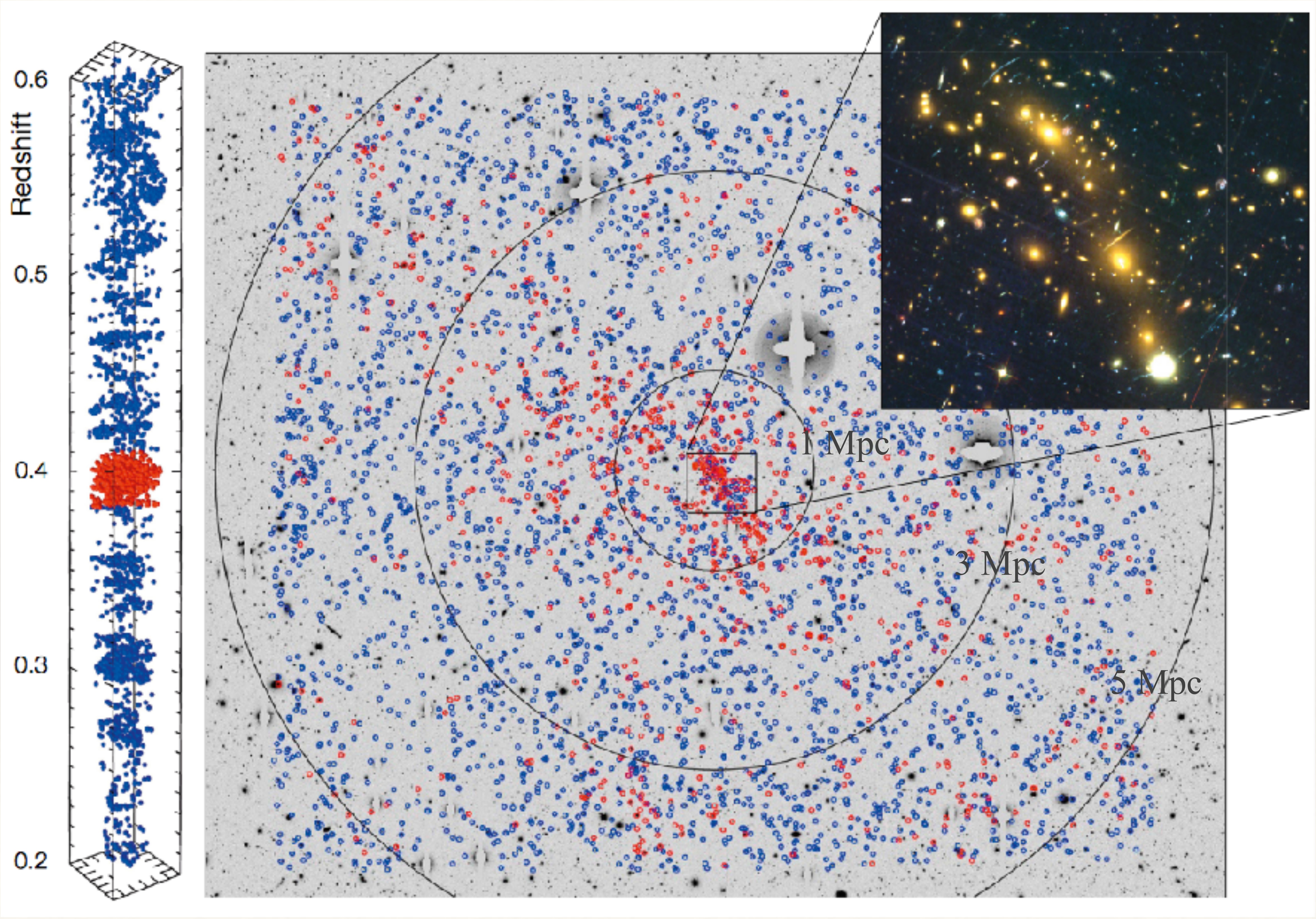

Balestra, Mercurio, Sartoris, et al. 2016, ApJS, 224, 33

The multiple-image spectra

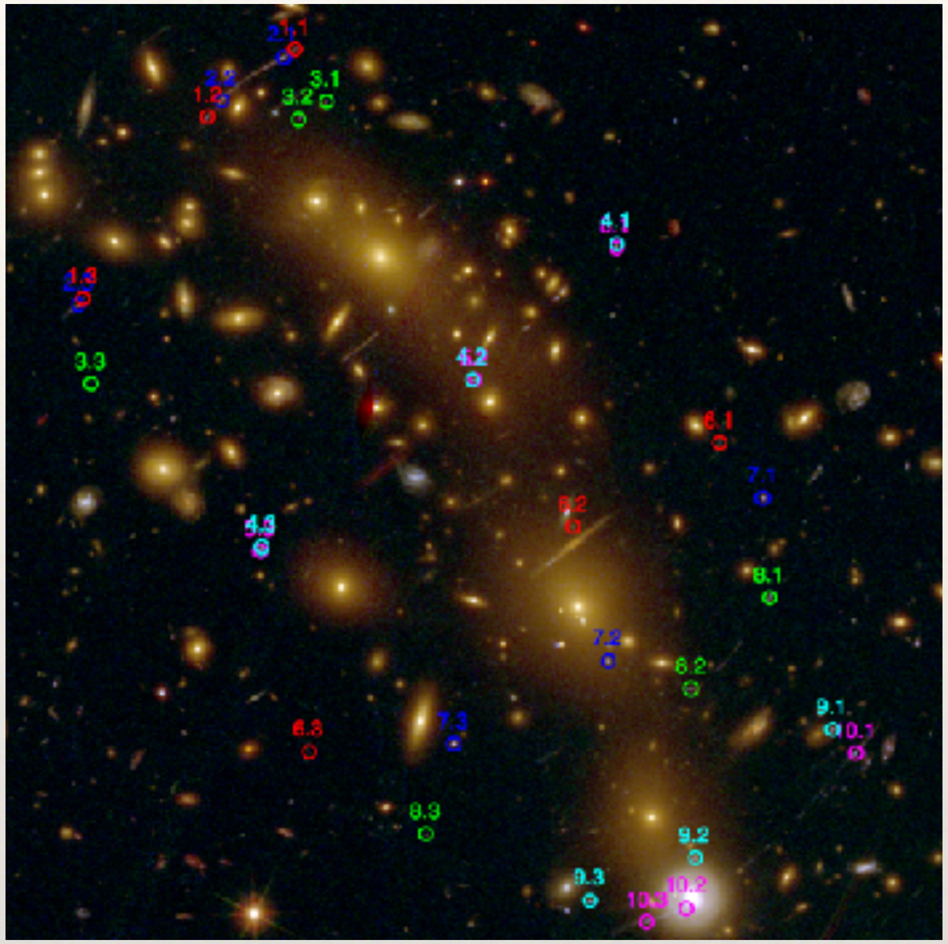

- For each system, at least 1 image has an either *secure* or *very likely* redshift
- If we have one *secure* and one *very likely*, we take the *secure*
- If we have two *secure*, we take the mean value

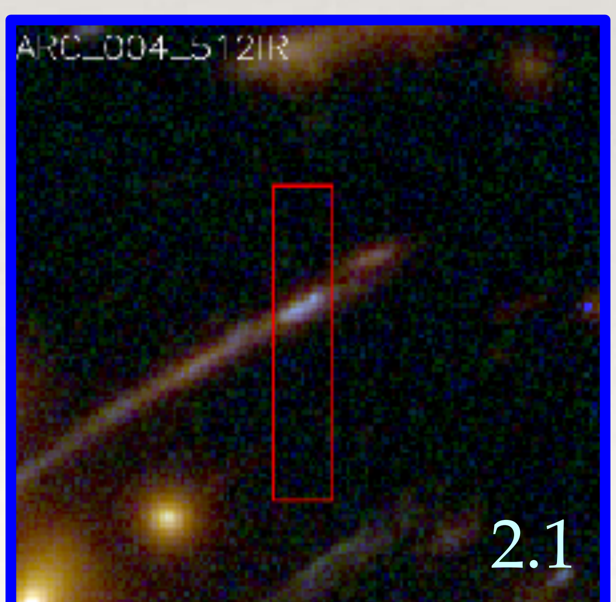

Grillo et al. (2005)

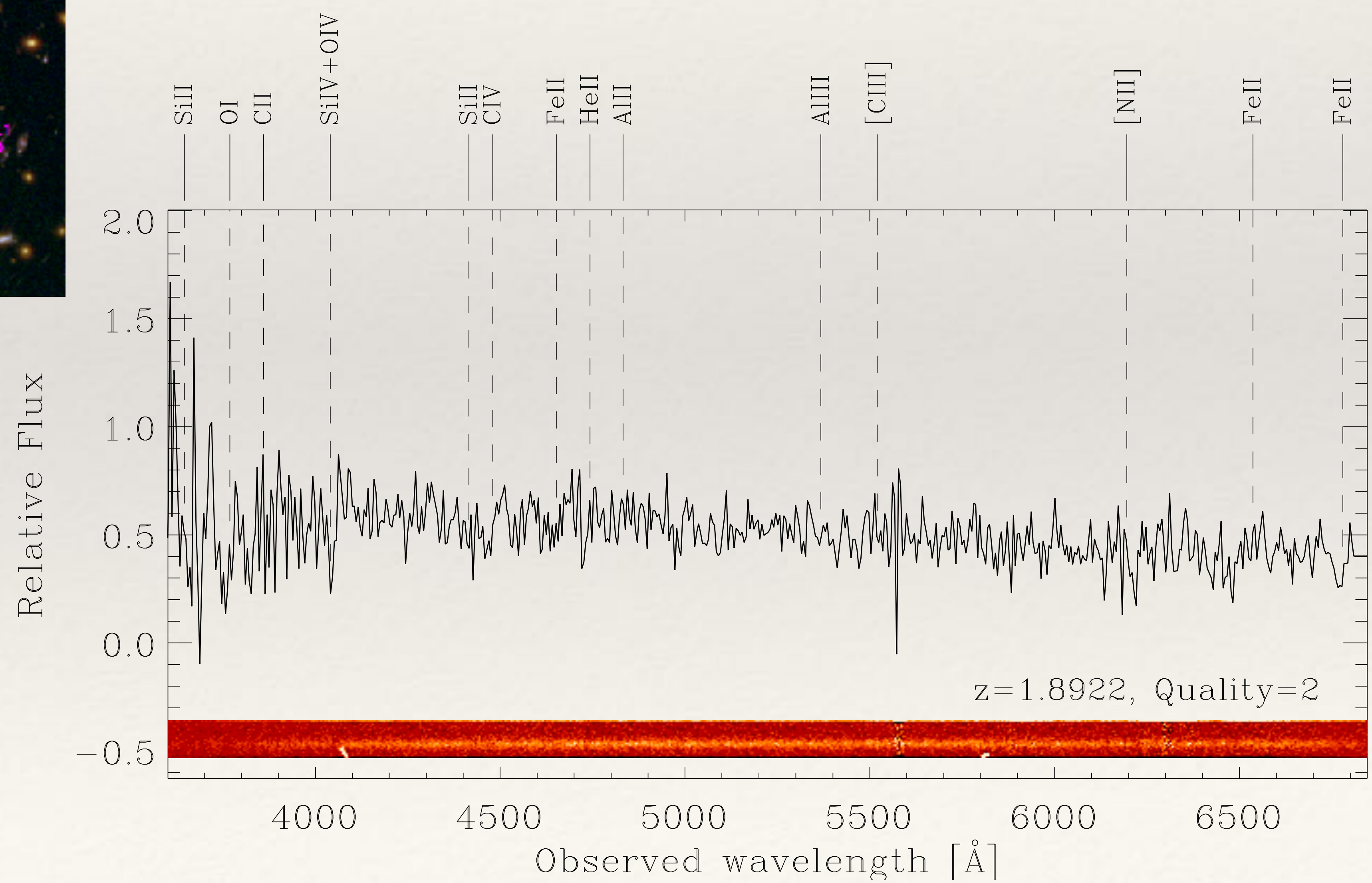

The multiple-image spectra

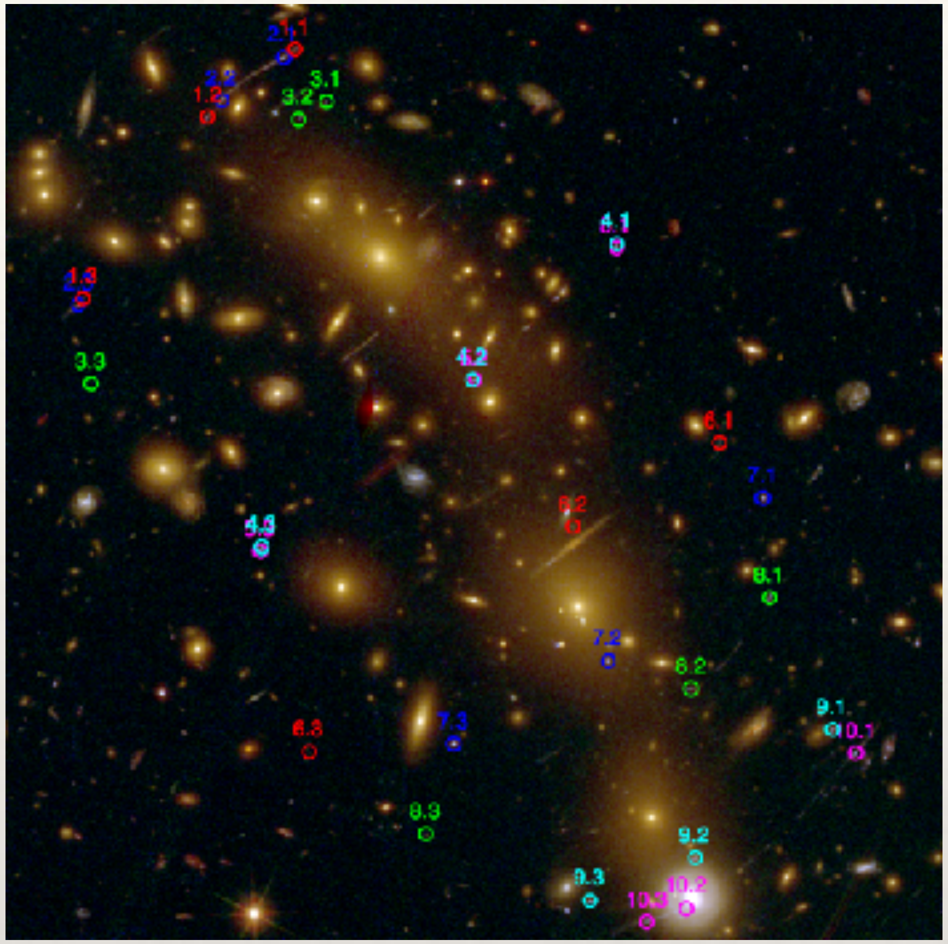

- For each system, at least 1 image has an either *secure* or *very likely* redshift
- If we have one *secure* and one *very likely*, we take the *secure*
- If we have two *secure*, we take the mean value

Grillo et al. (2005)

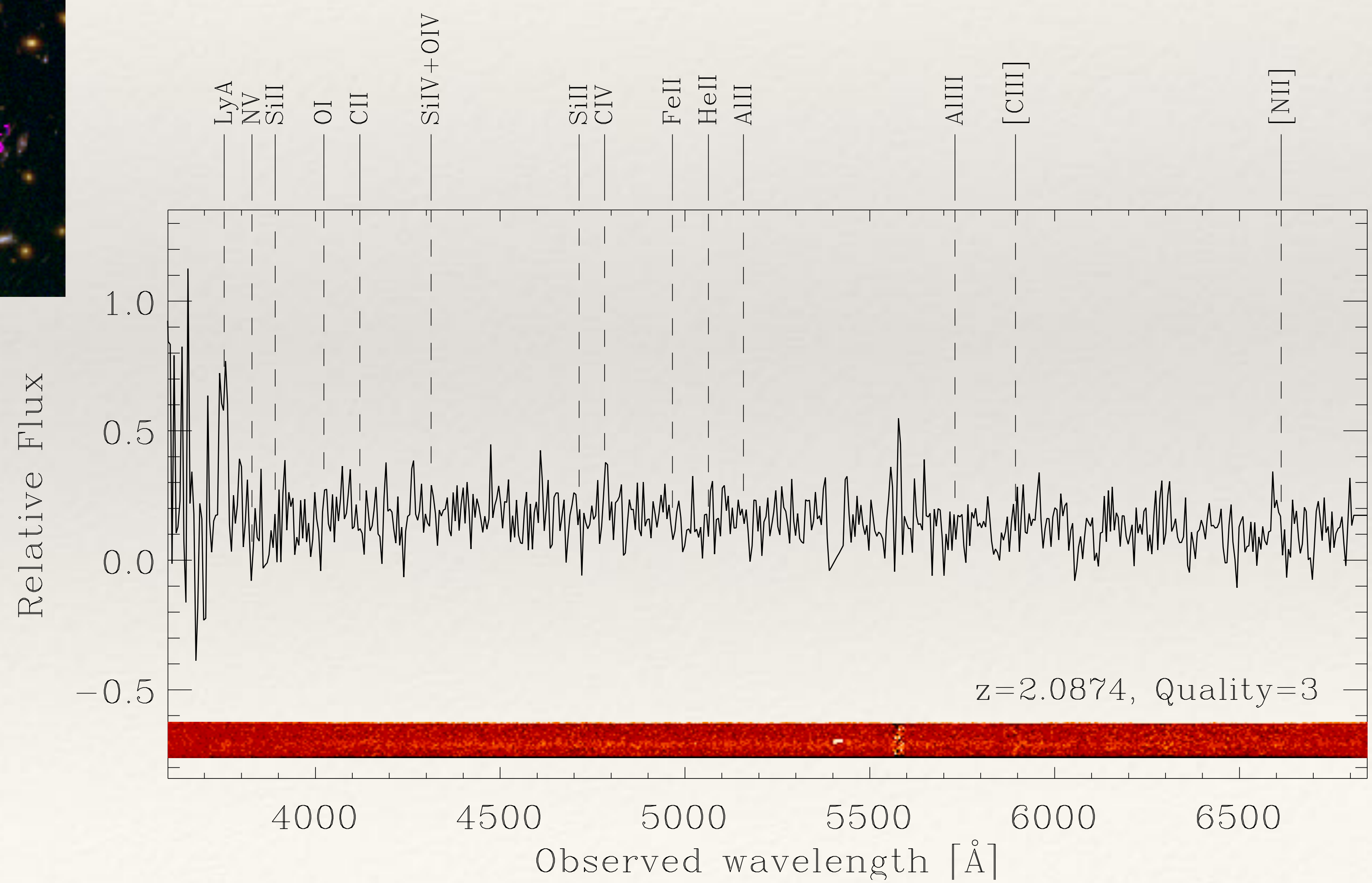

The multiple-image spectra

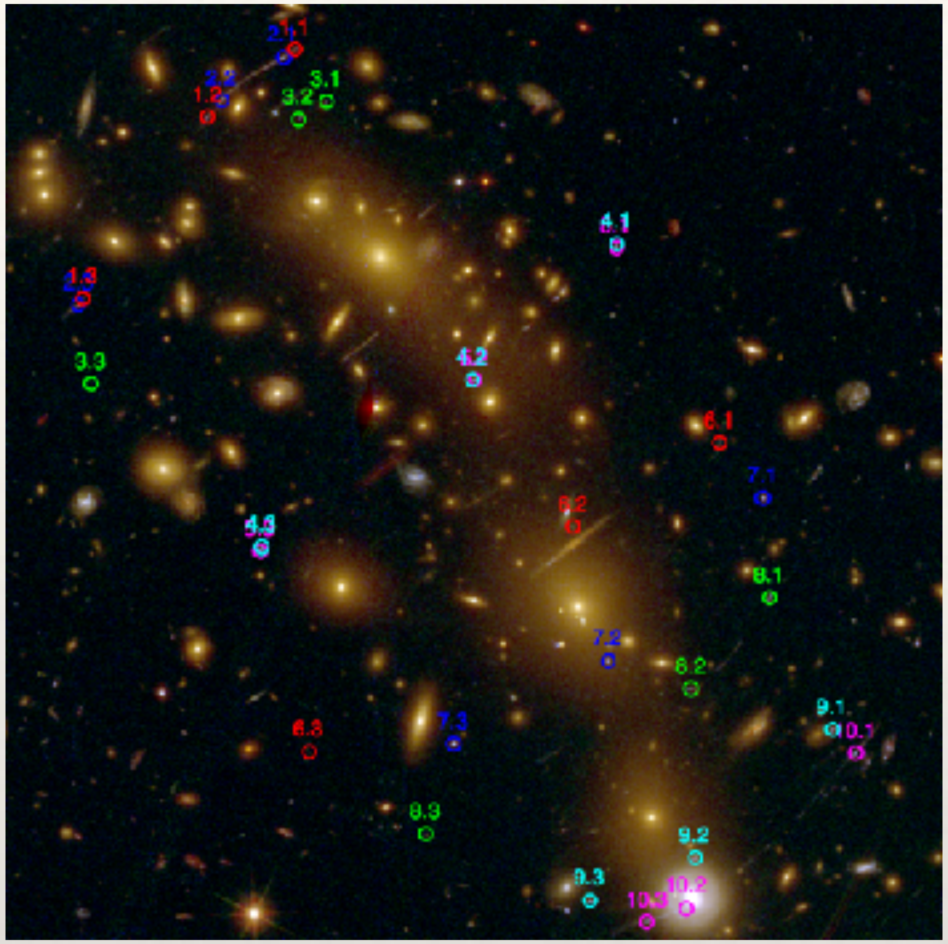

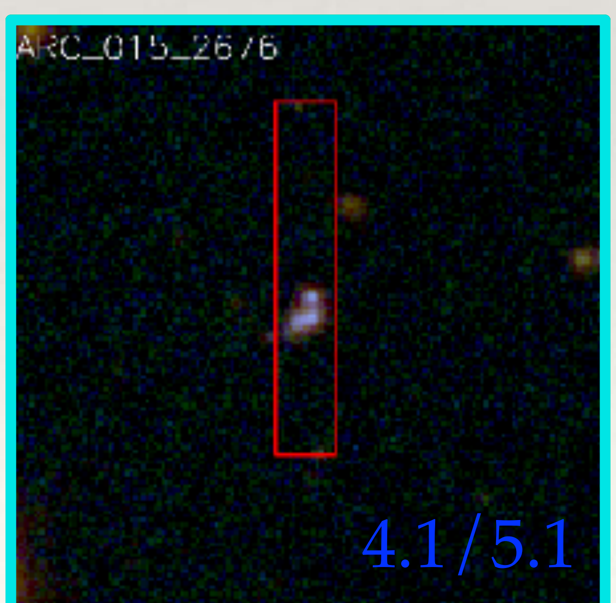

Grillo et al. (2005)

- For each system, at least 1 image has an either *secure* or *very likely* redshift
- If we have one *secure* and one *very likely*, we take the *secure*
- If we have two *secure*, we take the mean value

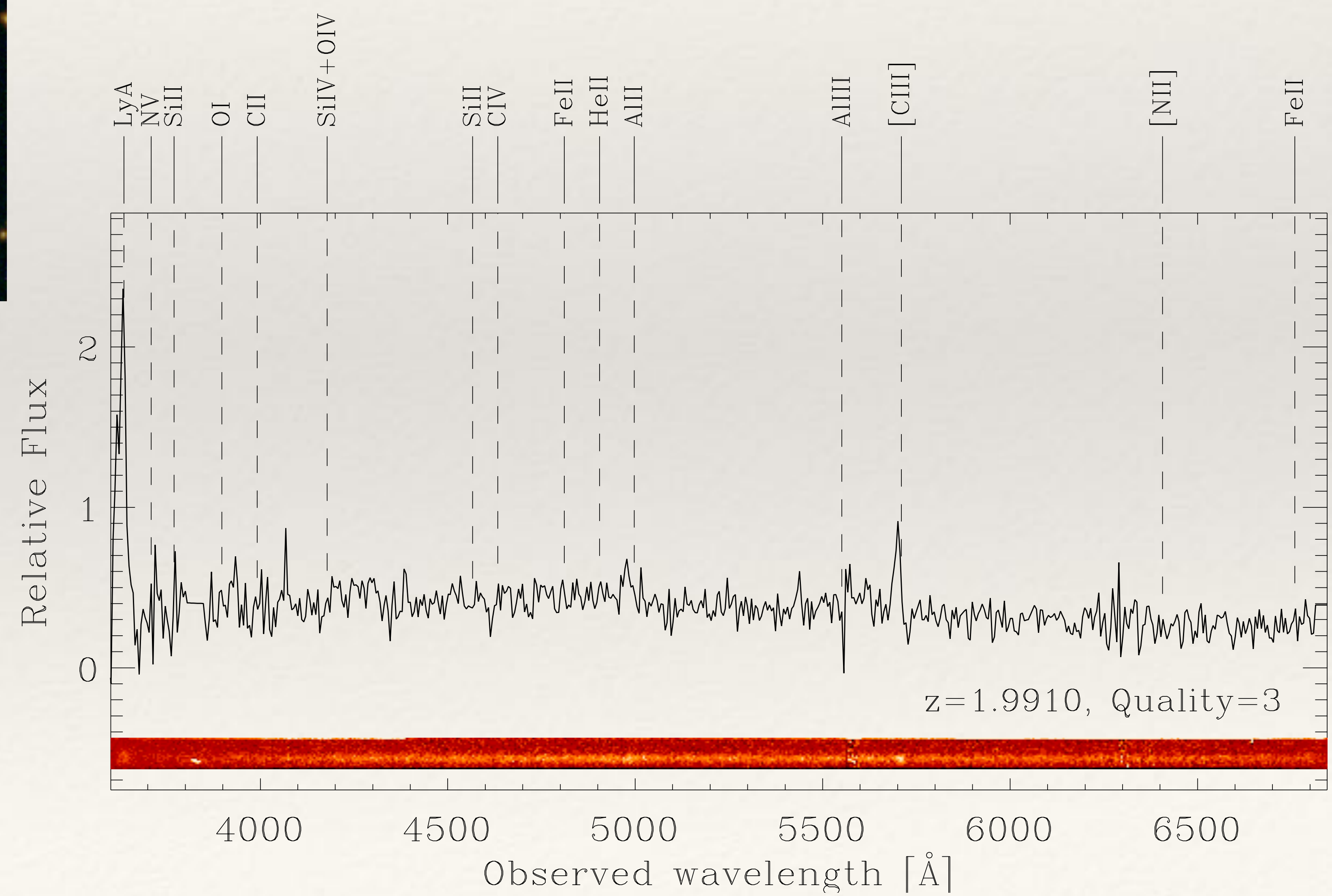

The multiple-image spectra

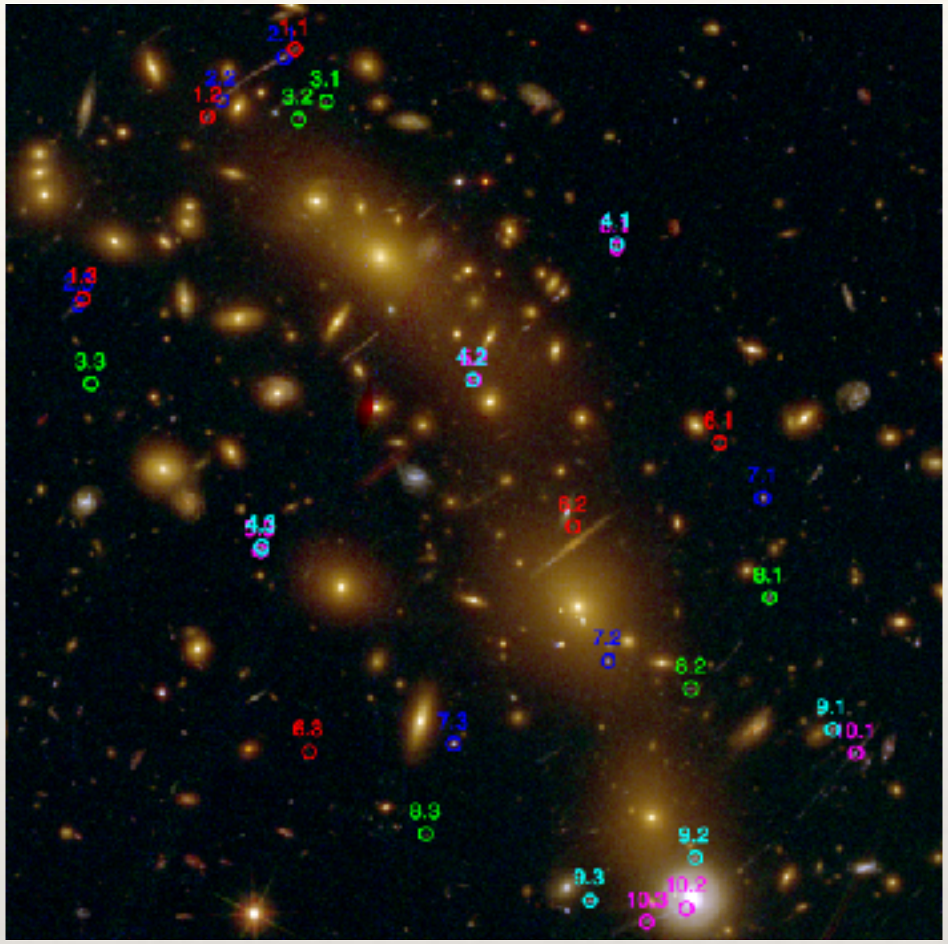

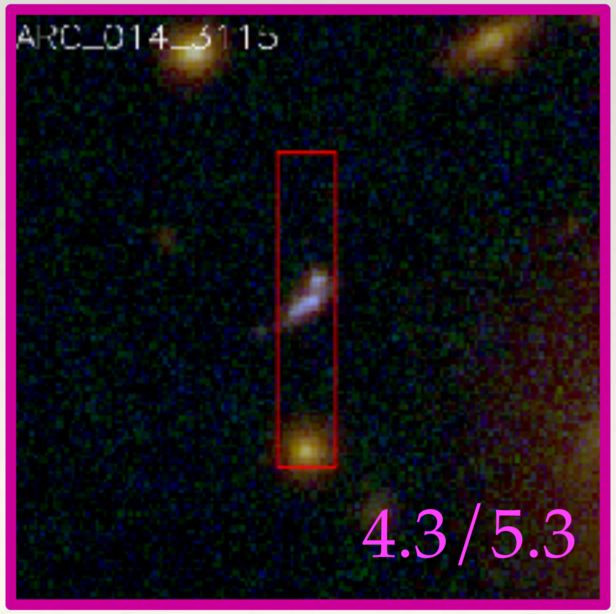

Grillo et al. (2005)

- For each system, at least 1 image has an either *secure* or *very likely* redshift
- If we have one *secure* and one *very likely*, we take the *secure*
- If we have two *secure*, we take the mean value

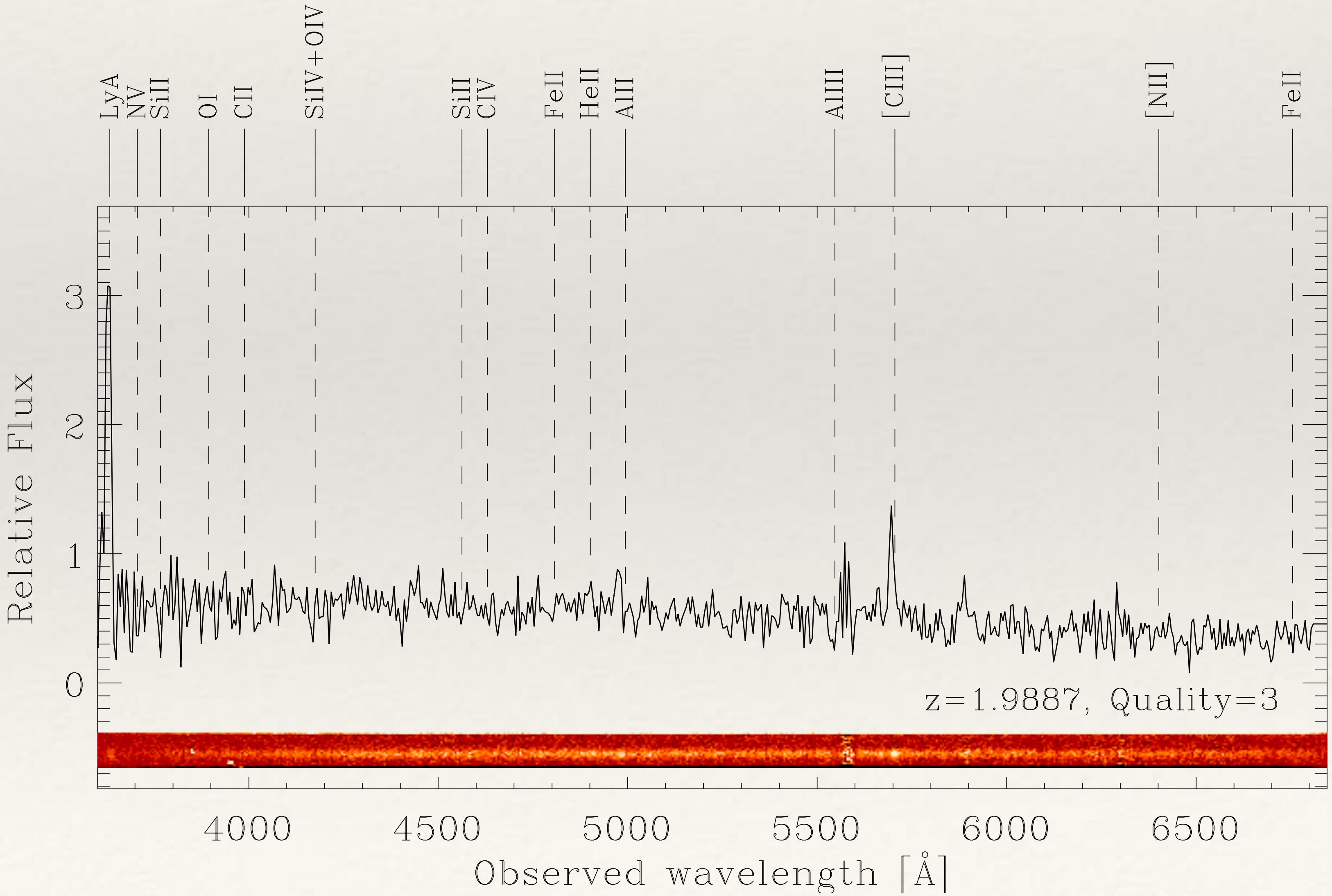

The multiple-image spectra

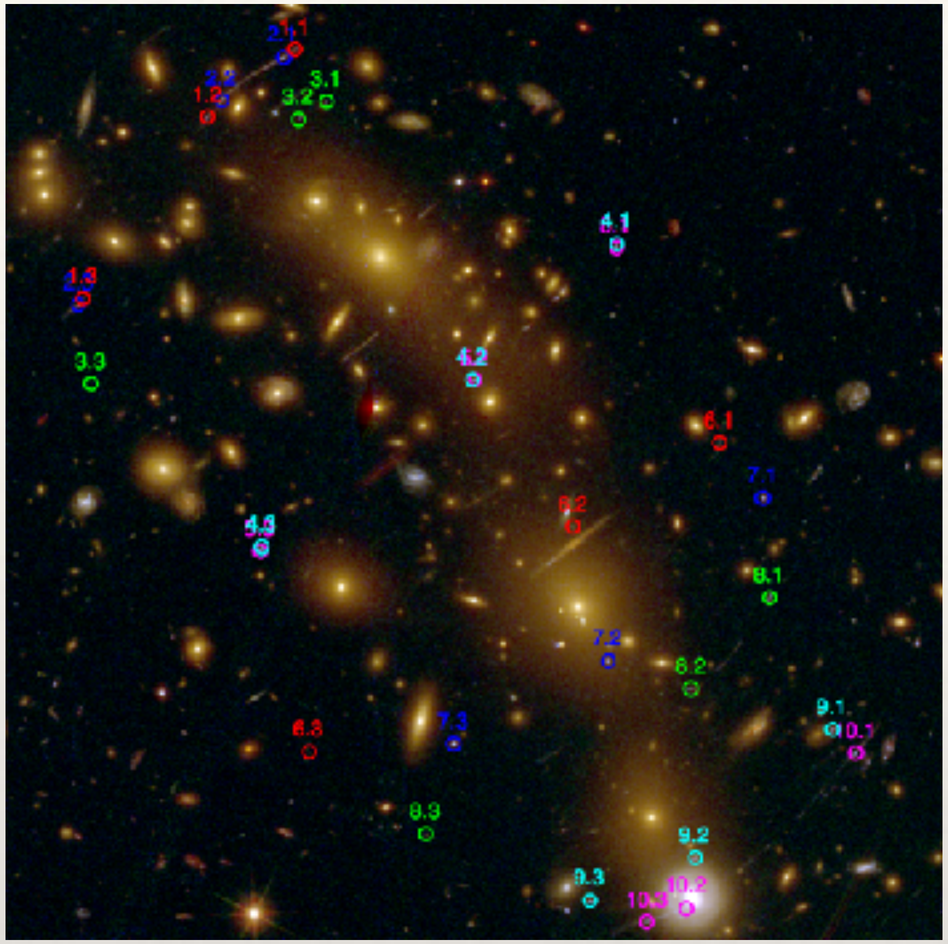

- For each system, at least 1 image has an either *secure* or *very likely* redshift
- If we have one *secure* and one *very likely*, we take the *secure*
- If we have two *secure*, we take the mean value

Grillo et al. (2005)

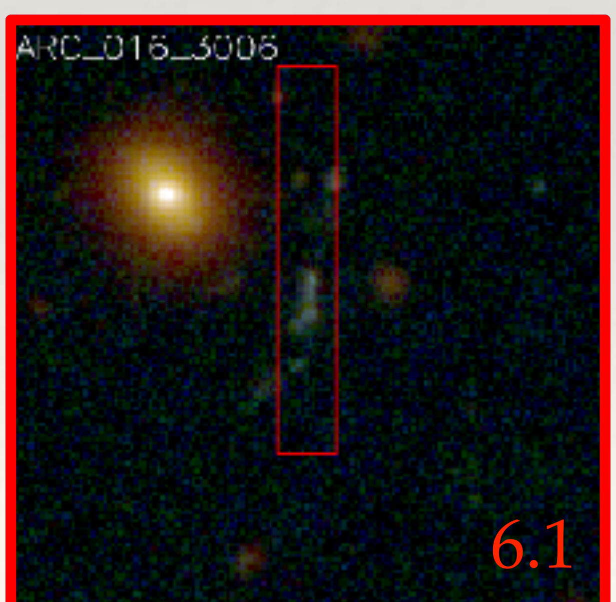

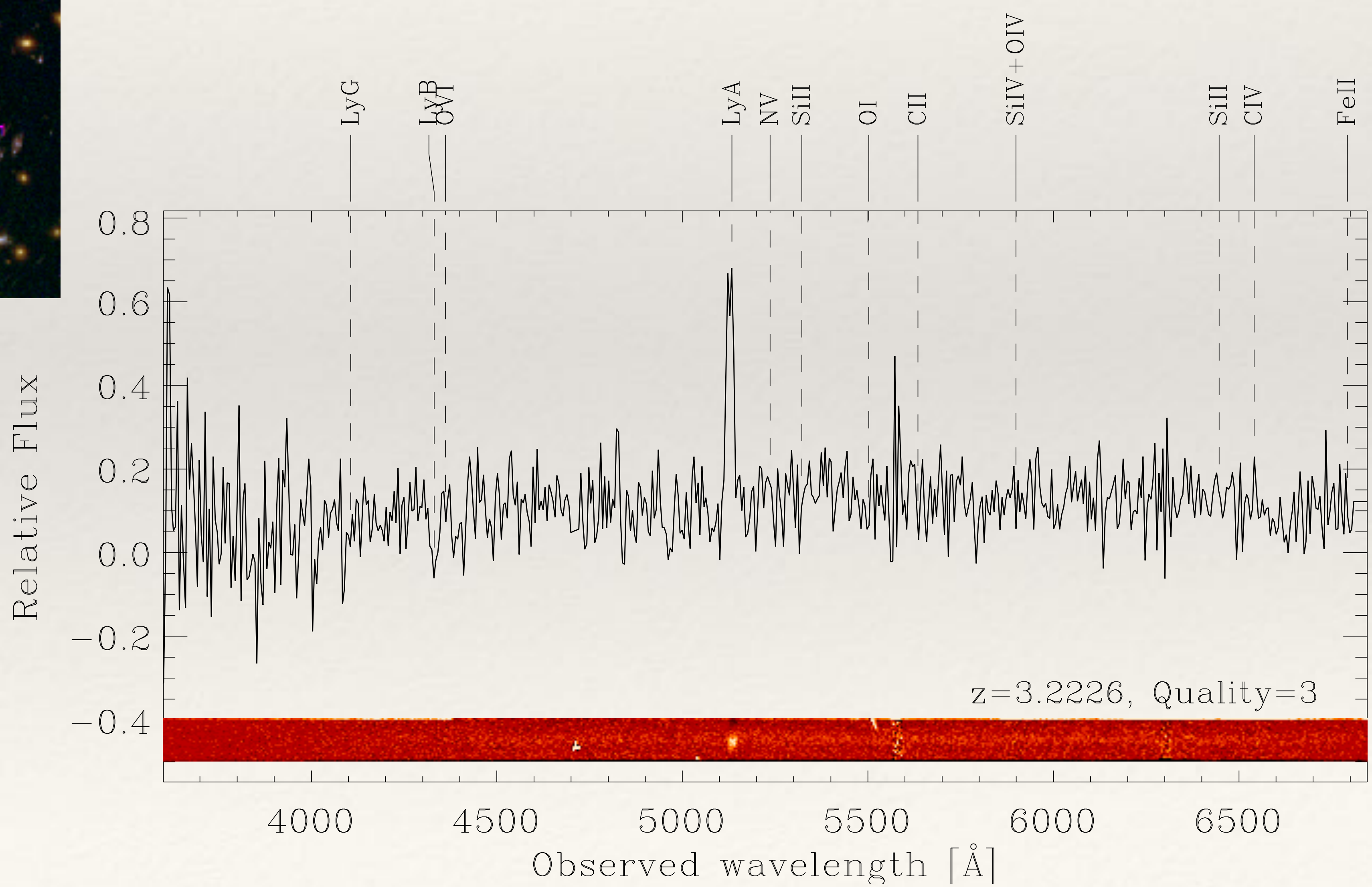

Hubble Frontier Fields and MUSE

- 24 IFU, 1 $arcmin^2$, resolution 0.2″, $R = 3000$, 4800–9300 Å, total efficiency ~25%

Hubble Frontier Fields and muse

- 24 IFU, 1 arcmin^2, resolution 0.2″, R = 3000, 4800–9300 Å, total efficiency ~25%
- **RXJ 2248** (Karman et al. 2015, 2017)
  - 4 x 1hr OB in the SW (SV; PI: Caputi, Grillo, Clement)
  - 6 x 1hr OB in the NE (PI: Caputi)

Hubble Frontier Fields and muse

- 24 IFU, 1 arcmin^2, resolution 0.2", R = 3000, 4800–9300 Å, total efficiency ~25%
- **RXJ 2248** (Karman et al. 2015, 2017)
  - 4 x 1hr OB in the SW (SV; PI: Caputi, Grillo, Clement)
  - 6 x 1hr OB in the NE (PI: Caputi)
- **MACS 1149** (Grillo et al. 2016)
  - 6 x 1hr OB in the core (obtained with DDT; PI: Grillo)

Hubble Frontier Fields and MUSE

- 24 IFU, 1 arcmin^2, resolution 0.2″, $R = 3000$, 4800–9300 Å, total efficiency ~25%
- **RXJ 2248** (Karman et al. 2015, 2017)
  - 4 x 1hr OB in the SW (SV; PI: Caputi, Grillo, Clement)
  - 6 x 1hr OB in the NE (PI: Caputi)
- **MACS 1149** (Grillo et al. 2016)
  - 6 x 1hr OB in the core (obtained with DDT; PI: Grillo)
- **MACS 0416** (Caminha et al. 2017)
  - 2hr in the NE (GTO; PI: Richard)
  - 11 hr in the SW (PI: F.E. Bauer)

RXJ 2248 (2 MUSE pointings)

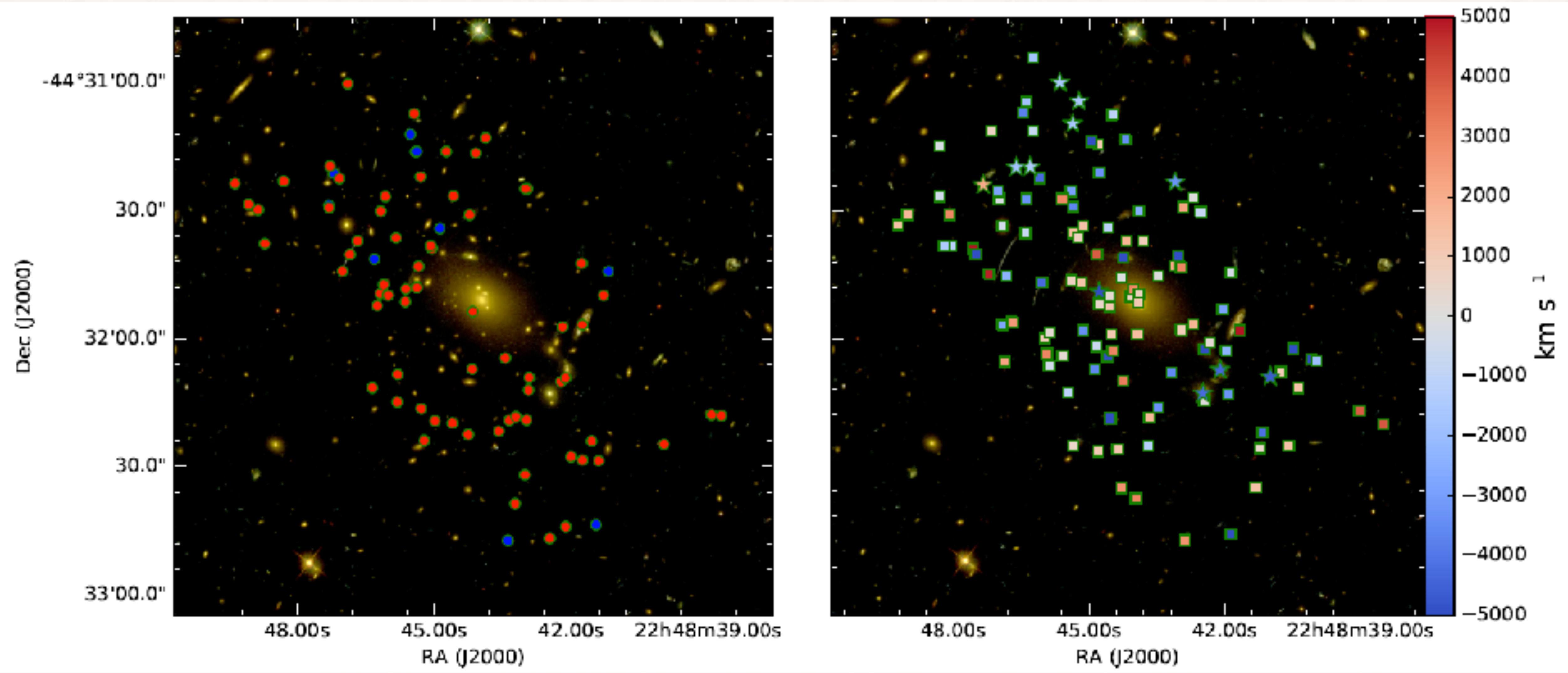

- 10 foreground galaxies
- 120 cluster members
- 42 background galaxies
- 17 multiple-image systems
- 43 images
- $z_{max} = 6.107$

MACS 1149 (1 MUSE pointing)

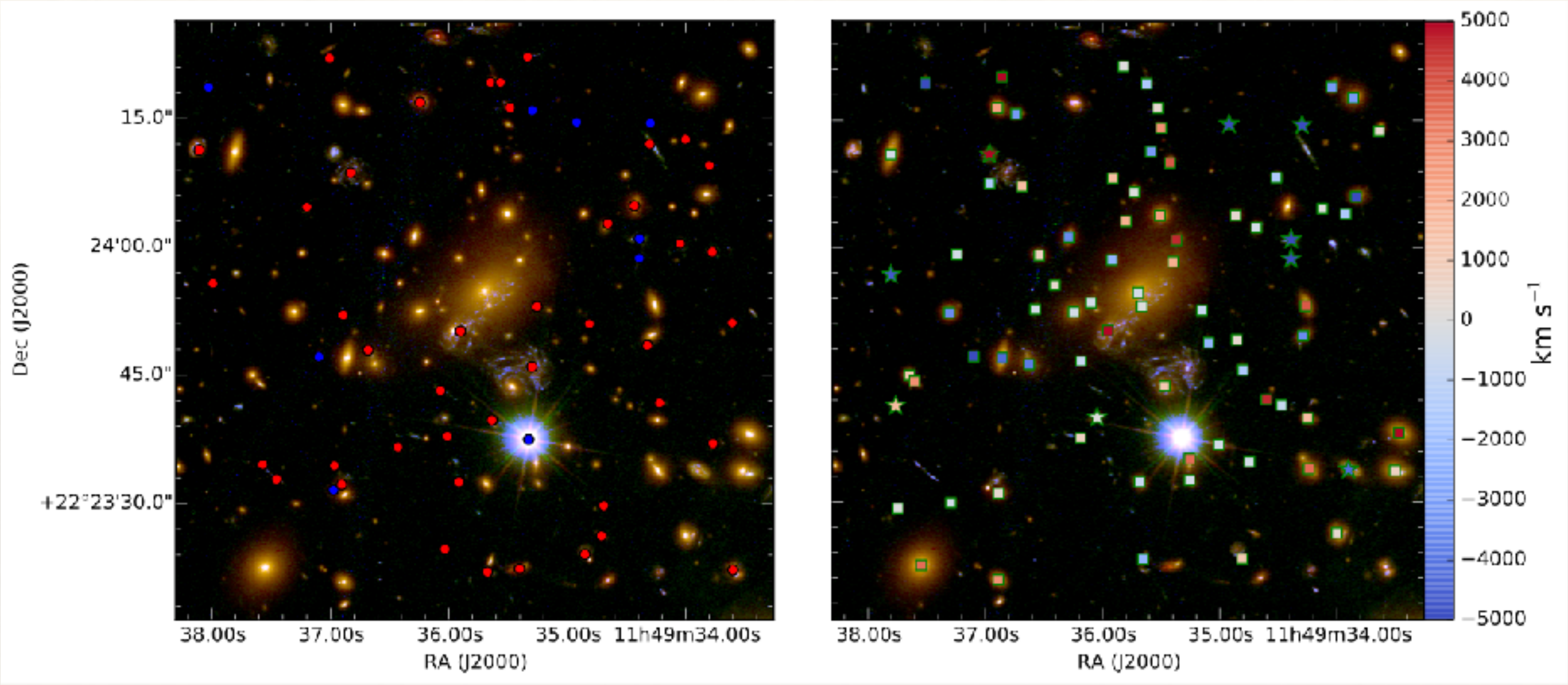

- 5 foreground galaxies
- 68 cluster members
- 30 background galaxies
- 7 multiple-image systems
- 18 images
- $z_{\max} = 3.703$

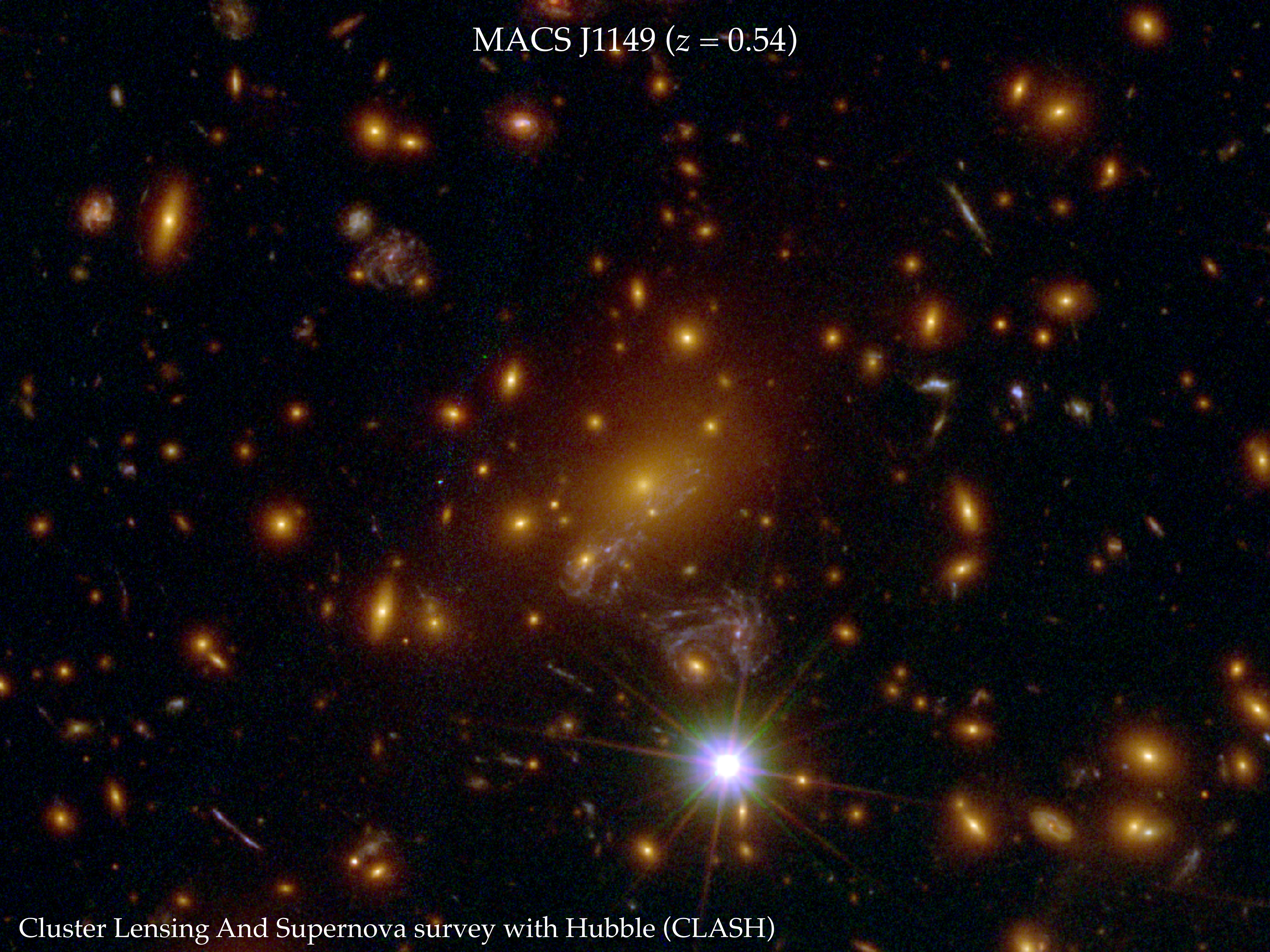
MACS J1149 (z = 0.54)
Cluster Lensing And Supernova survey with Hubble (CLASH)

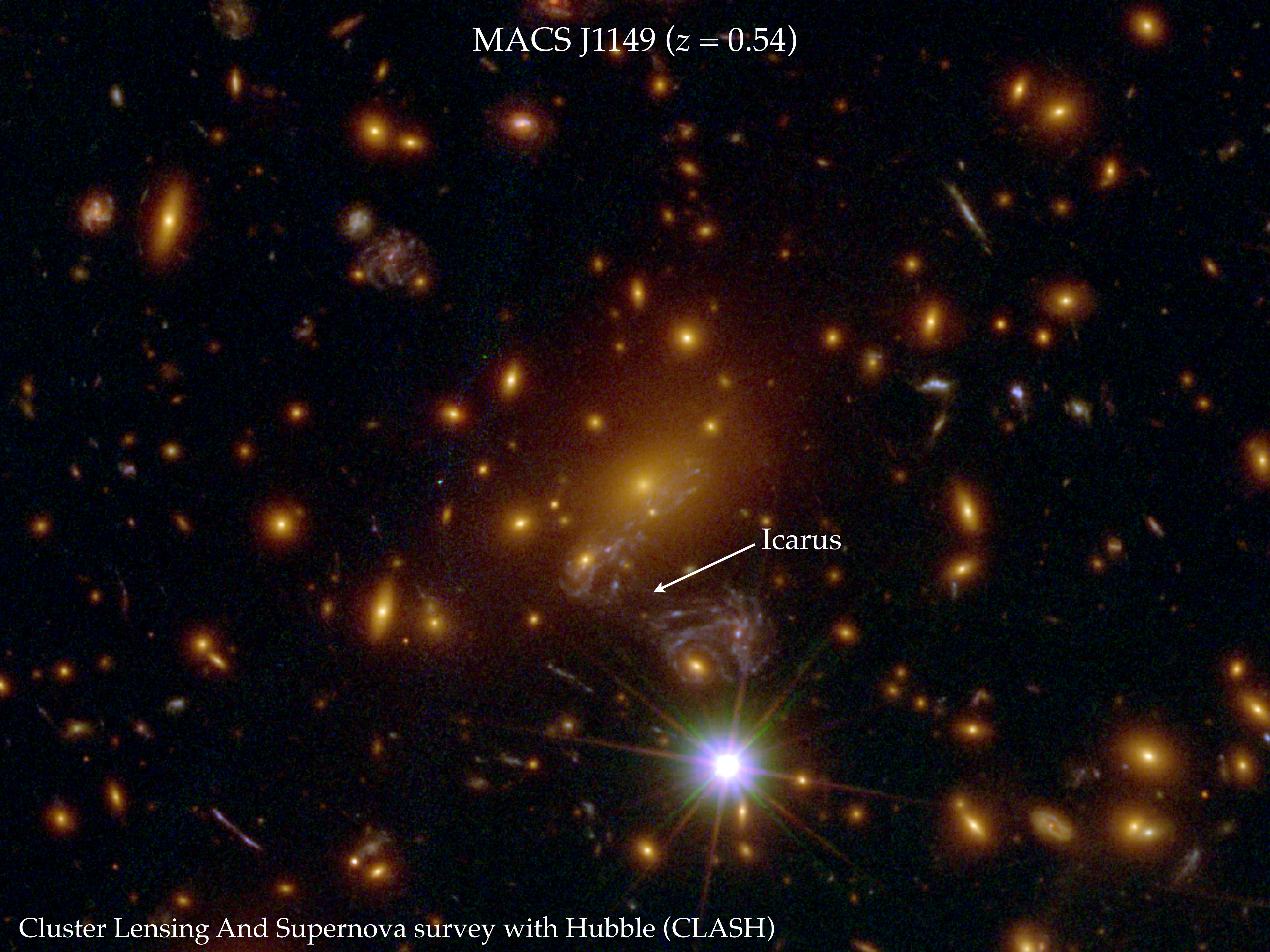
MACS J1149 ($z = 0.54$)
Icarus
Cluster Lensing And Supernova survey with Hubble (CLASH)

MACS J1149 ($z = 0.54$)

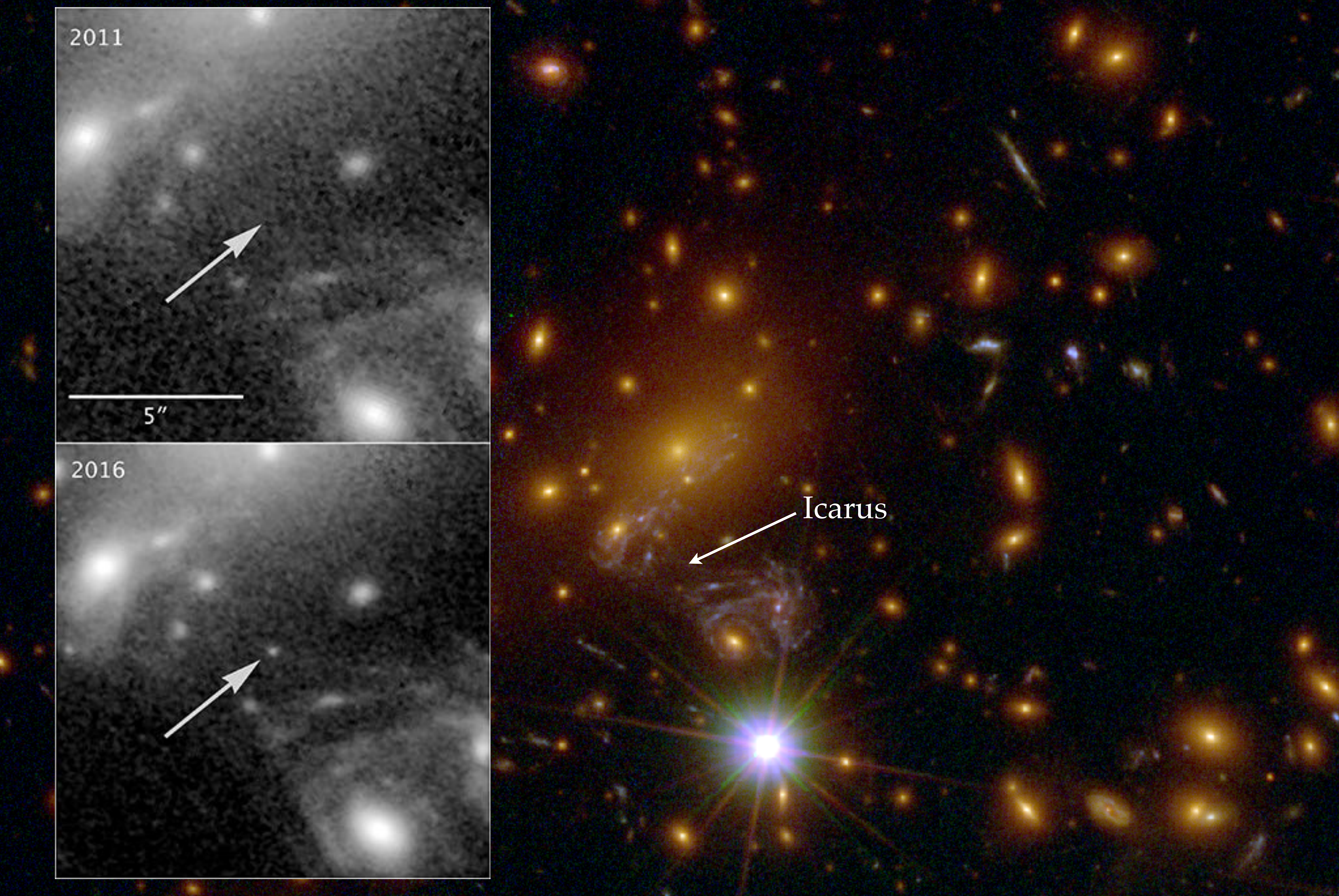

Cluster Lensing And Supernova survey with Hubble (CLASH)

Refsdal (1964)

ON THE POSSIBILITY OF DETERMINING HUBBLE'S PARAMETER AND THE MASSES OF GALAXIES FROM THE GRAVITATIONAL LENS EFFECT*

Sjur Refsdal

(Communicated by H. Bondi)

(Received 1964 January 27)

Summary

The gravitational lens effect is applied to a supernova lying far behind and close to the line of sight through a distant galaxy. The light from the supernova may follow two different paths to the observer, and the difference Δt in the time of light travel for these two paths can amount to a couple of months or more, and may be measurable. It is shown that Hubble's parameter and the mass of the galaxy can be expressed by Δt, the red-shifts of the supernova and the galaxy, the luminosities of the supernova " images " and the angle between them. The possibility of observing the phenomenon is discussed.

First multiply-lensed SN “SN Refsdal”

Kelly et al. (2015, Science)

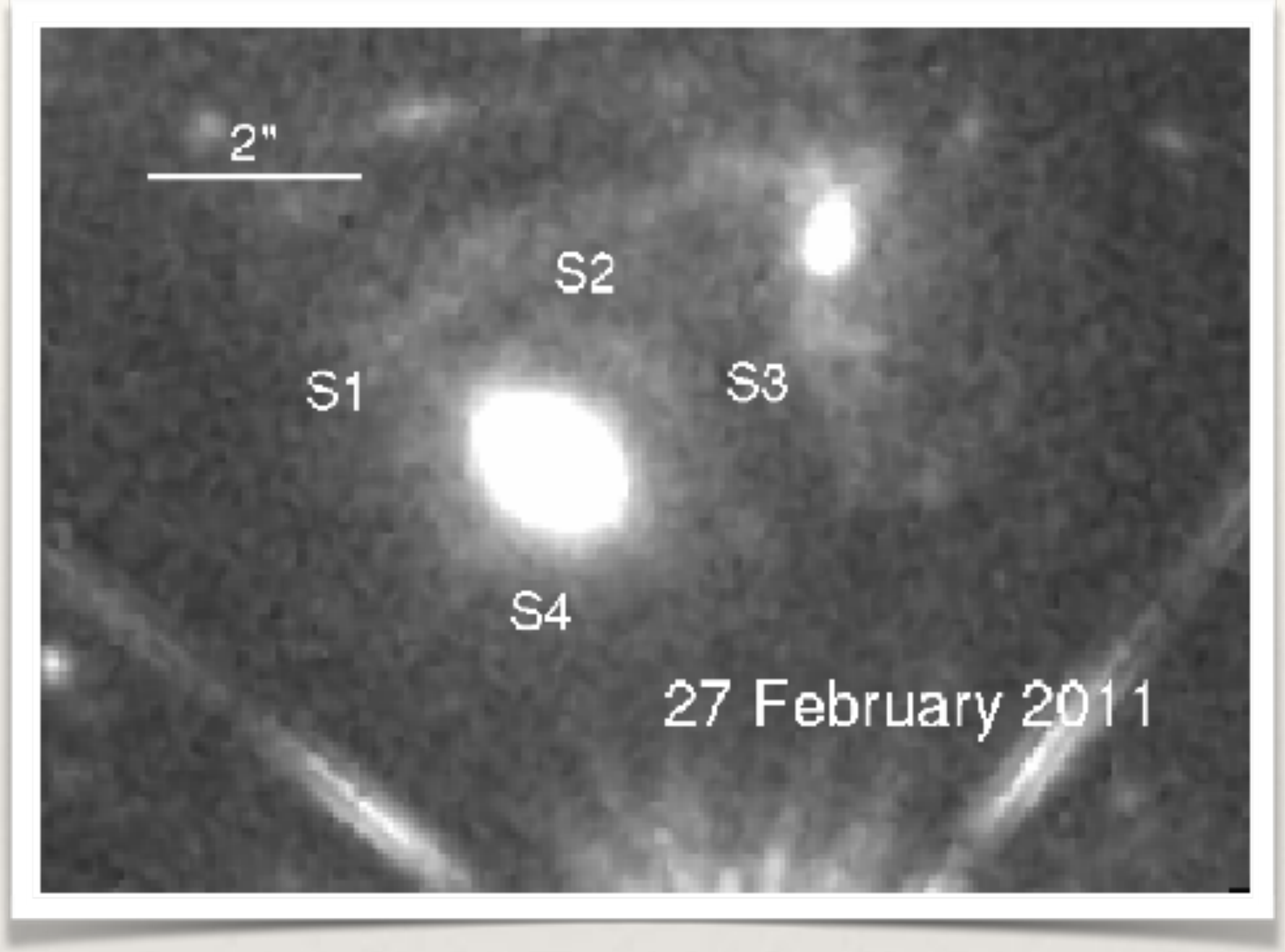

First multiply-lensed SN "SN Refsdal"

Kelly et al. (2015, Science)

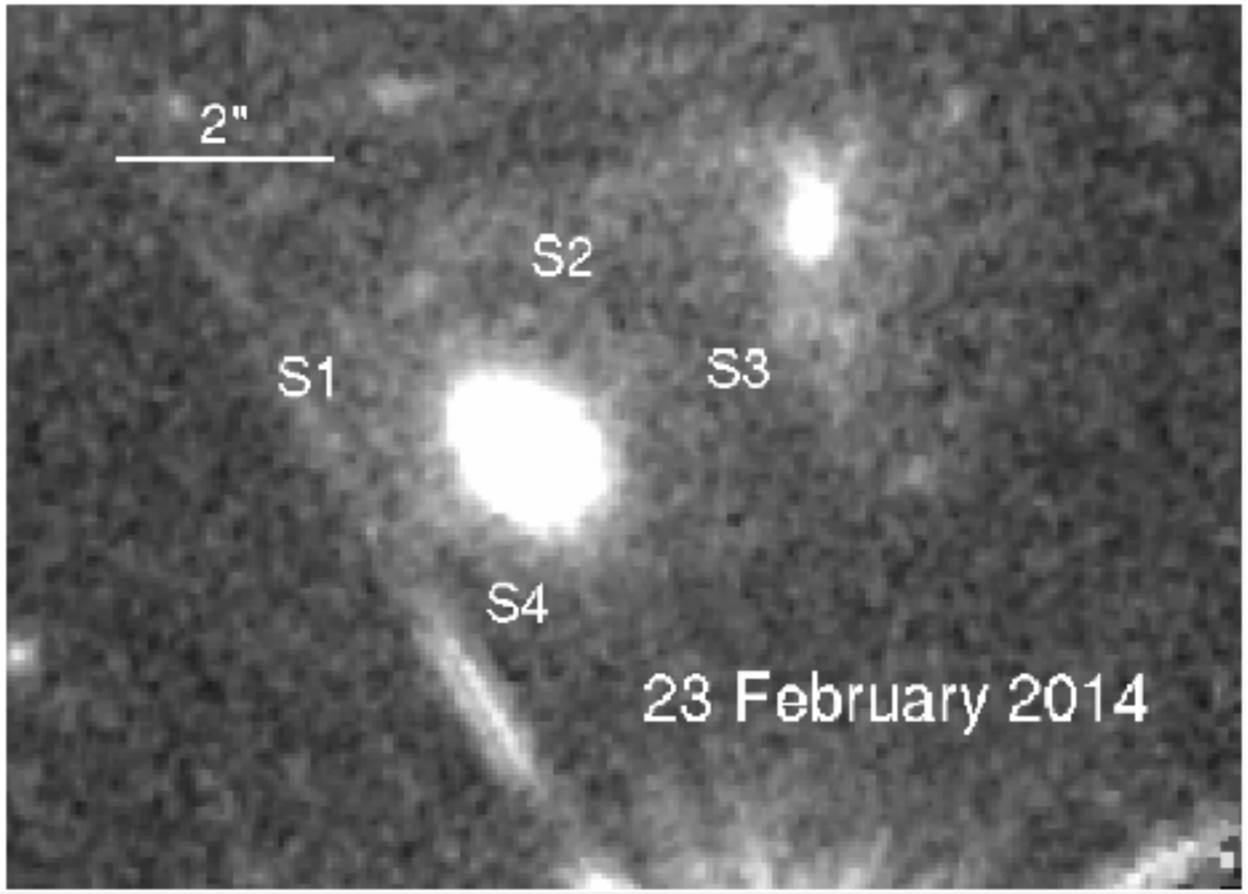

First multiply-lensed SN "SN Refsdal"

Kelly et al. (2015, Science)

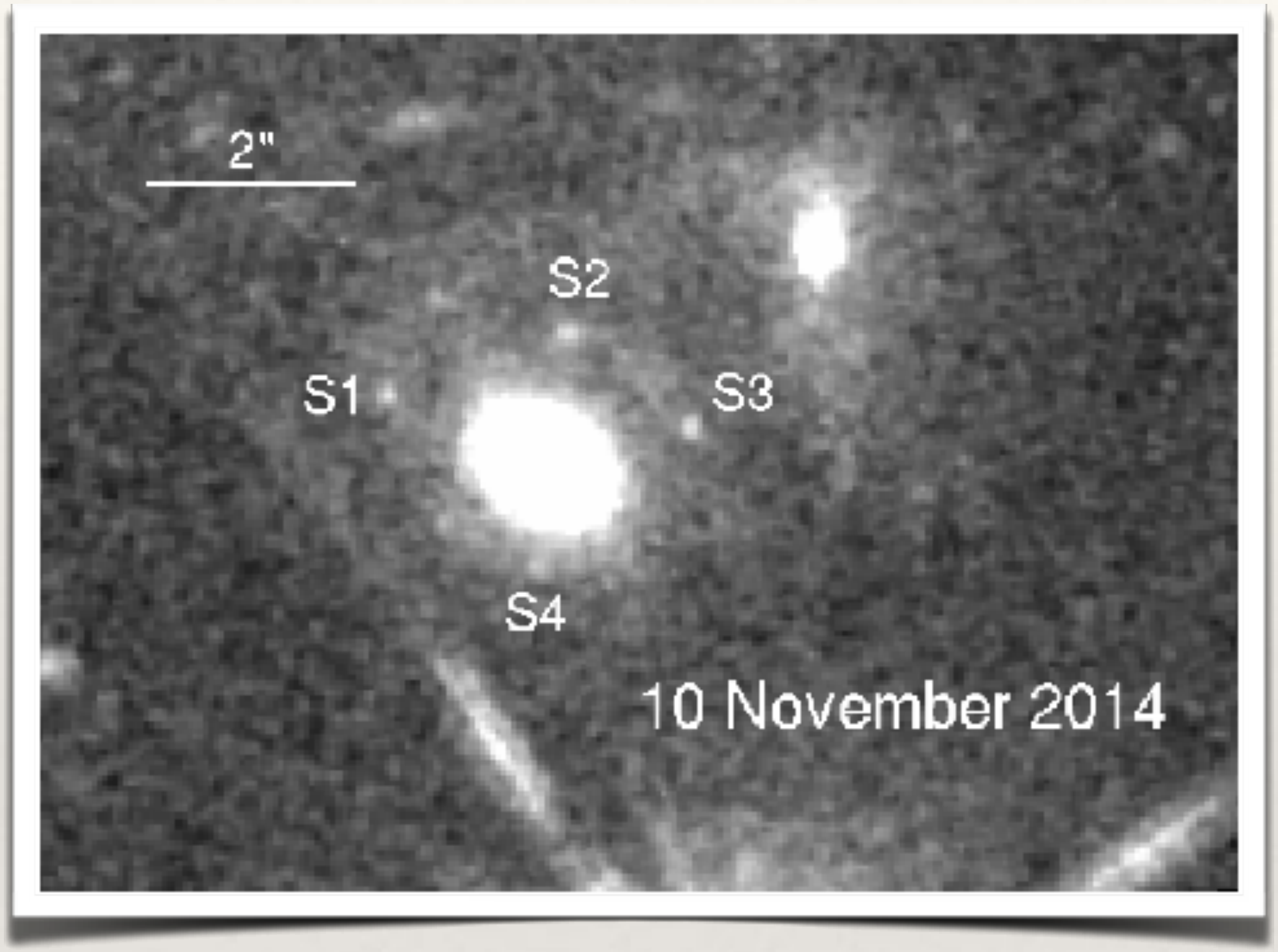

First multiply-lensed SN "SN Refsdal"

Kelly et al. (2015, Science)

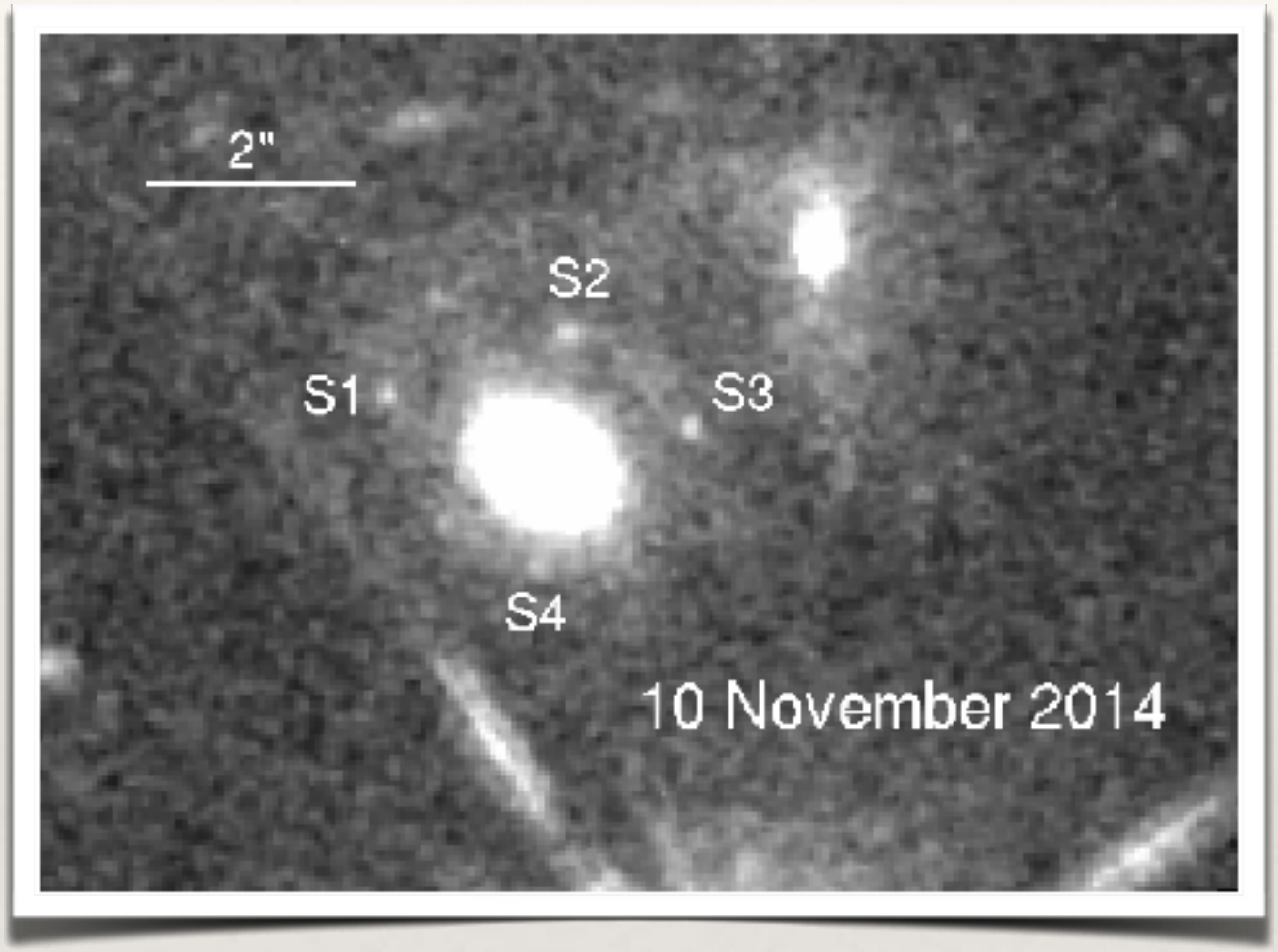

- Typical Einstein cross configuration (4 images)
- Main lens: elliptical cluster member
- Source: spiral galaxy
- Nucleus of the blue lensed spiral offset by ~ 3.3" from the red lens elliptical

First multiply-lensed SN “SN Refsdal”

Kelly et al. (2015, Science)

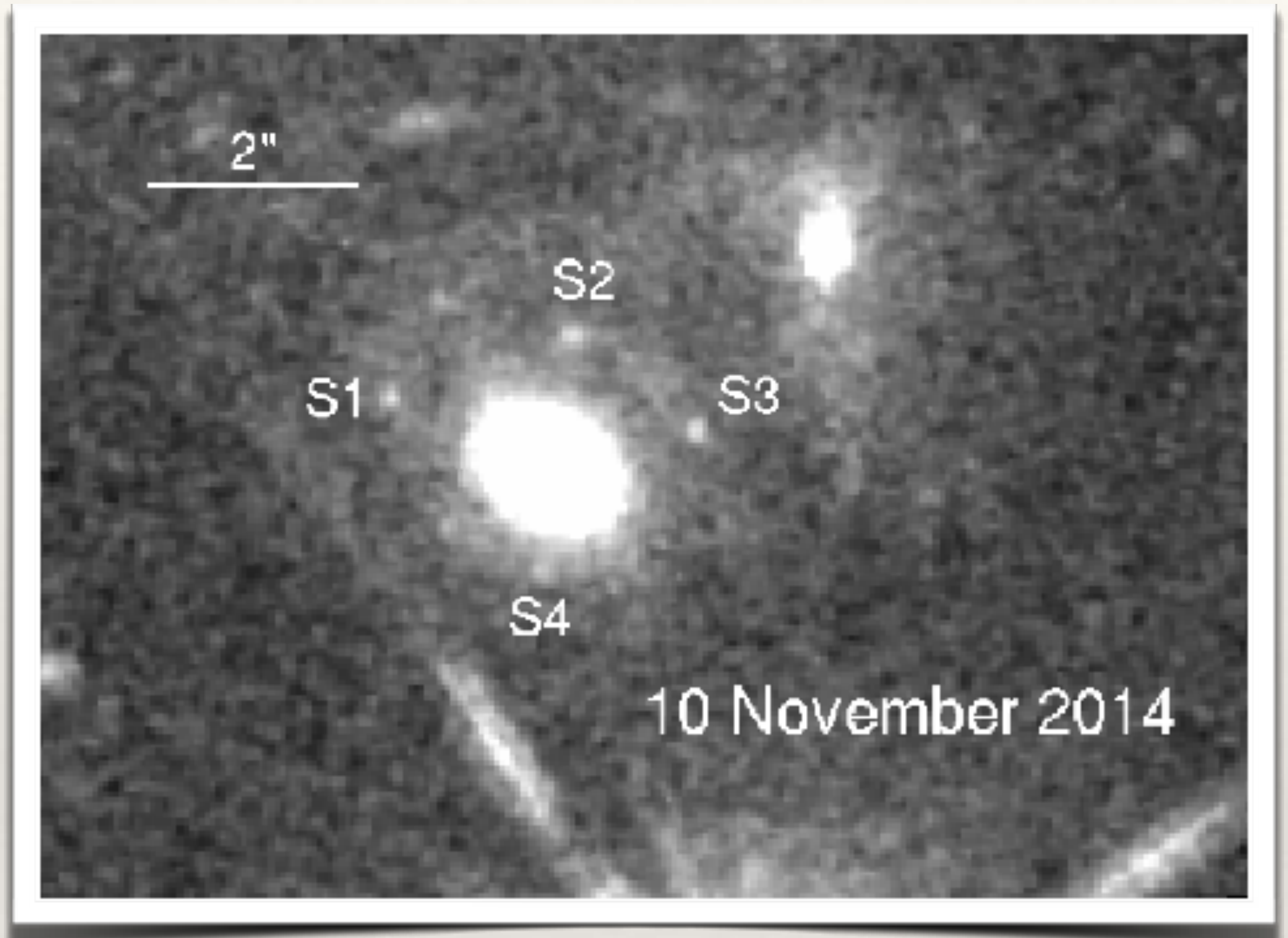

- Typical Einstein cross configuration (4 images)
- Main lens: elliptical cluster member
- Source: spiral galaxy
- Nucleus of the blue lensed spiral offset by ~ 3.3″ from the red lens elliptical

- Reapperance of the SN predicted by SL models…
- …and observed!

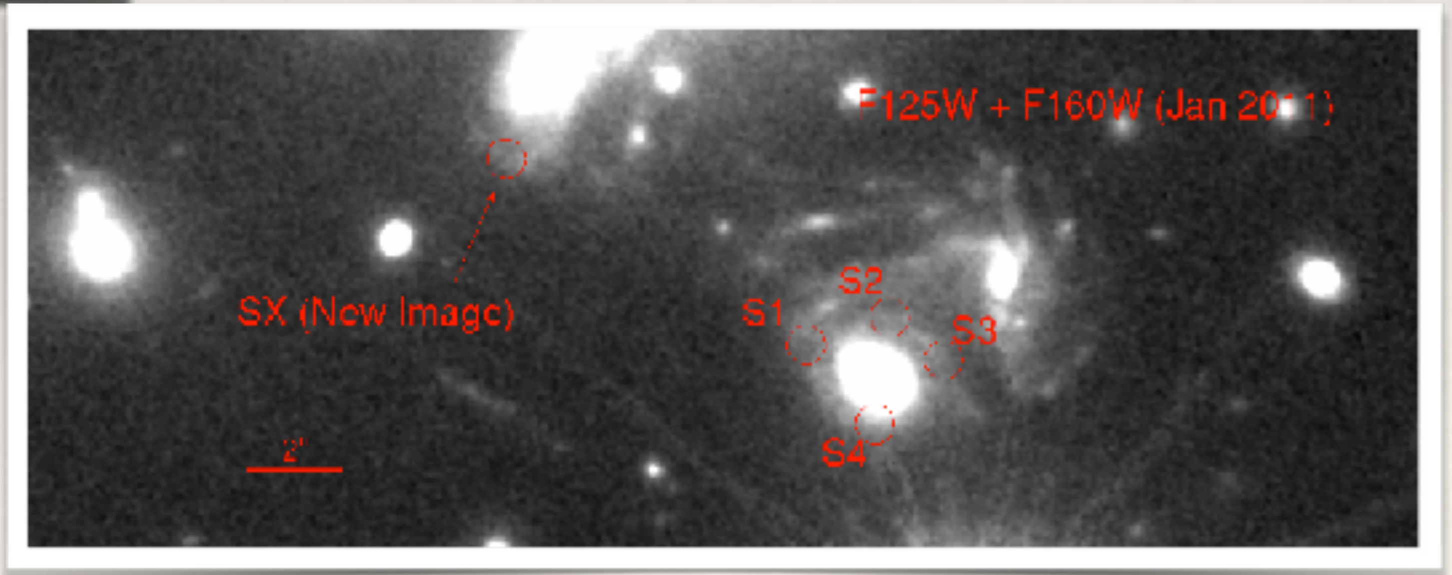

First multiply-lensed SN "SN Refsdal"

Kelly et al. (2015, Science)

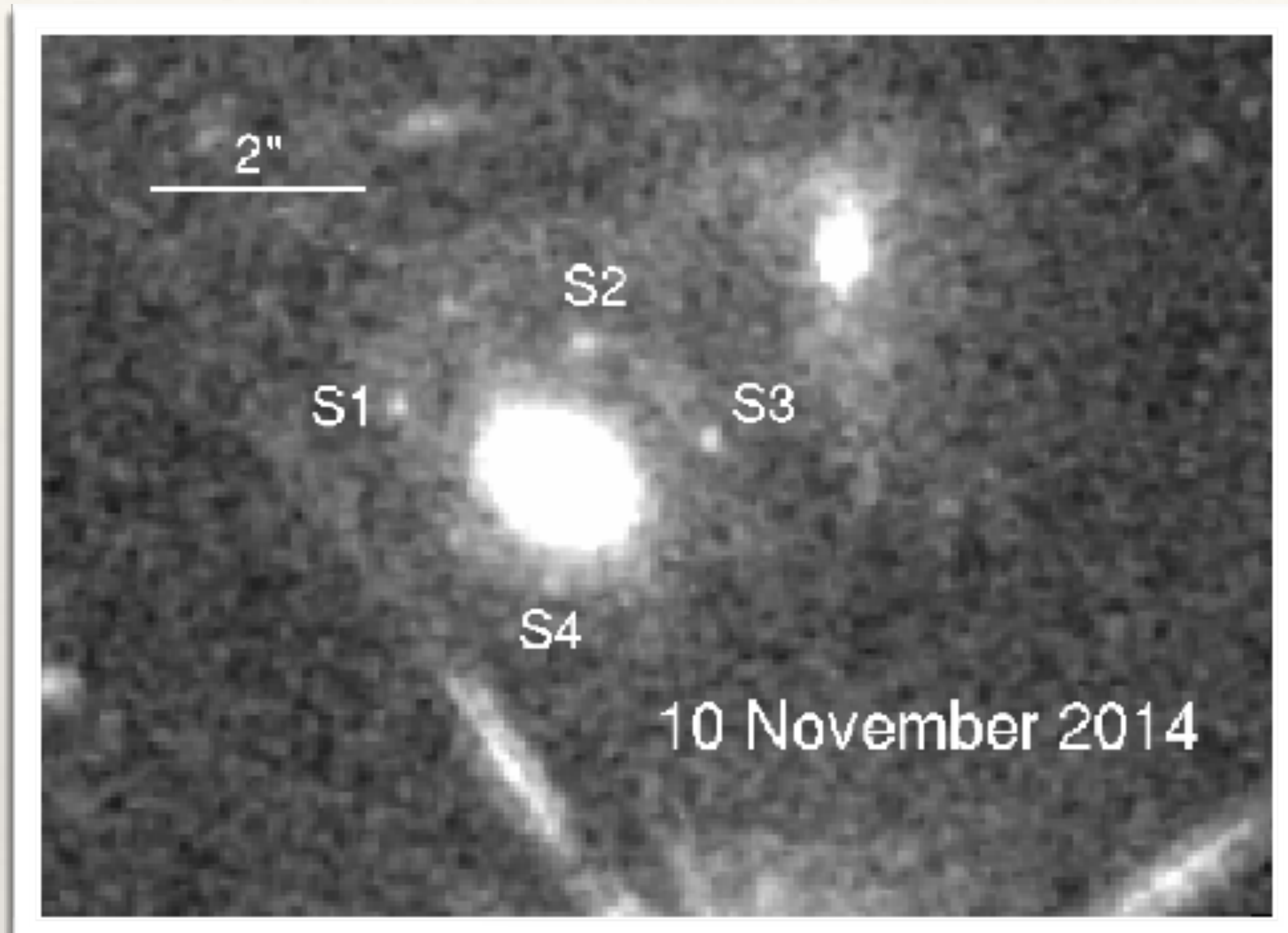

- Typical Einstein cross configuration (4 images)
- Main lens: elliptical cluster member
- Source: spiral galaxy
- Nucleus of the blue lensed spiral offset by ~ 3.3″ from the red lens elliptical

- Reapperance of the SN predicted by SL models…
- …and observed!

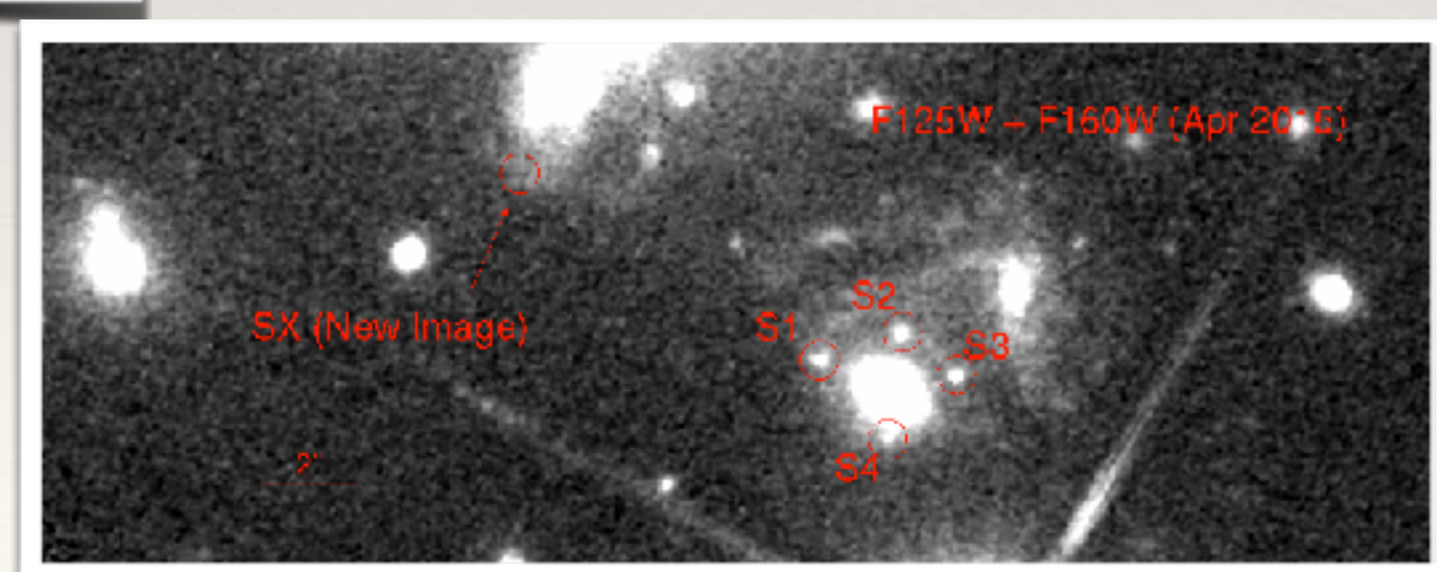

First multiply-lensed SN "SN Refsdal"

Kelly et al. (2015, Science)

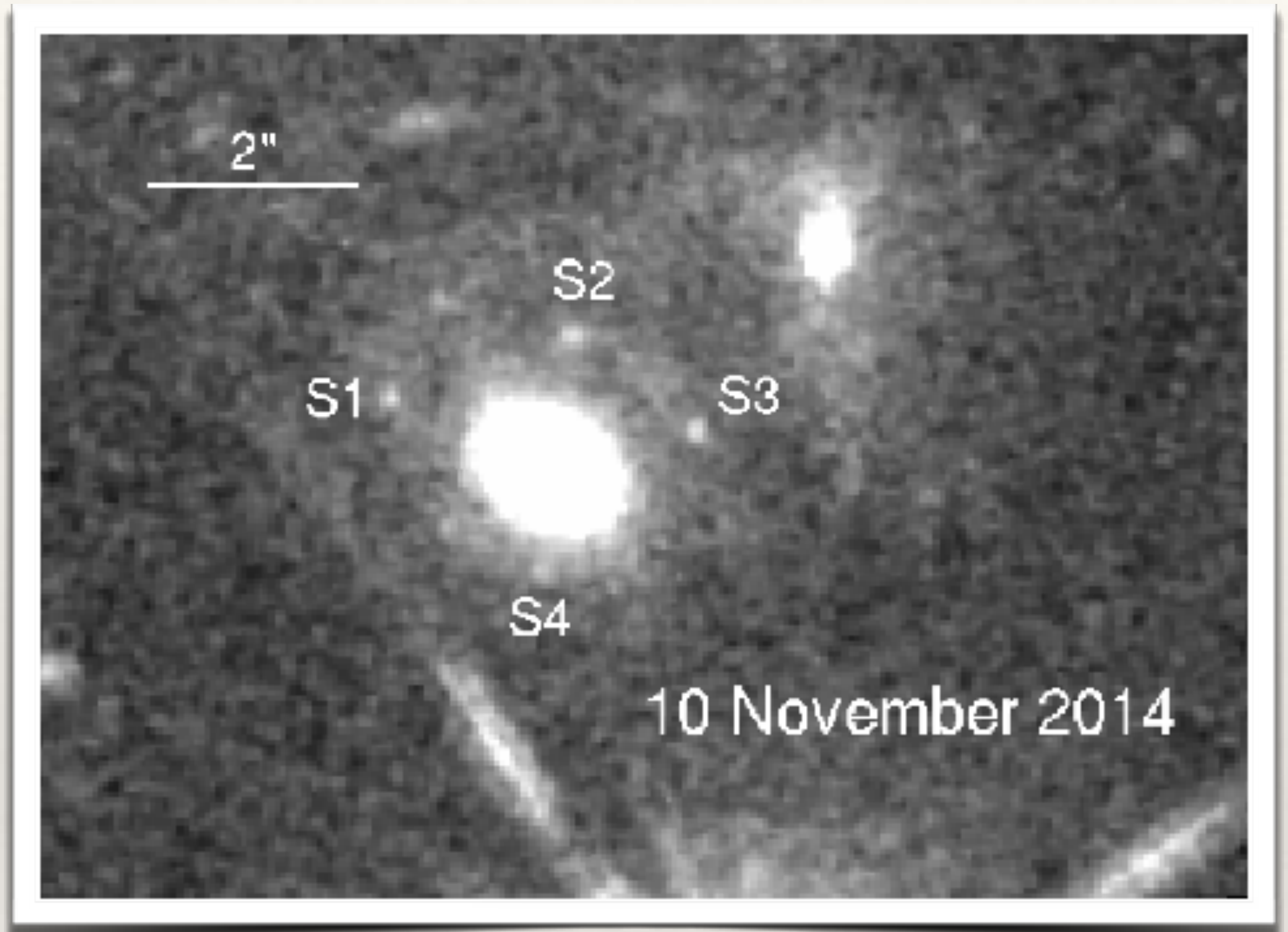

- Typical Einstein cross configuration (4 images)
- Main lens: elliptical cluster member
- Source: spiral galaxy
- Nucleus of the blue lensed spiral offset by ~ 3.3″ from the red lens elliptical

- Reapperance of the SN predicted by SL models…
- …and observed!

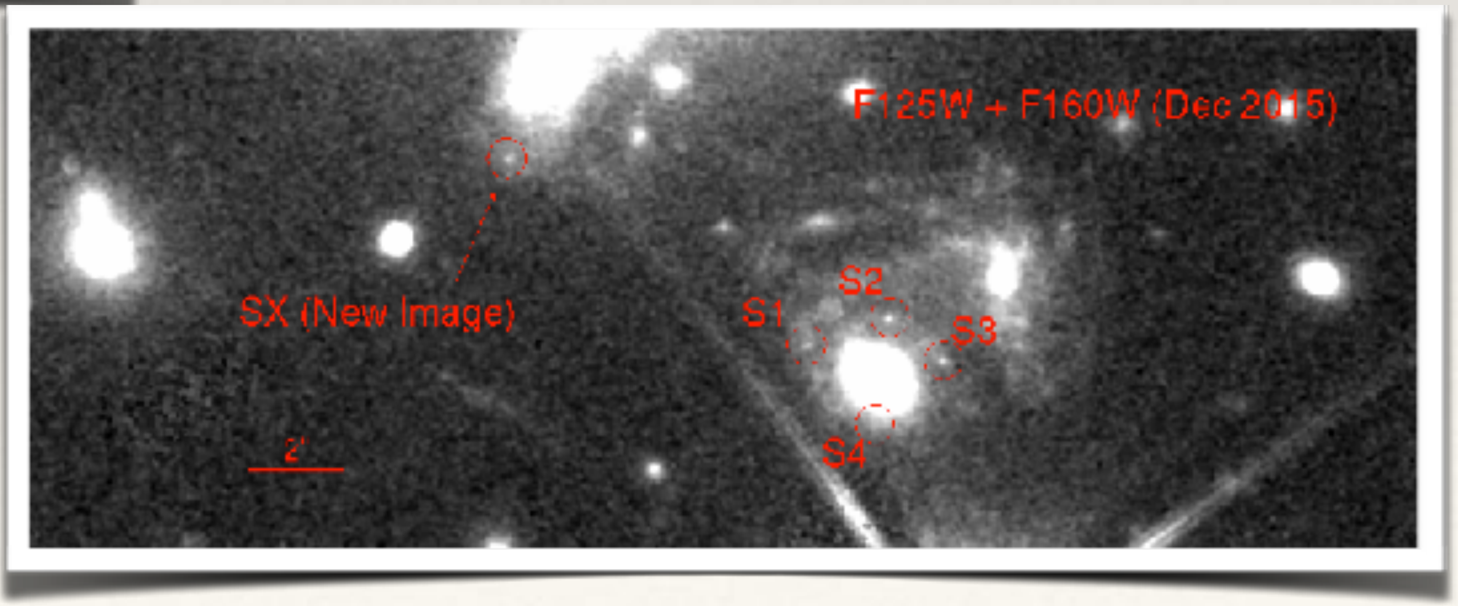

SN Refsdal's follow-up and true blind tests

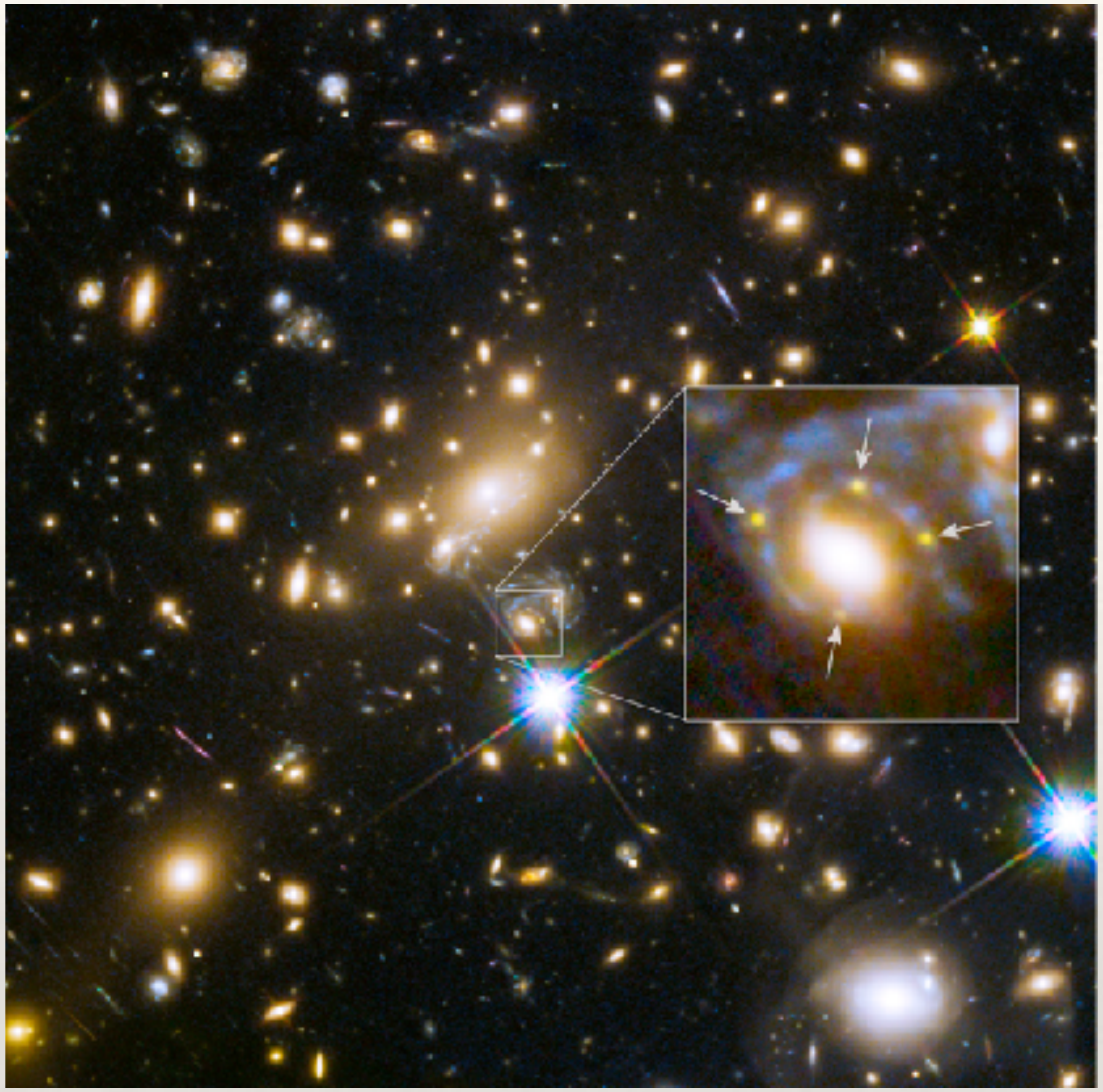

- MUSE and GLASS data to build refined strong lensing models and predict SX
- S1-4 time delays and magnifications measured (Treu et al. 2016)
- Excellent agreement with the model predictions (Rodney et al. 2016)

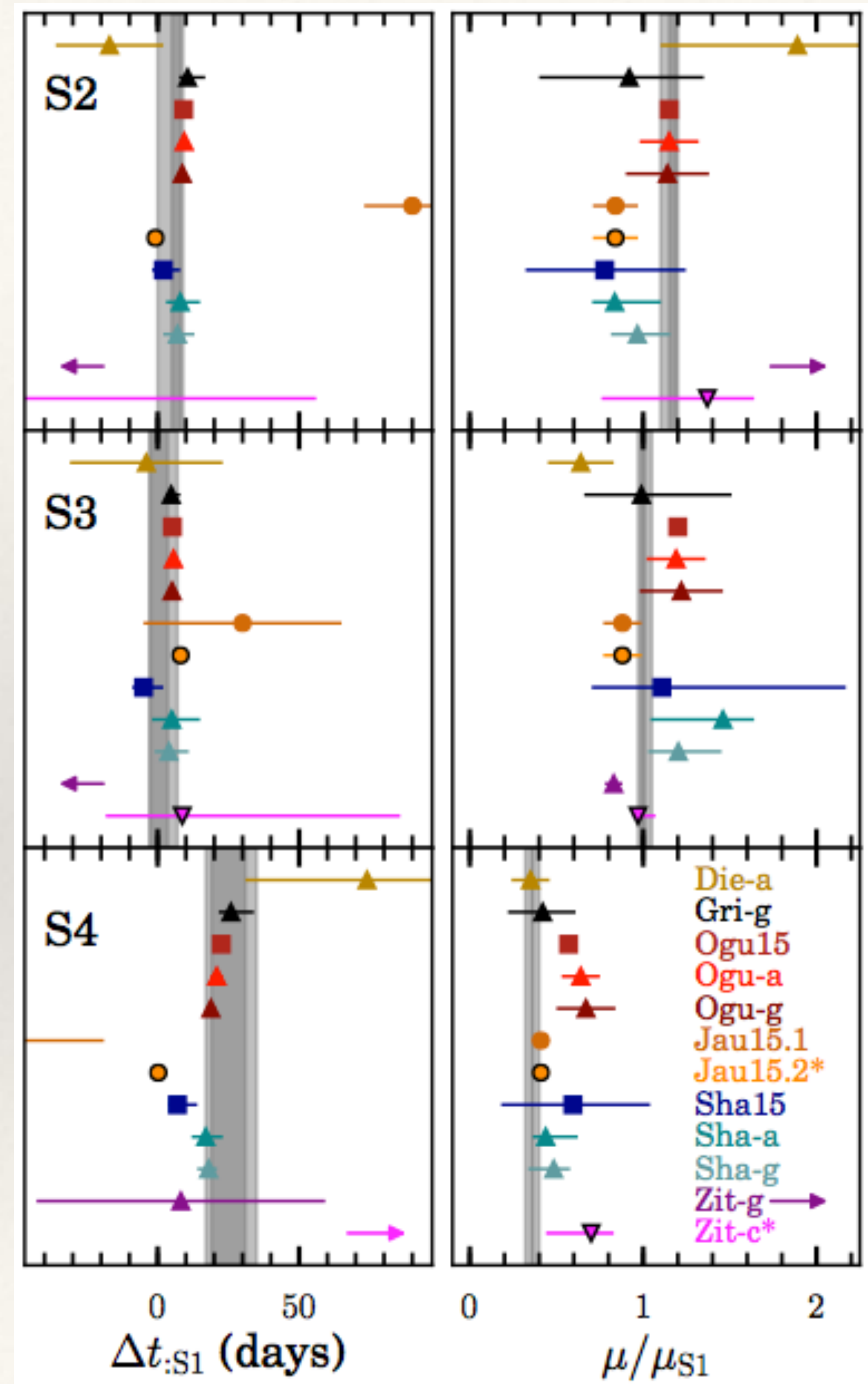

SN Refsdal's follow-up and true blind tests

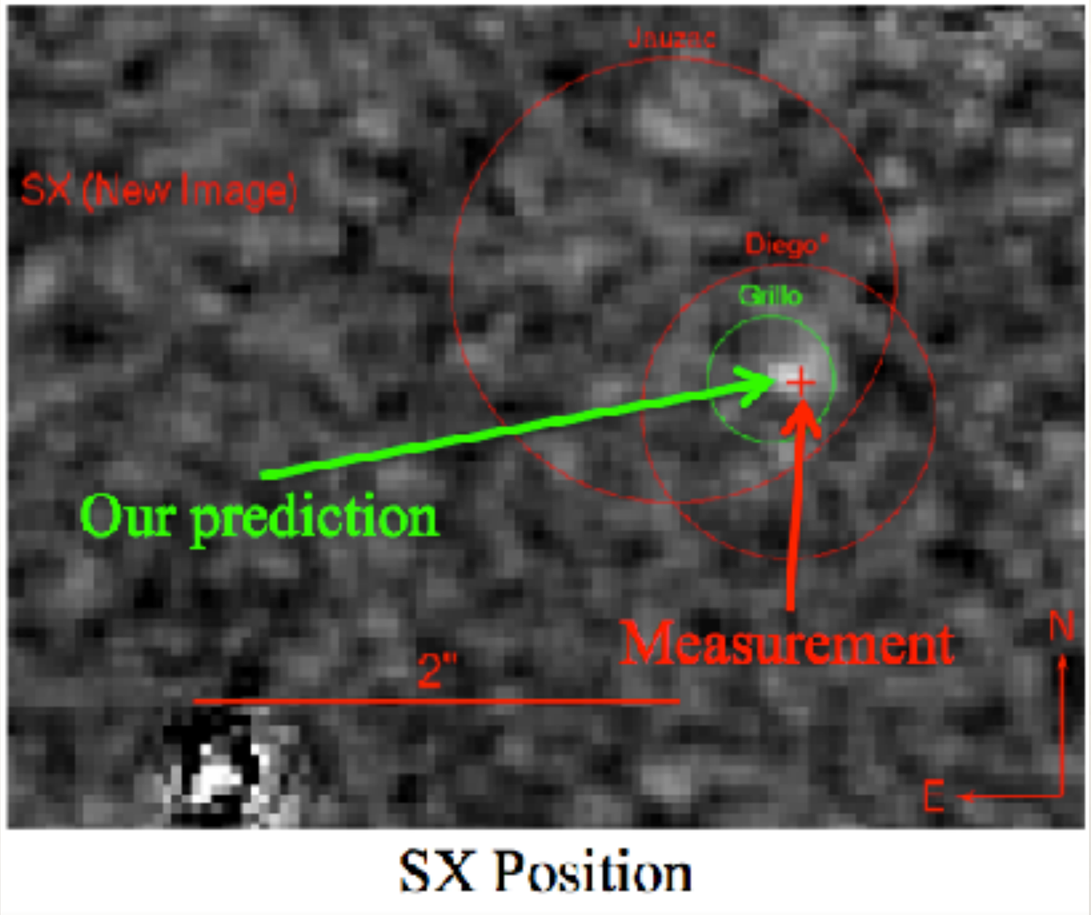

Grillo et al. (2016); Kelley et al. (2017)

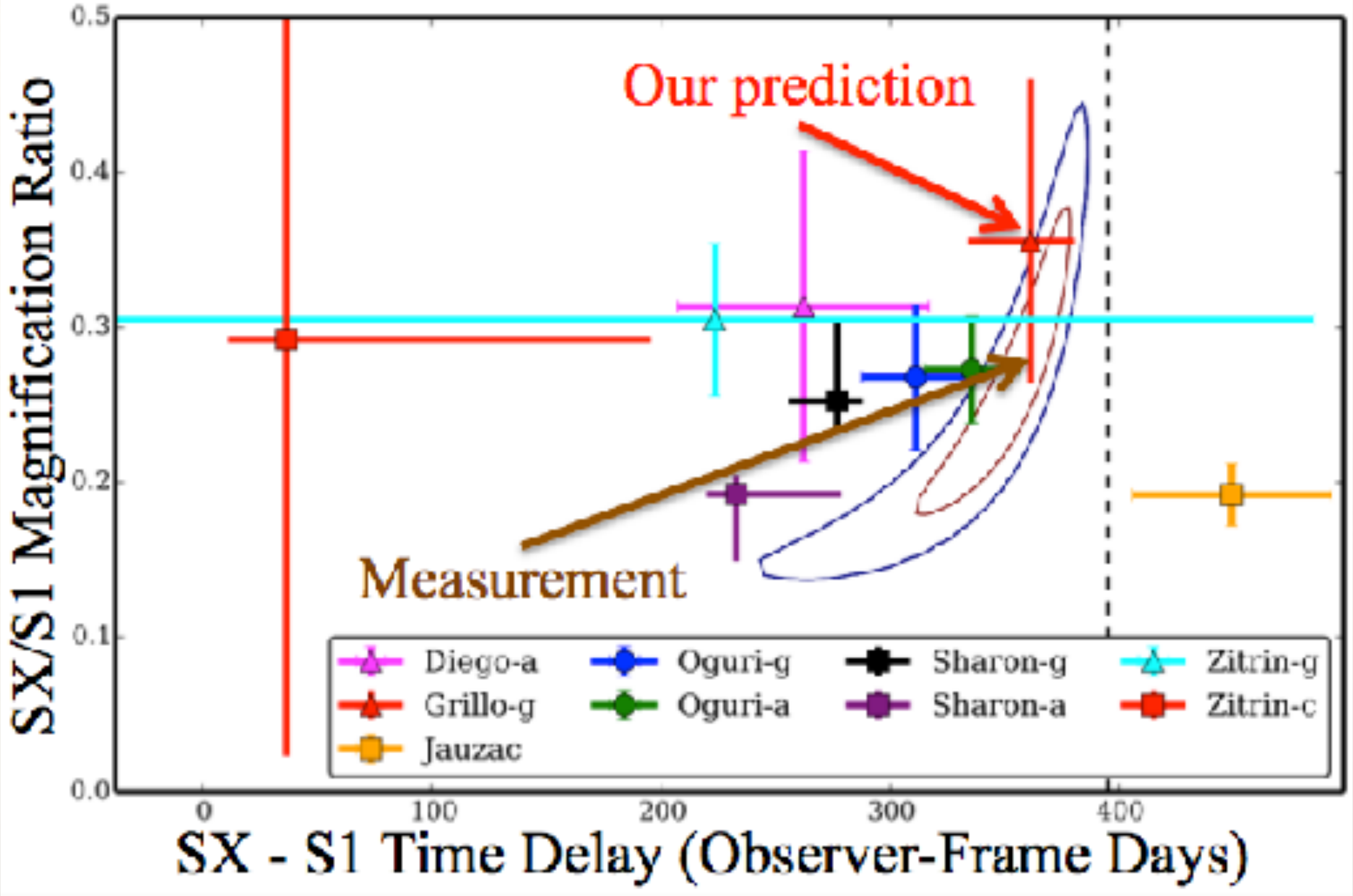

Treu et al. (2016)

- The appearance of a distant supernova at a specific sky position and time successfully predicted in advance!
- If our strong lensing models can provide accurate predictions, our cluster total mass (dark matter+baryons) mapping are likely to be very accurate!

The SN Refsdal host galaxy

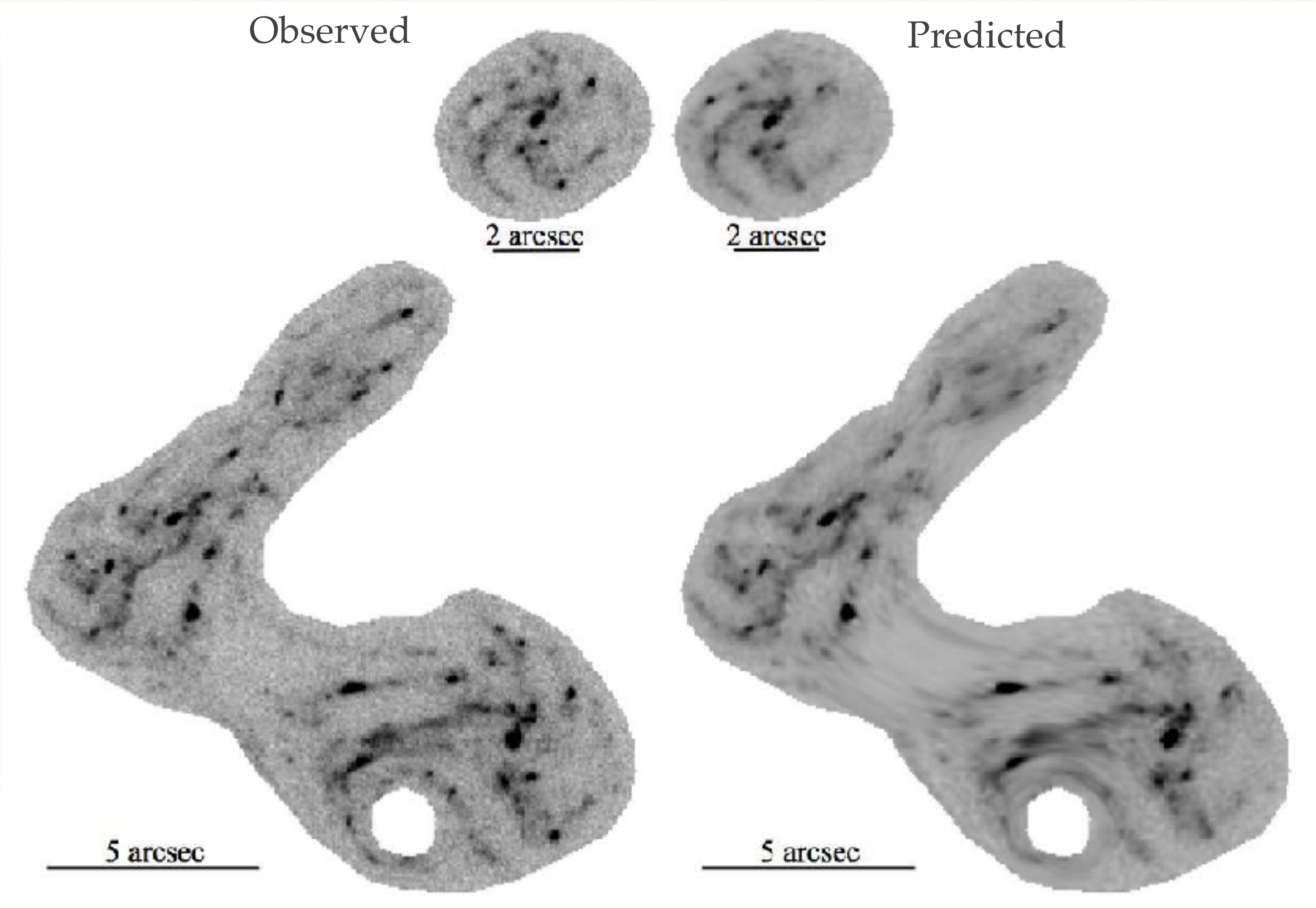

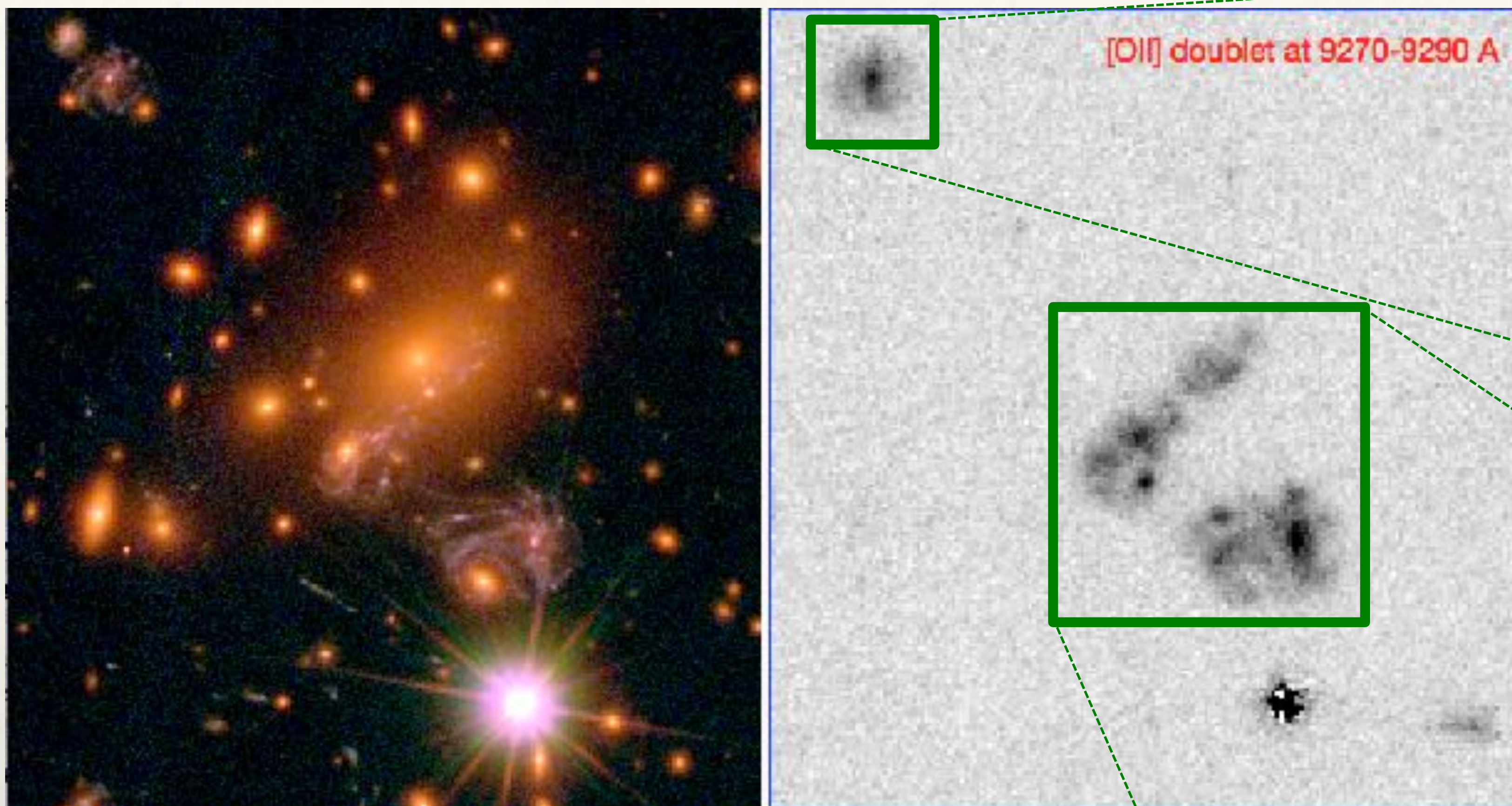

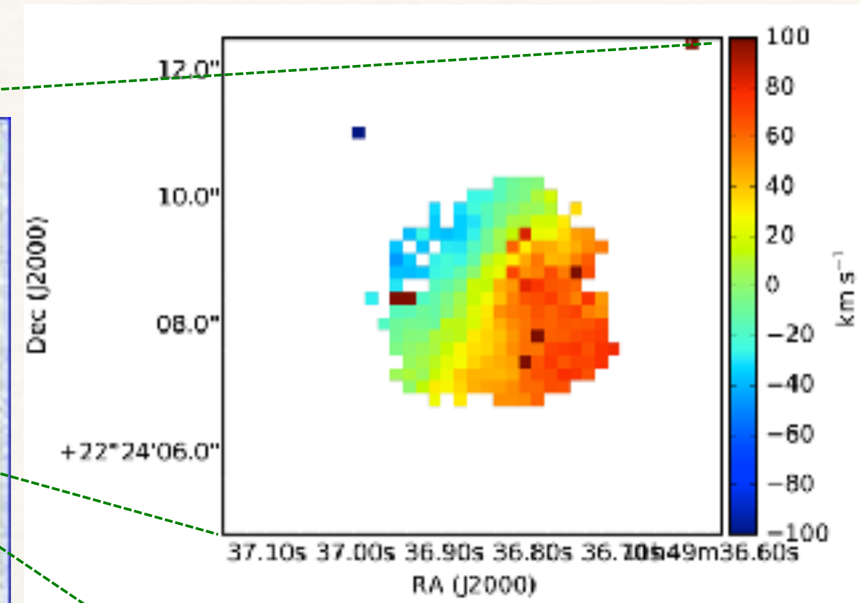

Di Teodoro et al. (2018)

- Strong [OII] emission at $z = 1.488$
- The [OII] velocity map shows a clear and symmetrical rotation pattern with peak values of ~100 km s^{-1}
- In principle the full MUSE cube could be used for the SL model!

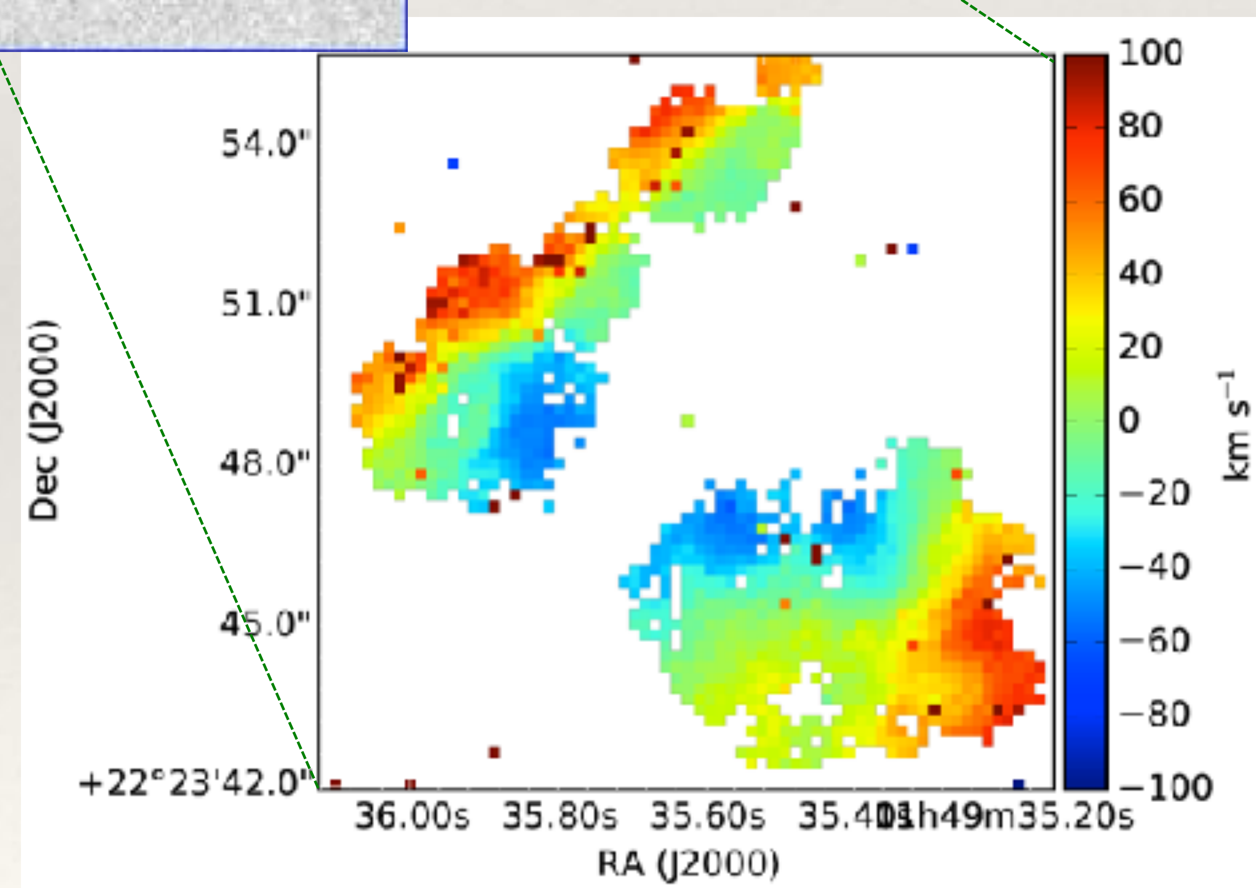

Measuring the Hubble constant

We include the S2-S4 and SX time-delay measurements in the modeling and optimize both the cluster mass distribution and the cosmological model

ID	$\Delta t_{S2:S1}$ [a] (days)	$\Delta t_{S3:S1}$ [a] (days)	$\Delta t_{S4:S1}$ [a] (days)	$\Delta t_{SX:S1}$ [b] (days)	χ^2_{pos}	χ^2_{td}	χ^2_{tot}	dof
Δt(t)	4 ± 4	2 ± 5	24 ± 7	345 ± 10	88.1	1.4	89.5	93
Δt(p)	7 ± 2	0.6 ± 3	27 ± 8	345 ± 10	88.9	1.2	90.1	93

ID	H_0	1σ	2σ	3σ
Δt(t)	73.5	$^{+4.6}_{-4.7}$	$^{+8.4}_{-8.8}$	$^{+12.4}_{-13.1}$
Δt(p)	72.8	$^{+4.3}_{-4.1}$	$^{+9.5}_{-8.0}$	$^{+14.1}_{-11.5}$

In a flat ΛCDM model, we can infer the value of H0 with a ~6% statistical error, **without any priors from other cosmological experiments**

Grillo et al. (2018)

Measuring the Hubble constant

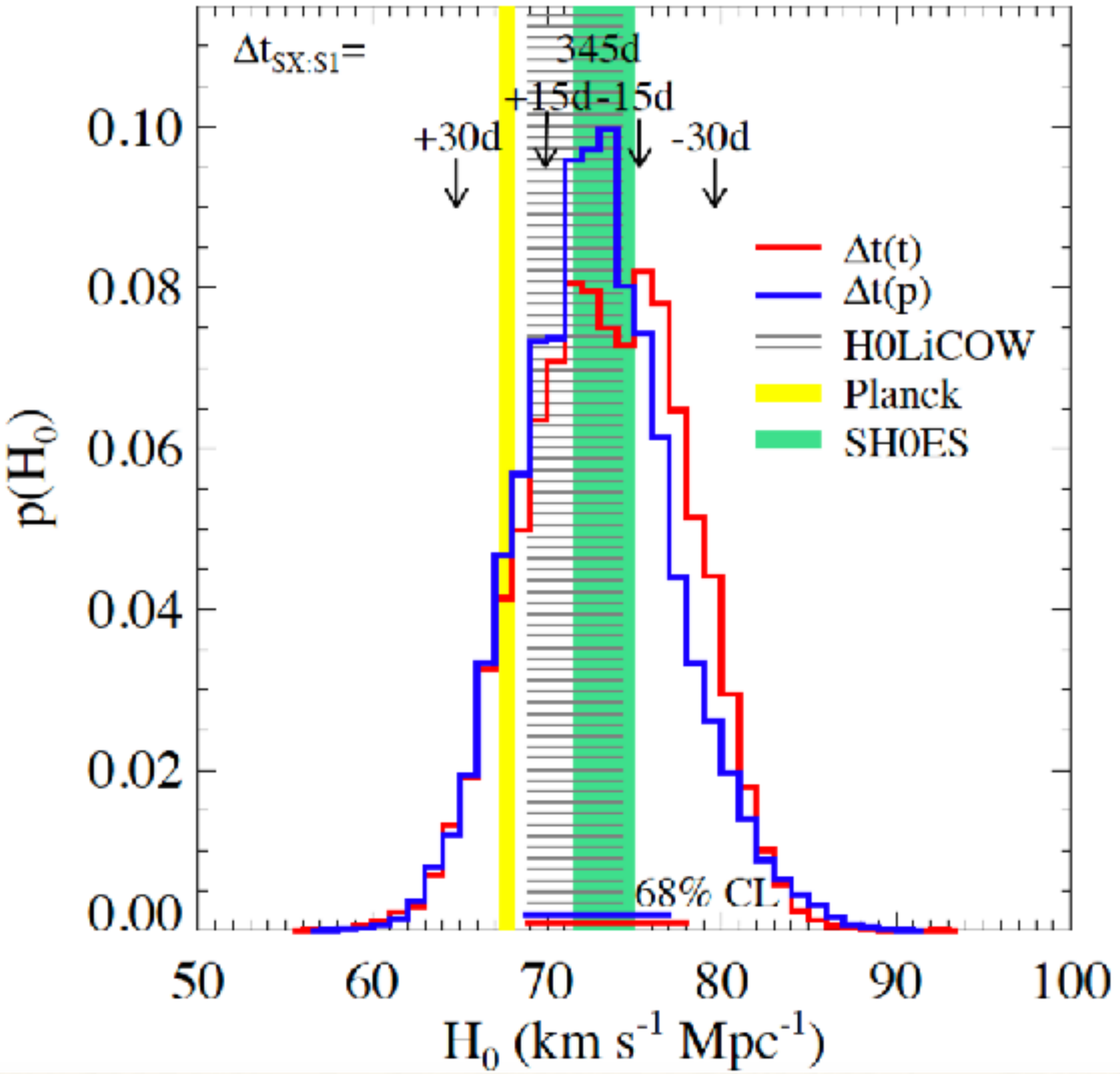

- Results complementary and potentially competitive to other techniques

Measuring the Hubble constant

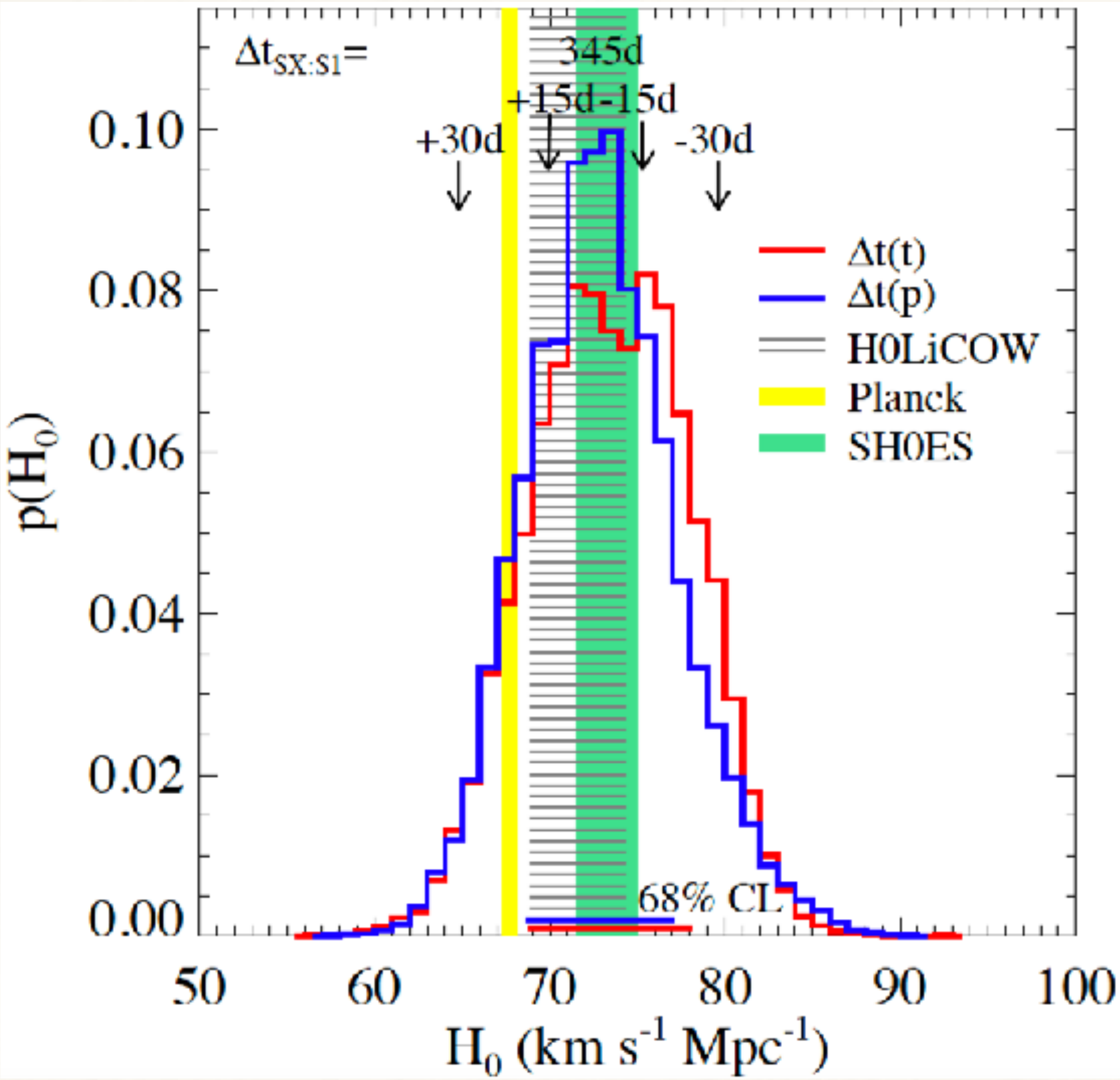

- Results complementary and potentially competitive to other techniques
- Shifts of ~4% (15d) or ~9% (30d) in the time-delay of SX translate into ~4% or ~9% differences in the estimate of H_0

Measuring the Hubble constant

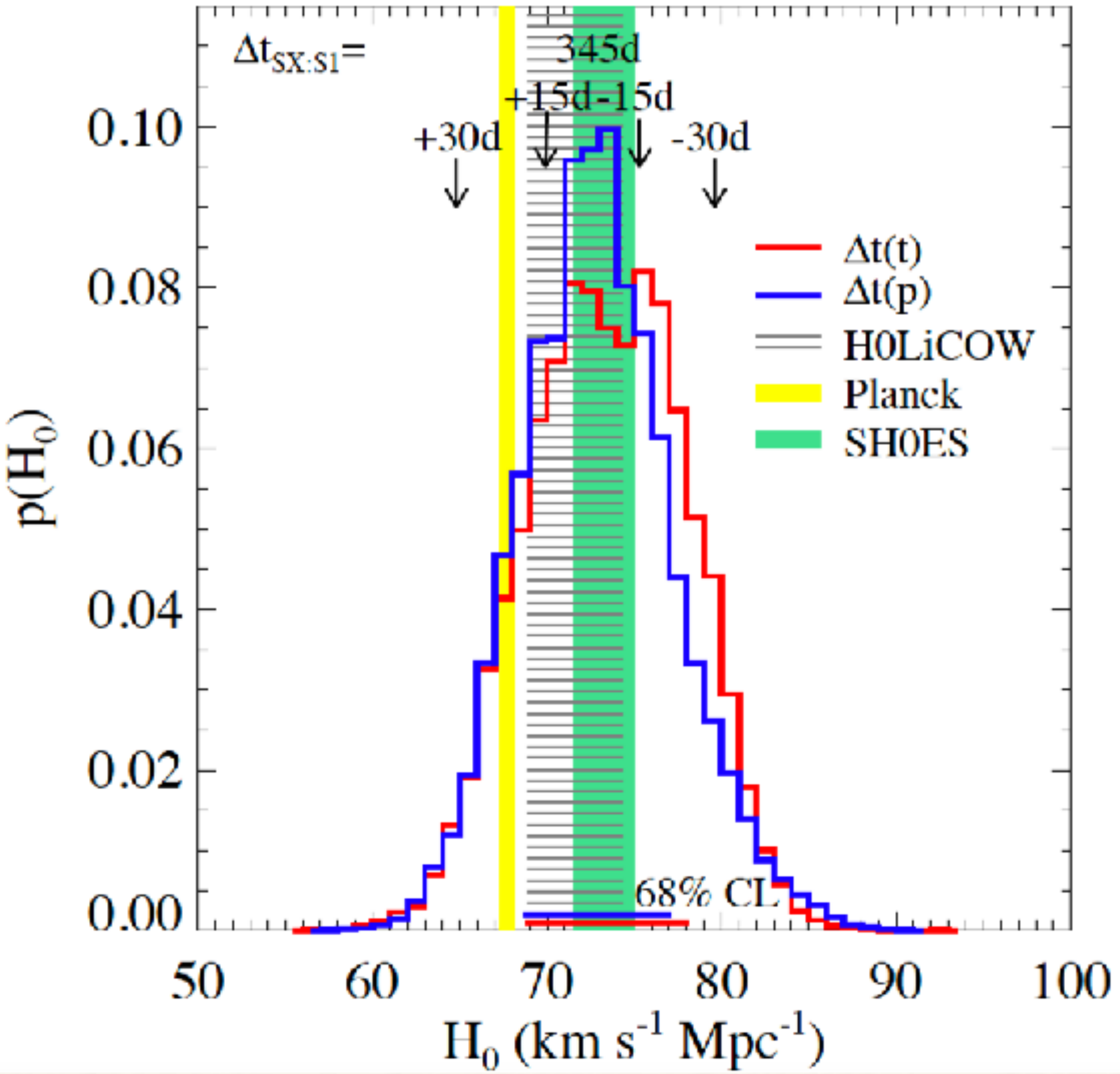

- Results complementary and potentially competitive to other techniques
- Shifts of ~4% (15d) or ~9% (30d) in the time-delay of SX translate into ~4% or ~9% differences in the estimate of H_0
- Reducing the error to ~2% or ~1% on the time-delay of SX decreases the error on the estimate of H_0 to ~5%

Measuring the cosmology

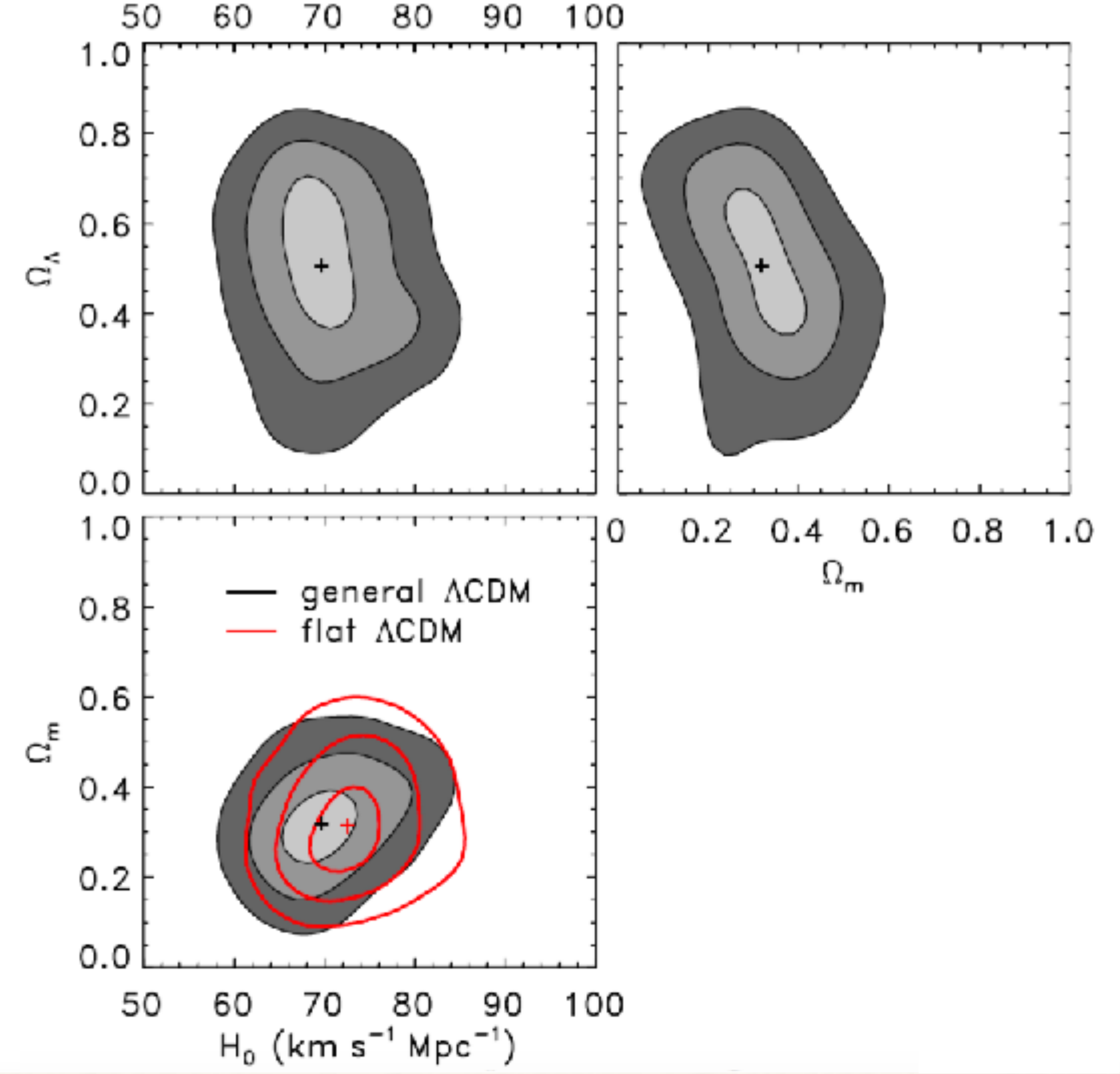

- In a flat ΛCDM model, H_0 and Ω_m can be measured with ~6% and ~31% statistical errors

Measuring the cosmology

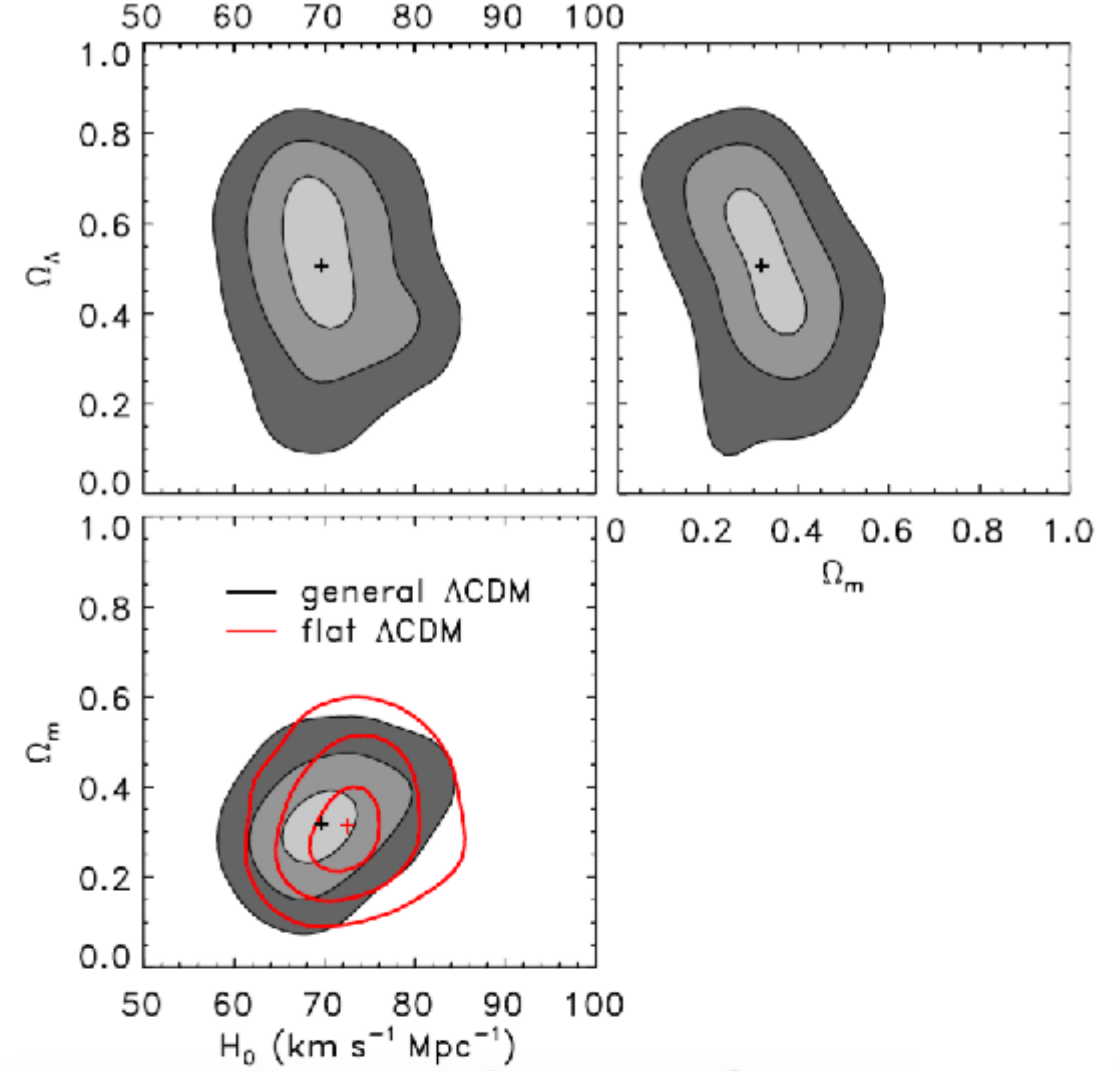

- In a flat ΛCDM model, H_0 and Ω_m can be measured with ~6% and ~31% statistical errors
- In a general ΛCDM model, H_0 and Ω_m can be measured with ~7% and ~26% statistical errors

Measuring the cosmology

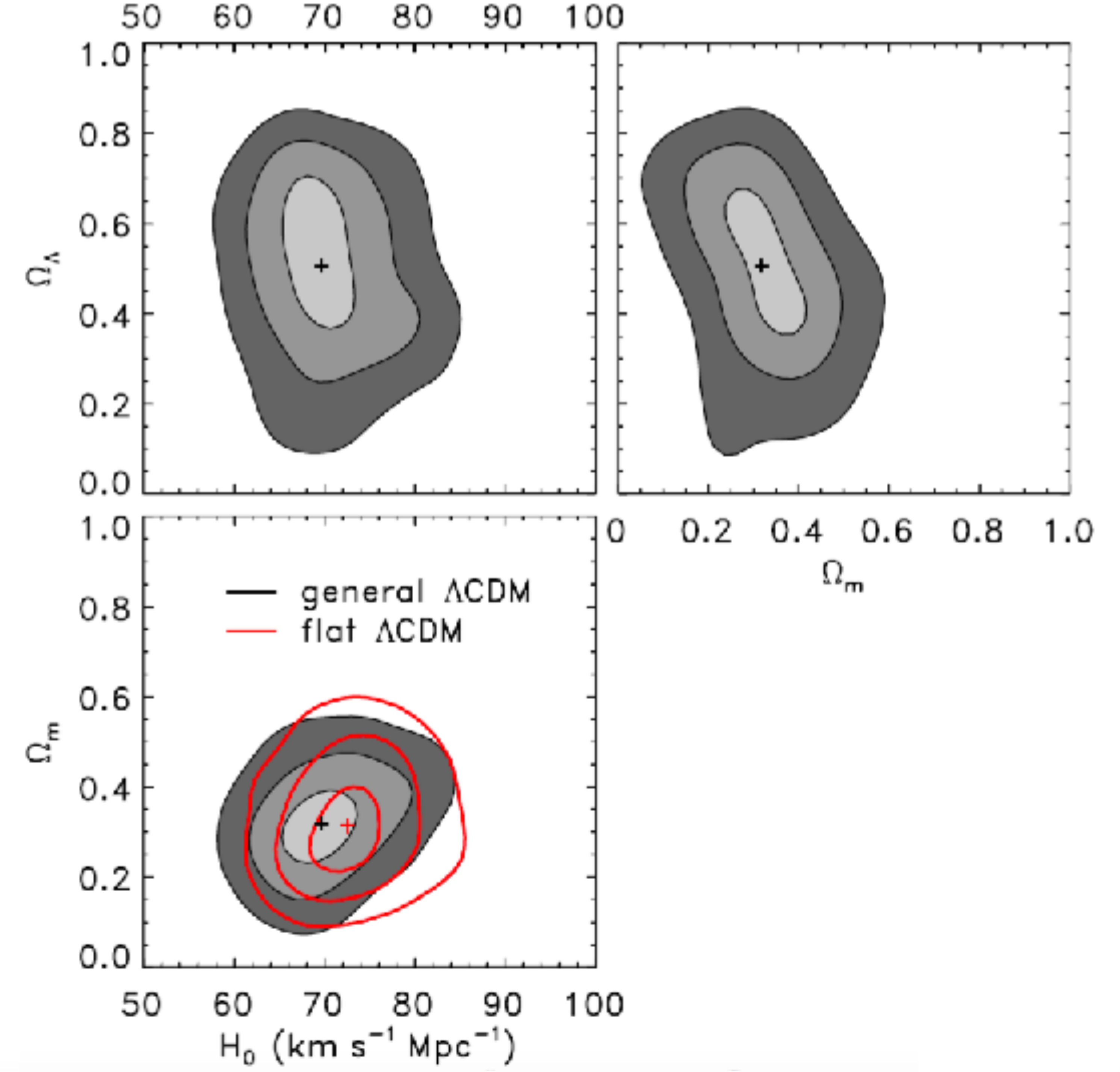

- In a flat ΛCDM model, H_0 and Ω_m can be measured with ~6% and ~31% statistical errors
- In a general ΛCDM model, H_0 and Ω_m can be measured with ~7% and ~26% statistical errors
- Time delays in lens galaxy clusters can become an important alternative tool for measuring the expansion rate and the geometry of the Universe

The HFF and MUSE

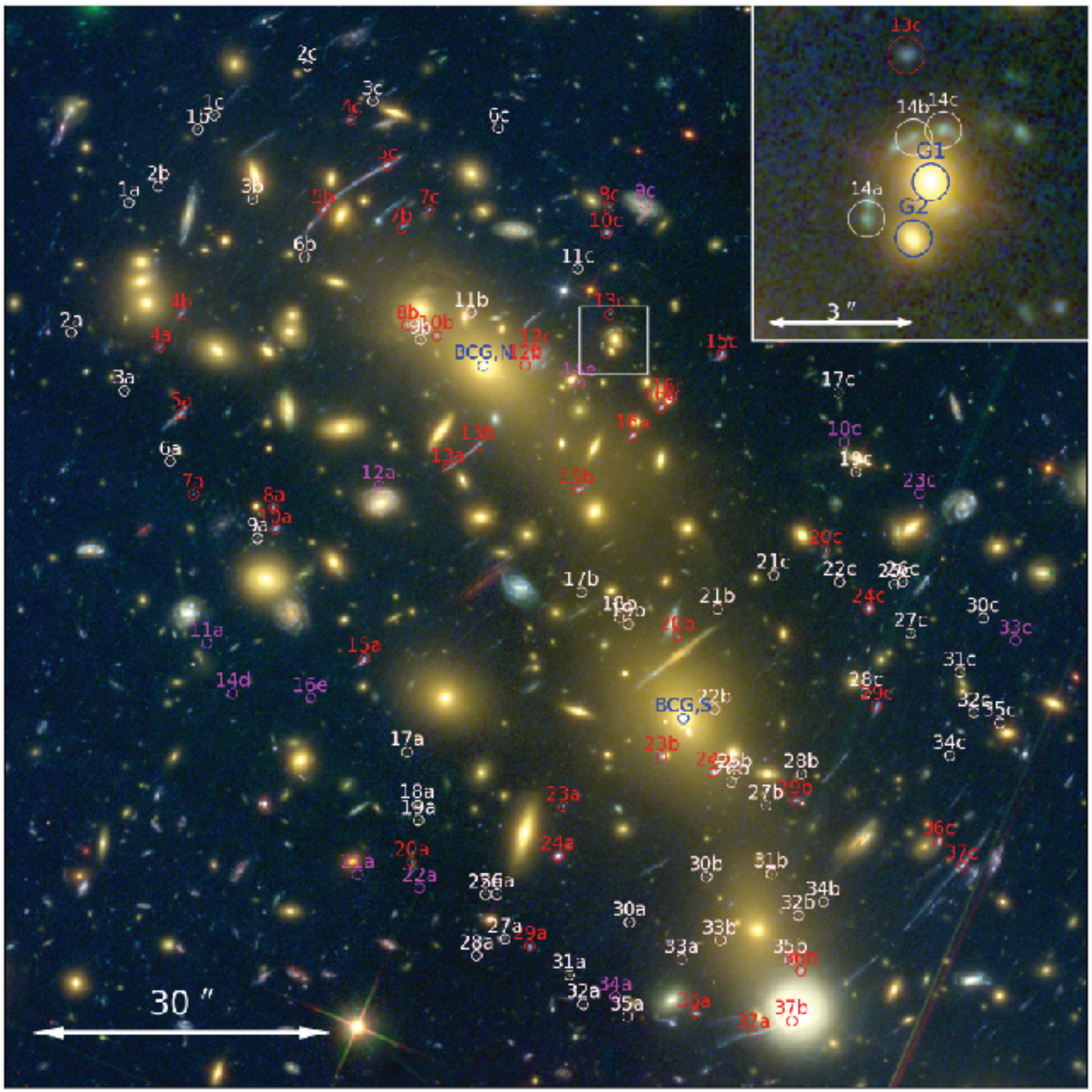

MACS 0416

- 2 MUSE pointings
- 22 new multiply lensed sources
- *z* between 3.077 and 6.145
- most of them are low-luminosity Ly-*α* emitters

Caminha et al. (2017)

The HFF and MUSE

Caminha et al. (2017)

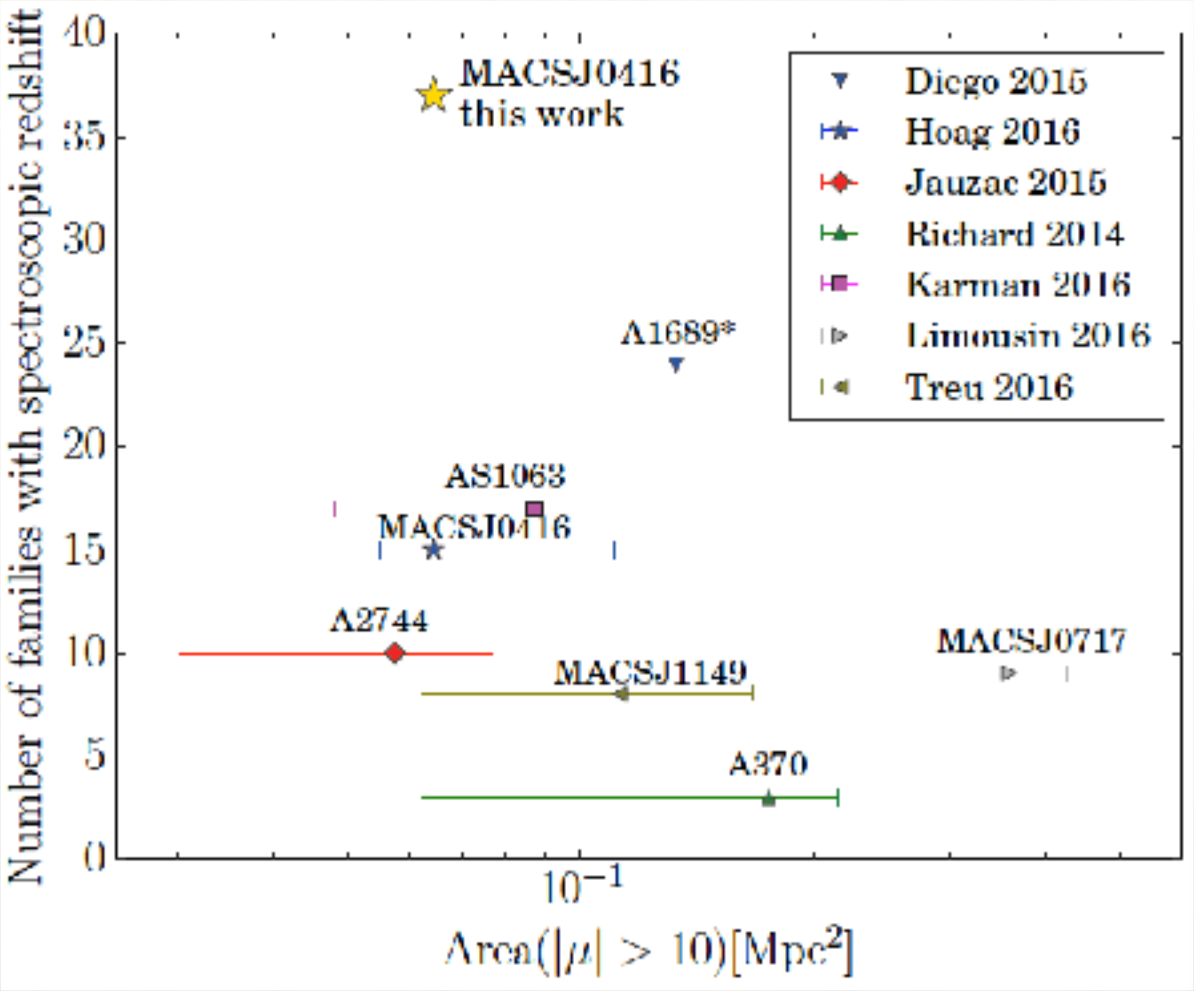

MACS 0416

- 102 secure multiple images
- 37 systems with measured redshifts
- largest sample of strong lensing families to date

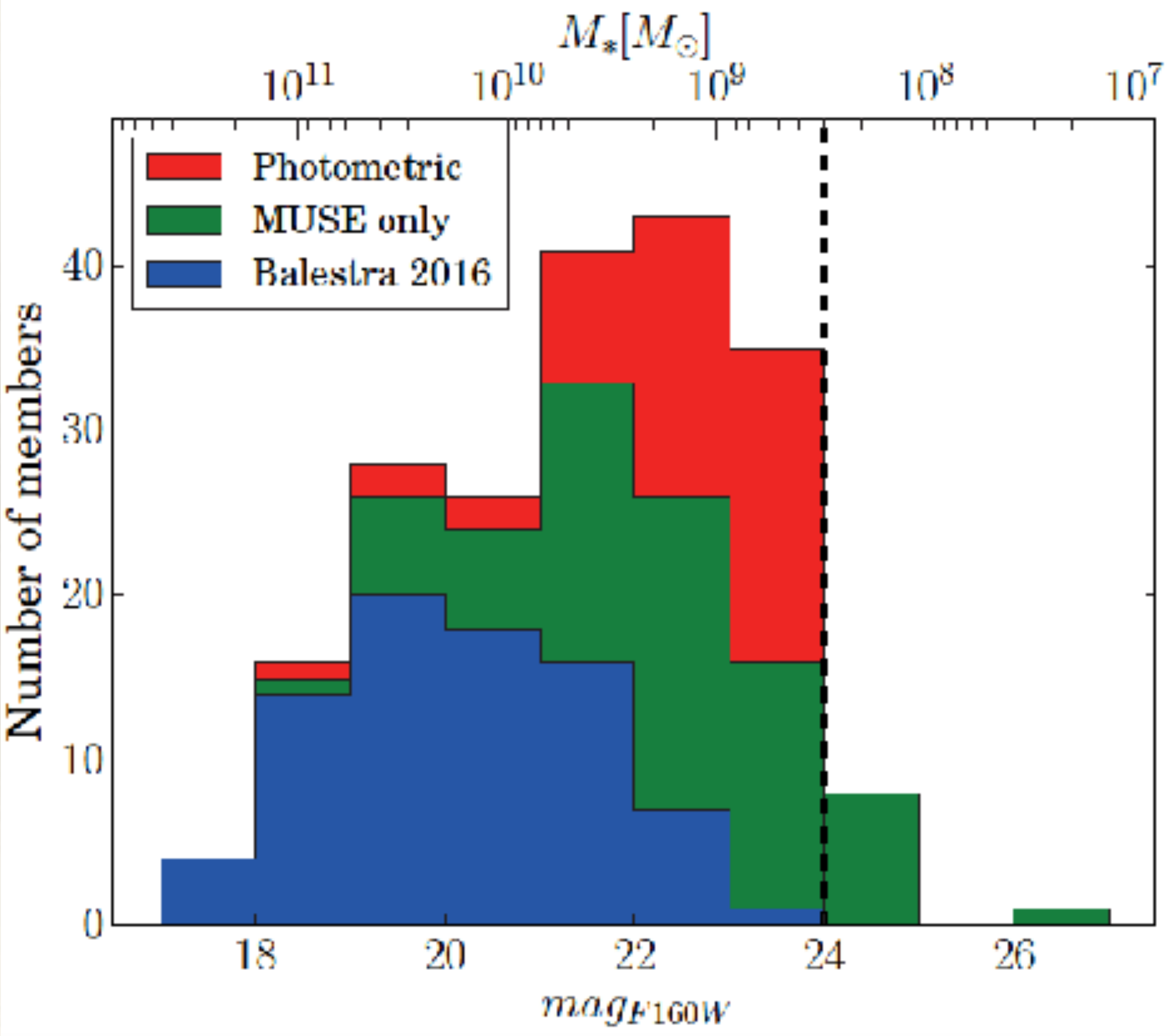

- 144 spec. member galaxies down to F160W 24 mag ($M_\star \sim 3\times10^8\ M_\odot$)
- Accurate determination of the projected total mass distribution
- Cored isothermal dark-matter haloes found

The strong lensing models

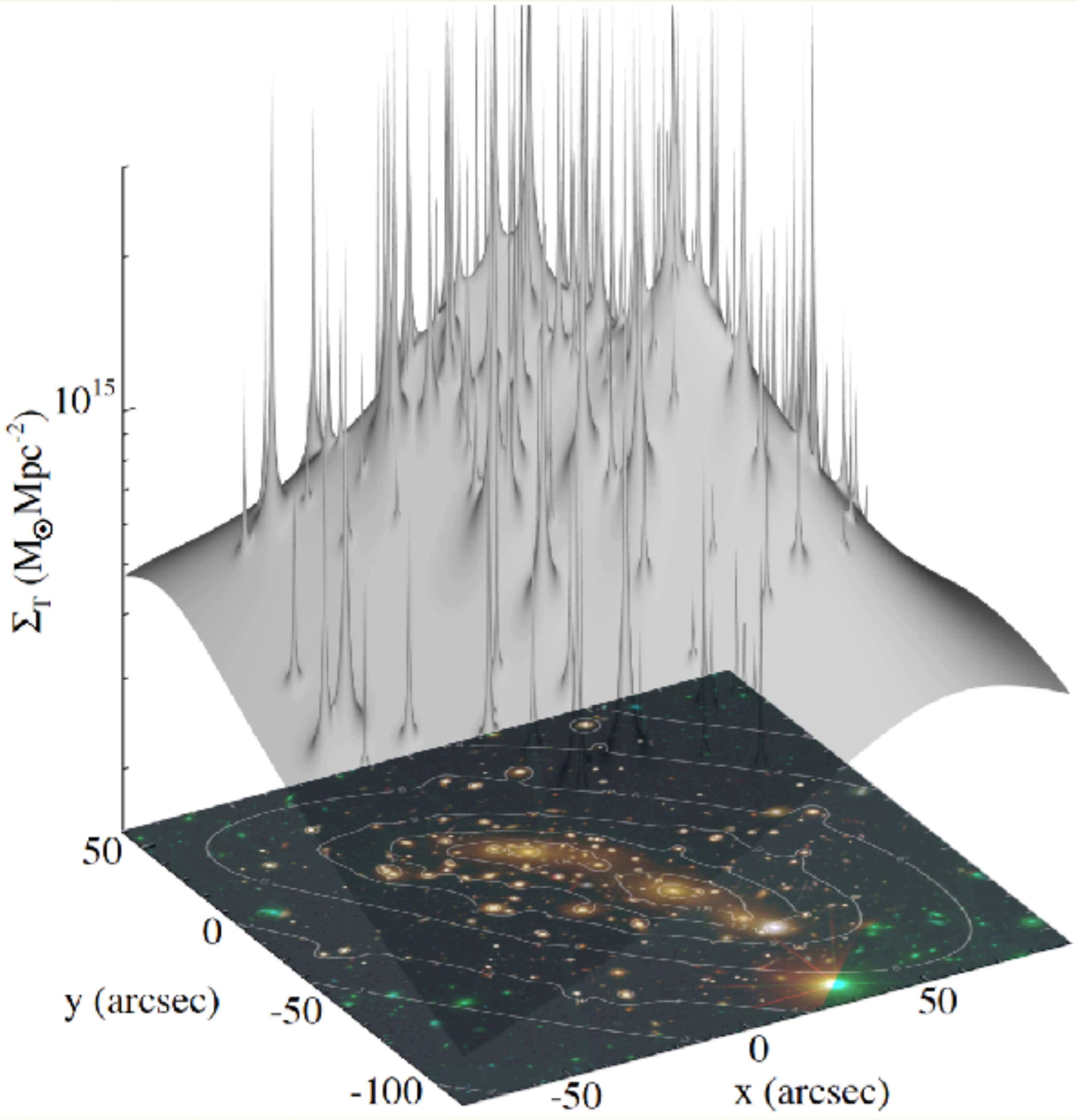

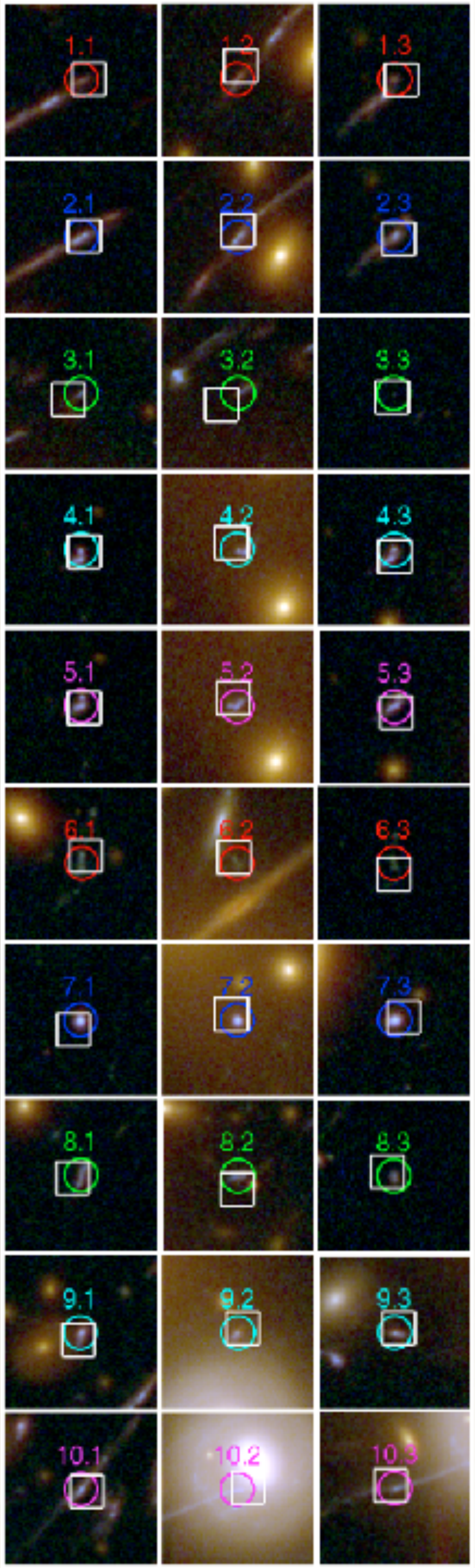

Grillo et al. (2015)

The strong lensing models

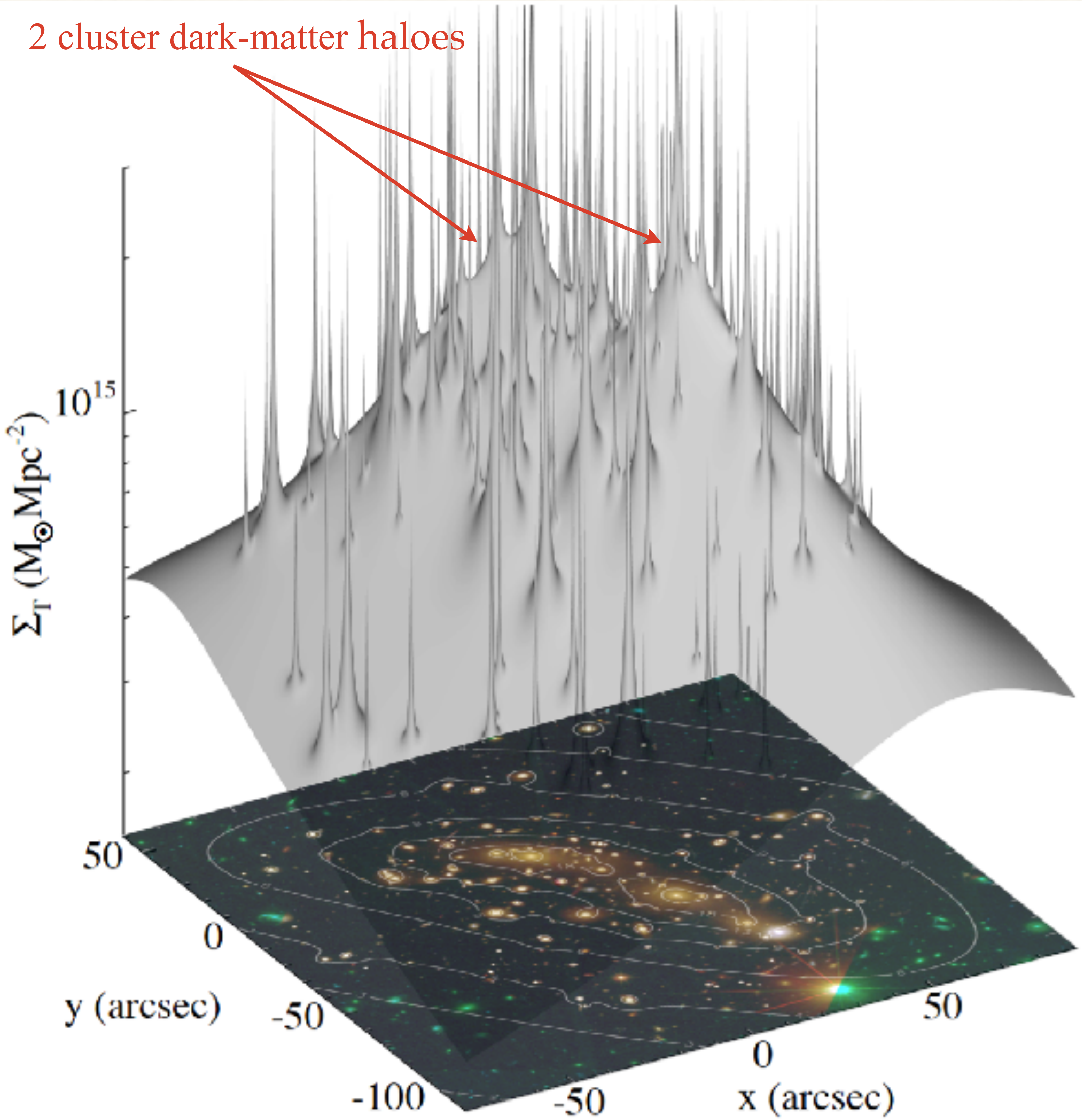

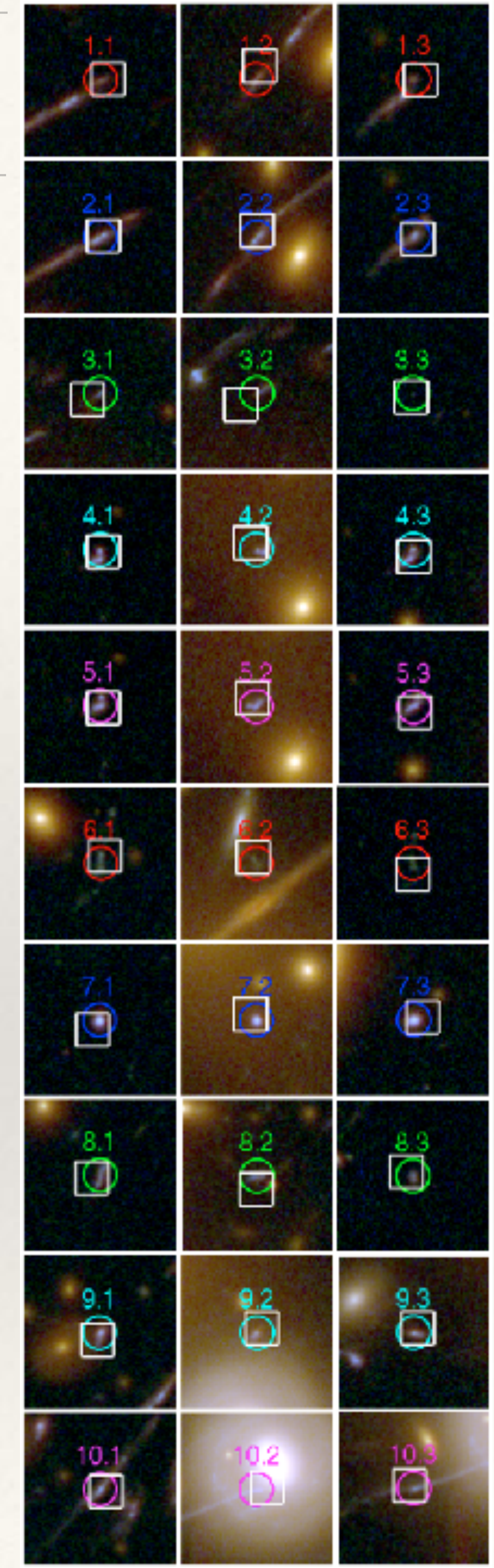

Grillo et al. (2015)

The strong lensing models

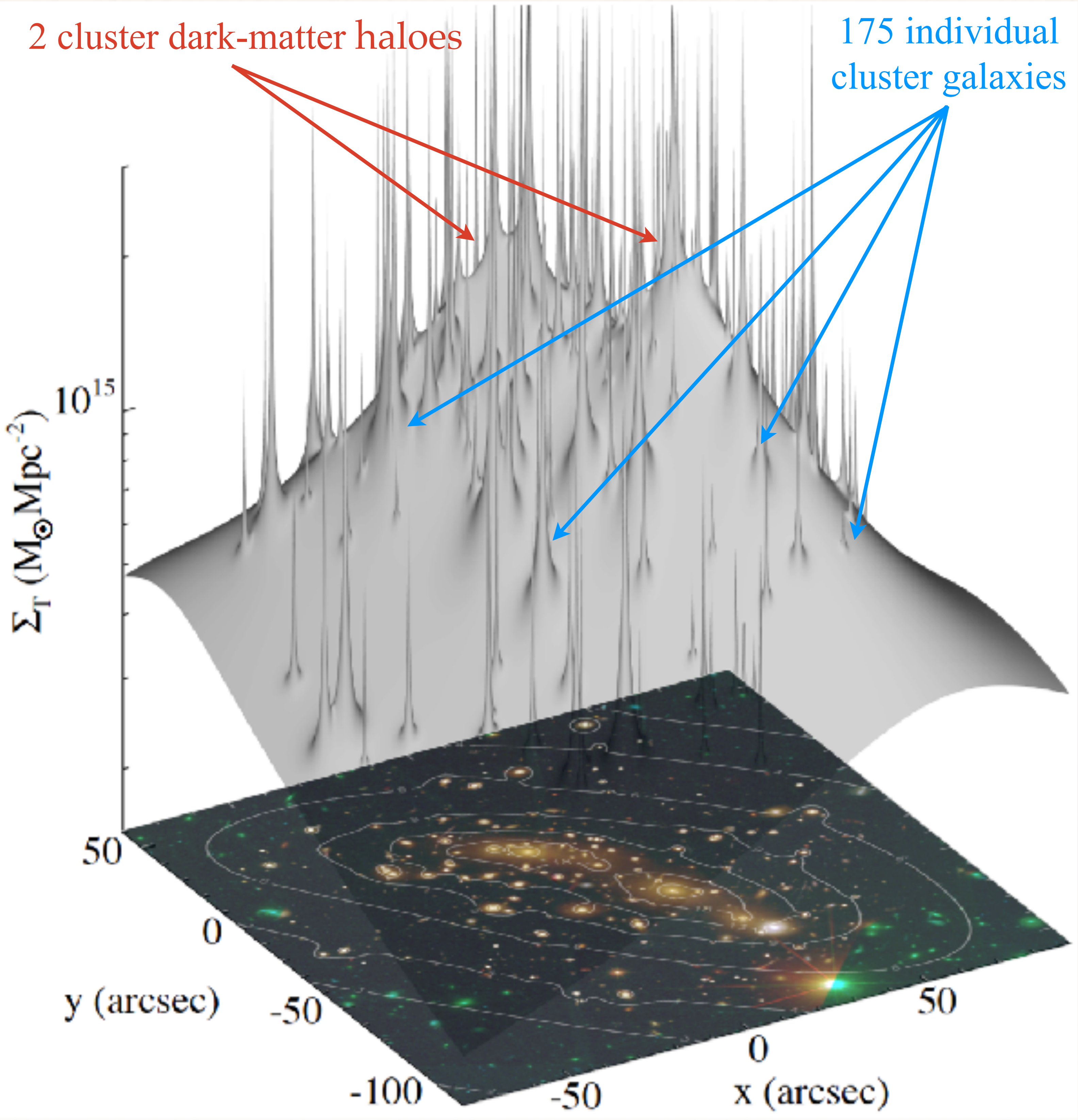

Grillo et al. (2015)

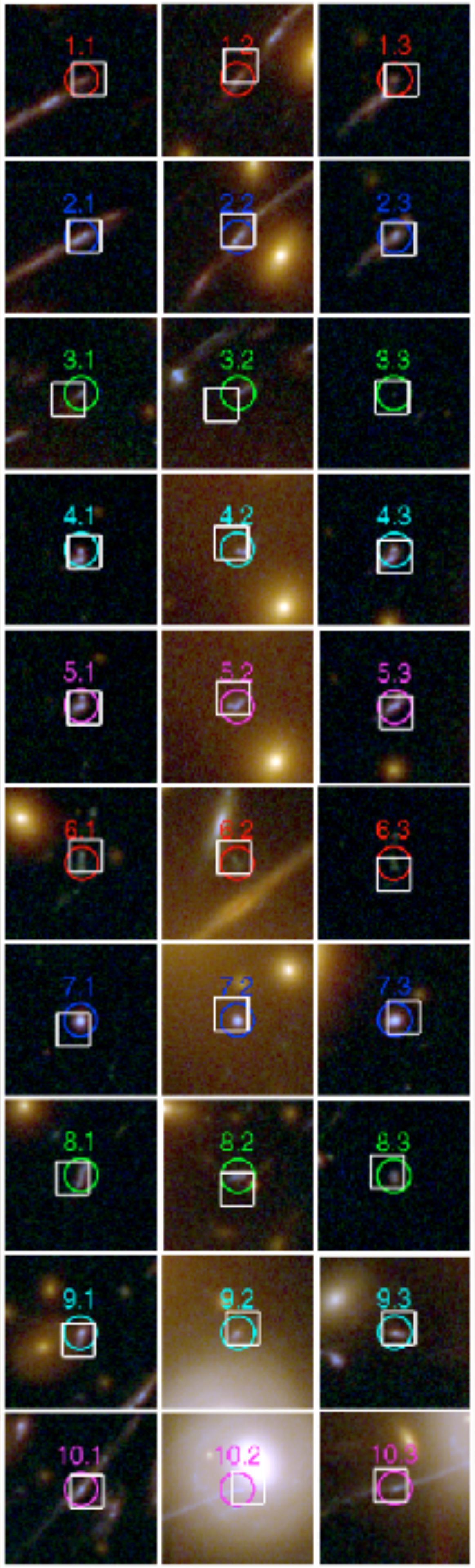

The galaxy cluster subhalo population

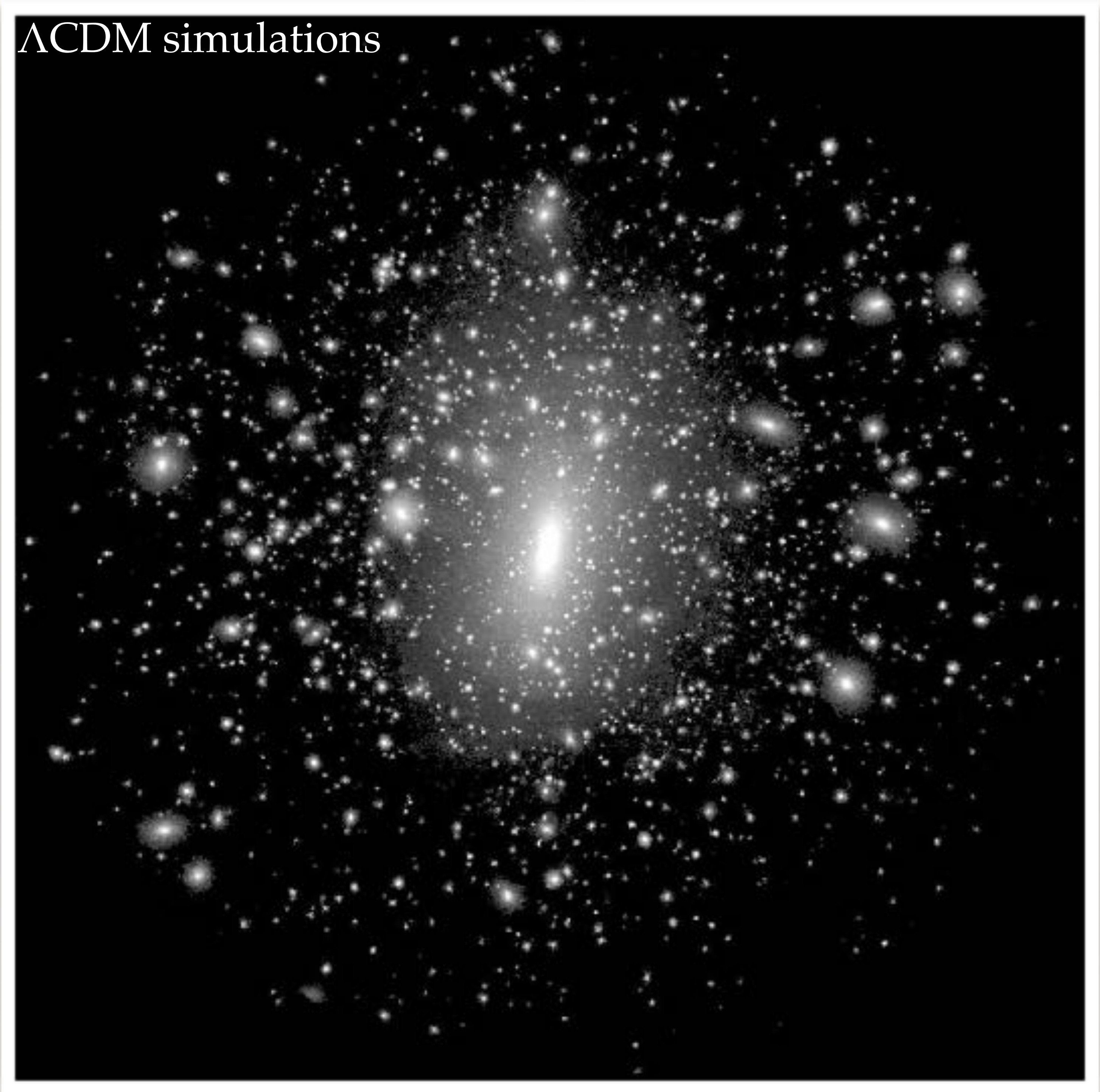

DM from high-resolution simulations, virial radius 1.7 Mpc
(Diemand et al. 2005)

The galaxy cluster subhalo population

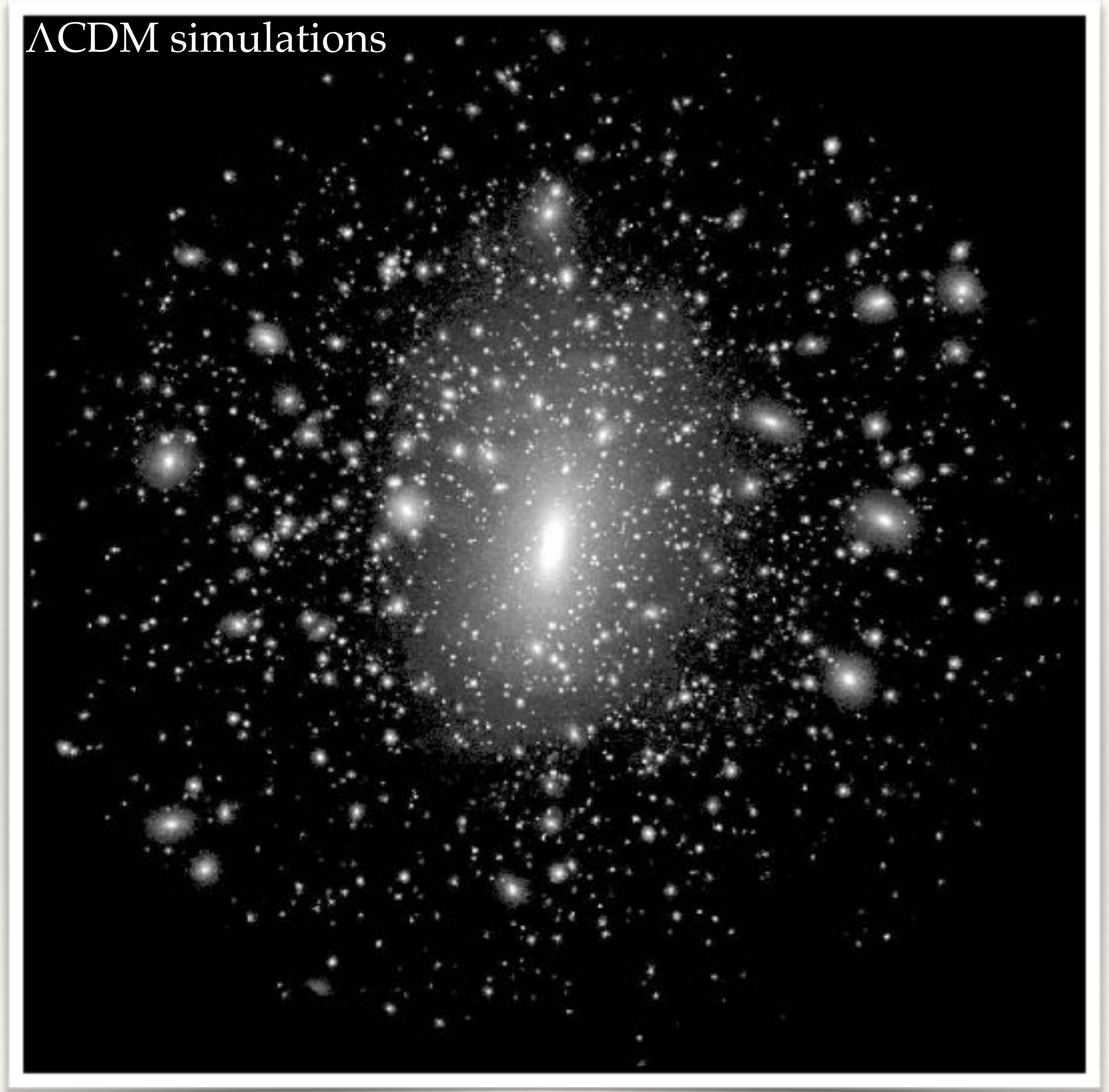

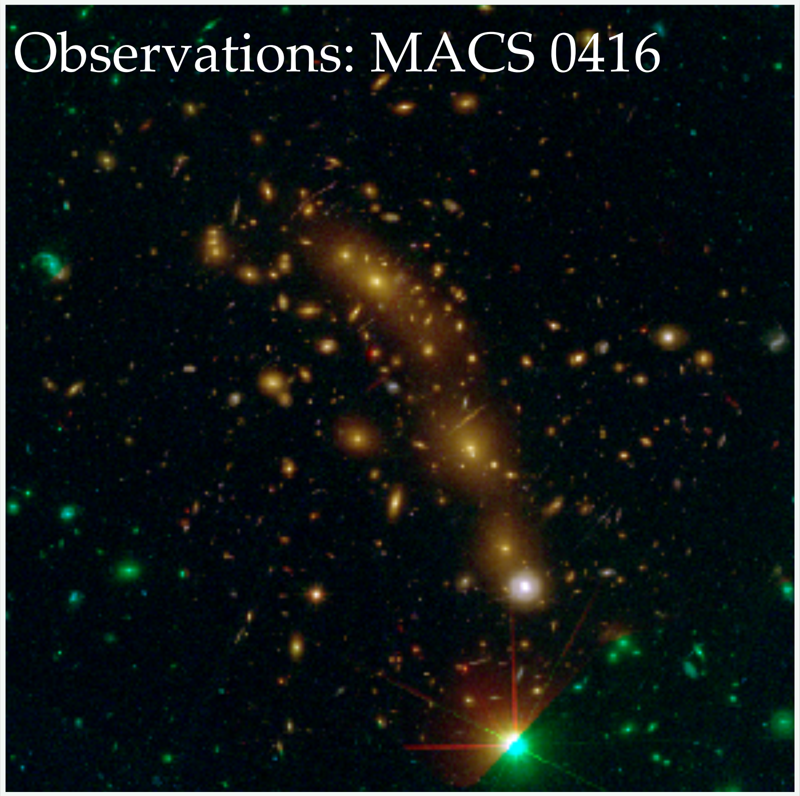

DM from high-resolution simulations, virial radius 1.7 Mpc (Diemand et al. 2005)

The galaxy cluster subhalo population

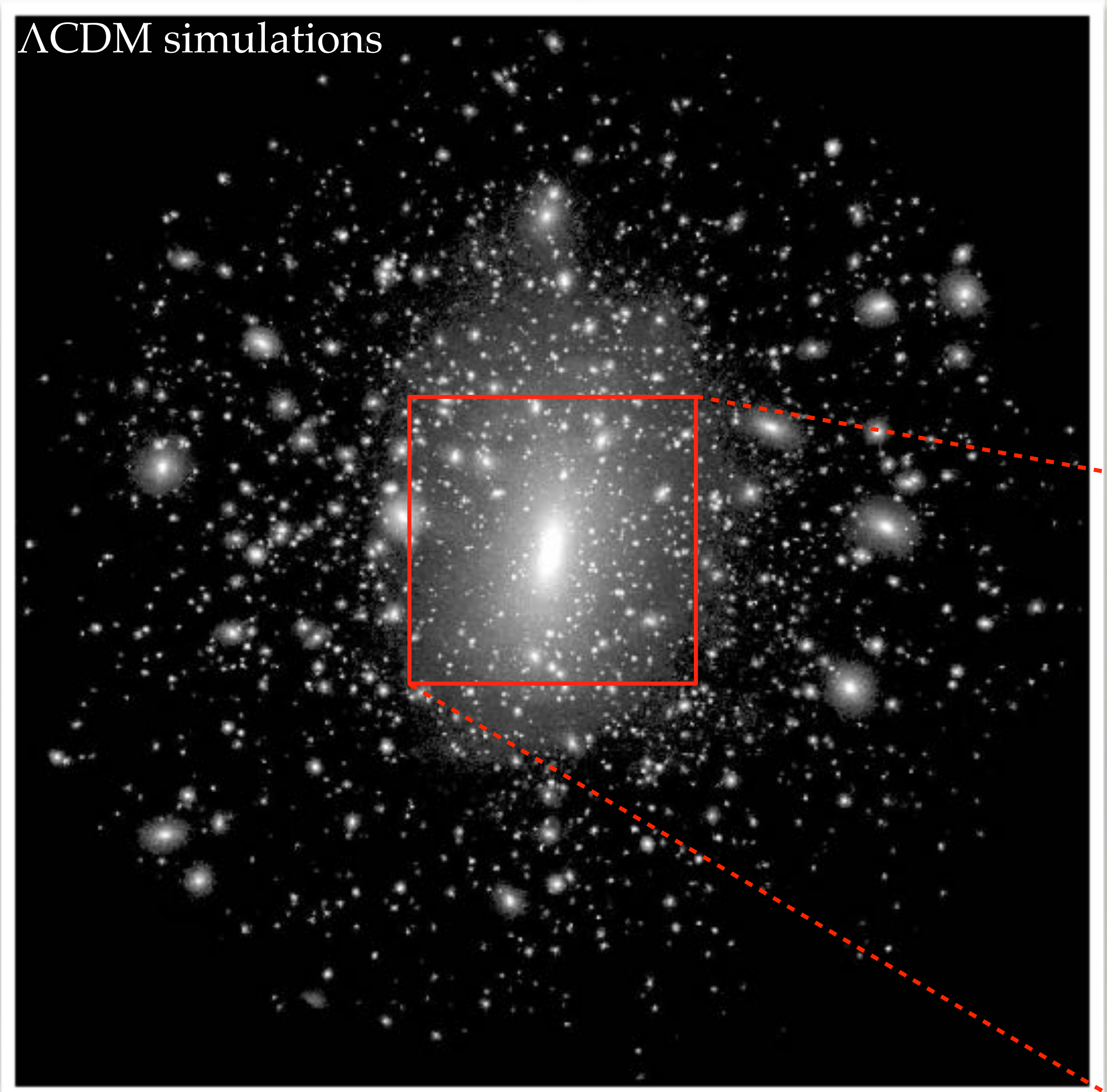

DM from high-resolution simulations, virial radius 1.7 Mpc
(Diemand et al. 2005)

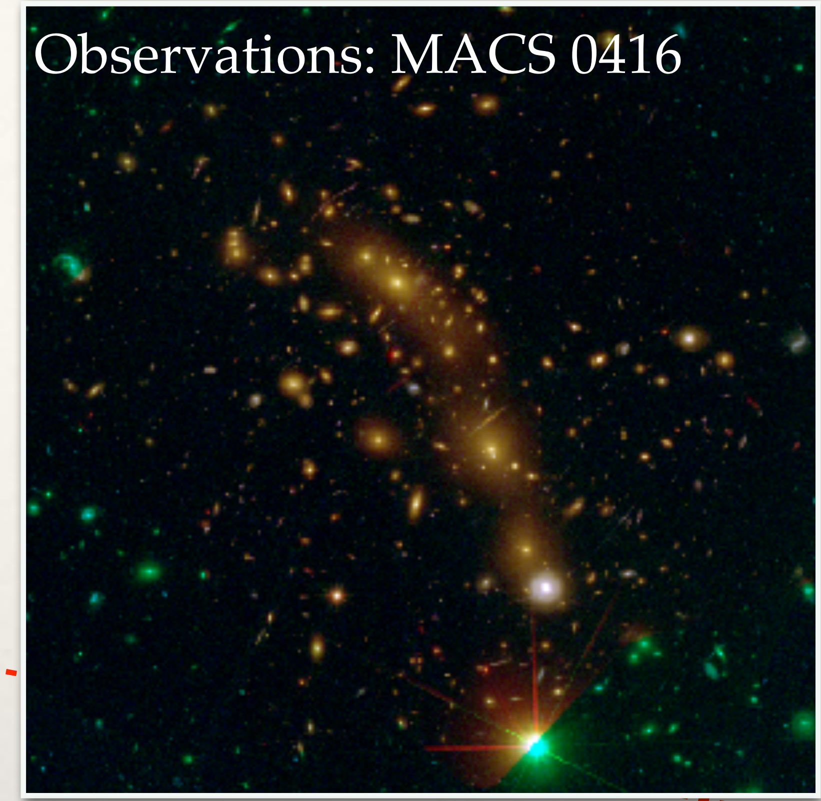

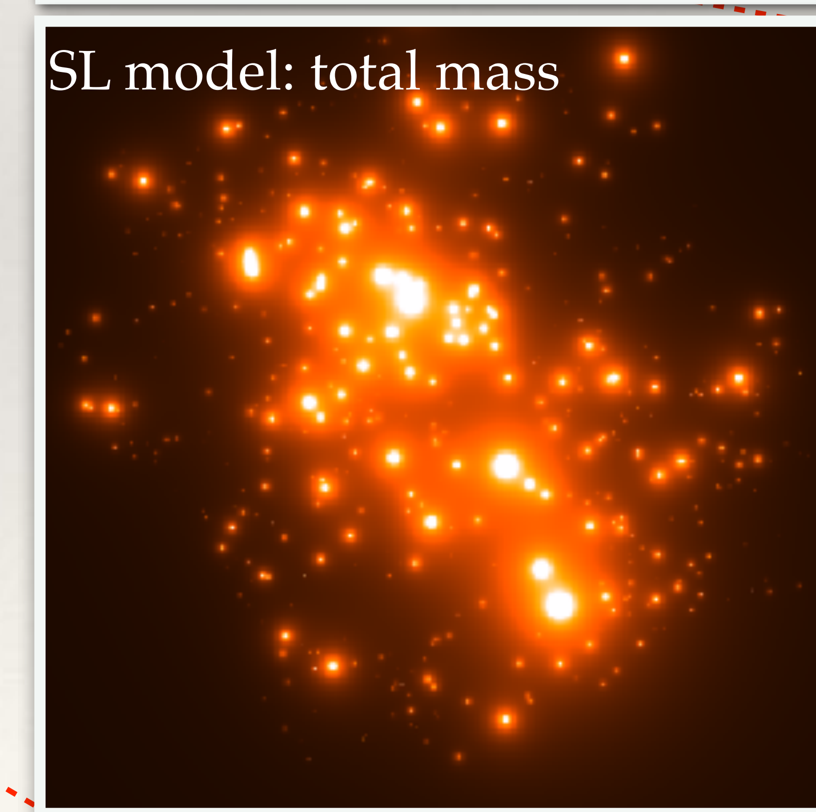

Grillo et al. (2015)

The galaxy cluster subhalo population

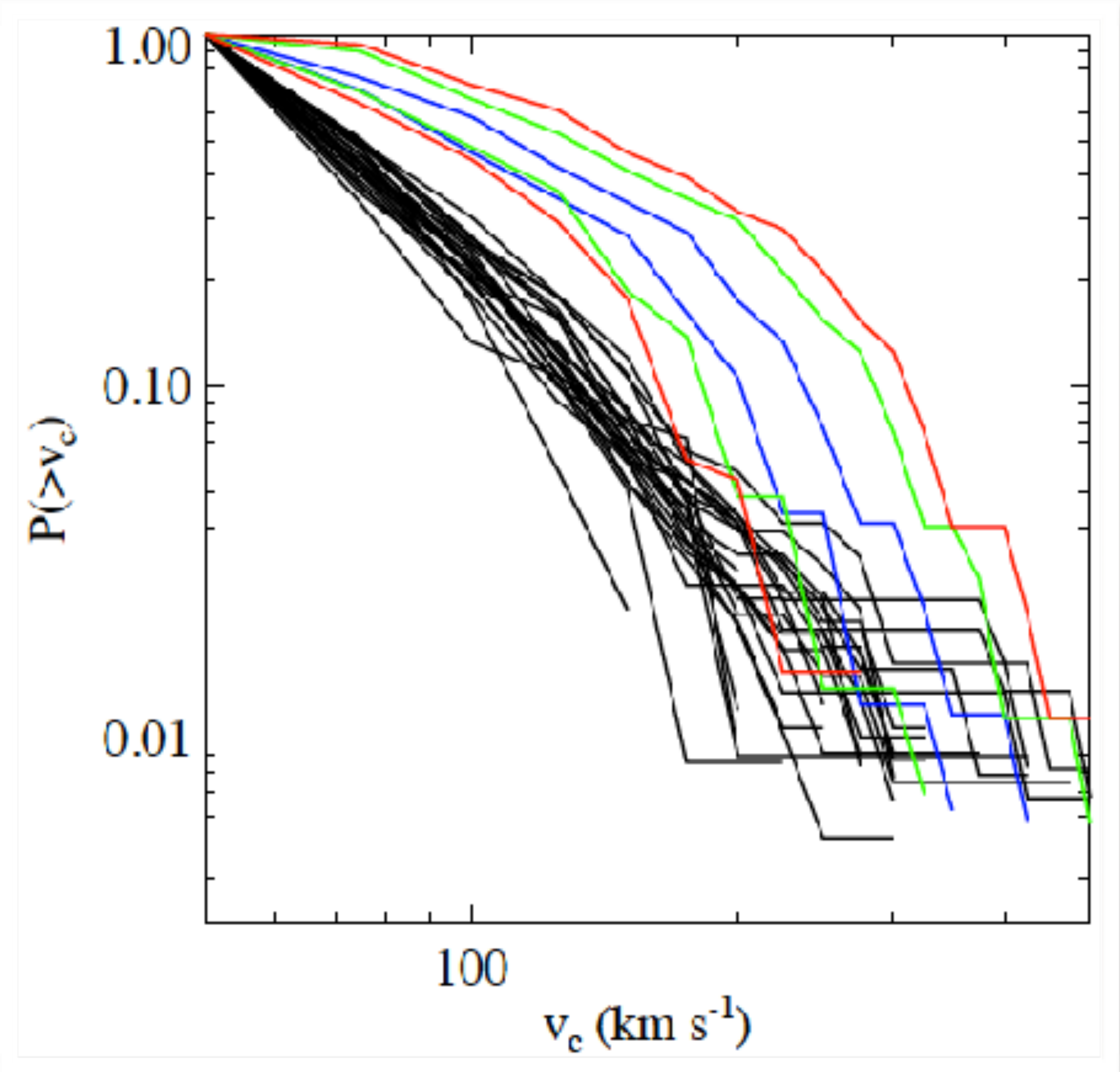

The velocity function of substructure in MACS 0416 from strong lensing at 1σ, 2σ, and 3σ.

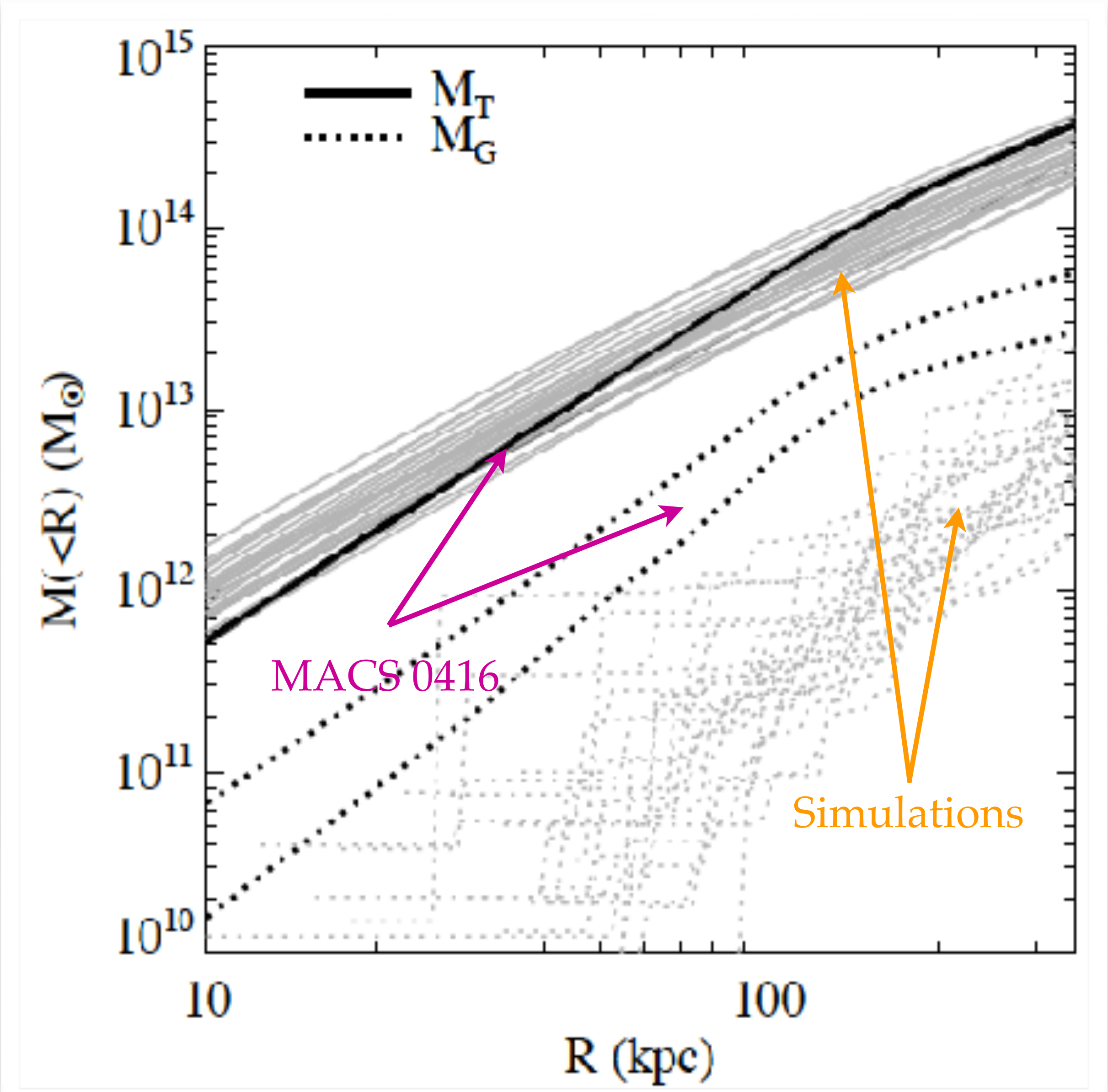

The galaxy cluster subhalo population

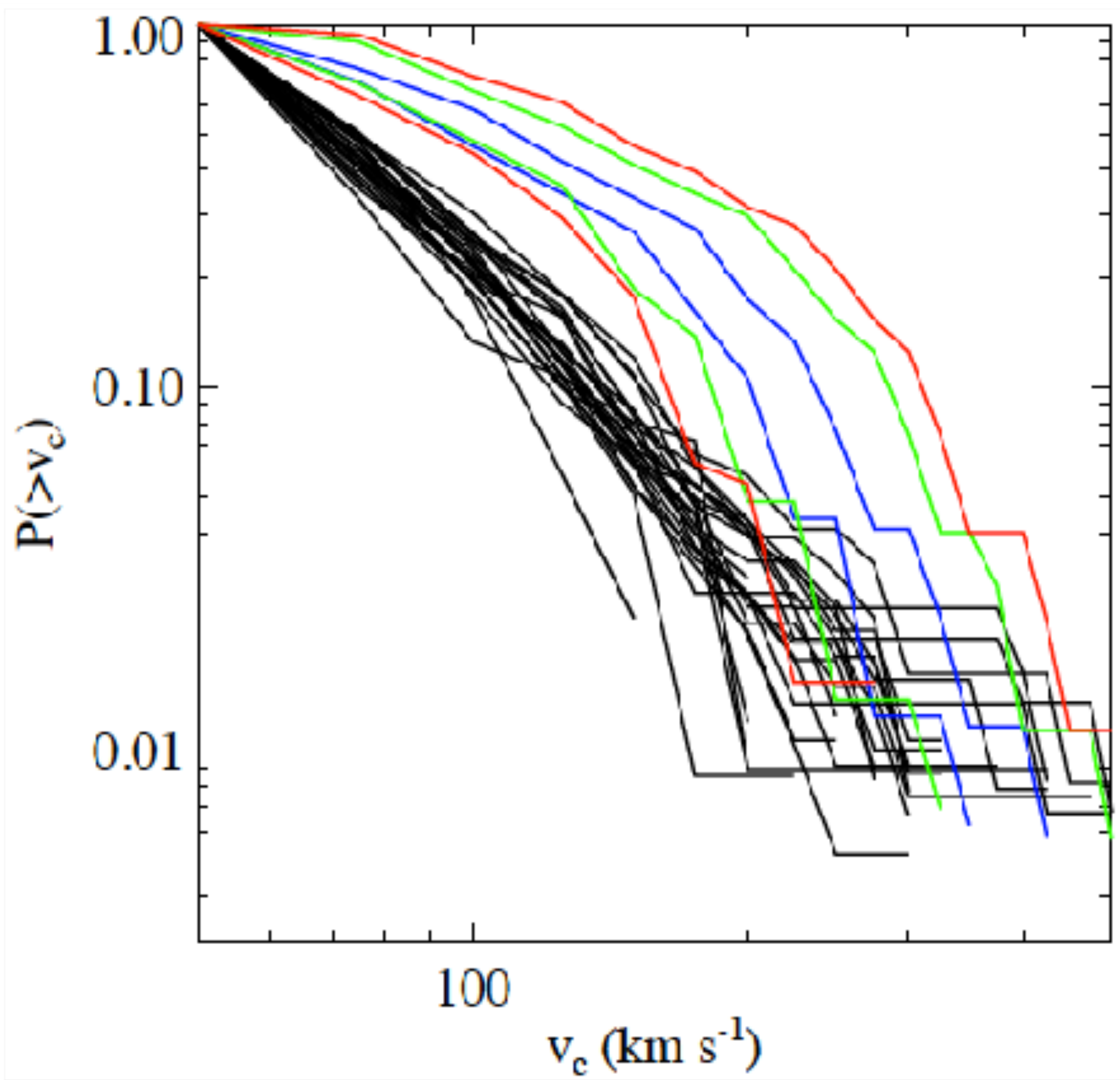

The velocity function of substructure in MACS 0416 from strong lensing at 1σ, 2σ, and 3σ.

- **Higher** and with **different shape** than for 24 simulated clusters with total mass similar to that of MACS 0416.

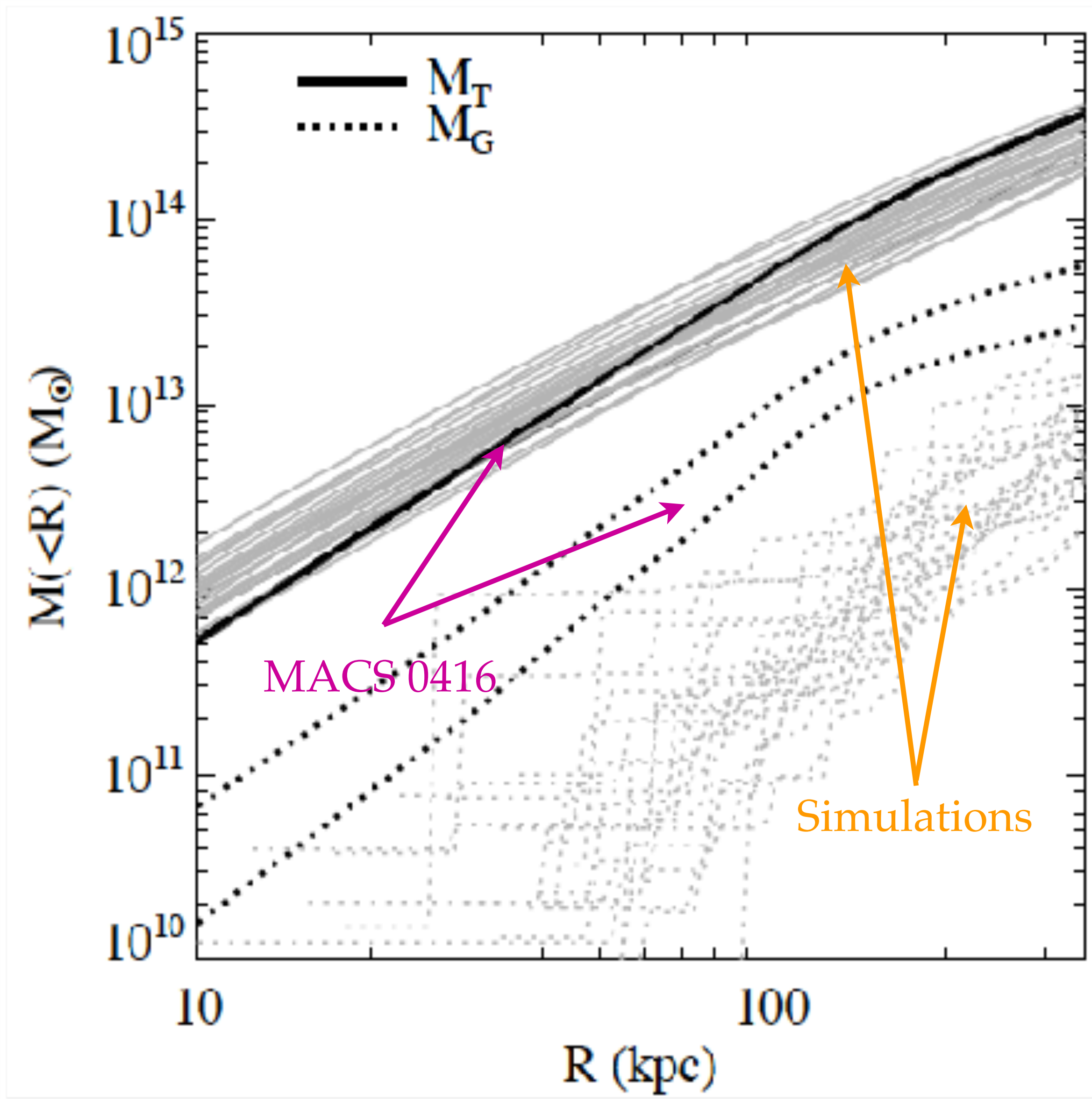

The galaxy cluster subhalo population

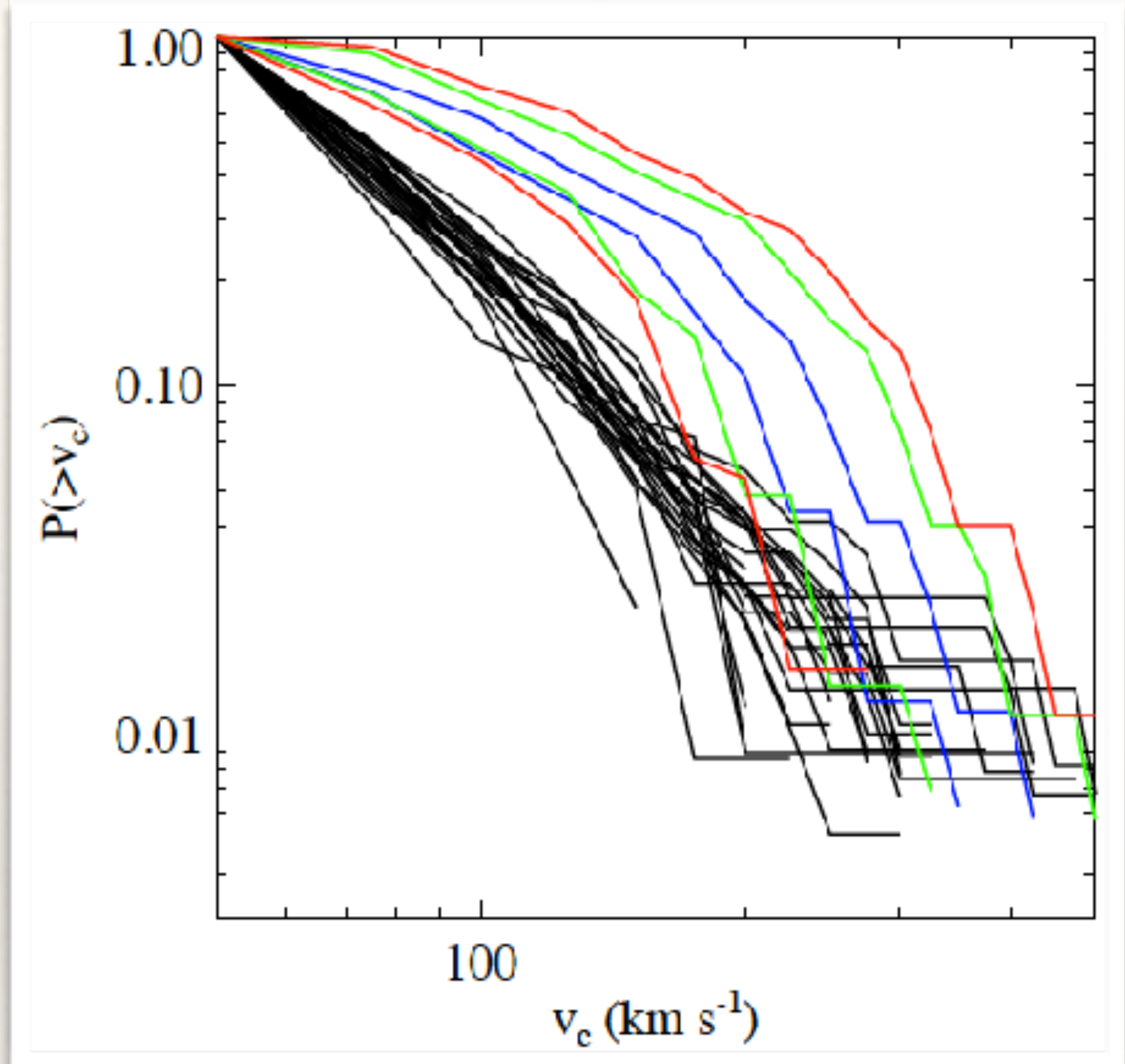

The velocity function of substructure in MACS 0416 from strong lensing at 1σ, 2σ, and 3σ.

- **Higher** and with **different shape** than for 24 simulated clusters with total mass similar to that of MACS 0416.

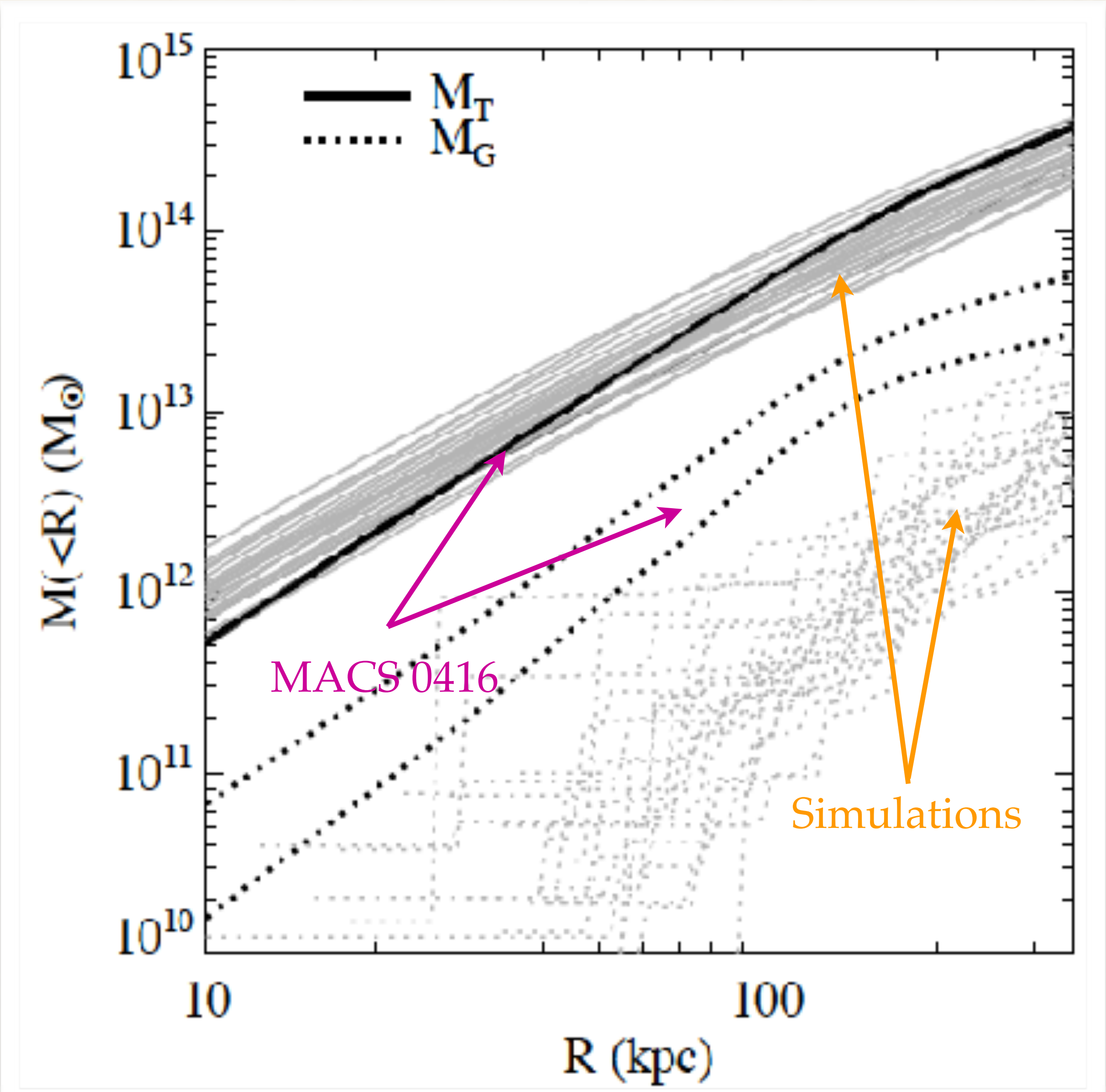

- Simulated galaxy clusters have less mass in substructure in the inner regions

The galaxy cluster subhalo population

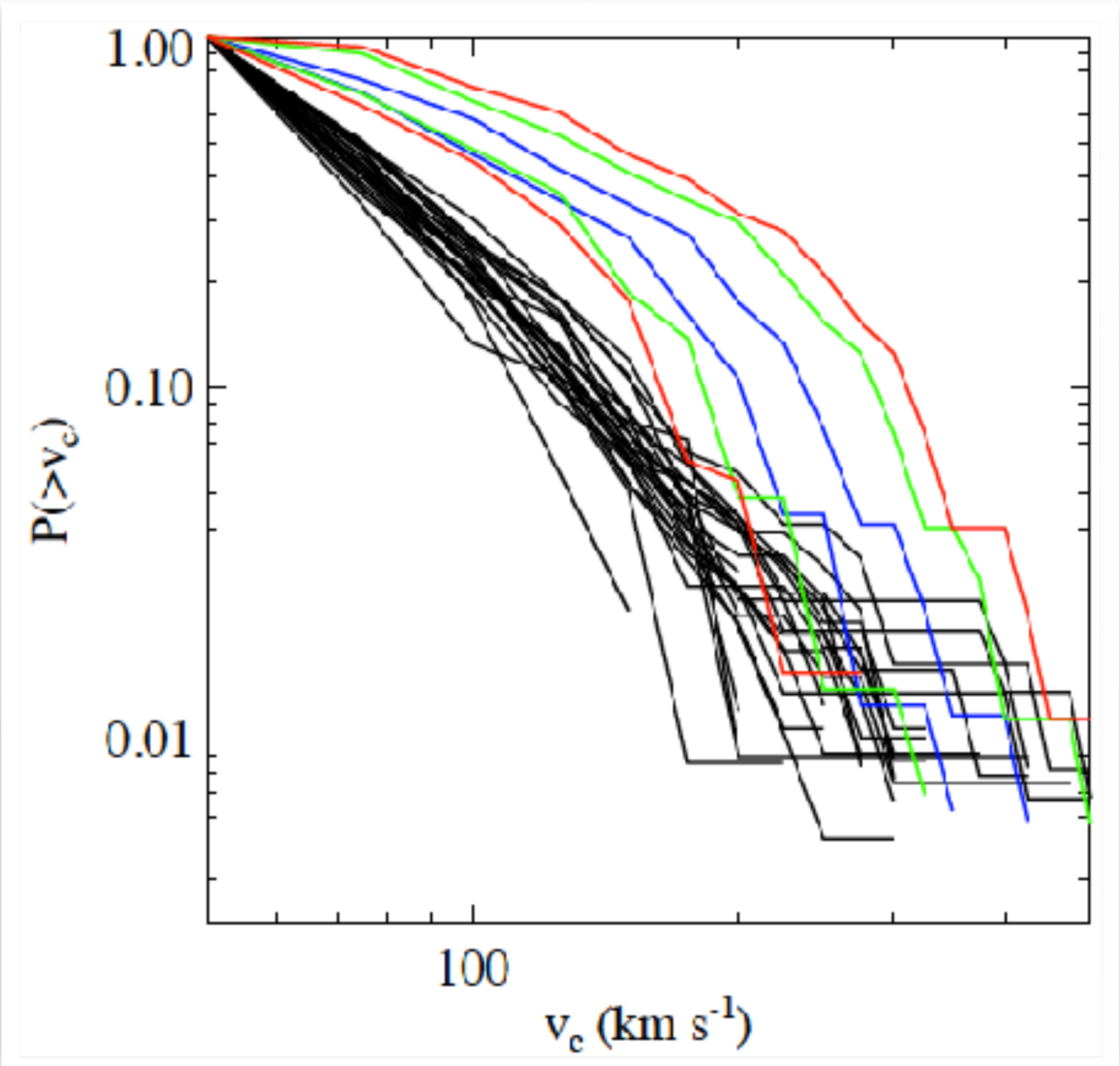

The velocity function of substructure in MACS 0416 from strong lensing at 1σ, 2σ, and 3σ.

- **Higher** and with **different shape** than for 24 simulated clusters with total mass similar to that of MACS 0416.

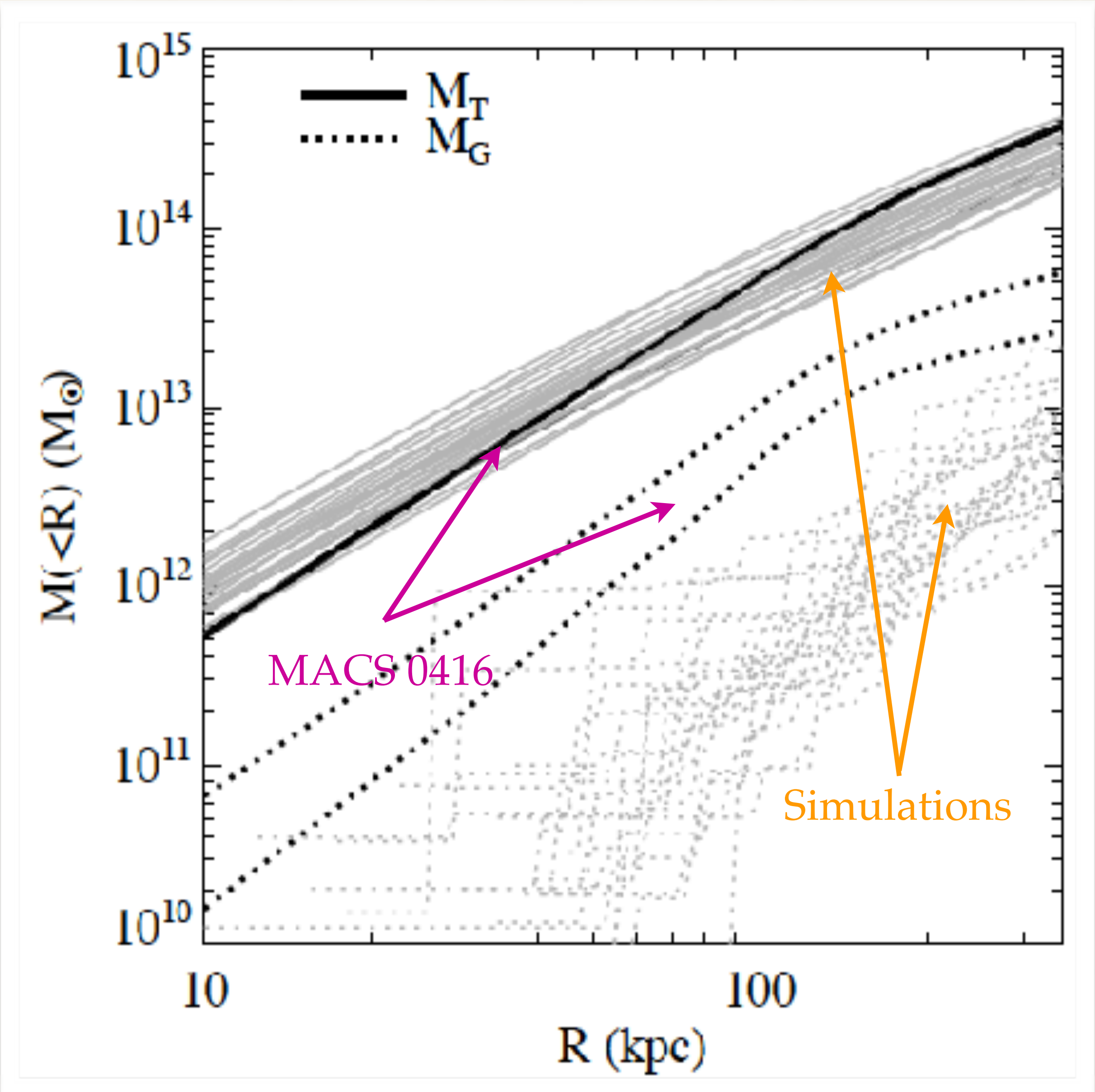

- Simulated galaxy clusters have less mass in substructure in the inner regions
- Perhaps the effect of dynamical friction and tidal stripping effects in DM-only cosmological simulations

The galaxy cluster subhalo population

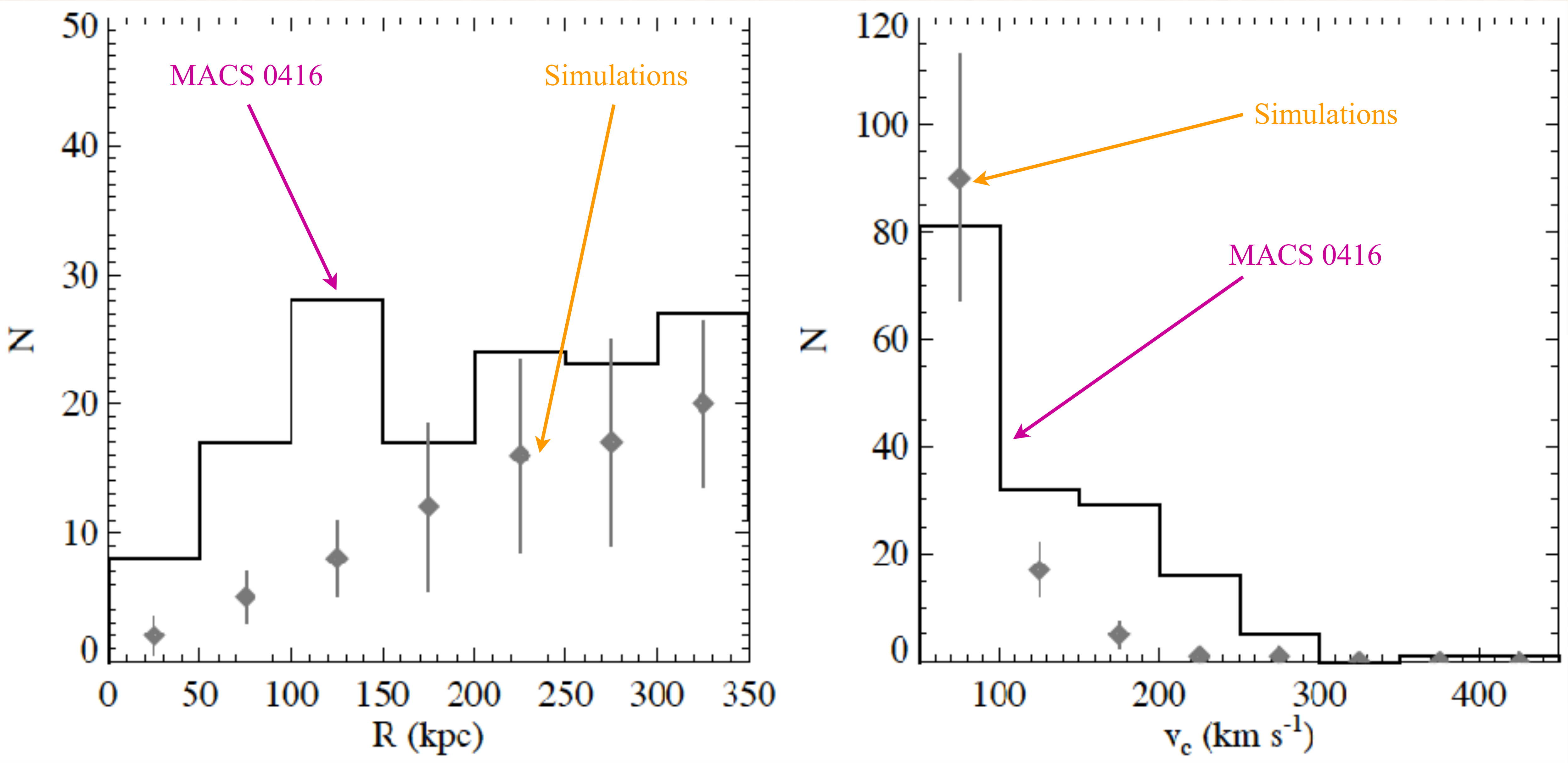

- Simulated halos consistently underpredict the number of subhalos on all radial scales (particularly in the inner 150 kpc)

The galaxy cluster subhalo population

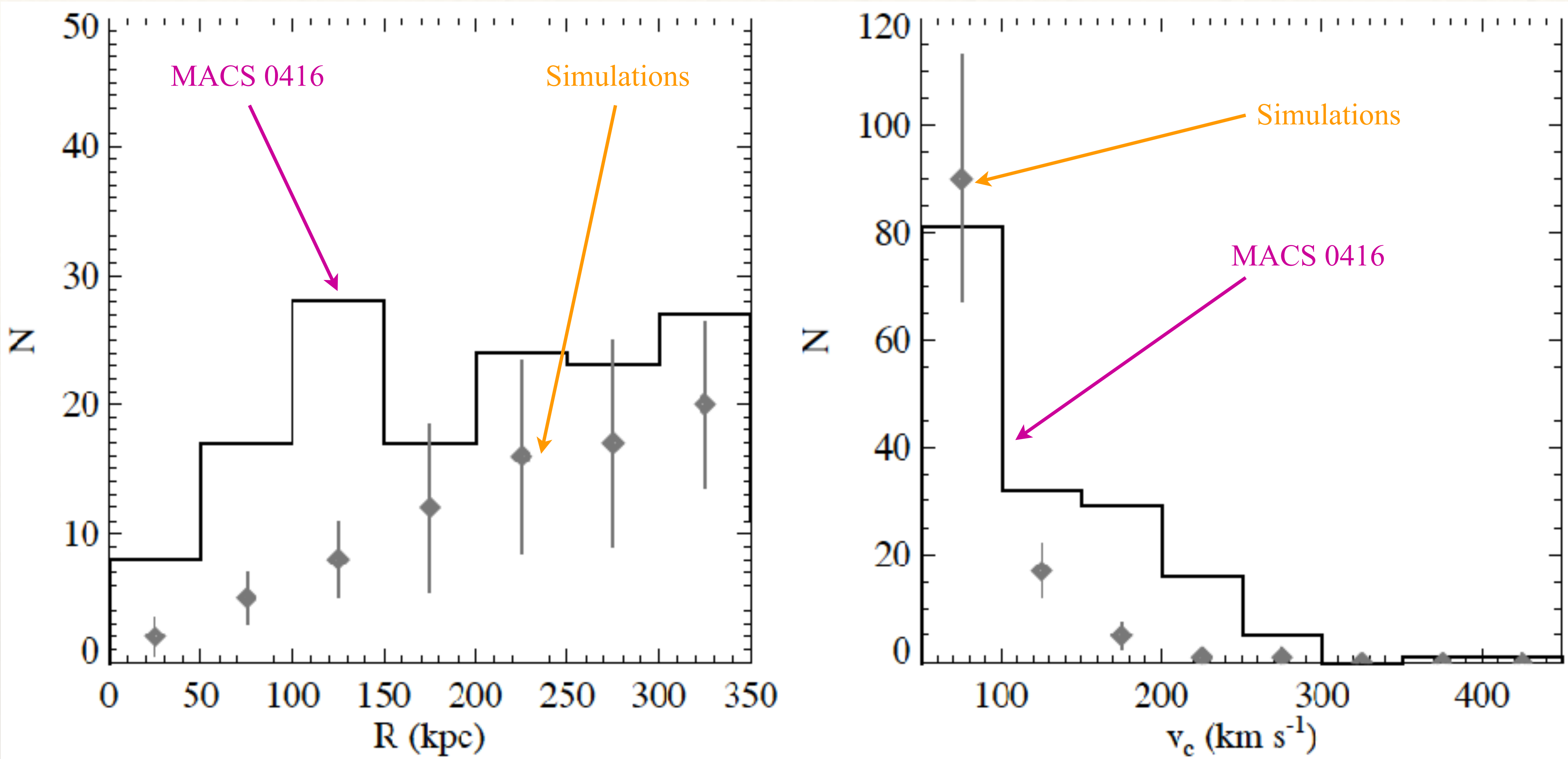

- Simulated halos consistently underpredict the number of subhalos on all radial scales (particularly in the inner 150 kpc)
- Simulated clusters have fewer substructures with v_c within ~100-300 km / s (observational results robust here)

The galaxy cluster subhalo population

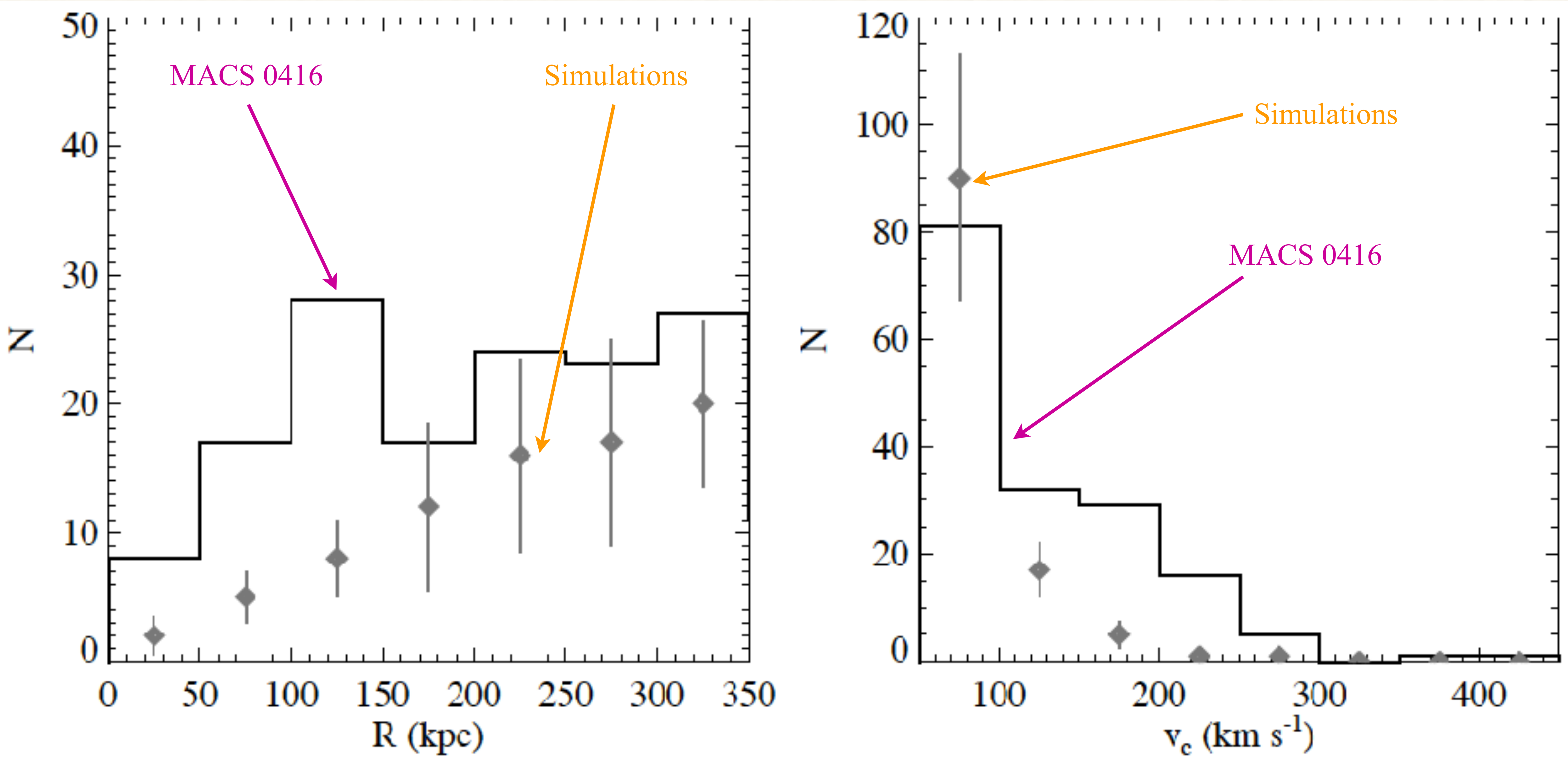

- Simulated clusters have fewer substructures with v_c within ~100-300 km/s (observational results robust here)
- Massive subhalos not formed or accreted so fast into the simulated clusters?

The galaxy cluster subhalo population

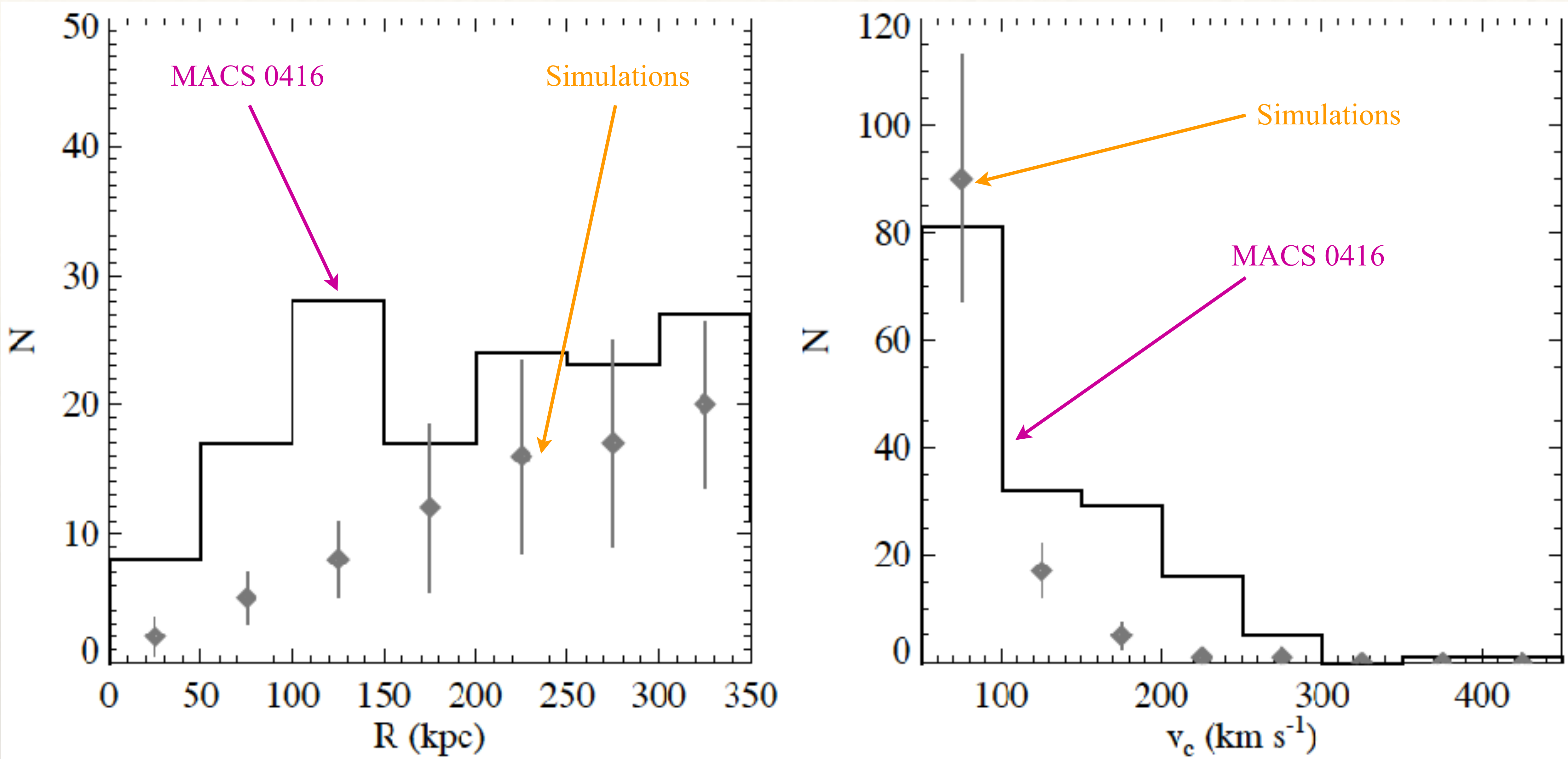

- Massive subhalos not formed or accreted so fast into the simulated clusters?
- Tidal stripping of massive subhalos more efficient than observed?

Cluster mass decomposition

- Combined analysis of X-ray and strong lensing data

Cluster mass decomposition

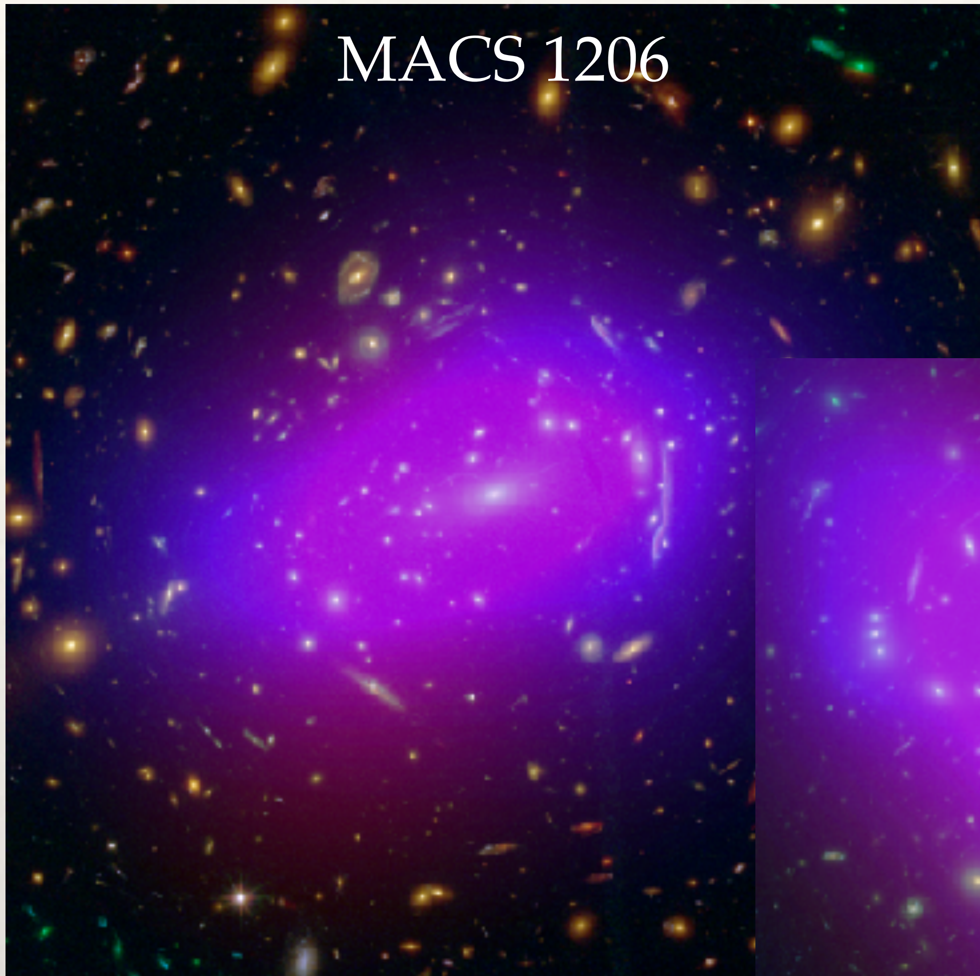

Bonamigo et al. (2017)

- Combined analysis of X-ray and strong lensing data

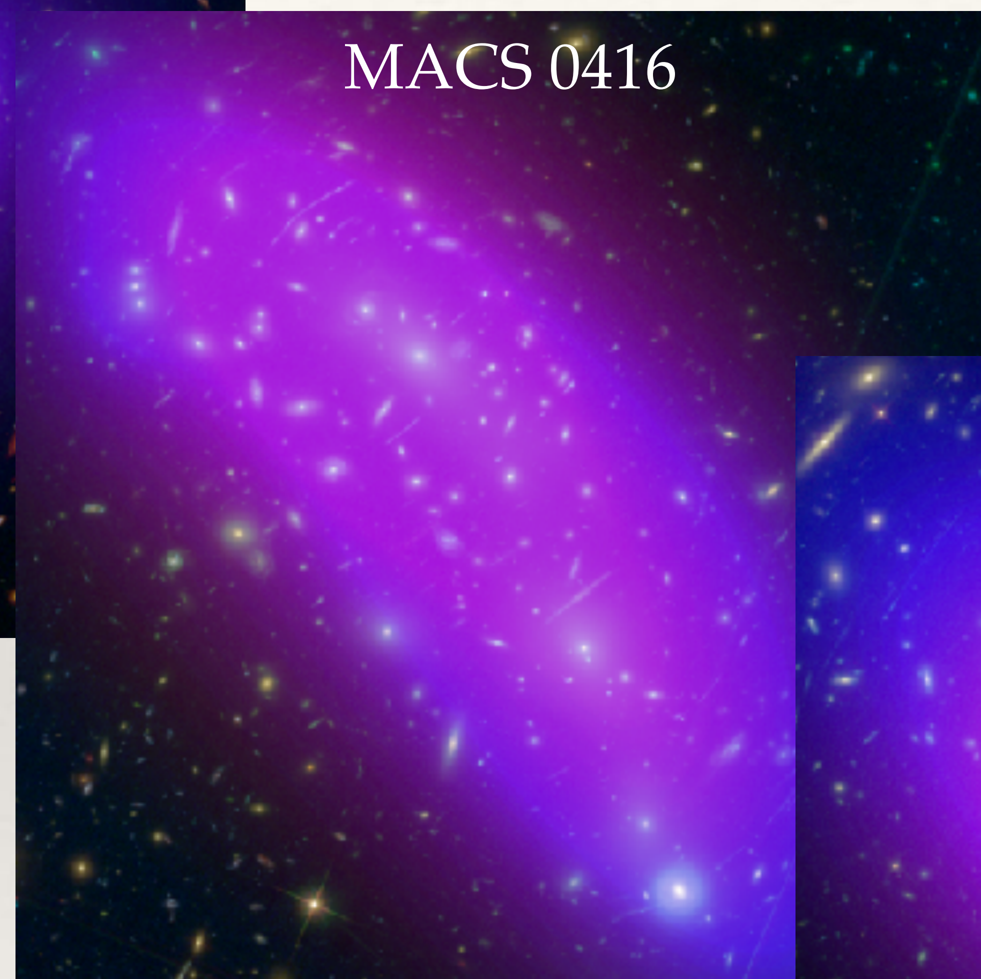

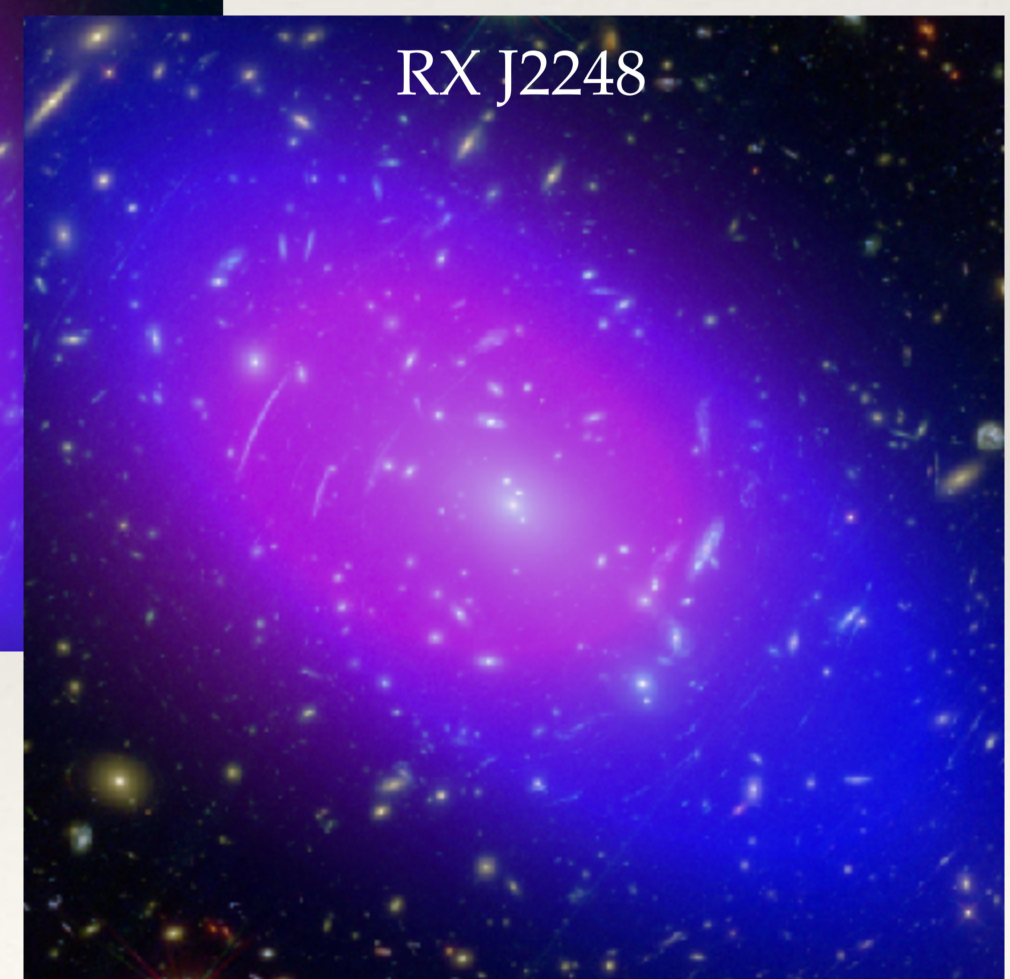

- Dissection of the hot gas and dark matter components

Cluster mass decomposition

Cluster	z	M_{200c} ($10^{15} M_{\odot}$)	R_{200c} (Mpc)	N_{mem}	N_{im}
RXC J2248	0.348	2.03±0.67	2.32±0.26	222	55
MACS J0416	0.396	1.04±0.22	1.82±0.13	193	102
MACS J1206	0.439	1.59±0.36	2.06±0.16	265	82

- Deep Chandra data
  - 123 ks for RXC J2248
  - 293 ks for MACS J0416
  - 23 ks for MACS J1206
- High temperatures
  - 12.8 keV for RXC J2248
  - 10.4 keV for MACS J0416
  - 13.0 keV for MACS J1206
- Modelling of the hot-gas mass distribution with multiple mass components to fit the X-ray SB

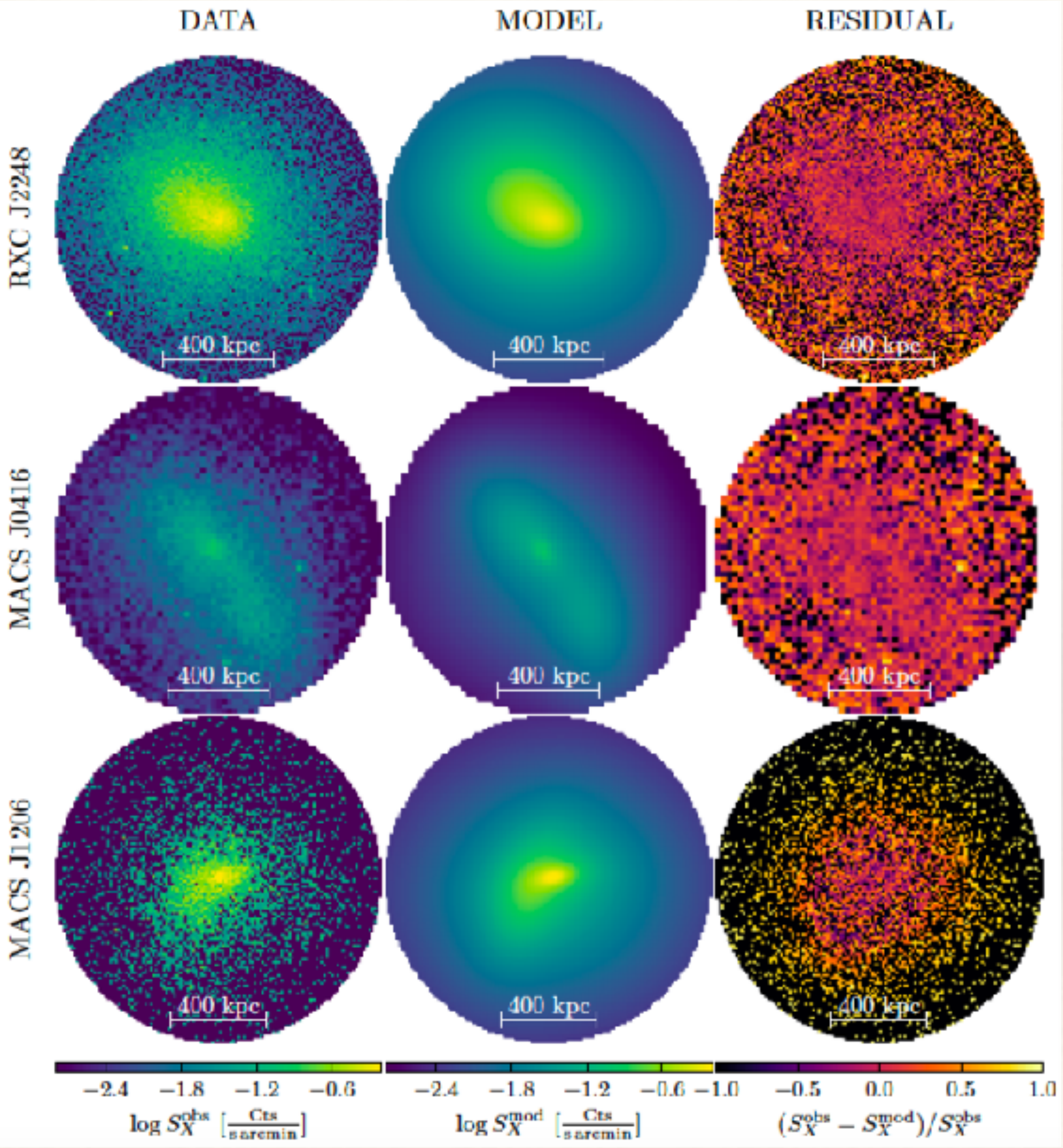

Bonamigo et al. (2018)

Cluster mass decomposition

- Dissection of the total mass distribution into the diffuse DM and hot-gas components
- The diffuse DM and hot-gas components have slightly different centers and shapes
- No significant offsets between the BCG positions and the peaks of the diffuse DM components

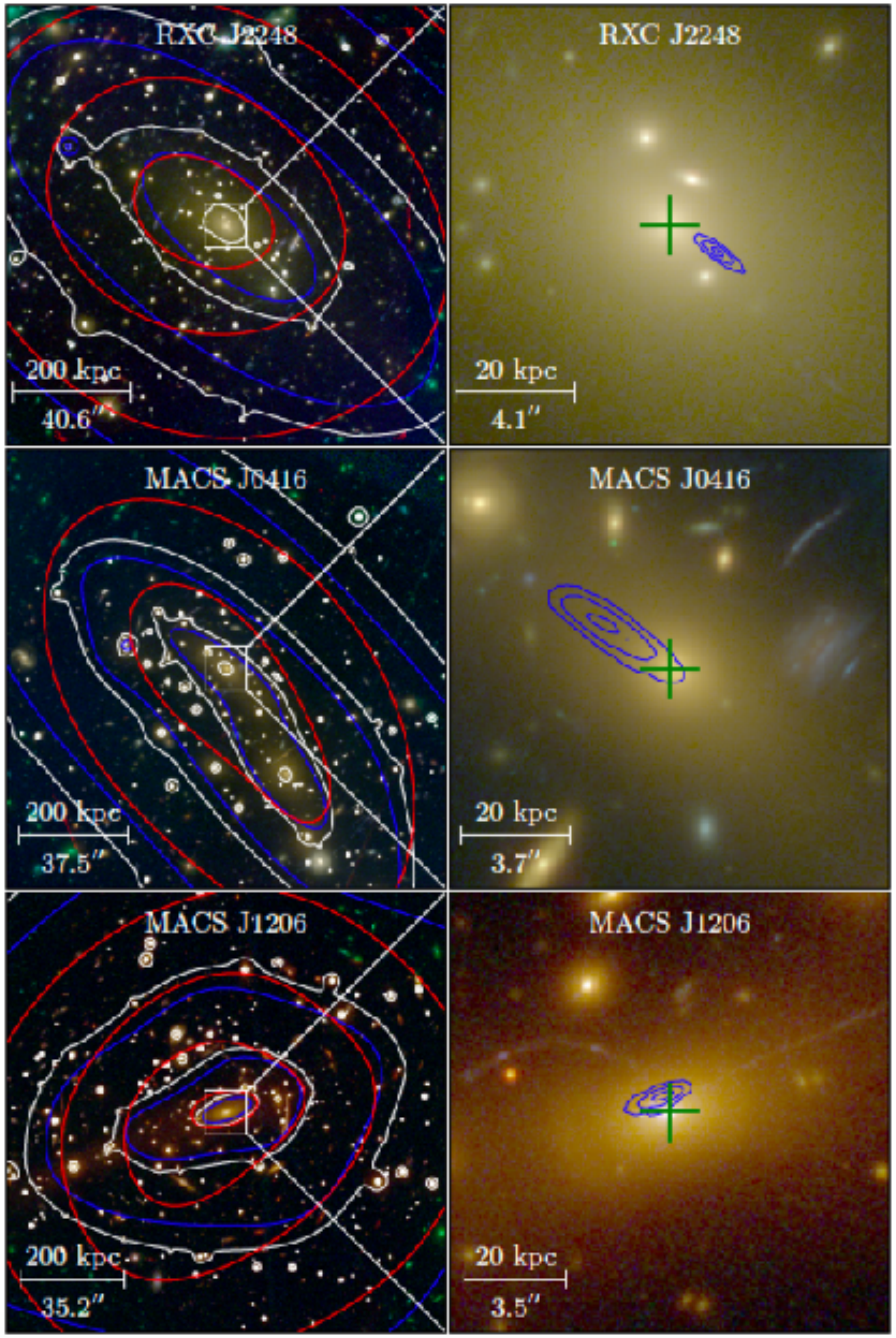

Bonamigo et al. (2018)

Cluster mass decomposition

- Dissection of the total mass distribution into the diffuse DM and hot-gas components
- The diffuse DM and hot-gas components have slightly different centers and shapes
- No significant offsets between the BCG positions and the peaks of the diffuse DM components

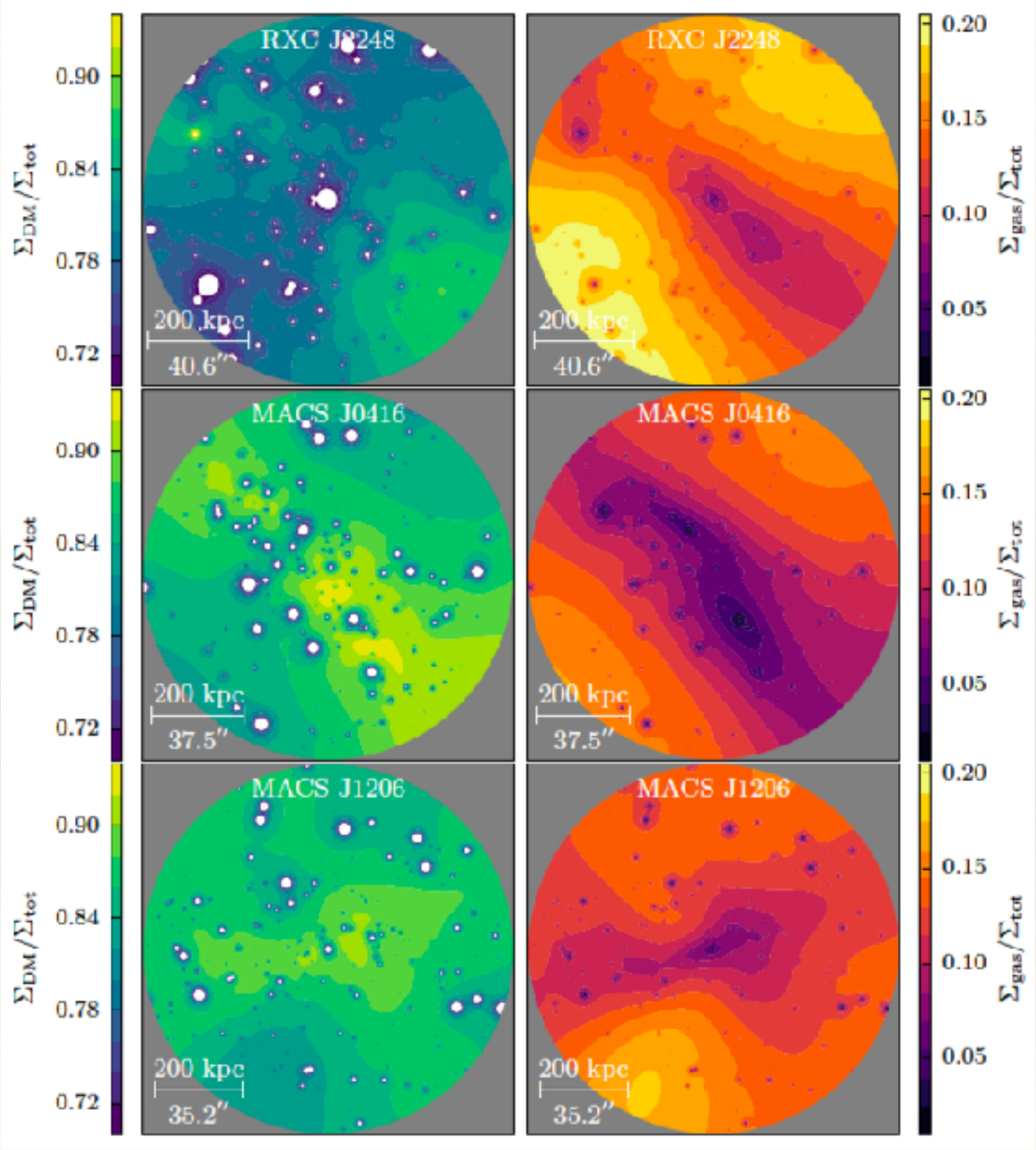

Bonamigo et al. (2018)

Cluster mass decomposition

- Dissection of the total mass distribution into the diffuse DM and hot-gas components
- The diffuse DM and hot-gas components have slightly different centers and shapes
- No significant offsets between the BCG positions and the peaks of the diffuse DM components

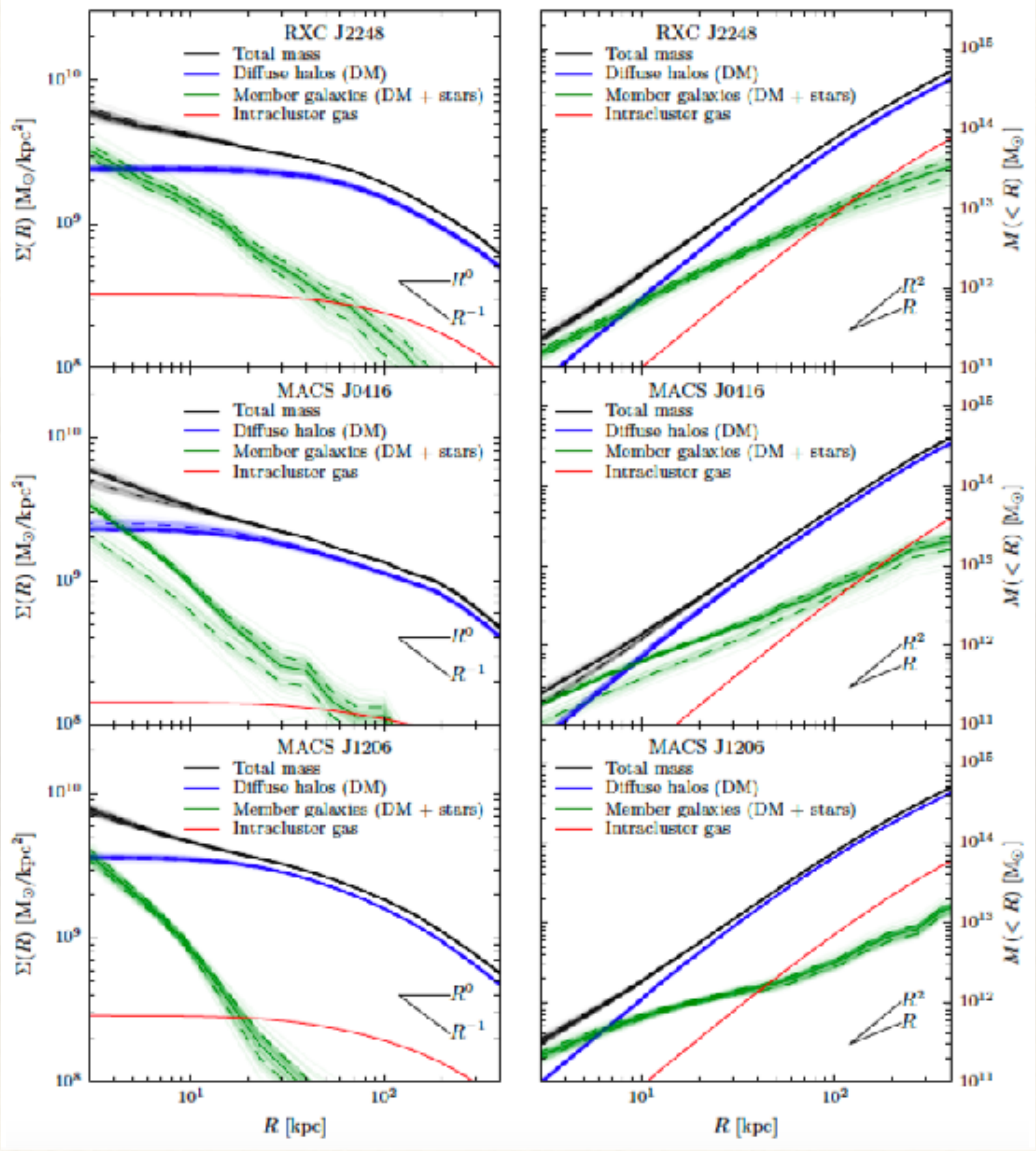

Bonamigo et al. (2018)

Cluster mass decomposition

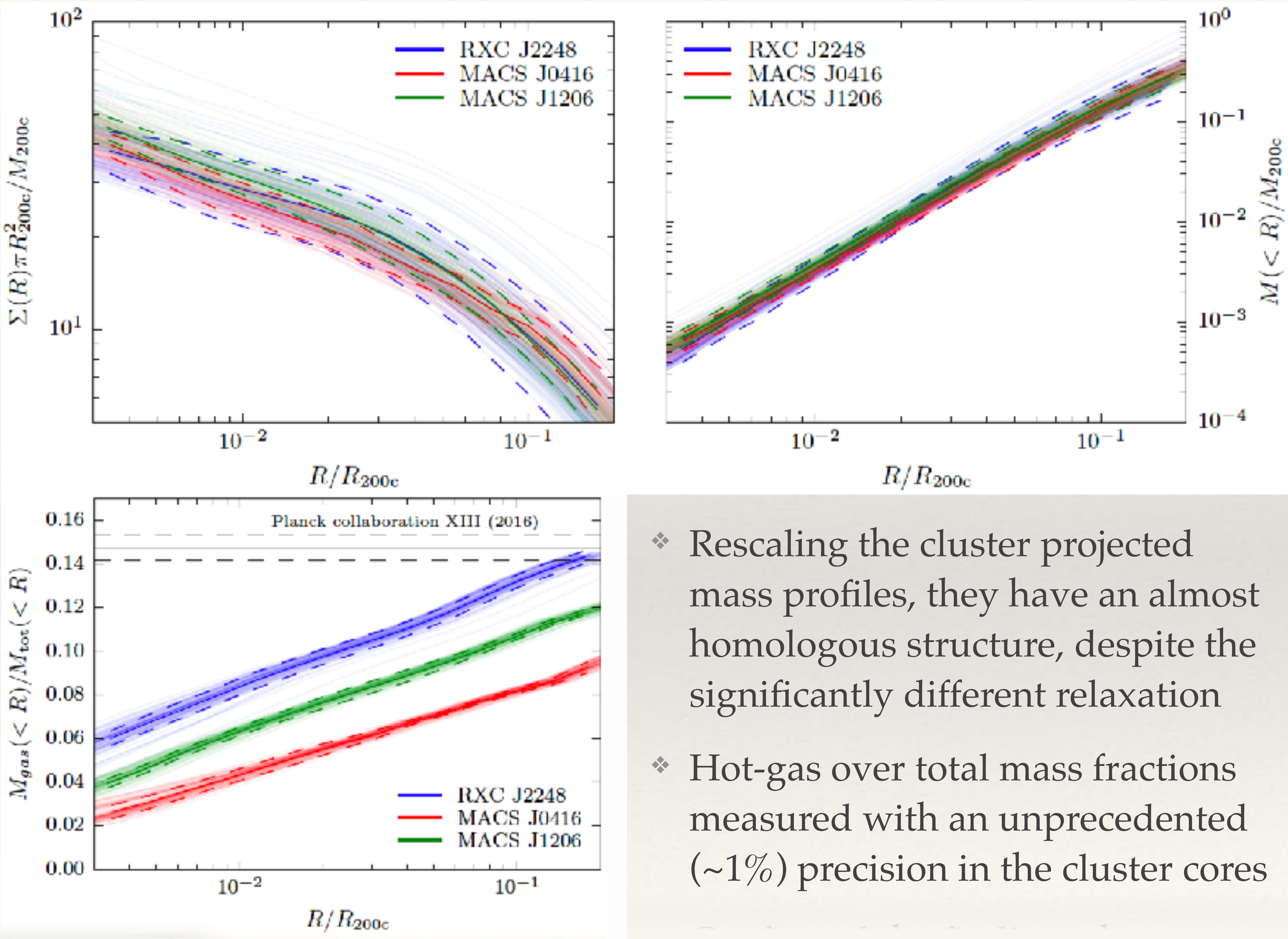

- Rescaling the cluster projected mass profiles, they have an almost homologous structure, despite the significantly different relaxation
- Hot-gas over total mass fractions measured with an unprecedented (~1%) precision in the cluster cores

Cluster mass decomposition

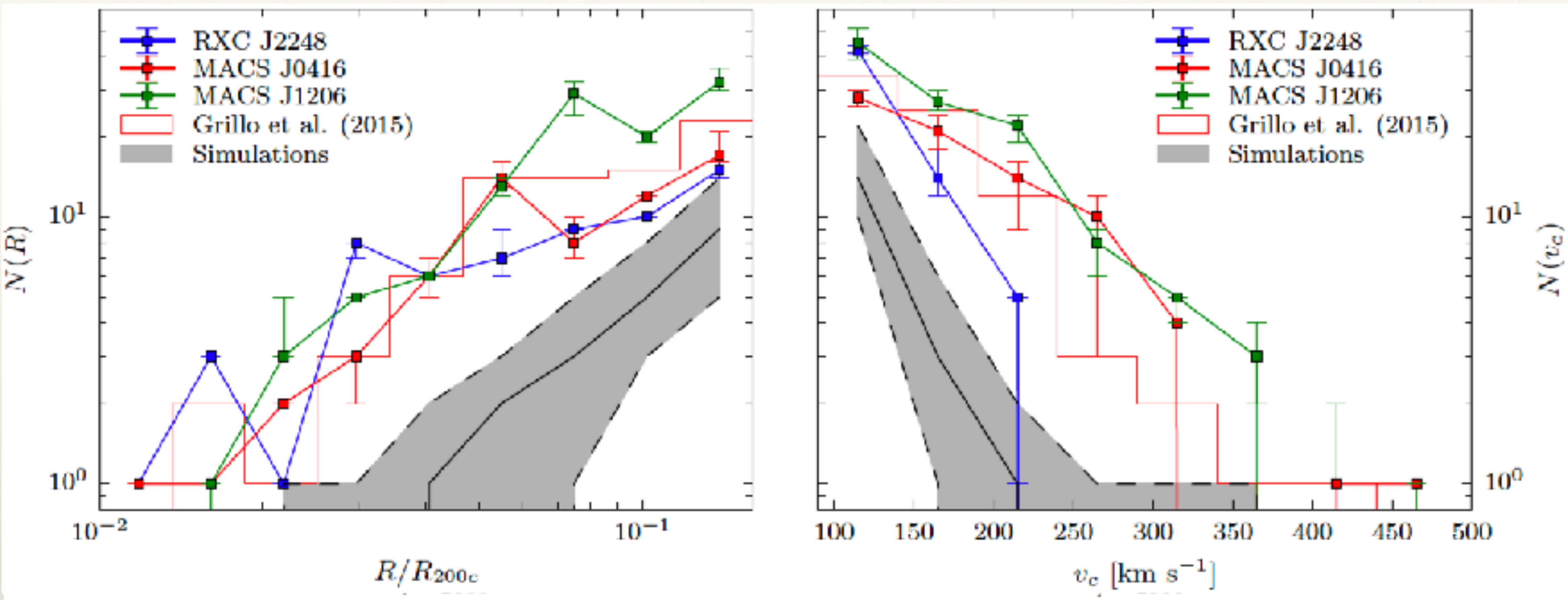

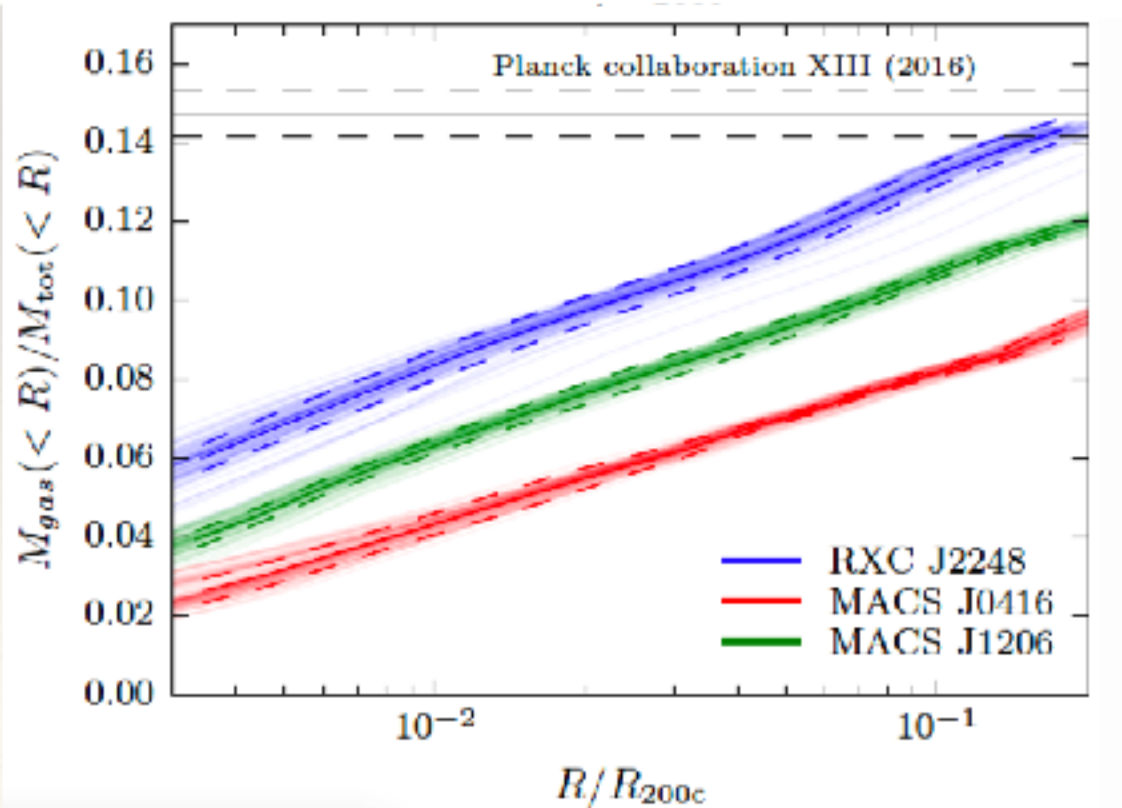

- Hot-gas over total mass fractions measured with an unprecedented (~1%) precision in the cluster cores
- Confirmed the findings that current N-body simulations under-predict the number of massive sub-halos in the cores of massive clusters

MACS 0416 mass decomposition

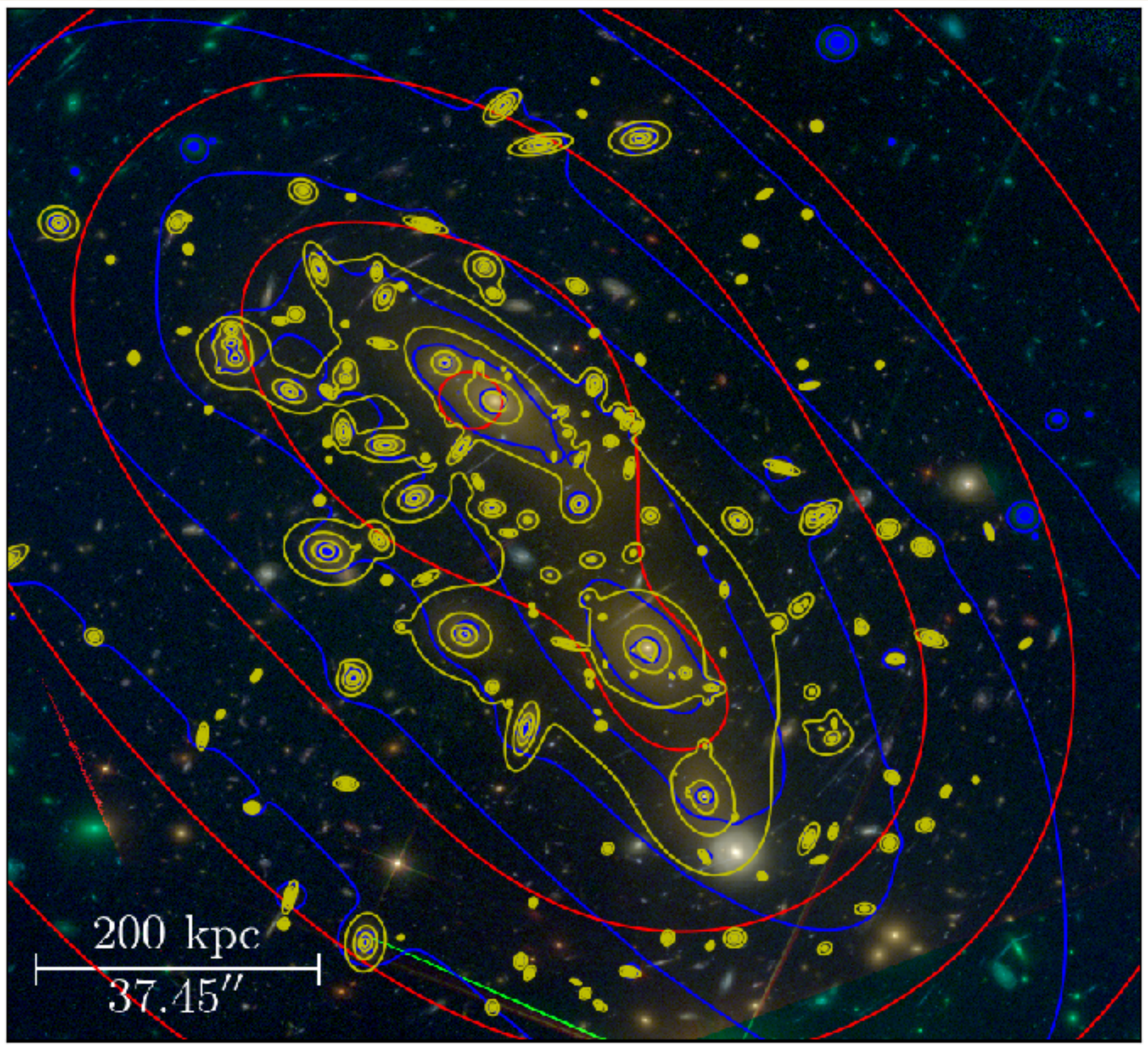

Bonamigo et al. (2017), Annunziatella et al. (2017)

MACS 0416 mass decomposition

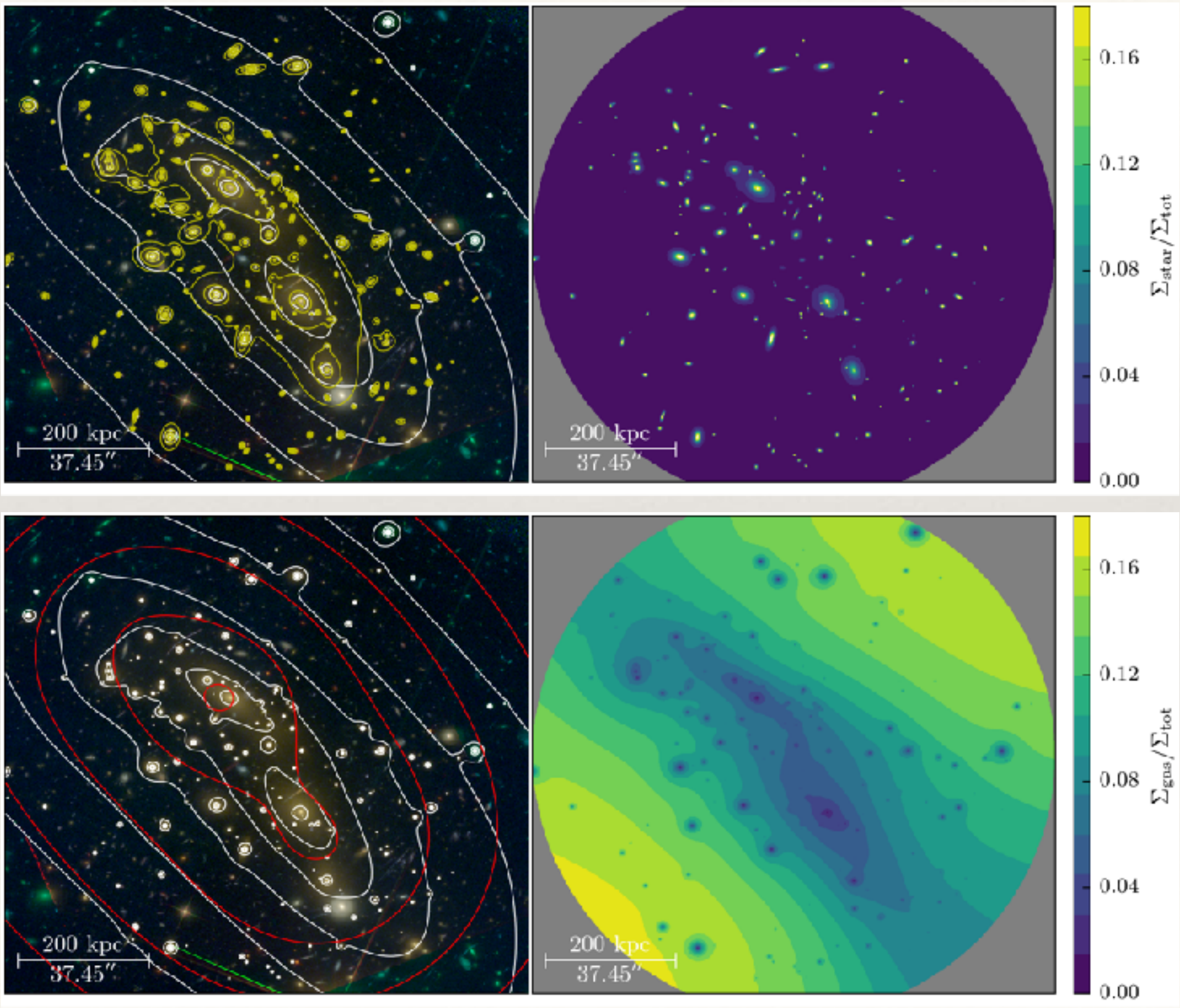

Bonamigo et al. (2017), Annunziatella et al. (2017)

MACS 0416 mass decomposition

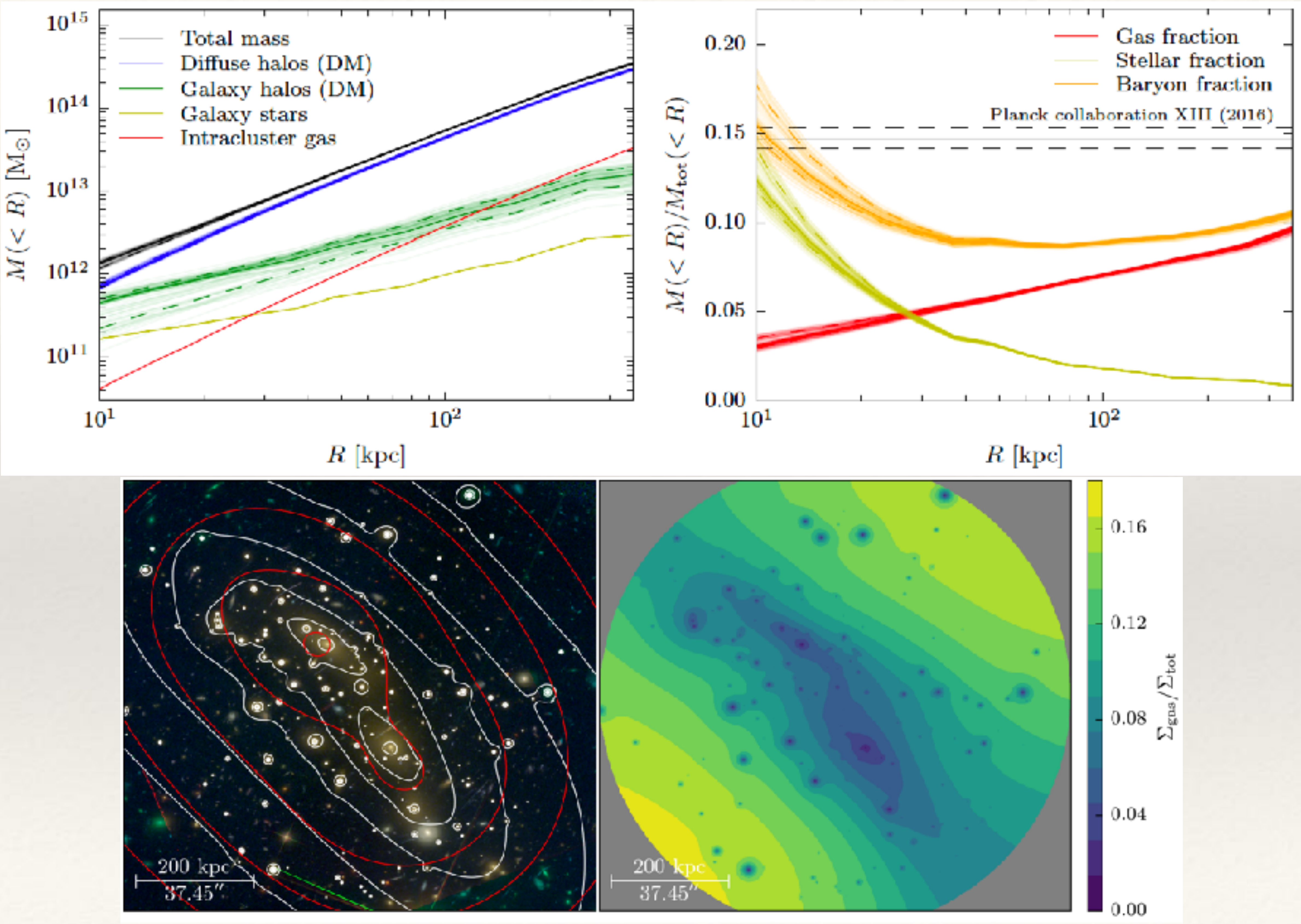

Bonamigo et al. (2017), Annunziatella et al. (2017)

MACS 0416 mass decomposition

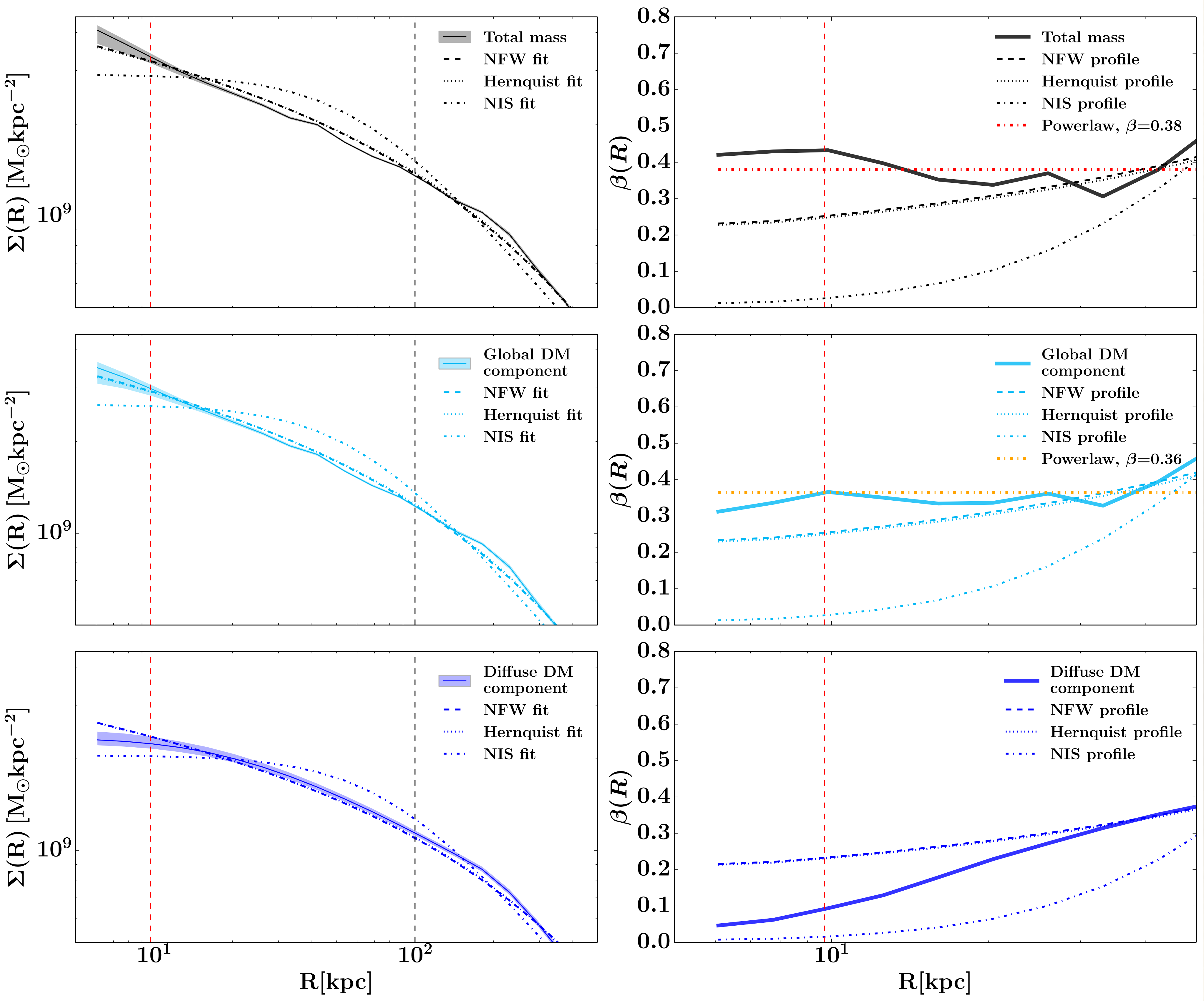

Bonamigo et al. (2017), Annunziatella et al. (2017)

Final remarks

- Careful strong lensing analyses of galaxy clusters can lead to new exciting results on their **dark matter halos** and **subhalo population**
- HST **angular resolution** and **multiband coverage** + VLT **spectroscopy** vital to
  - Select and model the cluster members, for both accurate dynamical and lensing analyses
  - Confirm several multiple image systems, allowing unbiased estimates of the cluster modeling parameters
  - Study in detail the physical properties of background lensed sources
- The new era of **high precision strong lensing modeling** will allow us to
  - Build robust high-resolution mass maps of the galaxy clusters
  - Test the ΛCDM model (e.g., DM mass profiles, substructures…)
  - Exploit the lensing signal to probe the background cosmology